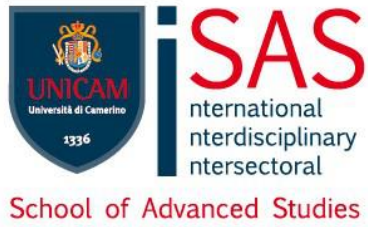

UNIVERSITÀ DEGLI STUDI DI CAMERINO

School of Advanced Studies

DOCTORAL COURSE IN

Chemical Sciences

XXVI cycle

ADVANCED SYNTHETIC STRATEGIES FOR THE PREPARATION OF KEY SMALL MOLECULES AND BIOLOGICALLY ACTIVE COMPOUNDS

PhD Student

Benedetta Bassetti

Supervisors

Prof. Alessandro Palmieri

Co-supervisors

Dr. Federico Peterlongo

Chiari mattini,
quando l'azzurro è inganno che non illude,
crescere immenso di vita,
fiumana che non ha ripe né sfocio
e va per sempre,
e sta – infinitamente.

Sono allora i rumori delle strade
l'incrinatura nel vetro
o la pietra che cade
nello specchio del lago e lo corrùga.
E il vocìo dei ragazzi
e il chiacchiericcio liquido dei passeri
che tra le gronde svolano
sono tralicci d'oro
su un fondo vivo di cobalto,
effimeri…

Ecco, è perduto nella rete di echi,
nel soffio di pruina
che discende sugli alberi sfoltiti
e ne deriva un murmure
d'irrequieta marina,
tu quasi vorresti, e ne tremi,
intento cuore disfarti,
non pulsar più! Ma sempre che lo invochi,
più netto batti come
orologio traudito in una stanza
d'albergo al primo rompere dell'aurora.

E senti allora,
se pure ti ripetono che puoi
fermarti a mezza via o in alto mare,
che non c'è sosta per noi,
ma strada, ancora strada,

e che il cammino è sempre da ricominciare.

A galla, Altri versi e poesie Disperse, Eugenio Montale

Occorre diffidare del quasi-uguale (il sodio è quasi uguale al potassio:
ma col sodio non sarebbe successo nulla), del praticamente identico, del pressappoco,
dell'oppure, di tutti i surrogati e di tutti i rappezzi. Le differenze possono essere piccole,
ma portare a conseguenze radicalmente diverse, come gli aghi degli scambi;
il mestiere del chimico consiste in buona parte nel guardarsi da queste differenze,
nel conoscerle da vicino, nel prevenirne gli effetti.
Non solo il mestiere del chimico.

Il sistema periodico, Potassio, di Primo Levi

Author's Declaration

I declare that the work presented in this dissertation was carried out in accordance with the requirements of the University's Regulations and Code of Practice for School of Advanced Studies, and that it has not been submitted for any other academic award. Except where indicated by specific references in the text, the work is the candidate's own work. Work done in collaboration with, or with the assistance of others, is indicated as such. Any views expressed in the dissertation are those of the author.

Camerino, 10/01/2024

Benedetta Bassetti

Table of Contents

Preface

The present manuscript gathers many topics I dealt with during my PhD research period. The first chapter includes an overview on how sustainability is getting more and more relevant in chemistry and, in particular, in the development of chemical processes, since the outbreak of Green Chemistry concepts until now. Moreover, some of the most important enabling technologies in organic synthesis are detailed, such as one-pot processes, microwave irradiation, flow chemistry and photochemistry, with a final section dedicated to combined techniques.

The second and third chapters encompass the research work I conducted at University of Camerino (Chemistry Interdisciplinary Project, ChIP, Camerino, Italy) in the Green Chemistry Group, under the supervision of Prof. A. Palmieri, with the collaboration of Indena S.p.A., and in Prof. C. O. Kappe's research group (CCFLOW lab) from April 2022 to October 2022, at the University of Graz, Institute of Chemistry, under the supervision of Dr. C. Hone.

In particular, the second chapter focuses on the importance of nitro compounds as key building blocks in organic synthesis. In this context, nitroolefins were exploited, during my PhD, to achieve the synthesis of polysubstituted carbazoles and conjugated (*E,E*)-dienones under mild conditions, two important compounds that find application in drug molecules and materials science. Furthermore, their hydroalkylation was accomplished under photocatalytic conditions, both in batch and flow, in a project conducted in collaboration with the PhotoGreen Lab of University of Pavia.

The third chapter is devoted to explore the relevance of natural products in organic chemistry, with particular attention on the development of synthetic procedures to access valuable compounds. With this aim, we envisaged a simple four-step sequence for the preparation of flavonoid Luteoloside, often present in natural sources only in traces, in the context of a project carried out in collaboration with Indena S.p.A.

The last section of the chapter describes the work realized during my abroad period at the University of Graz, in which a continuous flow protocol was developed, after an extensive batch investigation, for the selective synthesis of two cannabinoids, Δ^9-THC and Δ^8-THC.

1 New approaches and technologies in organic synthesis

Recent times force us, researchers, academics, and industrial experts, to interrogate us and care about what we do, but most of all about *how* we do it. The question come directly from the world that surround us. We must directly face the problems and accommodate us in this new reality where no one is allowed to look the other way, especially if we are part of a community that play an important role in it. Chemistry itself acknowledged this necessity long time ago, pioneers foresaw it all, but we continuously struggled to remember how a single person, or a small group of people is at the base of that necessity, of that change that the world needs.

The revolutionary concept of alternative reaction pathways to tackle environmental hazards and pollution were first conceptualized by Paul Anastas and Roger Garrett in **1991**, and later evolved in the more structured "Green Chemistry" paradigm, thank to Joe Breen, but the concerns regarding the impact that chemistry had on nature and human health started years before that important date.[1]

1.1 Green Chemistry: the evolution of an idea

Chemistry permeates every aspect of our life but its image all over the world has been long compromise, starting from the publication of Silent Spring in 1962. The book outlined the devastation that some chemicals had on local ecosystems and gave a boost to the modern environment movement. The attention was put on the growth of industrial activities and their waste dumping practices, and on the damages caused by pesticides like DDT.[2]

In order to face environmental problems and concerns, companies started to think about changing their processes and important actions were taken directly by the President of the United States itself, Richard Nixon, who introduced the Nation Environmental Policy Act (1969) and established the U.S. Environmental Protection Agency (EPA) at the beginning of the new decade. Their goals were "…to examine the full range of variables which affect environmental quality", considering that pollution control as major actor.[3]

Recognizing the need to move from "end-of-pipeline" mindset to actual pollution prevention, by the 1980s the EPA established the Office of Pollution Prevention and Toxics, and in 1990 emitted the Pollution Prevention Act, created to enforce sustainable approaches to productivity. Moreover, provided grants to states to reduce source waste, but one of the significant shifts began to occur among chemists. Scientists, growing in the new era of environmental awareness, started to research innovative strategies, while leaders of both industries and governments opened international conversations to face the problems and looking for preventative solutions.

By the end of the 1990, EPA launched a research program which was expanded in 1993 and named "Green Chemistry Program", where the brand-new term **Green Chemistry** made its first appearance, coined by Anastas and his team at US EPA.

Green chemistry is herein defined as "**the design of chemical products and processes that reduce or eliminate the generation of hazardous substances**",[4] where "design" represent the most important word, because it expresses the true essence of the sentence: it must be something

that is not done by accident, but a true "thoughtful endeavor, it is a statement of human intention", with an highlight on novelty, planning and systematic conception.[5,6]

The effort put in the Green Chemistry Program and the crucial presence of Dr. Joseph J. Breen, among others, led not only to the publication of "*Green chemistry: Theory and Practice*", where the famous Twelve Principles of Green Chemistry are postulated as guidelines for designing green products and processes, but also to the foundation of the Green Chemistry Institute (GCI), which few years later became part of the American Chemical Society (ACS GCI).

Within those years the green chemistry movement began to gain ground internationally, and conferences were held all over the world building a real community, a bridge that linked institutions and universities from United States to Italy and Japan. The divulgation of the new direction taken by scientists was of primary importance, and in 1999 the journal of Green Chemistry was launched by Royal Society of Chemistry in UK. Another main achievement was the inauguration of the pharmaceutical roundtable promoted by ACS GCI in 2005, with the aim to improve efficiency of the processes and to promote safety in drug designing among companies.[7]

In 2016, Green Chemistry celebrated its 25th birthday: ideas and principles evolved during decades, following innovations and discoveries. Now, the task is not yet completed, and many new challenges need to be faced (**Figure 1.1**). The same Anastas is conscious that green chemistry is still very much an emerging field that needs not only to be open but fused together to other disciplines, such as biology, engineering, and physics.[7,8]

Looking forward to the 2030 Agenda for Sustainable Development, the universal call to action see chemistry, and in particular green chemistry, as central.[9]

Chemistry may have an impact for at least 7 of the 17 aspirations goals established by the agenda, such as Zero Hunger (**2**), Good Health & Well-being (**3**), Clean Water & Sanitation (**6**), Affordable & Clean Energy (**7**), Industry, Innovation & Infrastructure (**9**), Responsible Consumption & Production (**12**), Climate Action (**13**).[10] Just an example: today more than 98% of all organic chemicals are still derived from petroleum.

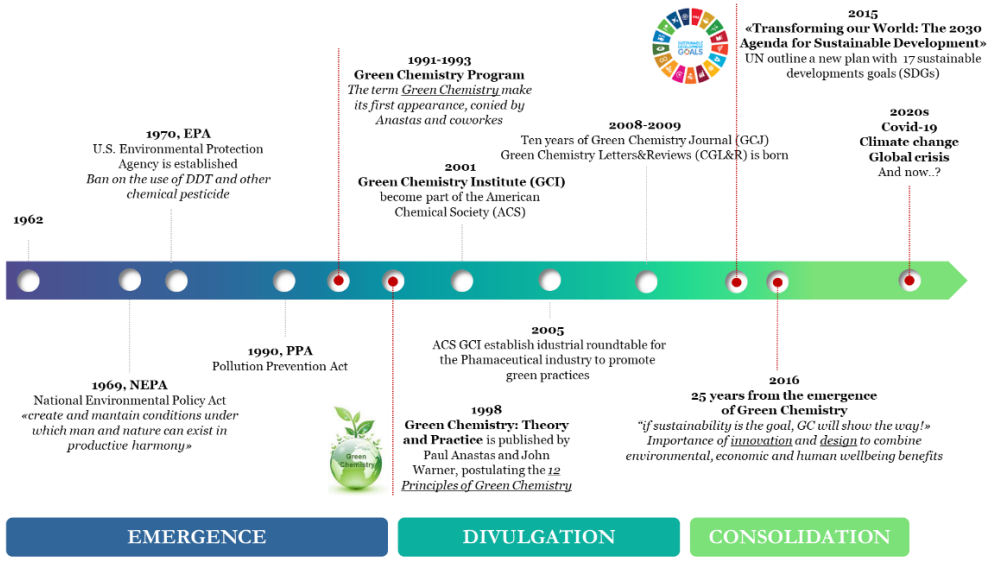

Figure 1.1 Green Chemistry evolution timeline[11]

Sustainable development goals have been proposed to achieve a harmonious development for the future, for the survival of humanity and protection of world's resources. A concerted effort by applying both green chemistry principles and the ones proposed by circular economy, such as the 5 R Rules (**Reuse, Reduce, Renew, Recycle, Redesign**), is necessary for sustainable production to advance, and it can be the starting point for re-directing the course of our evolution.

1.1.1 The Twelve Principles of Green Chemistry

In 1998, Paul Anastas and John Warner introduced a list of Twelve Principles that should be at the basis of Green Chemistry. They were interpreted as guidelines to help the design of safer, sustainable syntheses and processes, developed to look across their entire life-cycle stages of the product. These principles were envisaged to be general enough to be applied to the wider range of chemistry, with the final aim to reduce the intrinsic hazard and wastes of a chemical transformation.
Risks for human and environment coming from these hazards should be minimized at every level of the process, and this objective revealed to be also economically profitable.[6]

1. **Prevention —** It is better to prevent waste than to treat or clean up waste after it has been created.

This first principle is related to waste prevention, since this is the preeminent parameter that defines the impact of a process. Waste can be considered as everything that is not included in the final product, such as materials, solvent, side-products, unutilized energy. It can harmfully impact human

health and environment in different ways, depending on its nature, its toxicity, amount, or in the way it is released.

It is also important, when it is not possible to prevent their formation, to think of transformations in which these wastes could be recovered and return to life, be utilized in others production processes, introducing them in a virtuous circular stream. This can also represent a gain from the economic point of view.[12]

Roger Sheldon introduced in 1992 some metrics that are now widely used, based on the necessity of measuring the environmental acceptability of processes and contemporarily filling the lack of common languages between different industrial actors.[13]

Green metrics such as *E*-factor,[14] PMI,[15] and EQ are useful parameters to quantify the sustainability and impact of a synthetic design.[16]

USEFUL GREEN METRICS

E(nvironmental)-factor

It represents the actual amount of waste produced, from the raw material to the final product. It is calculated dividing the kg of waste produced in a process by the kg of recovered product. In this way, everything that is not the product will be considered part of the waste, such as organic solvents and purification materials. Yield and energy required are taken into account in the calculation, but the water produced usually is not included (and the comparison between processes become difficult), although the current trend in the pharmaceutical industry is to include it.

The ideal E-factor is 0, which correspond to 0 kg of waste. When it was first introduced in 1992, the analysis of different sectors of chemical industries pointed out the pharmaceutical one was the most impactful, with values from 25 to > 100, while oil refining produced less than 1kg of waste for kg of product (<0.1).

The concept was later expanded with the introduction of the environmental quotient (EQ), which asseses the environmental impact of the waste. EQ is calculated using the equation: EQ = (E-factor) · Q, where Q is an arbitrary parameter that consider the "unfriendliness" (eg. toxicity, persistency, ease of recycling) of the waste.

$$E\text{-factor} = \frac{\text{kg of waste}}{\text{kg of product}}$$

Process Mass Intensity

$$\text{PMI} = \frac{\text{kg input materials}}{\text{kg product}}$$

PMI is similar to the *E*-factor, and in fact it is related to it by an arithmetical relationship: PMI = *E*-factor + 1. It expresses the ratio of weight of all materials used in the process and weight of the product produced. Materials include reactants, reagents, solvents used in the reaction and purification. The best PMI for a process is equal to 1.

However, mass-based metrics like this and reaction mass efficiency (RME) are usually not sufficient to measure the environmental impact of waste or the economic viability of products and processes, and they need to be used in combination to others, such as life cycle assessment (LCI /A). Nevertheless, PMI has been adopted as key metrics from GCI ASC Pharmaceutical Roundtable.

Life Cycle Inventory and Assessment

LCI/A is a methodology that allows a precise estimation of the cumulative environmental impacts associated with all materials, equipments, processes of manufacturing used to make a final product. It provides a more accurate and comprehensive view of the "greenness" of a product or process through the entire life cycle, often including impacts not considered in other analysis. It is very useful analysis, but also more time consuming if compared to the others.

2. **Atom Economy —** Synthetic methods should be designed to maximize the incorporation of all materials used in the process into the final product.

This term was first introduced by Berry Trost in 1991, presented as an "exciting challenge" for organic synthesis, and it can be considered as another metric able to measure the mass efficiency of chemical processes.[17] Atom economy (AE) is calculated by dividing the molecular wight of the product by the total sum of the molecular weights of all substances used and formed in the stoichiometric equation from the reaction involved. It is a theoretical number that assumes the use of exact stoichiometric quantities of material and a 100% yield. It is important to date that, in this equation, solvents and chemicals used in the work-up are not considered.[18]

$$AE = \frac{\text{MW product}}{\text{MW reagents}}$$

The ideal chemical reaction should be as selective as possible, like a simple addition, which avoids the formation of any side products, or produces the most innocuous one. In this sense, catalytic hydrogenations are seen as one of the best examples of atom economy if compared to traditional synthetic methods (**Scheme 1.1, a-b**), although it is the Diels-Alder reaction that more accurately represent the epitome of the concept, with its theoretical 100% atom economy (**Scheme 1.1, c**).[19]

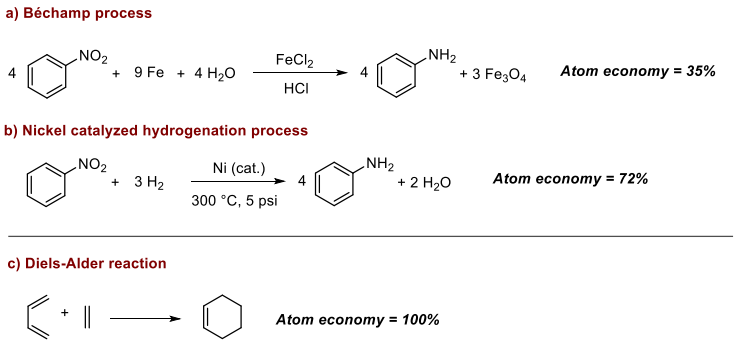

Scheme 1.1 a) Atom economy comparison among Béchamp processes ad Nickel catalyzed hydrogenation b) General Diels-Alder reaction.

3. **Less Hazardous Chemical Syntheses** — Wherever practicable, synthetic methods should be designed to use and generate substances that possess little or no toxicity to human health and the environment.

Redesigning processes with the aim to be cleaner and greener is also represented by finding alternatives to the use of toxic and hazardous chemicals. The pathway that leads to a final product is often composed by different steps, where each one can possibly contain toxic chemicals or produce risk of contaminations. There are different ways to avoid that or at least minimize it and, in this context, recent advances in synthetic strategies and technological innovation could be of great help,

such as one-pot synthesis, cascade of tandem reactions, multi-component couplings, the so called "click chemistry", rearrangements, cycloadditions, C-H activation, enzymatic catalysis, the use of solid supported catalysts and continuous flow technology. Some of these will be discussed in the next chapters.

4. **Designing Safer Chemicals —** Chemical products should be designed to affect their desired function while minimizing their toxicity.

Generally, toxicity depends on three factors: intrinsic toxicity of a substance, bioavailability, and exposure. Nowadays, the attention has shifted from efficacy to toxicity, and the harmfulness of chemicals, drugs, and pesticides, is a central topic of discussion, even more if we consider the perception of chemistry among people. This is a matter of undoubted great importance and concerns, for both producers (academia and industry) and consumers.
The infamous – but very important - case of Thalidomide in 50s gave a boost to toxicity studies in drug development and marked out the relationship between chirality and activity, stressing the urgency of studying SAR (Structure-Activity Relationship) to design chemicals that were less toxic. This claimed a change of mindset and precise training, and resulted in new knowledges and practice, with the flourishing of medicinal chemistry field.[20] Asymmetric synthesis, the importance of isosteres, the investigation of the relationship between chemical structure and biological effects, the definition of a toxicological profile, the careful control of absorption and the analysis of the metabolites produced, are at the basis of daily drug research.[21] Now, the attention is also focused on the studies concerning environmental impact of pesticides, plastics and polymers, and on the synthesis of new ones, with the effort to make them also degradable after disposal.

5. **Safer Solvents and Auxiliaries —** The use of auxiliary substances (e.g., solvents, separation agents, etc.) should be made unnecessary wherever possible and innocuous when used.

Solvents are still the main source of waste, pollution, and energy consumption in a process, hence influencing costs, safety and impact. Many of the common organic solvents are harmful, toxic and environmentally damaging,[22] so in the last decades a range of sustainable solvents have been developed and is now in use today. Among them, we find bio-based solvents, ionic liquids, deep eutectic solvents, supercritical fluids, liquid polymers, and water.[23,24] Each of them presents some advantages and drawbacks, but generally evaluations need to be done about the use of a solvent in a given application, as the economic factor is also important (eg. energetic costs regarding solvent recovery), and finally, some discrepancies among small and big scale syntheses still need to be filled. Another approach is to perform reactions in solvent-free conditions; in this case the reactants can be used alone without any solvents, or they can be absorbed on mineral support (alumina, silica, clays) or polymer support (polystyrene, polyethylene glycol).[25]
Auxiliaries are substances used in the reaction system that do not participate in the reaction, such as purification or separation agents. Their use can be avoided by eliminating intermediate purification step and using technologies that allow to have cleaner reaction profiles, with the production of side products minimized. In this sense, continuous flow chemistry can often represent a useful tool.

6. **Design for Energy Efficiency —** Energy requirements of chemical processes should be recognized for their environmental and economic impacts and should be minimized. If possible, synthetic methods should be conducted at ambient temperature and pressure.

Energy is and will be a key issue for our and next generations. The costs are escalating, and the resources are not infinite, plus most of the energy is still based on fossil fuels and most of it is lost in conversion and transmission. Nowadays, one of the focuses is reduce the overall energy consumption in any sector, but is also important the search of renewable energies. Several of these solutions have been found in biofuels production, solar power, wind power, hydro power, and hydrogen fuel cells.

In organic chemistry, there are different viable options to try to be more energy efficient: design methods that don't require hight temperatures, substitute conventional hearting with technologies that guarantee homogeneous heating, like microwave-assisted irradiation, the use of catalysis to reduce the thermal barrier, or the use of enzymes. Alternatives could also be represented by ultrasound. It is important to remember that a large amount of energy is used after the reaction is finished, like in the removal of solvents.[26]

7. **Use of Renewable Feedstocks —** A raw material or feedstock should be renewable rather than depleting whenever technically and economically practicable.

Most of the manufacturing products are still derived from feedstock, natural gas, and extracted mineral, non-renewable resources that have been depleted intensively.
Since the evaluation of sustainability of a process starts from the raw materials, turning toward renewable ones is now of primary importance.[6] Nature itself produces about 170 billion tons of plant biomass (eg. wood, crops, agricultural residue, food) per year, containing useful material such as carbohydrates, lignins, oils and fats, proteins, alkaloids and terpenes, and it has been estimated that we use just the 3.5% of it for human needs.[27] For this reason, the evaluation of bio-mass such as lignin and chitin,[28] has growth a lot of interest in recent years: the first has found application as source of energy in production site but also as raw material for the production of chemicals, whereas the latter can be used after being deacetylated into chitosan, useful for water purification and biomedical applications, like as nanoparticles in drug delivery systems.[29,30]

8. **Reduce Derivatives —** Unnecessary derivatization (use of blocking groups, protection/deprotection, and temporary modification of physical/chemical processes) should be minimized or avoided if possible, because such steps require additional reagents and can generate waste.

Since most of the processes are often made of subsequent steps, one of the goals should be to reduce the formation of derivatives and the use of protecting groups, and to prioritize a one-pot processes or a multicomponent one, in respect to conventional synthesis. In fact, every step of derivatization

might include a following step of deprotection and purification, leading to the production of waste and to more energy consumption.
Another way is to use enzymes, which are substrate specific. A great example is the industrial enzymatic synthesis of β-lactam antibiotics. In this way protecting groups are not needed and the reactions can be often conducted in water at just above room temperature.[31]
Finally, if the derivatization is necessary, non-covalent derivatization could be preferable, where the derivative is formed exploiting Van der Waals interactions or H-bond formation.[32]

9. **Catalysis —** Catalytic reagents (as selective as possible) are superior to stoichiometric reagents.

Catalysis has an important role in current organic synthesis. A catalyst is defined as "a substance that changes the velocity of a reaction without itself being changed in the process". So, it can improve the efficiency of a reaction by lowering the activation energy required. Catalysts can be use in sub-stoichiometric amount and, as they are more selective, this often resulting in less energy consumption, less feedstock used, and less waste produced.[33] Catalysis can involve different approaches, such as heterogeneous, homogeneous, organocatalysis, photocatalysis and biocatalysis.[34] To cite one example, the use of heterogeneous catalysis can bring some advantages like the reduction of work-ups to simple filtration, thus avoiding liquid-liquid extraction or distillation of the product.

10. **Design for Degradation —** Chemical products should be designed so that at the end of their function they break down into innocuous degradation products and do not persist in the environment.

As anticipated in principles 3 and 4, the goal must be the conscious design of chemicals, with an overall view of the entire life cycle of the product, from the origin of the raw material to its final degradation into innocuous derivatives. Pollution and persistency are problems strictly related to this. Decades of studies and investigations are now able to tell us which chemical feature might make the product more resistant and persistent, and so difficult to degrade into safe compound: halogens, especially chlorine and fluorine, branched chains, tertiary amine, nitro, nitroso, azo and arylamino groups, quaternary carbons, polycyclic residues, and others. Whereas functional groups such as esters and amides are generally more susceptible to enzymatic degradation, but also hydroxyl groups, aldehyde and carboxylic acids.[35]

11. **Real-time analysis for Pollution Prevention —** Analytical methodologies need to be further developed to allow for real-time, in-process monitoring and control prior to the formation of hazardous sub- stances.

The principle of prevention opposed itself to the firstly adopted approach of remediate after the damage is already done. In this sense, real-time and in particular "in-line" analysis is essential for the detection and elimination of eventual hazardous substance formed during a process. Analytical chemistry and troubleshooting analysis are of common use in manufacturing, but the direct continuous monitoring of a process could actually be able to solve problems before they go out of

control. Nowadays, the search of process analytical techniques, and their implementation in organic synthesis and multistep processes, is taking big steps forward. In fact, it is now possible to integrate NMR, UV/Vis, IR and UHPLC real time analysis for the better understanding and control of reactions.[36]

12. **Inherently Safer Chemistry for Accident Prevention —** Substances and the form of a substance used in a chemical process should be chosen to minimize the potential for chemical accidents, including releases, explosions, and fires.

The prevention starts also with the identification and assessment of the hazards: intrinsic toxicity, explosivity, flammability, corrosivity, mutagenicity, and others. So, whenever its possible, we should prioritize the use of safer and greener reagents, also for the health and safety of workers. Accidents can happen, but we should minimize the possibility to make them happens, also by carefully choosing the materials and the design of processes.[37] Of course, scale of production and the storage is something to remember. The ammonium nitrate explosion in the port of Beirut in 2020 stands out as the most recent and tragic event.

1.1.2 Green organic synthesis vs conventional organic synthesis

The aim of green chemistry extends beyond simply reducing hazardous substances and minimizing the environmental impact. It also involves the continuous search for new, improved and more efficient methods and techniques for chemical synthesis.
The synthesis of a final compound usually involves many steps, the use of large volume of organic solvents, long reaction time and tedious work-ups and purification. New approaches and technological progress can impact and reduce the usage of solvents, minimize purification steps, formation of side products, with the result of a more efficient, reliable e reproducible protocol. Green chemistry techniques can often improve the reaction rate, the total yield of the reaction and enhance purity of final products (**Figure 1.2**).

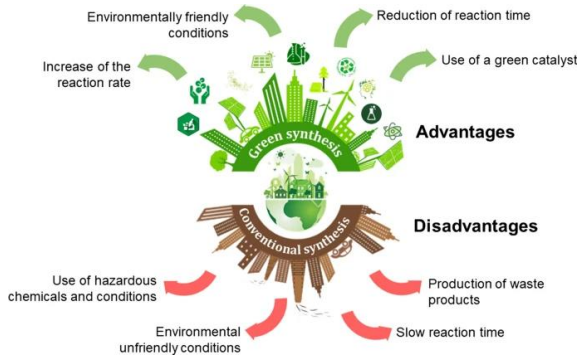

Figure 1.2 Green synthesis vs Conventional synthesis[38]

Green methods in this field involves the development of one-pot protocols, multicomponent reactions (MCRs) or solvent-free conditions, the use of alternate energy inputs, such as mechanochemistry, sonochemistry or microwave irradiation, but also organic electrosynthesis, photochemistry and continuous flow processes.

Multicomponent reactions, a type of one-pot process, involve the simultaneous reaction of three or more starting materials to form a desired product in a single step. MCRs are highly atom-efficient, as they allow the synthesis of complex molecules without the need for multiple synthetic steps or the generation of significant waste.

Ball milling is another example of green and efficient method for chemical synthesis. In fact, mechanochemistry can promote reaction at room temperature and without the use of solvent, thus increasing reaction rates, selectivity and energy efficiency. Ball milling can be applied in a wide range of reactions, including C-C bonds, cycloaddition reactions, reduction and oxidations.[39]

Ultrasound sonication and microwave irradiation have emerged as increasingly utilized green techniques in organic synthesis, in opposition to traditional methods that often lead to long reaction time, more solvent usage and mediocre yield. Ultrasound sonochemistry offers increased chemical reactivity, improved mass transfer, high efficiency, lower waste generation and energy requirements.[40]

Microwave-assisted organic synthesis (MAOS) is now a well-known and established tool in laboratories and industries, thanks to its many advantages, such as rapid and homogeneous heating, the possibility to operate above the solvent's boiling point, the precise control of parameters and temperature/pressure continuous monitoring, the dramatic reduction of reaction time, the cleaner reaction profile and generally higher yield of products.[41,42]

The use of continuous flow processes instead of batch ones often offer some advantages, like better control of reaction parameters, enhanced safety, and reduced waste generation. Flow chemistry can also enable reactions that are challenging or impossible to perform in batch processes.

Photochemistry, despite being more than 100 years old, is now living his renaissance period in synthetic organic chemistry and photons have been declared a 21st century reagent. Actually, the photon is one of the greener reagents at our disposal, as it is absorbed leaving no residue.[43] They generate electronically-excited molecules, which a generally more reactive, and they induce transformations without using harsh condition, ensuring clean reaction and good atom economy. Nevertheless, field has faced many challenges over the years, such as reproducibility, scalability, and the maximization of efficiency. However, this could be overcome by coupling the technology with continuous flow platforms.[44]

Over the past decades, organic electrosynthesis emerged as promising methodology that addresses critical aspects of green chemistry by substituting toxic oxidizing and reducing agents (electrons are inertly clean reactants), by the use of mild condition, the reduction energy consumption, and the in-situ generation of unstable of hazardous species within the reaction system, thus enhancing safety and reducing potential risks.[45] As electrochemistry offers a precise control of applied potential, it is possible to regulate reactivity and tailor selectivity, leading to more efficient chemical transformations.[46] As confirmation of its increasing importance, recently the IUPAC committee enlisted synthetic electrochemistry among the 2023 Top Ten Emerging Technologies in Chemistry.

As briefly shown, the employment of these methods allows researchers and industries to reduce the environmental footprint of chemical production, to enhance process efficiency and to promote the design and development of sustainable and greener chemicals, processes, and reactors.
It is undoubtable, and for this reason inevitable to mention, that progresses in **process analytical technology (PAT)**, **automation** and **digitalization** are already changing, and will change in the future, the way to conceive and to do chemistry.[47,48]

Some of the above-mentioned techniques will be extensively discussed in the next chapters (**1.2 One-pot processes, 1.3 MAOS, 1.4 Flow chemistry, 1.5 Photochemistry**), as they were efficiently applied during my PhD.

1.2 One-pot processes

A one-pot synthesis is a methodology in which multiples reactions are combined in one single vessel, where is ultimately possible to add reagents, change solvents and reaction conditions, but without any purification or isolation of intermediates.

One-pot approach offers several advantages for achieving efficient organic synthesis:

- **efficiency**: the integration of different transformations into a single step allows to minimize possible intermediates isolation, work-ups, purification, leading to a more straightforward and efficient process;
- **time and cost saving**: performing multiple reactions in one-pot reduces the overall reaction time and eliminates the need for additional reaction vessels and other equipment;
- **selectivity and yield**: the conduction of a reaction in a sequential manner can promote the formation of the desired product and limit the side products formation, thus improving yield and selectivity;
- **versatility**: the synthesis of complex molecules with different features and functionalities is allowed in a more efficient and practical way.

This is in line with several principles of green chemistry, like the reduction of synthetic steps and purification, the use of unnecessary atoms, and the final achievement of a better overall process efficiency.[49]
One-pot processes allow to condense different bond-formation steps, which is particularly useful when intermediates are toxic or they are unstable, and the isolation could lead to their degradation and lower yield; when there is an equilibrium between two intermediates, but both of them can be converted into the desired final product; or when there is an equilibrium between the starting material and an intermediate; but also when side-products can be converted into the desired product and, finally, when some of the reagents are involved in more than one reaction step.
Of course, this methodology in not universally applicable. The main drawbacks are due to very inherent characteristic of the process: the fact that is conducted in one "pot". Every reagent used remain in the same vessel and this means that every excess should be avoided, as also the formation of salts, or other side-products who may interfere within the following reaction mechanisms. The advances in computational methods could help in defining actual compatibility and final viability of a one-pot process.[50]

Multicomponent reactions (MCRs) are an example of one-pot process. It is a convergent approach in which three or more compounds react to form a single product, and where all or most of the atoms involved contribute to its formation (**Scheme 1.2**).[51] This is generally achieved through a cascade of elementary chemical reactions forming a network of reaction equilibria. Ultimately, the reactions culminate in an irreversible step that produces the target product. In this way, simple but differentiated substrates can be combined efficiently forming a way more complex molecule, in a

limited number of synthetic operations. Moreover, the application of this methodology guarantees a rapid access to a very large chemical and scaffold space, therefore gaining in the generation of diversity, such as in the synthesis of different and relevant biologically active compounds.[52] MCRs find also application in combinatorial synthesis, agro- and polymer chemistry.[53]
MCRs are now one of the key assets in the sustainable synthesis toolbox, as they can bring together many of the green chemistry principles, from atom and step economy, efficiency, mild condition, and to general compatibility with green solvents.[54]

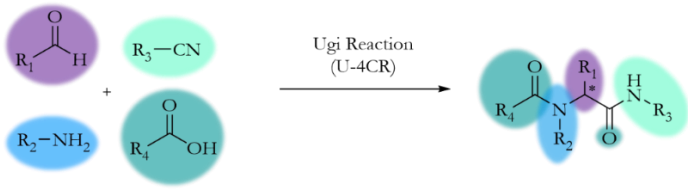

Scheme 1.2 Example of multicomponent reaction (U-4CR)

Cascade or **domino reactions** are another subclass, defined as processes involving two or more bond-formation steps, which can occur under the same reaction conditions in a single vessel and in a sequential manner. The crucial point is that at least two transformations must happen, and each reaction flows into the next one.[55] The idea first came to mind in chemists at the beginning of XX century and evolved in the 90s, inspired to mimic what nature does every day, with high efficiency.[56]
Cascade reactions are usually divided in three stages: an initiation, a relay, which coincides with one or more sequential steps, and a termination, where the product is formed.
Cascade reactions are very challenging but useful for total synthesis, as they can provide specific molecules with structural and stereochemical complexity, with the advantages already enlisted for one-pot processes.[57]

Tandem reactions are similar to the cascade one, but the subsequent transformations happen in two distinguished parts of the molecule, by addition of only one reagent.

A brief mention to **telescoped processing**, that can be defined as a multistep synthetic procedure in which intermediates extractions and filtrations are allowed. In this case, the intermediate crudes are held in the solution, used for the subsequent reaction without their direct isolation.[58] For this reason, telescoped reactions not always coincide with one-pot reactions.

One of the best examples of one-pot methodology applied to the production of pharmaceutical products was given by Hayashi and co-workers in 2013, with the synthesis of **(-)-Oseltamivir**, one of the most effective drug for the treatment of influenza, in 36% overall yield.[59] The compound was obtained in a one-pot fashion synthesis, without any evaporation or solvent exchange (**Scheme 1.3**).

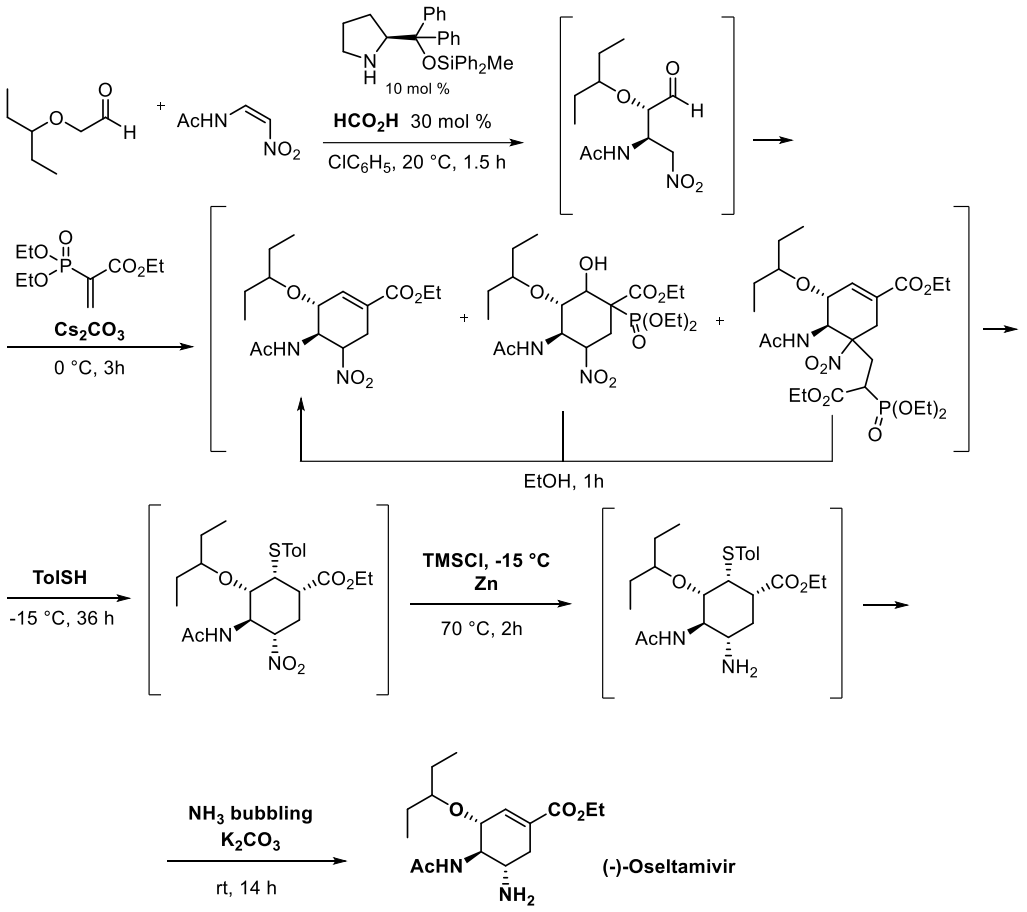

Scheme 1.3 One-pot synthesis of (-)-Oseltamivir

During my PhD, this methodology was successfully applied for the synthesis of polysubstituted carbazoles (**Chapter 2.2**), and for the preparation of (*E,E*)-conjugated dienones (**Chapter 2.3**), starting from *β*-nitro-*β,γ*-unsaturated ketones.

1.3 Microwave-Assisted Organic Synthesis (MAOS)

Microwave (MW) radiations correspond to that portion of the electromagnetic spectrum with a frequency range of 0.3 - 300 GHz, which correspond to wavelengths of 1 mm - 1m. Their region is located between infrared radiation and radio waves (**Figure 1.3**). Since a big part of the band frequencies within this region are used for telecommunication and radar equipment, to avoid interference, domestic and industrial microwave apparatus generally works to a frequency of 2.45 GHz (12.25 cm).

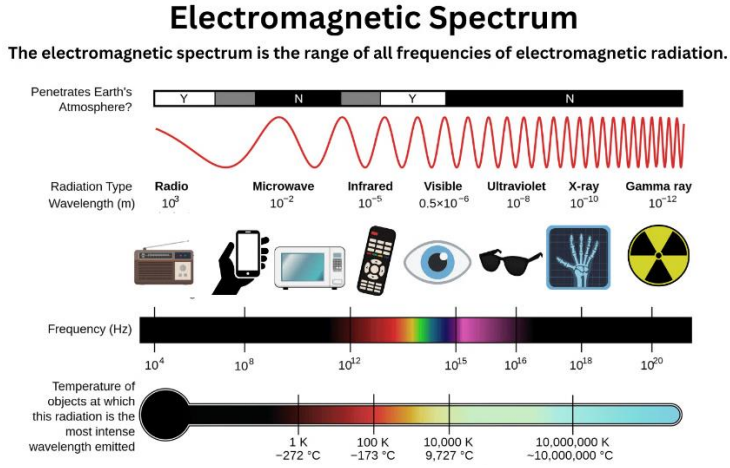

Figure 1.3 Electromagnetic spectrum[60]

Microwave technology began to gain attention during World War II, mostly for the need of RADAR devices. The two events that pinpointed significantly that time were the invention of the magnetron, designed to generate fixed frequency microwaves, and the serendipitous discovery of the cooking potential of microwave energy. Further investigations revealed that microwaves could rapidly increase the internal temperature of food compared to conventional ovens.

Nevertheless, the exploration of microwave irradiation effects in organic synthesis did not begin until the mid-1980s. The first two papers on the topic were published in 1986,[61,62] leading many organic chemists to recognize the advantages of utilizing microwave energy to drive synthetic reactions, like a significant decreasing in reaction time. At that time, most of the research were conducted using domestic MW ovens, with all the correlated challenges, such as the quick corrosion when exposed to acids and solvents, lack of safety controls and no temperature and pressure monitoring. The need of instruments, tailored for laboratory and industrial need, that pushed manufacturers to design and built specialized ovens, the transition from multi-mode system to single-mode processors, and the use of sealed vessels, marked a significant breakthrough in technology advancements and a rapid expansion for this research field.[63]

1.3.1 Microwave theory

Traditionally, most organic reactions have been heated through conductive heating with an external equipment, such as oil bath, sand bath and heating jackets. However, these methods present many drawbacks: they tend to be slow and inefficient, temperature variations can occur within the sample, and the transfer of energy into the system is strictly dependent on the thermal conductivity of the material that need to be penetrated. Moreover, localized overheating may lead to the decomposition of reagents or products.

In contrast, microwave heating is based on a different approach. The energy is coupled directly with the molecules and solvents inside the reaction mixture, with minimum heating of the vessel. The apparatus guarantees the temperature increases, and distributes it uniformly throughout the sample, thus reducing the formation of by-products and the composition of targeted compounds. Moreover, in pressurized systems with sealed vessels, microwave irradiation allow to operate beyond the boiling point of the solvent used, providing enhanced control in reaction conditions (**Figure 1.4**).[64]

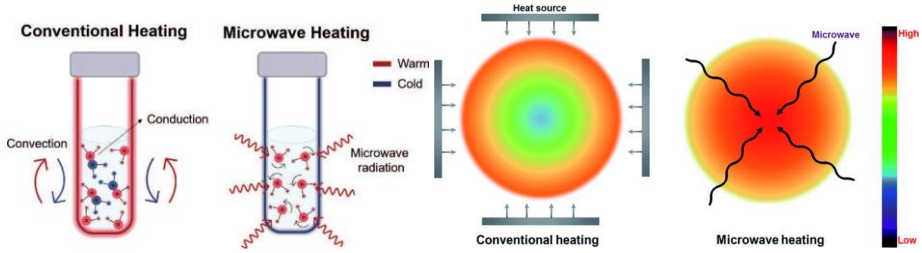

Figure 1.4 Temperature distribution: conventional heating vs microwave heating. [65,66]

The instantaneous dielectric heating provided by microwaves is due to two main mechanisms, **dipolar polarization** and **ionic conduction**, which depend on the ability of a specific materials (i.e., a solvent or reagent) to absorb microwave's energy and convert it into heat.

1) Dipolar polarization: a substance with a dipole moment, on exposure to electromagnetic field, try to follow and align themselves with the alternate electric field; these rotations result in frictions that causes loss of energy, which is released as heat.
The energy lost is described by the Loss Tangent (tan δ)

$$\tan \delta = \frac{\varepsilon''}{\varepsilon'}$$

ε" corresponds to the dielectric loss, which is the efficiency of a solvent to convert the radiation into heat
ε' is the dielectric constant (or relative permittivity), which measure the polarity of a material, and display its ability to store electrical potential energy

What we can imply from this equation is that reaction media with hight tan δ will convert more efficiently radiation into heat. For this reason, these solvents are usually preferable when performing a reaction using MW. Nonetheless, also the low absorbing solvents can be used if

some of the reactant or catalyst are polar and able to enhance the overall dielectric properties of the mixture, or if a proper polar additive, like alcohols or ionic liquids, is used to promote the warming.

Solvent's microwave absorbance can usually be classified according to their value of tan δ (**Table 1.1**).[67]

Table 1.1 Loss factor of selected solvents (20 °C, 2.45 GHz)

- High: tan δ > 0.5
- Medium 0.1 > tan δ > 0.5
- Low: tan δ < 0.1

Solvent	ε' (25 °C)	tan δ
Ethylene Glycol	37.0	1.350
Ethanol	24.3	0.941
DMSO	45.0	0.825
Methanol	32.6	0.659
DMF	37.7	0.161
Water	80.4	0.121
Chloroform	4.8	0.091
Acetonitrile	37.7	0.062
Ethyl Acetate	6.0	0.059
Tetrahydrofuran	7.4	0.047
Dichloromethane	9.1	0.042
Toluene	2.4	0.040
Hexane	1.9	0.020

Substances with high dielectric constant not always have the highest absorption capacity. In fact, ethanol (ε' = 24.3), which possesses a lower dielectric constant in respect to water (ε' = 80.4), heats much more rapidly than water in a microwave field, thanks to its higher loss factor (tan δ: ethanol=0.941, water=0.121).

Since reaction vessels are typically made of microwave transparent materials, like glass or Teflon (tan δ < 0.01), only the reaction mixture will be heated, while the vessel remains relatively unaffected.[68]

2) Ionic conduction: the motion and oscillation of free ions or ionic species present in the mixture, generated from the electric field, generates heat; the transfer of energy is more efficient as the temperature increases.

This is why, if two samples of tap and distilled water are heated by microwave irradiation, the first one will be more rapidly heated. The presence of ions in tap water enhances its ability to conduct electricity. The conductivity principle, driven by the presence of ions, has a much greater impact on heat generation compared to the dipolar rotation mechanism.

Microwave energy consists of a magnetic field and an electric field, but only the latter transfers energy to heat a substance. However, this energy seems to be not sufficient to ionize molecules or cleave molecular bonds, as opposed to what happens in photochemistry with ultraviolet and visible radiation. Microwaves cannot affect the structure of organic molecules and their excitation is purely

kinetic, although there are still some debates going on among scientists on the so called "non-thermal" and "specific" effects.[69]

Essentially, microwave-enhanced reaction rate is, as we just said, a thermal/kinetic effect. The rapid and uniform heating of the solvent, usually over the set temperature, accelerates synthetic processes or enhance the product yield, or both (**Scheme 1.4**). Naturally, such temperature profiles are very difficult, if not impossible, to reproduce by standard thermal heating, and the product distribution might change using MW. Therefore, comparisons with conventionally heated processes are inherently troublesome.

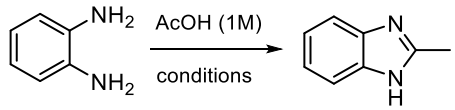

Heating	Temperature	Pressure	Time
CONV	25 °C	-	9 weeks
CONV	60 °C	-	3 d
CONV	100 °C	-	5 h
MW	130 °C	2 bar	1 h
MW	160 °C	4 bar	10 min
MW	200 °C	9 bar	3 min

Scheme 1.4 Synthesis of 2-methylbenzimidazole: thermal microwave effect.[70]

The Arrhenius equation well describes the kinetic (k) of a reaction as related to both activation energy (Ea) and temperature (T).

$$k = Ae^{\frac{-E_a}{RT}}$$

"A" is called frequency factor and represents the frequencies of collisions, $e^{\frac{-E_a}{RT}}$ is the fraction of collisions with enough energy to react.

As we can infer from the equation, the kinetic is directly proportional to the temperature and inversely proportional to the activation energy.

The supposition of the existence of some "specific microwave effects" arises from the distinctive heating (dielectric) mechanism associated with the instrument. Generally, these include the superheating effect of solvents at atmospheric pressure, the elimination of wall effects in the reaction vessel and an inverted temperature gradient in favour of the bulk liquid, the selective heating of strongly microwave-absorbing heterogeneous catalysts or reagents within a less polar reaction medium, which can lead to enhanced reaction rates or selective transformations, particularly in biphasic or multiphasic liquid-liquid systems, and the generation of localized "molecular radiators" or microscopic hotspots, formed by direct coupling of microwave energy to specific reagents in homogeneous solutions.[71] These hotspots can result in enhanced reactivity, or promote specific

reaction pathways. Today, it is generally agreed that most of these effects can be categorized as thermal direct or indirect phenomena.

Also, the presence of "non-thermal effects" in chemical reactions has been a subject of speculation and debate among researchers, but it appears to be difficult to rationalize. Some groups propose that these effects arise from specific and unique interactions between microwaves and materials or reactants, resulting in a decrease in activation energy or an increase in the pre-exponential factor in the Arrhenius equation, and so in altered reaction kinetics or selectivity beyond what can be explained solely by thermal effects. These effects could be attributed to the orientation of polar species in the orientation of polar species in the electromagnetic field. Though, in several instances where specific or non-thermal microwave effects have been initially claimed, subsequent rigorous investigations have unveiled that those were primarly due to inaccurate temperature measurements and agitation or stirring of the reaction mixture. One example is the use of an external IR temperature sensor, instead of an internal, fast responding fiber-optic (FO), that can more accurately monitor the reaction temperature during the process.[72]

The ongoing discussions and debates reflect the complexity of understanding the intricacies of microwave-assisted reactions, the diversity of chemical systems, and the need for further research to elucidate the underlying mechanisms. Different research groups may employ different experimental setups (in most paper this description is not even reported), conditions, and analytical techniques, leading to varying interpretations of the observed effects.

When considering microwave-irradiation heating, another important factor to take into account is the **penetration depth (d_P)**, defined as the depth at which the energy of the microwave irradiation decreases to 1/e of its initial value, which is determined by the absorption properties of the material and the dielectric properties of the medium being heated.[73] The limitation of penetration depth becomes particularly relevant when scaling up microwave-assisted syntheses. As the volume of the reaction mixture increases, the microwave energy may not be able to uniformly penetrate throughout the entire sample. This can result in uneven heating and temperature gradients, leading to inconsistent reaction outcomes and lower overall efficiency.[70]

1.3.2 Equipment and techniques

Many things have changed since the first kitchen microwave oven was used for synthetic purposes. Currently available dedicated microwave reactors for organic synthesis present specific features to enhance control, precision, and automation in microwave-assisted synthesis, such as built-in magnetic stirrers, direct temperature control, software that allow the real-time regulation of temperature and pressure, continuous power regulation and efficient and rapid post-reaction cooling systems.[63]

For what concerns microwave reactor design, there are basically two distinct types: monomode (single-mode) and multimode instruments. The latter are similar to domestic oven, with the waves entering the cavity and being reflected by the walls, while single-mode reactors, the most widely used, have a much smaller cavities and the microwaves are precisely directed and guided to the reaction

vessel, placed at a fixed distance from the source. Moreover, multimode allows for simultaneous irradiation of multiple samples, enabling parallel synthesis, whereas in monomode systems only one vessel can be irradiated at a time. In this case, robotics and autosamplers might overcome the issue and guarantee high throughput.[74] Additionally, the integration of different technology, such as continuous-flow or stop-flow reactors can solve penetration depth issues, holding promises for scaling up MAOS processes.[42] Generally, single-mode microwaves can operate volumes from 0.2 to 50 mL, temperature, and pressure around 300 °C and 30 bar, while higher volumes can be handled in multi-mode instruments (several liters), allowing kilogam-scale preparation in both cases.

Microwave-assisted organic synthesis can be accomplished using standard organic solvent, water,[75] or high-boiling microwave-absorbing solvents like DMSO, N-methyl-2- pyrrolidone (NMP), 1,2-dichlorobenzene (DCB) and ethylene glycol, under open or sealed-vessel fashion. The integration of rapid heating through microwaves with sealed-vessel (autoclave) technology has become the preferred method for conducting MAOS on a laboratory scale, because of the possibility of precise on-line monitoring of bulk temperature and pressure. In the last two decades, the use of ionic liquids as both solvents, reagents and additive in order to heat non-polar substances has increased significantly in microwave chemistry,[76] since they present many good properties for the scope: high boiling point, exiguous vapor pressure and their high thermal stability.[77] Also, soluble polymer matrices, such as polyethylene glycol (PEG) represent a viable and useful option.[78] Apart from classical protocol in solution, solid-phase microwave organic synthesis, with the use of the use of cross-linked macroporous or microporous polystyrene resins, can present some advantages. Frequently, MAOS can be perfomed also solvent-free,[79] with the reagents pre-adsorbed onto inorganic support, such as silica, alumina, clay or graphite, but in this case non-uniform heating, mixing and precise determination of the inner temperature might happen.[80] Phase-transfer catalysis (PTC) is also a widely used technique when performing organic synthesis using microwave irradiation.

1.3.3 Microwave heating in organic synthesis

In the last 30 years many different reactions were conducted exploiting the advantages of microwave irradiation. In particular, metal-catalyzed carbon-carbon and carbon-heteroatom bond-forming reactions and cross-coupling reactions, apart from being of great importance in organic synthesis, they can greatly benefit from the application of this technology. In fact, conventional protocols often require hours or days to undergo completion with conventional heating, usually under reflux condition and inert atmosphere.[81,82]

With this aim, MAOS has been efficiently applied to **Heck reactions**, using both homogeneous and heterogeneous catalysts, also in aqueous and solventless conditions.[83,84]

Suzuki couplings were one of the first studied reaction exploring microwave-assisted synthesis. Traditionally, they involved aryl halides and boronic acids but, with the recent advancements, this methodology has been extended to include coupling with alkyl-, alkenyl-, alkynyl halides and

alternative boron sources.[85,85] Recently, **Sonogashira cross couplings** gained a lot of interest in synthetic field and many examples are reported in combination with microwave irradiation.[86] In this context, methods have been developed to conduct these reactions also under transition metal-free condition.[87,88]

In recent years, significant advancements have been made in microwave-assisted C-N bond forming reactions, these includes **Ullmann couplings**,[89] and **Buchwald-Hartwig reactions**.[90]

The application of microwave irradiation has impacted **Ring-closing methatesis** by significantly improving reaction rates and conversion efficiencies, overcoming the drawbacks of conventional methods and enablig the efficient synthesis of macrocycles.[91,92]

One of the first and well-suited examples of microwave-assisted procedures were given by **cycloaddition reactions**, since conventional methods often require harsh conditions.[93] Also **cyclocondensation reactions** have found relevant space in the field.[94]

One-pot and **multicomponent reactions**, such as Ugi and Mannich, are considered hot topic and in the past years many different microwave-assisted procedures have been published.[95,96]

These are just few examples of the potential applications of MAOS.[97,98]

Microwave-assisted organic synthesis appeared to be revolutionary and suited to the increased demands in industry. Considering the many advantages they could provide in organic synthesis, like a uniform heating of the sample, shorter reaction times coupled with generally higher purity and yields, compatibility with solvents and easy removal, and lower energy usage,[99] it was often enlisted as the "technology of tomorrow" and "The Bunsen burner of the 21st century".[100]

Over the years, the attention of the scientific community to this technology has become someway timid and has slightly faded, favouring other advanced methodology, probably due to frequent scale-up problems. Nevertheless, microwave reactors are now standard equipment in organic synthetic laboratories, both in universities and pharmaceutical industries. Moreover, the combination of microwaves with enabling equipment such as continuous flow processing (MACOS) might represent the future road to industrialization of dielectric heating.[101,102]

During my PhD, microwave irradiation was exploited for the development of a one-pot protocol for the synthesis of polysubstituted carbazoles (**Chapter 2.2**). It was also explored for the optimization of different reactions, such as in a key step for the preparation of Luteoloside (**Chapter 3.2**), and to conduct some trials for the selective acidic-catalyzed conversion of CBD into Δ^9-THC and Δ^8-THC (**Chapter 3.3**).

1.4 Flow chemistry

Continuous flow chemistry is known as the procedure/technique of performing chemical reactions or chemical processes in a continuous manner with the use of small flow reactors (**Scheme 1.5**). Reagents, reactants and solvents (in A and/or B) are pumped together into tubes, reaching a mixing junction where reagent streams are combined and passed into a reactor (where the actual reaction occurs) to provide reaction residence time.

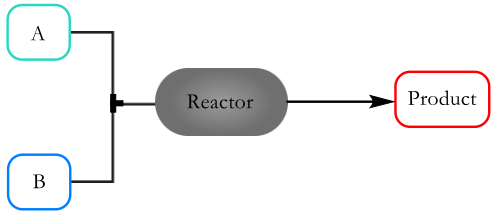

Scheme 1.5 General scheme for flow reaction

Then the reaction mixture may be fed into a column reactor that contains solid reagents, catalysts, or scavengers; the system can also be equipped with back pressure regulator and inline analytics, providing information about reaction performance.[103]

Flow chemistry has been primarily developed in the last three decades, establishing itself as a disruptive innovation for manufacturing active pharmaceutical ingredients (API) and small molecules, but microreactors chemistry was known since the 1960s, when technological progress and was not yet ready and developed to support it.[104] Flow technology presents the significant advantages of precise control of some key synthetic parameters, such as stoichiometry, temperature, pressure, and the contact time of molecules within a reactor, when compared to a batch process.[105] These principles often lead to improved product quality, safety, cost effectiveness and sustainability.[106]
Flow chemistry, in combination with several other enabling technologies, such as photochemistry, high pressure processing or electrochemistry, can allow a radical improvement of the existing chemical processes and of previously inaccessible materials.

1.4.1 Operating principles and advantages

Running a reaction under batch condition often comprehends a series of sequential actions: reaction-quench/work-up-evaporation-purification-evaporation-distillation/recrystallization to obtain the pure product. Whereas, to prepare and conduct flow reactions is quite different and requires knowledge of many reaction parameters, which calculations can differ from traditional synthesis.

- **Stoichiometry**

Under batch conditions the stoichiometry is set by the molar ratio of the reagents added to the reaction vessel/flask, and the reaction proceeds until the reagents are consumed and the desired conversion is achieved. In contrast, in a flow process, where the reaction takes place continuously as the reactants flow through a reactor, the stoichiometry is set by the correlation of parameters such as flow rates and molarities of the reactants. By a fine adjusting these parameters, which can be done real-time on the instrument, the desired stoichiometry can be achieved and maintained throughout the reaction.

- **Residence time as "reaction time"**

In batch mode synthesis the reaction time is determined by the time a vessel is stirred under fixed conditions, whereas the concept of reaction time in a flow process is expressed by the residence time, that is the time reagents spend in the reactor. The mean residence time is given by the ratio of the reactor volume (V) and the reaction flow rate (overall flow rate, ν).

$$t_{res} = \frac{V}{\nu}$$

Operatively, the residence time can be changed by modulating the flow rate or modifying the length/volume of the flow reactor. It is important to note that, while the mean residence time can be easily calculated, there is a distribution of residence times within the reactor, due to the non-uniform flow speed caused by axial convection and radial diffusion. In fact, the flow velocity near the centre of the channel is generally faster than that near the walls (parabolic velocity). This produces a significant difference between the overall conversion/yield of a transformation and the conversion/yield in steady-state conditions, where the system is stable (**Figure 1.5**). Fractionated collection at the outlet can particularly useful for determining when the concentration is invariant over time. However, if the diameter of the reactor channels or tube is sufficiently small, the radial diffusion time becomes shorten, for the reduced diffusion path, resulting in a narrower and uniform residence time distribution. The narrow residence time distribution in reactors with small diameters

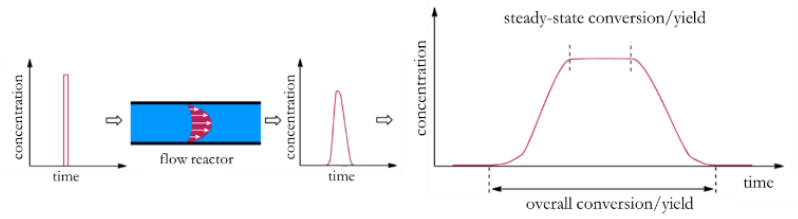

Figure 1.5 Parabolic velocity and residence time distribution (left); Differences between overall and steady-state conversion/yield (right) – scheme taken from ref[107]

has advantages, such as improved reaction selectivity, better control over reaction kinetics, and enhanced process efficiency and reproducibility.
Sometimes, especially when using reactors (typically tubes or columns) in which solid particles or pellets (catalysts) are packed, it is difficult to calculate the exact volume with the equation, because the formation of hotspot, as well as dead volumes derived from non-homogeneous packing, can broad residence time distribution. When using packed-bed reactors it is easier to manually measure the residence time.

- **Flow rate (ν)**

Under flow conditions reactions kinetics are controlled by the flow rates of the reagents streams. The flow rates of the reagents indeed influence the residence time of the reaction, and have an impact on the outcome of the transformation.
ν is usually expressed in units such as mL min^{-1}

Generally, the flow in a reactor can be of three different types: 1) laminar, 2) turbulent or 3) transitional, depending on the size of the tube, flow rate (low flow rate – high flow rate), viscosity or density of fluids. The determination of flow pattern is given by the Reynolds number (*Re*), a dimensionless indicator, defined as the ratio between the inertial forces and the viscous forces of a fluid flow.

$$Re = \frac{\rho \, u \, D_h}{\mu}$$

where ρ is the fluid density, u the fluid velocity, D_h the hydraulic diameter of the channel and μ the dynamic viscosity.

For low *Re* (*Re* < 2300), the flow regime is laminar and diffusive forces governs the mixing, whereas for high *Re* (*Re* > 4000), the flow is turbulent, characterized by convective mass transport. The flow is defined as transient when 2300 < Re < 4000.
In continuous flow reactor, the flow is also influenced by the different type of multiphasic systems that can be present in a reaction, such as gas-liquid, solid-liquid, liquid-liquid, solid-liquid-gas.

In order to measure and regulate the mass flow rate of a fluid per time, devices such as a mass flow meter or mass flow controller can be used. These can be a valuable tool in situations where there is uncertainty about the pump's operation at a desired setpoint or when fluctuations in flow rate may occur.

- **Volume vs space**

When considering a batch reaction, the reagent and product concentrations vary over the time, and mixing becomes a relevant aspect (especially when increasing the scale of the reaction) in order to reduce concentration gradients that affect the kinetics of a reaction. Reactant's concentration decay exponentially with time. Under flow conditions, each portion of the reactor is defined by specific concentrations of the starting material(s) and product(s): in this sense, the reaction profile within a

flow reactor can be defined within space rather than time. In a flow reactor, reactant's concentration decreases exponentially with distance along the reactor while product's concentration increases, till it reaches the outlet no back or forward mixing is possible and an optimal flow rate allow to obtain maximum concentration of the product.[108]

- **Mixing and mass transfer**

The overall movements of species (i.e., a reactant) due to diffusion and convection processes within the reactor, defines the mass transfer. This parameter plays a vital role in determining the degree of mixing within the reaction mixture. Efficient mass transfer influences the reaction kinetic and selectivity, leading to improved mixing, thus in enhanced reaction rates and overall reaction efficiency. In many processes, limitations in mass transfer can be a bottleneck for the efficiency of the process, such as in multiphase reactions, and flash chemistry.[109]
In conventional processes, reactants are usually mixed by a stirrer, which can lead to non-uniform and chaotic mixing. In contrast, continuously-flowing microreactors offer a solution by enabling rapid and homogeneous mixing due to the small channel dimensions, that guarantee reduced diffusion distances and faster molecular interactions.
The channels or capillaries in microreactors typically have diameters ranging from 0.05 to 0.5 cm, promoting laminar flow as the predominant mode of fluid motion.[110] Due to their compact size and laminar flow behaviour, microreactors can achieve complete mixing within microseconds.
Mixing in a flow process is highly advantageous, compared to batch mode, as it is determined by diffusion within very small volumes of reagents. Under flow conditions, mass transfer is considered very effective and determines the specific and enhanced kinetics observed.
In flow systems, the main mixing occurs when the reagents streams reach a mixing point. This can happen with different methods, that will be discussed in the next section.

- **Temperature control and heat transfer**

Heat transfer consists in the exchange of heat between the interior and exterior of a reactor, and for this reason surface-to-volume ratio plays a crucial role.
The heat transfer rate (q) is provided by the following equation:

$$q = UA\Delta T_{LM}$$

where U is the heat transfer coefficient, which depends on the properties of fluids, on the reactor wall properties and geometry, and on the fluid velocity, ΔT_{LM} is the logarithmic mean temperature difference along the reactor and A is the heat transfer surface area.

As the surface area is proportionally related to the heat transfer rate, we can infer that an increased surface area can allow a more careful control of temperature.
Temperature is a key parameter in organic synthesis and its relevance is highlighted in many transformations, such as reaction with slow kinetics, exothermic reactions, where runaway episodes are frequent and lead to safety concerns, but also in reactions where the product-to-side-product ratio is determined by a small difference in transition state energies.

In batch conditions, especially when performing reaction on a larger scale, it is quite difficult to obtain a homogeneous distribution of heat. Microchannels of flow reactors, with their smaller dimension compared to round bottom flask, presents enhanced and more efficient transfer of heat and smaller temperature gradients inside the reactor.
Moreover, reactors are made of highly thermal conductivity materials, such as stainless-steel or silicon. This means that the temperature can be accurately controlled, with the benefit of an improved selectivity, the possibility to safely handle exothermic reactions by continuous removing of heat from the system, and making possible to operate under isothermal conditions and also above the solvent's boiling point.[111] Reactions with slow kinetics can significantly enhance reaction rates thanks to process intensification, with the possibility of operating at high temperatures and pressures applying back pressure regulators.
Finally, the fine control of temperature can favour the reaction pathway that leads to the formation of the target product, suppressing, or at least minimizing, the formation of by-products.

The general possibility of changing quite easily different key parameters of a reaction, the reduced operating time, coupled with a real-time analytical monitoring, allow the almost simultaneous screening of conditions, which become more important when performing a process optimization. Automation, or the simple configuration of the flow system with a computer, permits to set a series of consecutive experiments without the need of any human intervention.

In recent years, the number and types of reactions performed with continuous flow chemistry have grown substantially, especially in pharmaceuticals, fine chemicals, and polymer chemistry.[112] Much of the growth resides in the possibility of safely use of those chemicals that are too problematic to be handled on larger scale by batch reactions. These include potentially hazardous reactions such as:

✓ Hydrogenation Reactions
✓ Oxidations
✓ Halogenations
✓ Nitrations
✓ Diazotizations
✓ Reactions with Grigrands
✓ Reactions that use toxic gases

Summarizing, amongst the advantages and benefits of continuous flow chemistry we find:
• **improvement in heat transfer, mass transfer and mixing;** these reaction parameters together with residence time can be more precisely regulated, the controlled contact among reactants leads to a better impurity control (limitation of side reactions) and final product yield;
• **better overall process control;** in-line analyses are often combined to flow equipment to evaluate step-by-step the trend of the process, following Principle 11 of Green Chemistry; in particular, technological advancement with computation and automation well integrates with the whole flow

system, and tools like Process analytical technology (PAT) can contribute to control, analyze and design better processes, with great impact on the optimization phase of products development.

• **tunability,** derived from the possible implementation of other enabling technologies or organic synthetic methods, like microwave irradiation, photochemistry or electrochemistry, with flow, enhancing also the energy efficiency of the whole process;

• **better scalability, productivity and reproducibility of reactions:** usually microreactors, which have channel sizes in the millimeter or sub-millimeter range, are often used in academic and industrial laboratories, thus providing the production of multiple g/h, but thanks to high surface-to-volume ratio compact, efficient and modular reactor design, processes can be easily scaled up to pilot or production scale; however, the requirements for mass transfer and heat transfer in larger reactors must be considered; reactors can work also in parallel (numbering up), thus leading to higher productivity.

• **a wider range of reaction variables are accessible;** for example, running a continuous reaction under pressure allows reactions to be run at higher temperatures than possible in batch reactions, where solvent reflux at ambient pressures is typical, and this can also provide higher products yield;

• **fast reaction time and diminution of wastes**; testing a range of reaction variables is far faster in flow processes, especially for an early screening stage, and less substrates and reagents are required; inline real-time analysis provides immediate feedback on the effects of variables on the reaction performance;

• **improved process safety and reduction of risk factors**; in fact, reactions that are considered too hazardous to carry out in batch are often considered acceptable in continuous flow, like the ones that are very exothermic or otherwise energetic; in flow reactors smaller amounts of reactants are in contact, but also the exposure to toxic substrates and reagents is minimized by the smaller volumes required in continuous flow systems. Beside a safer handling of toxic reactants (in line with Principle 12), flow technology allows to combine consecutive reactions (multistep flow synthesis) with multiple reactors and modules, thus also avoiding any manipulation of intermediates, which might be toxic or unstable.[113]

Although continuous flow processing has numerous benefits, it has also faced some challenges, that deter its widespread use in chemical processing, especially at large scale production.

One major problem is the formation and use of solids. The channel diameters of continuous flow reactors and tubes can barely tolerate the presence of solids in the system and hence, channel fouling leading to eventual blockage is a common phenomenon and a serious issue; also suspensions are prone to clogging channels. The compatibility of equipment materials (for example O-ring) with solvents is also something to consider when implementing an organic synthesis in flow.

Another relevant issue is the huge cost of flow equipment, that limits its use. Often, academic laboratories prefer to adopt "in-house built" or modular flow systems, since they are less expensive and more adaptable to different chemistries. In this context, 3-D printing technology and new affordable electronic toolkits came in help making flow chemistry more accessible.[114,115]

The development of laboratory equipment from continuous flow processes filled the gap between research and process chemistry development, but the lack of flow equipment dedicated for scale-up is still a problem that sizing up (in diameter or length) or parallelization procedures cannot solve on their own.[116]

1.4.2 Set-up, instrumentation, and technology

Generally, a continuous flow chemistry apparatus can be compact, like many pricy "off-the-shelf" or modular commercial systems, or home-built, less expensive and tailored to the laboratory needs.

However, generally it consists of common operating unit or modules (**Scheme 1.6**):

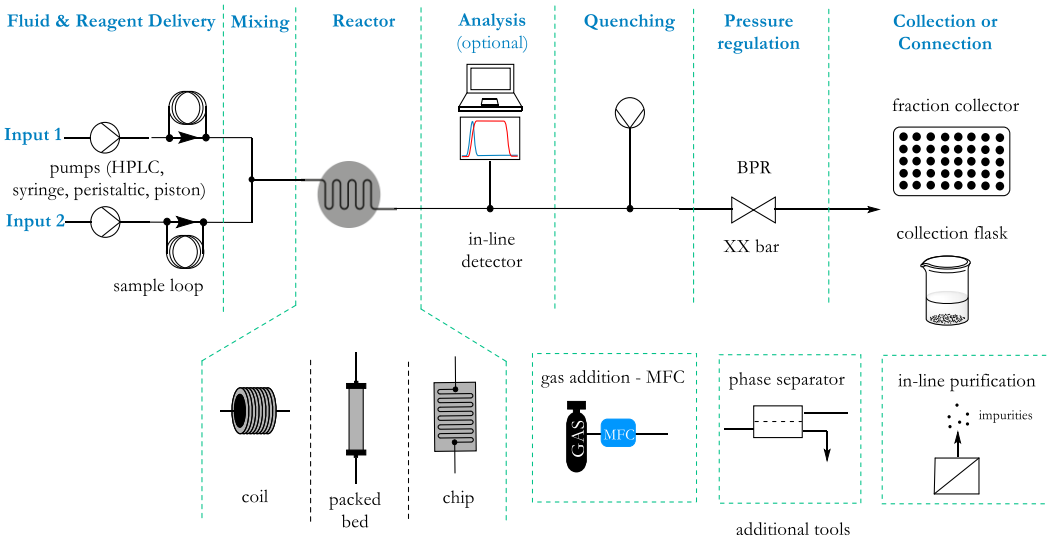

Scheme 1.6 General set-up for a flow apparatus

Fluid & Reagent Delivery

This module can deliver reproducible quantities of liquids (reagents, solvents) or gases, and it must be carefully calibrated to ensure a specific flow rate. Eventual pulsation in the pumping step can influence the overall reaction stoichiometry. Liquids are usually delivered by piston-, syringe-, peristaltic, or HPLC pumps (**Figure 1.6**), adequately chosen to suit a specific process. In fact, each pump has different characteristic, advantages, and disadvantages. Syringe pumps – single and dual - are very easy to use and suited for small-scale optimization; they present high precision at low flow rate (< 0.1 mL/min) but the reservoir is limited by the syringe volume. Peristaltic pumps can be very reliable, they guarantee no contact with the sample, and they are less susceptible to pressure changes; they can also deliver viscous and slurries feed, but they suffer pulsed flow and fast deterioration of tubing. HPLC pumps stably operates at flow rate 0.1 > mL/min and are suitable for the use of large-scale reservoir and solvent compatibility might be an issue, mostly for volatile one. In HPLC pump,

as well as in syringes, liquids are in contact with the pump, and clogging/blockage problems for precipitation of reagents can stop the flow.

Figure 1.6 Example of syringe, peristaltic and HPLC pumps

A compact device, such as a **mass flow controller**, capable of accurately controlling the flow rate, can be added to the system to supply one or more chemical compounds to the process.
Finally, **sample loops** and **injection valves** (usually 6 port valve) can be used to introduce small precise volumes of reagents. They are usually exploited during flow optimization step to minimize material consumption, and in case of very expensive reagents that need to be carefully dosed.
Generally, the introduction or formation of solid precipitates within the system causes fouling, but in some cases magnetically stirred slurries can be used.[117,118]

Mixing

In flow systems, the mixing occurs when the reagents streams reach a mixing point: usually this can happen with three different active or passive methods: a) for simple contacting, with a T-piece, Y-piece or and arrow-piece, b) in a split and recombine fashion, c) with multilamination micromixers (**Figure 1.7**)[119], but it can also occurs thank to the presence of flow obstacle or active mixers.

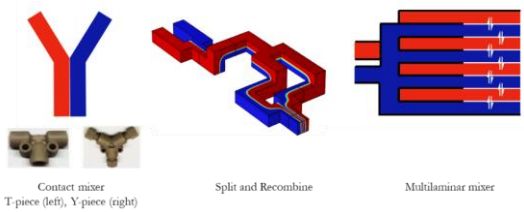

Figure 1.7 Example of different mixing unit

Additionally, in biphasic gas-liquid processes, one efficient and safe way for mixing the two steams is to use a semipermeable membrane in a tube-in-tube method, where only the gas can pass the membrane and interact with the substrate, or saturate the solvent (**Figure 1.8**).[120]

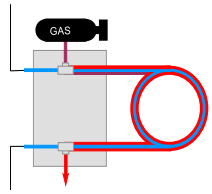

Figure 1.8 Tube-in-tube system

Reactor

In recent years, there has been significant attention toward the development of various types of reactors for flow chemistry applications. These units provide residence time for the reaction and offer advantages in terms of temperature adjusting during the reaction, process control, safety, and efficiency. Commonly used reactors are coil reactors, chip-based reactors, and packed bed reactors (**Figure 1.9**). **Coil reactors** are the simplest and more versatile type of reactors used in flow chemistry. They are typically made by a variety of materials depending on their applications: inert polyfluorinated polymers, such as polyetheretherketone (PEEK), polytetrafluoroethylene (PTFE), polyfluoroacetate (PFA), fluorinated ethylene propylene (FEP), are more suitable for low and medium pressure whereas, stainless steel or Hasteloy reactors are generally used for high pressure and temperature processes. **Packed bed reactors** usually contain a bed of solid reagent or catalyst or scavenger particles, facilitating the interaction between the reactants and the catalyst surface, offering high surface area contact, enhancing reaction rates and selectivity. Furthermore, after the reaction is occurred no quenching and separation steps are needed. Notwithstanding, heterogeneous catalysis be problematic, leaching episodes occurs frequently, turnover frequency of the catalyst is not easy to establish, leading to not uniform performance, and "chromatographic effects" might be detected.[107] This type of columns can be used downstream to achieve in-line purification. **Chip-based reactors** exploits microfluidic channels on a small chip, allowing for precise control over mass and heat transfer and efficient mixing (they often incorporate their own mixing unit). They are usually made of silicon, glass, ceramic, or stainless steel. As disadvantages, they possess generally low throughput and tend to clog easily.

All reactors can be designed with the ability to be heated or cooled, by fixing them to the flow system with a dedicated adaptor, allowing precise temperature control during the reaction. In other cases, a simple bath, in which the coil is immerse, can serve the purpose.

Figure 1.9 Coil reactors (left), packed bed reactor (centre), chip reactor (right)

Analytical units

Reaction mixtures in a continuous process can be analysed with three different approaches: offline, online, inline. The first one downstream analysis is the most commonly used in many laboratories: sample are collected from the outlet and subjected to different analysis, such as gas chromatography (GC), hight performance liquid chromatography (HPLC), nuclear magnetic resonance (NMR). On-line procedures include periodic automated sampling of the reaction mixture, transferring them to analytical instrument. This allows a fine monitoring of the reaction progress and quality control, and fastens the decision-making process for conditions optimization. The diagnostic capture information that can also be used to control further pumps and to carry multi-step sequences.

Inline analysis integrates the analytical unit directly into the flow process using an analytical flow-through cell. This is suitable for non-destructive techniques such as Fourier-transform infrared spectroscopy (FTIR), Raman spectroscopy, ultraviolet-visible (UV-vis) spectroscopy, and the use of benchtop NMR. In this way, continuous monitoring of the reaction can be achieved, providing immediate feedback on reaction parameters, and allowing for real-time adjustment.

Quenching

Chemical or thermal quenching procedures ensure the right reaction time for a reaction by halting the reactions, that could continue in the collecting flask and could generate side products. Rapid cooling can be used to immediately stop a reaction, and flow equipment, with enhanced heat transfer, guarantees efficient cooling. In most other cases, chemical quenching is required. This involves the addition of a quenching reagent to the reaction stream through a mixing unit (like a T-valve). Tools like in-line liquid/liquid phase separators and extractors can be connected to the set-up, with semi-permeable membranes able to separate liquids with similar density and that are usually miscible, like THF and water. Their application is useful also for catalyst recovery, for the separation of hazardous or toxic species generated in-situ and for solvent switching between two consecutive reactions.

Back-pressure regulator (BPR)

The integration of a Back Pressure Regulator (BPR) in a flow reactor enables precise pressure control in a flow reactor by opening a valve when a selected pressure is reached, and maintaining it constant during the whole process. The use of a BPR offers several advantages over conventional batch reactors: the possibility to operate above the solvent's boiling point, by keeping the solvent in a liquid state even at higher temperatures, an increased gas dissolution, by enabling gas-liquid transformations to occur more efficiently, to maintain a stable flow rate (especially for low boiling solvents) and minimize pressure fluctuations, improving the overall pump performance and reliability.

Generally, there are two types of BPR: one works at predefined pressure value, the other are adjustable (**Figure 1.10**). As the first are usually compact cartridge-type devices with a spring-loaded plunger, convenient and easy to use, the latter are membrane-based, more versatile and expensive; they use a reference pressure against a diaphragm to precisely set the system pressure, allowing fine-

tuning of the pressure during the reaction without the need to stop the flow. Additional pressure sensors can be integrated into the delivery system upstream.

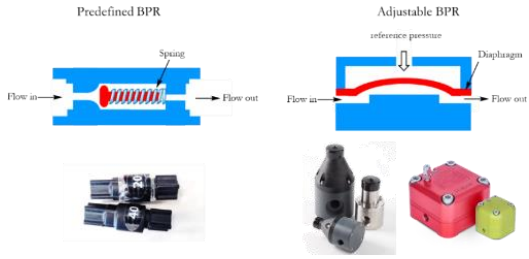

Figure 1.10 Predefined (left) and adjustable (right) BPR.

Collecting

The set-up can be endowed with different collection modules, like tanks or batch vessels, where the outlet of the reaction is collected. An automated fraction collector can be used to collect fractions at different time points during a process run. Differently, the reaction outlet could go into further downstream units.

Purification

Generally, organic synthesis of complex molecules and pharmaceuticals involves several transformation steps that often require time-consuming and tedious purification procedure, like separation by standard column chromatography. Continuous flow allows to conduct multistep reactions without isolating unstable or toxic intermediate but, as the complexity of mixtures profile increases over number of steps, many laboratories still rely on off-line conventional purification.
For this reason, continuous in-line purification strategies have not yet become an ordinary procedure for a flow process. The main used techniques are, liquid-liquid separation, that we already mentioned when talking about quenching procedure, tube-in-tube system, that can operate also as gas separator when connected to vacuum, and packed bed filled with scavenger materials. In recent years, microfluidic distillation, nanofiltration, as well as prototypes of in-line evaporators and continuous extractors, joined the picture with the aim of facilitating impurities removal, solvent switching, isolation of products and recycling of catalysts.[121] In this context, new straightforward but complex technologies have emerged, such as continuous crystallization and simulated moving-bed chromatography (SMB).[122,123] These methods could guarantee better performance, less solvent consumption and hight throughput compared to batch purification, but they still need to be fully implemented.

Connecting parts

Every operating unit or modules need to be connected to the other. This role is played by tubing and nonwetted parts, like nuts and ferrules, generally used in HPLC instruments, compatibly with the chemicals and solvents used, and the pressure reached by the system. Also, syringe-to-tube connectors, tube-to-tube fittngs and T-valves can be considered in this category. Usually, the

materials choice between polymers and stainless steel follows the same indication as the one previously showed for reactors material selection.

1.4.3 Flow chemistry in organic synthesis: advances and perspectives

Flow chemistry revolutionized many chemistry sectors, but one of the main impacts was registered in medicinal chemistry, where multidisciplinary efforts are put together to develop new, safe, and effective drugs.
The preparation of complex molecules starting from simpler building blocks was undoubtedly favoured by the disruptive growth of flow technology, so much that it now finds vast applications in the synthesis of heterocyclic compounds, natural products,[124] and active pharmaceutical ingredients (API).[125,126,127]

One advantage of continuous flow synthesis is possibility to conduct several transformations without the need of any purification and isolation of the intermediate.[128] In this context, one interesting example was provided by Petersen et al.. They presented a multistep flow sequence starting from a protected diamine and an isocyanate, followed by a Cbz-deprotection, and subsequent alkylation with different benzyl bromides, exploiting different supported scavenging cartridges and catalysts (**Scheme 1.7**). The process yielded a series of piperazines that target a receptor involved in inflammatory conditions.[129]

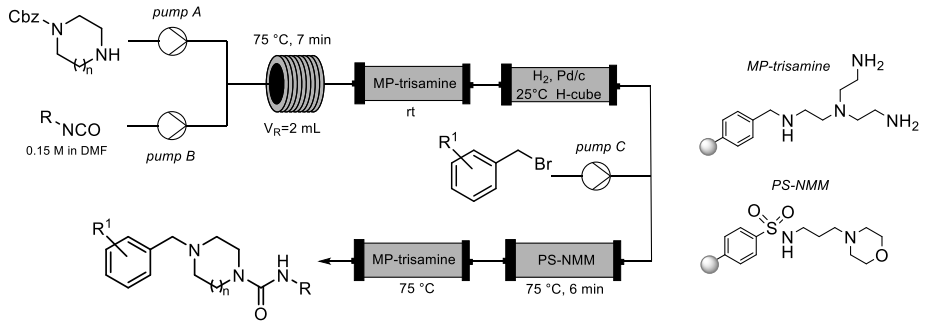

Scheme 1.7 Flow scheme for the multistep synthesis of piperazines

Multiple reaction steps combined into few continuous operations were also exploited to achieve the semi-continuous synthesis of Efavirenz, first-line treatment of HIV.[130]
The process starts with the lithiation of 1,4-dichlorobenzene and the subsequent trifluoroacylation. The following addition of lithium cyclopropylacetylide on the obtained intermediate affords a propargylicalcohol. The final step is a copper-catalyzed cyclization of an in situ generated arylisocyanate, which provides Efavirenz in 45% yield in less than two hours (**Scheme 1.8**).

Moreover, the system is provided with in-line purification, with scavenging columns to remove the byproducts from the stream. Overall, the process envisages the use of less toxic and less expensive reagents within a shorter reaction route, if compared to previous approaches.[131,132]

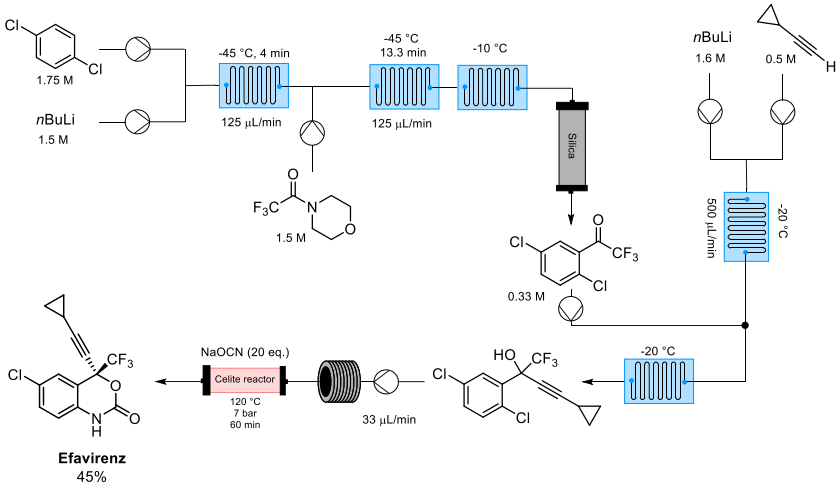

Scheme 1.8 New continuous flow synthesis of Efavirenz

Since I previously reported the one-pot procedure to achieve (-)-Oseltamivir (**Chapter 1.2**) presented by the Hayashi group, it seems interesting to also report their continuous flow approach. They developed few years later, attracted by the possibility of building an even more efficient, safe and reproducible process.[133]

This achievement was preceded by a batch optimization of the entire process, in order to obtain a faster reaction time and decrease the number of steps. Indeed, the group was able to perform the total synthesis of (-)-Oseltamivir within 60 minutes (with MW irradiation; 170 min without its use). Once optimized, they transferred the method in flow, in a multistep synthesis using five consecutive units (**Scheme 1.9**). The process involves a diphenylprolinol silyl ether mediated Michael reaction (1), a domino reaction of Michael and intermolecular Horner– Wadsworth–Emmons reactions (2), protonation (3), epimerization (4), and final reduction of the nitro group to an amine (5).

Another problem was the represented by the solubility of some of the reagents used in the previous approaches: Cs_2CO_3 was profitably substituted with *t*-BuOK in the flow process, and the reduction of the nitro using Zn and TMSCl was performed with Zn packed in a column, with Celite to avoid clogging issue. Unfortunately, after the last step, a traditional acid-base extraction and column chromatography was needed to afford the product.

The process leads to a 13% total yield of the product, by operating through a single flow, and with a residence time of 310 minutes. Even though this result cannot match the one obtained in the one-pot process, flow chemistry represents a stimulating tool for further investigation and scale-up.[134]

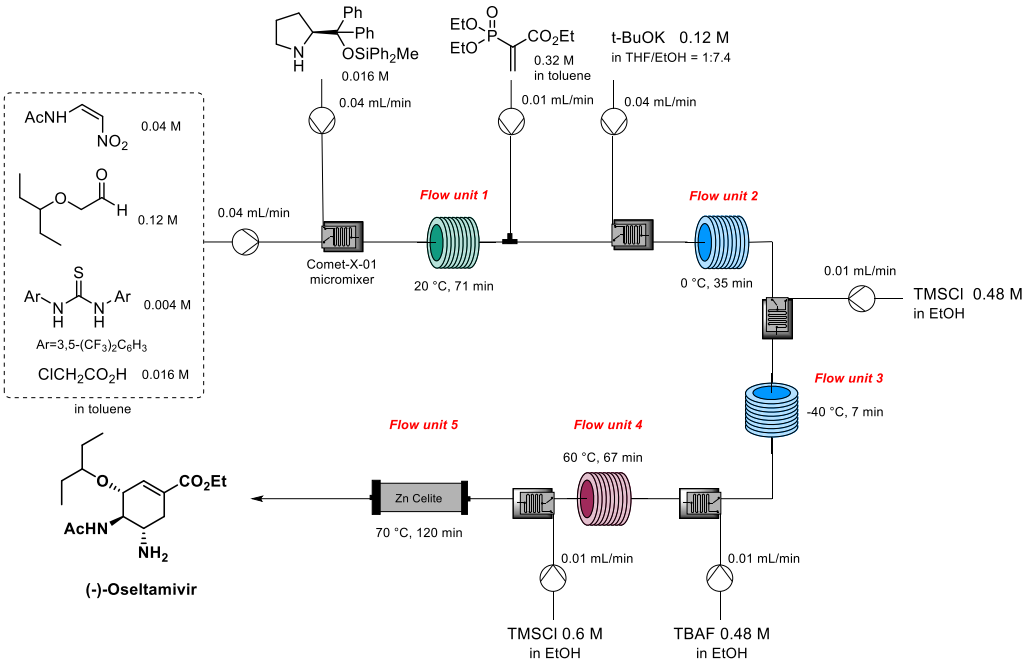

Scheme 1.9 Continuous flow approach for the preparation of (-)-Oseltamivir

Another interesting example of continuous flow process was reported by Jamison and Snead, involving the synthesis of important anti-inflammatory drug Ibuprofen, within an overall residence time of three minutes (**Scheme 1.10**). The method, that uses simple and inexpensive reagents, was also scaled up and provided the product at a rate of 8.09 g/h^{-1}.[135]

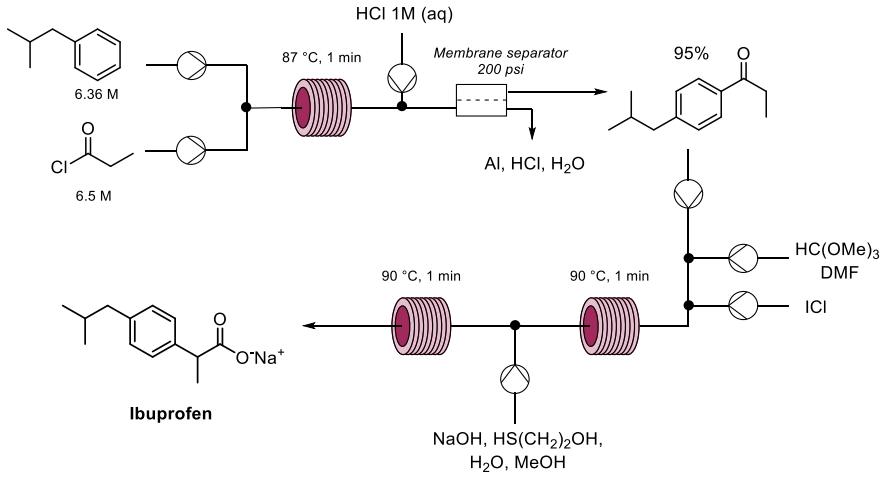

Scheme 1.10 Three minutes flow synthesis of Ibuprofen

The development of flow systems, integrated with automation and digitalization,[136] PAT,[137,48] and computational chemistry, boosted the creation of compound libraries and facilitated simultaneous screening, enhancing lead discovery and optimization.[138] Moreover, the emergence of advanced technologies for data acquisition, processing, and control, led to a significant increase in the amount of data generated, that can be profitably used to improve the quality, safety, cost-effectiveness, and sustainability of processes, especially in terms of energy consumption and wastes generated.[139] These data can be analysed using statistical methods, machine learning, and data visualization techniques to identify trends, correlations, and anomalies, to model and predict the behaviour of chemical reactions. This helps in optimizing process parameters, identifying of potential issues, and reducing the need for extensive experimental testing to find the optimum.[140]
The economic and social benefits of flow chemistry are particularly relevant in our society, particularly in this historical moment where the chemical manufacturing industry is a key driver of the economy, and a reduction in the footprint of processes is strongly demanded to the petrochemical, commodities and pharmaceutical sectors.[141]

Within this thesis work, continuous flow technology found application in the photocatalyzed hydroalkylation of nitroalkenes (**Chapter 2.4**), and in the development of a selective process for the synthesis of Δ^9-THC and Δ^8-THC from Cannabidiol (**Chapter 3.3**), conducted at the University of Graz.

1.5 Photochemistry

The history of light-induced reactions can be easily dated back to Earth early stages, even before the beginning of human life. It was plants work that created an atmosphere that shielded life from solar high-intensity UV irradiation, through the generation of the protective ozone layer. In this way, solar energy and light's interaction with matter have shaped the planet's course and continue to play a significant role in various natural, productive, and environmental processes. From photosynthesis, where the energy of absorbed photons is used to provide ATP for energy storage and NAPH, while oxygen is liberated into the atmosphere, to the many biological – physiological and psychic - processes in which is involved within our own bodies. Light is Life.

Nowadays, the field where its impact is of paramount importance is, without any doubt, energy production. World's demand is constantly growing and solar irradiation represents a clean, reliable and renewable source,[142] considering also the need of more sustainable solutions to modern challenges and crises. In fact, beside the progresses in photovoltaic systems development, photocatalysis can be employed to remove pollutants and contaminants from water and air.[143,144]

Photochemistry finds applications in healthcare, with the use of photosensitizing agents to treat cancer,[145] and in the development of new drugs and pharmaceuticals.

Light often allows to operate under mild conditions if compared to many chemical processes, and photons, unlike other activating agents or catalysts, leave no residue or byproducts to remove after their action. The high energy generated can be selectively delivered directly to an absorbing molecule, by carefully choosing the wavelength and intensity of light, allowing the formation of reactive intermediates in a controlled manner, therefore making processes safer. These advantages contribute to the growing importance of photochemistry in various fields, ranging from organic synthesis to materials science,[146] and beyond. In fact, another relevant application is in the development of new devices and technologies, ranging from electronic displays and sensors to advanced imaging techniques.

1.5.1 Origins of contemporary photochemistry (and green chemistry)

The knowledge of photochemical transformations has a long history, but some of the most important discoveries dates to the 18th century, like Priestley's initial encounter with the oxidation of mercury into a red solid, after focusing sunlight on a sample using a twelve-inch lens. In 19the century, Trommsdorff first, Sestini and Cannizzaro later, studied the wavelength dependence of photoreactions, the chemistry of Santonin and its photoproducts, and their work served as a foundation for further explorations in the field. In the same years, the contribution of academics such as William Henry Perkin, for the light-induced isomerization of olefins, and Heinrich Klinger, for the photoreduction of carbonyl compounds when exposed to sunlight, paved the way for the next generation of chemists.[147] It was in the 20th century that organic photochemistry emerged as a significant area of research, thanks to the contributions of scientists such as Giacomo Ciamician and

Paul Silber. Working on the terrace of the University of Bologna, they conducted experiments by exposing solutions of various chemical compounds to sunlight (**Figure 1.11**).[148]

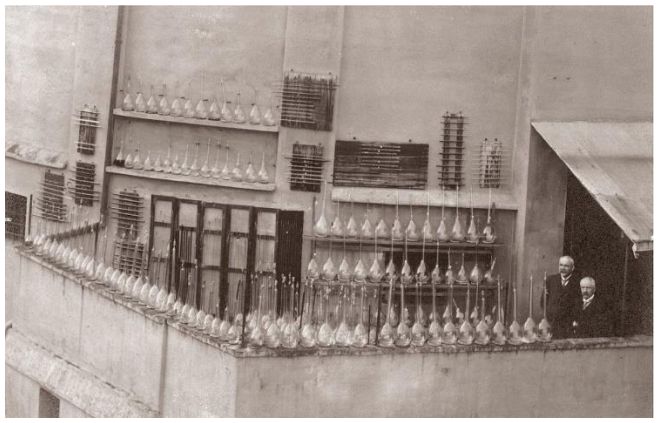

Figure 1.11 Ciamician and Silber: photochemistry on the rooftop of University of Bologna

Through their work, Ciamician and Silber made significant advancements in photochemical transformations, surpassing previous efforts, and showcasing the potential of utilizing light as a driving force for chemical reactions, becoming pioneers of not only solar energy conversion, but also of green chemistry. In fact, their work laid the ground for further investigations into the mechanisms and applications of organic photochemistry, demonstrating its power in enabling unique and selective transformations, and finally leading to its recognition as an essential field of study within chemistry. But, they also hold the merit to have focused, probably for the first time, the attention of the world on energetic problems. In his famous lecture "*The photochemistry of the future*" (**Figure 1.12**), given at the "*VIII International Congress of Applied Chemistry*" (New York, September 1912), and later published in 4 different languages,[149] Ciamician expressed his forward-thinking perspective, anticipating several of the fundamentals that now stands in the 12 Principles of sustainable chemistry (1, 2, 3, 5, 6, 7, 12, see **Chapter 1.1.1**).[150,151] He recognized the finite nature of fossil solar energy (i.e. fossil fuels, including coal and oil), enlisted and evaluated the contribution and impact of the various forms of energy, proposed the use of solar energy for producing electrical energy, and highlighted the importance of the use of renewable materials and reagents. He recognized that photochemistry provided a unique tool for driving chemical reactions, due to its resemblance to how nature and organisms operate every day, enabling reactions that may not occur readily under thermal conditions.

SCIENCE

FRIDAY, SEPTEMBER 27, 1912 THE PHOTOCHEMISTRY OF THE FUTURE[1]

Figure 1.12 Transcription of Ciamician's speech[149]

More than 100 years passed form that inspiring talk. The future toward which Ciamician was referring to is the one that we are living now, and photochemistry itself is living a renaissance.

1.5.2 Back to basics

Interactions between matter and visible or ultraviolet light were significantly clarified with the emergence of quantum theory at the beginning of last century. Quantum theory showed how electrons in matter can be described by wavefunctions, which represent their probability distributions, as they exhibit both wave-like and particle-like properties. Quantum theory also explained that light and the energy of matter are quantised, and there are only discrete energy levels available to electrons in atoms, molecules, and other materials. The energy levels are separated by specific energy differences, and these separations are on the same order of magnitude as the energy of visible or ultraviolet light. When matter interacts with visible or ultraviolet light, it can absorb **photons** of specific energies, corresponding to the energy differences between its quantized energy levels. This absorption can promote electrons from lower energy levels to higher energy levels, resulting in the creation of electronically excited species. These excited species possess higher energy, and they can exhibit distinct chemical or physical properties.

Planck's law defines the energy of a photon (E)

$$E = h\nu = hc/\lambda$$

Where h is Planck constant (6,63 x 10^{-34} Js) and v is the frequency of oscillation of the photon in units of s^{-1} or Hertz (Hz), c is the speed of light

This means that the energy of a photon is proportional to its frequency and inversely proportional to its wavelength (**Table 1.2**).[152]

Table 1.2 Visible and ultraviolet light's properties

Colour	λ (nm)	ν (10^{14} Hz)	E (kJ mol^{-1})
red	700	4.3	170
orange	620	1.6	193
yellow	580	5.2	206
green	530	5.7	226
blue	470	6.4	254
violet	420	7.1	285
ultraviolet	<300	>10.0	>400

Generally, light-matter interaction can be the result in three different processes:

- **Absorption**: where a photon, with an amount of energy equal to the energy difference that occurs between two electronic states, can transfer its energy to an electron, causing its transition from a lower energy state to a higher one.
- **Spontaneous emission**: it involves the spontaneous release of energy by an excited electron as it transitions from a higher energy state to a lower energy state; it emits a photon with energy equal to the energy difference between the two states.

– **Stimulated emission:** it occurs when an already excited electron is stimulated by an incoming photon of the same energy; the stimulated electron undergoes a transition from the higher energy state to the lower energy state, releasing a photon with the same energy, phase, and direction as the incoming photon.

When referring to an absorption process, other two laws that become essential to mention are Grotthuss-Draper law and Stark-Einstein law. As the first states that for a photochemical reaction to occur, the molecules or atoms involved must absorb light, the second postulates that the absorption of one photon results in the excitation of a single molecule, because light absorption is a one-quantum process. However, there are exceptions to this latter, particularly when very intense light sources like lasers are used to irradiate a sample, and concurrent or sequential absorption of two or more photons by a single molecule occurs, or when free radicals that can initiate chain reactions are generated.

In a photochemical reaction, the absorption of light, ranging from high-energy ultraviolet (UV) light to visible light and even low-energy infrared radiation, induces a chemical transformation. This process involves several photophysical processes, which can be represented in the Jablonski state diagram (**Figure 1.13**). This illustrates the energy levels and transitions of a molecule during a photochemical reaction: initially, the molecule is in its ground state, denoted as $\mathbf{S_0}$, where the highest occupied molecular orbital (HOMO) is fully occupied by two electrons; upon **absorption** of a photon, with the energy matching the HOMO-LUMO (lowest unoccupied molecular orbital) gap, the molecule is excited to its first excited state, $\mathbf{S_1}$, where one electron is promoted to the LUMO. Once in the excited state, several processes can occur. The excited electron can go back to the HOMO emitting light by **fluorescence**, or it undergo a non-radiative internal conversion (IC), where the energy is dissipated as heat, bringing the molecule back to the ground state, without emitting any light. Alternatively, through a process called intersystem crossing (ISC), the excited molecule can change the spin configuration of one electron, leading to its transition to a long-lived triplet state, denoted as $\mathbf{T_1}$. In this state the energy is lower than the one of the corresponding excited singlet state, in line with Hund's rule.

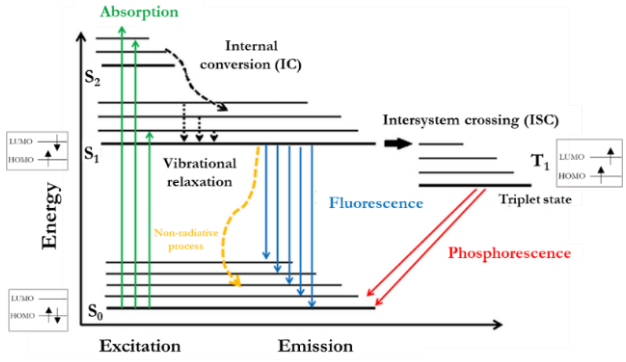

Figure 1.13 Jablonski state diagram[153]

From the triplet state, the molecule has two possible pathways to return to the ground state. It can undergo radiative decay, known as **phosphorescence**, where the electron transitions back to the ground state with the emission of light, or it can undergo a non-radiative internal conversion like the one observed from the singlet excited state.

The absorption of a photon and subsequent formation of an electronically excited state (**R^***) , that possess different electronic distribution and geometry, enhances electron donor or acceptor properties, and serve as the starting point for various processes. In photochemical reactions, the excited state can undergo chemical transformations, such as isomerization, dissociation, oxidation, or reduction, leading to the formation of new compounds (**P**). These reactions are driven by the energy gained from the absorbed photon. In photophysical transformations, besides fluorescence and phosphorescence, other processes include energy transfer, where the excited state transfers its energy to neighbouring molecules.

$$R + h\nu \rightarrow R^* \rightarrow P$$

Beer-Lambert Law describes the linear relationship between the concentration of a solute in a solution, the light absorbance as it passes through the solution and path length.

$$A = \varepsilon\, c\, l$$

where A represents the absorbance of the solution, which is a dimensionless value, as it can be also written as the negative logarithm of relative absorption (I_{out}/I_{in}), ε is the molar absorption coefficient, which is a constant specific to the absorbing substance and the wavelength of light being used, c is the concentration of the solute in the solution, expressed in mol/L, l is the path length of the light through the solution, usually measured in cm.

As the molar absorption coefficient varies at wavelengths (λ), a plot of these two can provide an absorption spectrum of a specific substance. This helps determining the wavelength (λ_{max}) at which the compound exhibits its maximum molar absorption coefficient (ε_{max}), meaning the highest probability of absorbing light. By identifying λ_{max}, the photoexcitation process of the compound can be optimized, as it can be more efficient and effective.

When molecules absorb photons and transition to electronically excited states, that are inherently transient and have a limited lifespan, they acquire excess energy. The loss of the excess energy can occur through various physical deactivation processes, ultimately resulting in the returning to a ground-state configuration of the molecule. If the dissipative process is accompanied by the formation of a new chemical species or modification of the molecular structure, it can be considered a chemical process. Differently, if the excess energy is dissipated through luminescence or non-radiative processes, that involve energy redistribution within the molecule or energy transfer to the surrounding environment, it does not result in the formation of new chemical species.

When the excited molecule undergoes a photochemical reaction, the excess energy is utilized to drive the chemical transformation, resulting in the creation of different chemical bonds, isomerization, or other chemical rearrangements. In this case, intermolecular processes occur, such as: vibrational relaxation, where a molecule is in an electronically excited state with excess vibrational energy can

rapidly collide with other molecules, including solvent molecules, thus producing molecules in the lowest vibrational level; energy transfer, where the energy from an electronically excited state of one molecule (the donor) is transferred to another molecule (the acceptor); or electron transfer, in which a photoexcited donor transfers an electron to the acceptor molecule, resulting in the formation of an ion pair. Nevertheless, the line between physical and chemical processes in photochemistry can sometimes be blurred, as certain reactions involve a combination of both. For example, excited-state proton transfer or electron transfer reactions involve both physical and chemical phenomena.

Generally, the transition from ground states to upper electronic states (excited) in a system can be depicted also in term of changes in the potential energy of reactants, intermediates, and products during the reaction (**Figure 1.14**). This usually comprehend at least two energy surfaces, the ground-state surface and the excited state surface, in contrast to thermal reactions, where a single energy surface is sufficient to describe the process. To start and finish in ground-state surface, the key step is transitioning through a "photochemical funnel" from an excited state to a lower one to reach the appropriate electronic and vibrational state for the desired products or reaction pathway.[152]

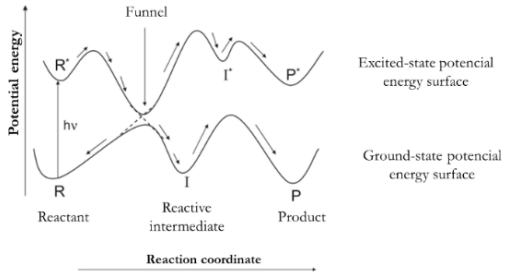

Figure 1.14 Potential energy surfaces for excited - state and ground - state molecules

In this point, the excited-state and ground-state potential energy surfaces come into close proximity, allowing for efficient transitions between the two states. The conversion from an electronically-excited state $\mathbf{R}^*$ can lead to the target product either in a concerted single step process, or through the formation of a reactive intermediate **I**, like a radical species.

As we anticipated, one difference between a photochemical reaction and a thermal one is the energy state of the reagents involved, but another important characteristic is that temperature does not have marked effect on the rate of light-initiated reactions. Furthermore, in conventional thermal reaction heat is generally applied to the whole system indiscriminately, thus leading to random collision which can result in favouring alternative reaction pathways and byproducts, whereas a photochemical reaction is able to generate excited species selectively, especially when a monochromatic light of the appropriate wavelength is used.
Another difference resides in Gibbs free energy between thermal and photochemical processes. In fact, the difference in Gibbs free energy (ΔG) is primarily determined by the difference in enthalpy (ΔH) and entropy (ΔS) between the reactants and products, so a thermodynamically favourable and

spontaneous reaction in the thermal process is characterized by a negative ΔG. In thermal processes, the rate of reaction is primarily governed by the necessity of overcoming the activation energy barrier. In photochemical processes, Gibbs free energy also considers the energy of the photons absorbed during the excitation process, and the reaction rate is primarily determined by the intensity and wavelength of the light source, the absorption cross-section of the molecule, and the efficiency of energy transfer processes. So, even if the ΔG is positive, the reaction may still occur spontaneously, as the absorption of light energy can drive reactions that would not be thermodynamically favourable based solely on the ground-state thermodynamics.
Finally, the formation of electronically excited states, which have different energy levels and reactivity compared to the ground state, can broadened the number of accessible reactions.

1.5.3 How to conduct a photochemical reaction

General consideration to take into account when approaching a photochemical reaction are the importance of the determination of the absorption band of the reagent or a no-competitive region to guarantee the chromatically orthogonality, the absence of any physical interferences between the photon source and the target substrate or reagent (generally, vessel's walls and solvents selected need to be transparent to the desired range of wavelengths), and of chemical interferences in the excited states, that could provoke premature quenching and no reaction.[154]

Another important aspect is the configuration of the system, with the light source placed at the correct distance to the reaction mixture so that there are no non-irradiated zone nor lost irradiation, and the maximum light intensity can reach the medium, accordingly to the inverse-square law of light. If not possible, reflective surfaces or mirrors strategically placed around the reaction vessel could help redirect and enhance light intensity, ensuring more uniform illumination of the reaction mixture. Therefore, also the reactor design and geometry play an important role. Several advancemens in the matter, and consequent advantages provided by the combination of photochemistry and flowchemistry (i.e. photoflow) will be discussed in the next chapter (**1.6 Combining technologies**).
In the early stages of photochemical investigations, the absence of artificial light sources posed a significant challenge. Researchers had to rely on sunlight as the sole source of irradiation for their reactions. This limitation resulted in long irradiation times, as reaction flasks were exposed to direct fluctuant sunlight (i.e. insolation process) for extended periods, with impact of external factors such as temperature variations, whether and geographic location that could change reaction rate. The advent of specialized lamps, such as mercury vapor lamps, and more recently LED lamps, allowed researchers to overcome these obstacles and achieve greater control over reaction conditions, thus tackling reproducibility problems and leading to more precise investigations and advancements in the field of photochemistry.

Light sources

In organic chemistry, the wavelength range of interest generally corresponds to ultraviolet (UV) and visible (Vis) light, between 200 and 1000 nm (near IR).

Common light sources used in photochemistry include mercury vapor lamps, xenon lamps, halogen lamps, and UV lamps. Light-emitting diodes (LEDs) are becoming increasingly popular due to their energy efficiency and tuneable but narrow spectra.

UV light provided by medium- and low-pressure mercury lamps, with his high energy, was profitably used for the direct activation of organic compounds that allow many important reactions such as [2+2] cycloaddition, Norrish-type reactions and the homolytic cleavage of C-C bonds, but it can be more challenging to handle, and by-products formation is enhanced. The same outcome, with the potential formation of byproducts, is provided by the use of high-pressure mercury lamps, that emits light across a broad range of wavelengths from UV to visible light.

In this context, the advent of compact LEDs, constructed using layered crystalline semiconductor materials which form a p-n junction at the interface of two types of semiconductors and that generates light through and electroluminescence process, provided number of advantages.[155] Their small size enables precise alignment with reactants, ensuring efficient light absorption and interaction with the desired chemical species, they consume less power and generate less heat, resulting in reduced energy costs and better temperature control within the reactor. Moreover, they have a narrow wavelength range, typically around 10-30 nm, that guarantees precise and specific emission, and since the wavelength of the emitted light depends on the material characteristics, they can be very versatile. Finally, LEDs intensity can be easily tuned, and they can be easily integrated into different reactor designs, thanks to the overmentioned characteristics (**Figure 1.15**).

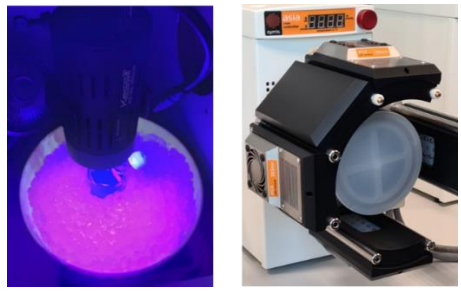

Figure 1.15 Kessil LED light irradiating a reaction (left), 385 nm LEDs on Syrris Asia Photochemistry module (right)

Solvents

Solvents used in photochemical reactions are typically chosen to be transparent to the specific range of wavelengths required for the reaction. Common solvents used in organic chemistry, such as acetonitrile, methanol, or dichloromethane, are generally transparent to a wide range of UV and visible light (**Table 1.3**). A useful parameter is the λ_{lim}, the wavelength at which a 1 cm layer of solvent absorbs 90% of the of the light.[156] The choice of the solvent must be in accordance with the reagent used, taking into account that reagents at their excited state present different properties compared to

the corresponding ground state. Important factors such as solvent stabilization of transition states and intermediates need to be considered.[157]

Table 1.3 Cut-off wavelength of common solvents

Solvent	λ_{lim}
acetonitrile	190
n-hexane	195
methanol	205
diethyl ether	215
ethyl acetate	255
dimethylsulfoxide	265
benzene	280
pyridine	305
acetone	330

Reactors

Transparent materials, such as borosilicate glass or quartz, are commonly used to construct reaction vessels for photochemical experiments. The λ_{lim}, wavelength at which a 1mm layer of the glass absorbs 90% of the light is around 300 nm for Pyrex glass.

Simple Pyrex vessel or immersion well reactors are exploited in batch photochemistry.

Whereas, different materials and configurations are adopted if the photochemical reaction is conducted in combination with other technologies (i.e. flow chemistry), that exploits pumps for circulating the solution. For example, fluorinated ethylene propylene (FEP) tubing coiled around the light source, parallel tube reactor, and microchip reactors with LED modules irradiating both sides. In the latter case, problems related to mixing, and the volume irradiated in larger-diameter reactors (as in scale-up), derived from Bouguer−Lambert−Beer law, can be minimized.[158]

1.5.4 Photochemistry in synthesis

There are several different types of photochemical reactions that can occur when molecules or compounds are exposed to light. Some of the major types include photo-induced rearrangements, isomerization, photo-addition, -dissociation or -substitution, redox reaction, photolysis, photopolymerization, but a more general distinction can be done by identifying the role of the photoexcited molecule:

1) **Direct photochemical reactions**, where the substrate or a reagent that can directly absorb light subsequently undergo a chemical transformation (bond breaking, bond formation, rearrangements, or other chemical processes); two examples of these activation mode are carvone intramolecular [2+2] cycloaddition (**Scheme 1.11, Example a**),[159] firstly reported by Ciamician in 1908, and cis-trans isomerization of stilbene (**Scheme 1.11, Example b**).[160]

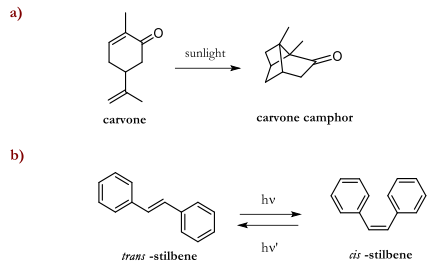

Scheme 1.11 Examples of two direct photochemical reactions

In certain cases, direct activation in photochemical reactions can involve the formation of an electron donor-acceptor (EDA) complex. In this case, there is a strong interaction between an electron donor molecule and an electron acceptor molecule, that reduces gap HOMO-LUMO thus favouring the activation.[161]

2) **Sensitized photochemical reactions**: a photocatalyst (also called photosensitizer) absorbs the incident photon and transfers its energy – generally by emission of a photon - to a substrate or the reagent, which then undergoes the chemical transformation. The sensitizer serves as an intermediary, efficiently absorbing light energy, characterized by a longer excited-state lifetime, enhancing the efficiency of energy transfer to the substrate or reagent. This type of reaction expands the range of compounds that can undergo photochemical reactions by enabling species that do not absorb at the desired wavelength. This process is commonly achieved through non-radiative energy transfer pathways, such as Förster resonance energy transfer (FRET) or Dexter energy transfer. In the latter, direct electrons exchange occurs after donor and acceptor's orbitals overlap.[162]

3) **Photoinduced electron transfer reactions**: the photocatalyst (i.e. photoredox catalyst) undergoes an electron transfer and participates in a redox reaction, resulting in a change in their oxidation states. The absorption of light by the photocatalyst molecule generates an excited state that can undergo electron transfer with a suitable electron donor or acceptor molecule (catalysts can act as both an oxidant and reductant in their excited state), leading to the formation of radical species (anions or cations, or even neutral) or the generation of charged intermediates, which can subsequently undergo various chemical reactions. Metal-based ruthenium(II) and iridium(III) photoredox catalyst complexed with several homoleptic or heteroleptic polypyridyl ligands have been commonly used for the scope,[163] but recent interests in this research field are directed to the use of organic dyes as photoredox catalysts, as they presents enhanced tunability, functional group compatibility, and ease of modification. Moreover, the exploitation of more earth abundant metals, such as copper, molybdenum, chromium and iron is being explored, as well as the development of multicatalytic strategies.[164]

Photocatalysis is experiencing a renaissance in recent years, and a remarkable attention is put in the discovery of new activation patways, that result in an expanded scope for synthetic protocols development by harnessing the power of visible light.[165] This allows the selective activation of specific bonds or functional groups, enabling the formation of molecules previously challenging to access using traditional thermal methods.[166] These techniques include processes such as single-electron transfer (SET) and hydrogen atom transfer (HAT),[167] which is able to provide the straightforward activation of R–H (R = C, Si, S) bonds. An example of HAT reaction, applied to the hydroalkylation of nitroolefins will be presented within this thesis work (**Chapter 2.4**).
Generally, synthetic methodologies enabled by photocatalysis are in continuous expansion. These go from the formation of challenging C-C,[168,169] and C-N,[170] α-amino functionalizations,[171] cross-coupling reactions,[172] cyclization reactions,[173] to the generation of a vast array of reactive intermediates such as radicals, carbenes, and nitrenes under mild reaction conditions.[174]

As anticipated when exploring the reactors used in photochemistry, one of the main challenge in the field is related to scalability. New alternatives, new reactors and systems can be found in literature daily,[175,176] as well as guidelines for the correct draft of sectorial articles, with important and technical details of the set-up required for reproduce an experiment, aimed toward a standardization of processes.[177]
Challenges related to versatility, availability of different systems and lamps, and therefore in the reproducibility of experiments, are highlighted in different literature papers. One example is the effect of total supplied energy dose and light intensity on reaction kinetics (Bunsen-Roscoe law), which is not often considered.
Photoflow technology can be an option to tackle some of the problems, and there is a lot of excitement around this theme. More details will be given in **Chapter 1.6**, dedicated to combined technologies. This approach can be useful to address critical aspects, and to transfer procedures from laboratory to pharmaceutical industry, making this powerful tool a well-established, reliable technique.

1.6 Combining technologies (let them flow!)

As continuation of the previous chapter, some insight and details over combined photo and flow processes – will be given, as they were also profitable applied in one of the projects presented in this thesis work (**Chapter 2.4**).
Following, an overview of some others combined enabling techniques, already singularly discussed, will be provided, as they constitute one of the main recent advances in organic synthetic strategies.

Photo-flow

One of the reasons of this new flourishing era that photochemistry is living is also due to the possibility of a synergic combination with continuous flow chemistry. The simultaneous exploitation of the two techniques holds the credit for an enhanced light penetration and homogeneous energy distribution, derived from microtubings that ensures that a larger fraction of the reaction mixture is exposed to the light source; fast mixing, due to the small size of the reactor; efficient heat dissipation, preventing unwanted side reactions or degradation; precise control over reaction parameters, thus allowing for a rapid optimization and fine-tuning of conditions; improved reaction selectivity and reproducibility, as consequence of the enhanced mass, heat and photon transfer provided microchannels; straightforward scalability, that can be achieved with longer operating times and continuous introduction of starting materials or by a numbering-up (internally or externally) using parallel reactors; improved safety, thanks to the confined reaction volume and minimized risk of accidental exposure to high-intensity light sources. Another advantage is provided by recent advances in LEDs technology, that provide compact and easily adaptable light source for flow reactors.[178]
Moreover, several reactors were developed for specifically handling multiphase reactions in flow and can be adapted also for photochemical processes, such as basic single channel microreactors with transparent polymer-based capillaries, falling film, continuous stirred-tank reactor, or membrane microreactors.[179] In addition, thin layers of semiconductor heterogenous species in reactors are increasingly being used as photocatalyst, such as TiO_2, Bi_2O_3, cadmium sulfide/ selenide and graphitic carbon nitrides.[180,]
Finally, several efforts have been made in the development of integrated platforms for high-throughput experimentation of photochemical transformations, as well as the integration with algorithms for self-optimization and automation.[155]
The importance of this continuously expanding research field is also endorsed by the possibility to pinpoint many of the 12 Green Chemistry Principles through these combined techniques.[181]

To report an example of light driven reaction coupled with continuous flow conditions, in **Scheme 1.12** is described an enantioselective α-alkylation of aldehydes, a recent work by Molnár et al.,[182] that I have seen developing during my abroad period at Graz University. To this aim, no photoredox catalyst was used, but a chiral organocatalyst (diarylprolinol) responsible for enamine-mediated activation of the aldehyde.

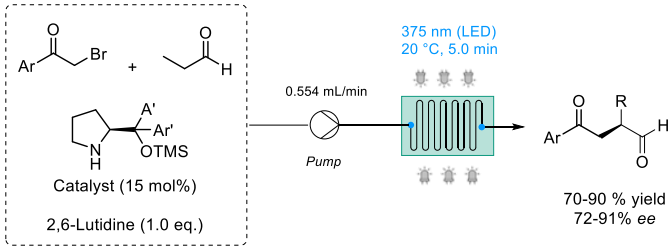

Scheme 1.12 Enantioselective α-alkylation of aldehydes

One-pot flow

Already intrinsically advantageous one-pot strategies can be further expanded when conducted in flow, in particular one-pot stepwise synthesis of small molecules or cascade reactions.[183] Complex synthesis pathways can be achieved, enabling the synthesis of intricate compounds that may be challenging or impractical to pursue using traditional batch methods. Overall enhancements in efficiency and productivity, reaction control, and excellent mixing and heating complete the picture.

An example of continuous-flow one-pot processes is represented by 1,3 polar cycloaddition of alkynes with $TMSCH_2NH_2$, reported in the below **Scheme 1.13**.[184] In particular, the method involves the continuous flow formation of trimethylsilyldiazomethane from the corresponding amine, and subsequent alkyne addition to the obtained crude reaction mixture, affording the synthesis of different pyrazones in good yield.

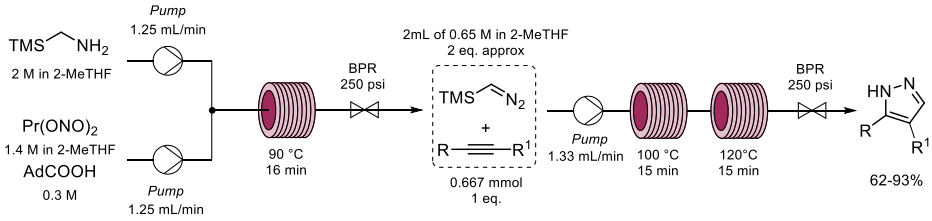

Scheme 1.13 One-pot cycloaddition of alkynes with $TMSCH_2NH_2$

Flow-microwave

The application of continuous flow technologies changed the future perspectives of microwave chemistry. The possibility to minimize limited penetration depth of microwaves into absorbing media, that strongly mined scale-up processes, can be accomplished by the development of glass-based microreactor, Kevlar-reinforced coils, or microcapillary reactor positioned in a microwave cavity. On the other hand, microwave irradiation provides high temperature very quickly, and uniform heating.[185] This increase the energy efficiency, reliability and reproducibility of processes. These two synergistic processes are often coupled with the use of immobilized catalyst, coated onto the capillaries.[186]

One example of microwave-flow synthesis was provided by Musio et al.,[187] involving the synthesis of β-lactams starting from 2-diazoketones reacted with amines and imines, after the in-situ generation of highly reactive ketenes (**Scheme 1.14**). The products were obtained in moderate to good yields and with a preferential *trans*-configuration.

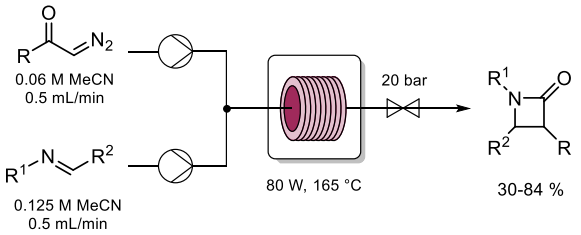

Scheme 1.14 Flow synthesis of *β*-lactams

Solid supported catalysis and flow

Heterogeneous catalysis in flow was already briefly discussed when presenting the general instrumentation used in continuous synthesis (**Chapter 1.4.2**).

Solid-supported species are inert materials, generally organic or inorganic polymers that can be functionalized with different catalyst, such as organic, organometallic, metallic or enzymatic.

Beside packed-bed flow reactors, heterogeneous catalysis can be achieved using wall-coated flow reactors, where the catalyst is immobilized on the walls of the reactor, and monolithic flow reactors, that present a honeycomb-like structure of polymeric or inorganic materials with interconnected channels through where the solution flows.[188] Each of these methods present advantages and disadvantages: in packed-bed reactors a high catalyst loading that can provide enhanced reaction rate can be deterred by a fluid dynamic often unpredictable, frequent leaching or deactivation of the catalyst; wall coated reactors provide good mass transfer and reduces occurrence of clogging episodes, but the catalyst loading is quite low if compared to the others techniques; monolithic reactors present high efficiency in mass transfer and tolerance of high flow rate, on the other hand pores clogging can occur. Alternative approaches in the field of biocatalysis have been recently presented, utilizing heterogeneous biocatalysts as a mobile phase, with the development of segmented hydrogel/organic solvent system.[189]

Herein, it is reported a remarkable and efficient combination of continuous flow and different column-packed heterogeneous catalysts, to achieve the multistep enantioselective preparation of (R)- and (S)-rolipram, achieved by Kobayashi and co-workers (**Scheme 1.15**). The product was obtained after eight steps conducted in flow, without any separation co-products, by-products, and excess reagents and without isolation of intermediates, exploiting real-time monitoring during the process.[190]

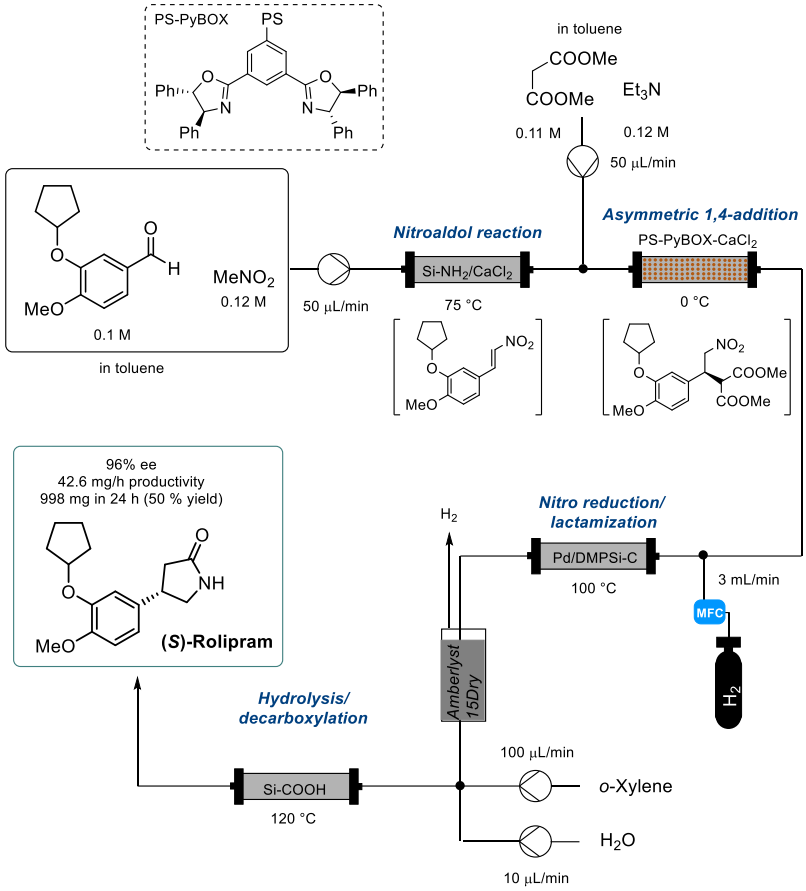

Scheme 1.15 Multistep flow synthesis of (*S*)-Rolipram

The above-enlisted technologies are often cross-linked, integrated like puzzle pieces, and simultaneously exploited, thus demonstrating that the synergic combination of enabling technologies is one of the hot topics in organic synthesis, and an exciting road toward future advancements in research field.

1.7 References

(1) Kar, S.; Sanderson, H.; Roy, K.; Benfenati, E.; Leszczynski, J. Green Chemistry in the Synthesis of Pharmaceuticals. **2022**. https://doi.org/10.1021/acs.chemrev.1c00631.

(2) Boerner, L. K. The Birth of Green Chemistry. *C&EN* **2023**, *101* (26), 42–44.

(3) ACS. *Green Chemistry History*. https://www.acs.org/greenchemistry/what-is-green-chemistry/history-of-green-chemistry.html (accessed 2023-10-04).

(4) Anastas, P. T.; Warner, J. C. *Green Chemistry: Theory and Practice*; Oxford University Press, 1998, 1998.

(5) Anastas, P. T. Origins and Early History of Green Chemistry. *Advanced Green Chemistry: Part 1: Greener Organic Reactions and Processes* **2017**, 1–17. https://doi.org/10.1142/9789813228115_0001.

(6) Anastas, P.; Eghbali, N. Green Chemistry: Principles and Practice. *Chem Soc Rev* **2010**, *39* (1), 301–312. https://doi.org/10.1039/b918763b.

(7) Marques, C. A.; Machado, A. A. S. C. An Integrated Vision of the Green Chemistry Evolution along 25 Years. *Found Chem* **2021**, *23* (3), 299–328. https://doi.org/10.1007/s10698-021-09396-6.

(8) Warner, J. C.; Cannon, A. S.; Dye, K. M. Green Chemistry. *Environ Impact Assess Rev* **2004**, *24* (7–8), 775–799. https://doi.org/10.1016/j.eiar.2004.06.006.

(9) ACS. *Chemistry & Sustainable Development Goal.* https://www.acs.org/sustainability/chemistry-sustainable-development-goals.html (accessed 2023-10-09).

(10) Anastas, P.; Nolasco, M.; Kerton, F.; Kirchhoff, M.; Licence, P.; Pradeep, T.; Subramaniam, B.; Moores, A. The Power of the United Nations Sustainable Development Goals in Sustainable Chemistry and Engineering Research. *ACS Sustain Chem Eng* **2021**, *9* (24), 8015–8017. https://doi.org/10.1021/acssuschemeng.1c03762.

(11) Linthorst, J. A. An Overview: Origins and Development of Green Chemistry. *Found Chem* **2010**, *12* (1), 55–68. https://doi.org/10.1007/s10698-009-9079-4.

(12) Ivanković, A. Review of 12 Principles of Green Chemistry in Practice. *International Journal of Sustainable and Green Energy* **2017**, *6* (3), 39. https://doi.org/10.11648/j.ijrse.20170603.12.

(13) Sheldon, R. A. No Title. *Chem. Ind.* **1992**, 903–906.

(14) Sheldon, R. A. The: E Factor 25 Years on: The Rise of Green Chemistry and Sustainability. *Green Chemistry* **2017**, *19* (1), 18–43. https://doi.org/10.1039/c6gc02157c.

(15) Jimenez-Gonzalez, C.; Ponder, C. S.; Broxterman, Q. B.; Manley, J. B. Using the Right Green Yardstick: Why Process Mass Intensity Is Used in the Pharmaceutical Industry to Drive More Sustainable Processes. *Org Process Res Dev* **2011**, *15* (4), 912–917. https://doi.org/10.1021/op200097d.

(16) Sheldon, R. A. Metrics of Green Chemistry and Sustainability: Past, Present, and Future. *ACS Sustain Chem Eng* **2018**, *6* (1), 32–48. https://doi.org/10.1021/acssuschemeng.7b03505.

(17) Trost, B. M. Atom Economy—A Challenge for Organic Synthesis: Homogeneous Catalysis Leads the Way. *Angewandte Chemie International Edition in English* **1995**, *34* (3), 259–281. https://doi.org/10.1002/anie.199502591.

(18) Constable, D. J. C.; Curzons, A. D.; Cunningham, V. L. Metrics to "green" Chemistry - Which Are the Best? *Green Chemistry* **2002**, *4* (6), 521–527. https://doi.org/10.1039/b206169b.

(19) Dicks, A. P.; Hent, A. Atom Economy and Reaction Mass Efficiency. **2015**, 17–44. https://doi.org/10.1007/978-3-319-10500-0_2.

(20) Garrett, R. L. Pollution Prevention, Green Chemistry, and the Design of Safer Chemicals. *ACS Symposium Series* **1996**, *640*, 2–15. https://doi.org/10.1021/bk-1996-0640.ch001.

(21) Devito, S. C. On the Design of Safer Chemicals: A Path Forward. *Green Chemistry* **2016**, *18* (16), 4332–4347. https://doi.org/10.1039/c6gc00526h.

(22) Joshi, D. R.; Adhikari, N. An Overview on Common Organic Solvents and Their Toxicity. *J Pharm Res Int* **2019**, *28* (3), 1–18. https://doi.org/10.9734/jpri/2019/v28i330203.

(23) Clarke, C. J.; Tu, W. C.; Levers, O.; Bröhl, A.; Hallett, J. P. Green and Sustainable Solvents in Chemical Processes. *Chem Rev* **2018**, *118* (2), 747–800. https://doi.org/10.1021/acs.chemrev.7b00571.

(24) Sherwood, J. Bio-Based Solvents for Organic Synthesis, **2014**

(25) Sahoo, B. M.; Banik, B. K. *Solvent-Less Reactions: Green and Sustainable Approaches in Medicinal Chemistry*; Elsevier Inc., 2020. https://doi.org/10.1016/B978-0-12-817592-7.00014-9.

(26) Mandal, B. Alternate Energy Sources for Sustainable Organic Synthesis. *ChemistrySelect* **2019**, *4* (28), 8301–8310. https://doi.org/10.1002/slct.201901653.

(27) Tripathy, D. B.; Mishra, A. Renewable Plant-Based Raw Materials for Industry. *Encyclopedia of Inorganic and Bioinorganic Chemistry* **2016**, 1–16. https://doi.org/10.1002/9781119951438.eibc2432.

(28) Kühlborn, J.; Groß, J.; Opatz, T. Making Natural Products from Renewable Feedstocks: Back to the Roots? *Nat Prod Rep* **2020**, *37* (3), 380–424. https://doi.org/10.1039/c9np00040b.

(29) Unnati Garg, Swati Chauhan, Upendra Nagaich, N. J. Current Advances in Chitosan Nanoparticles Based Drug Delivery and Targeting. *Advances Pharmaceutical Bulletin* **2019**, *9* (2), 195–204. https://doi.org/10.15171/apb.2019.023.

(30) Vigani, B.; Valentino, C.; Sandri, G.; Listro, R.; Fagiani, F.; Collina, S.; Lanni, C.; Bonferoni, M. C.; Caramella, C. M.; Rossi, S.; Ferrari, F. A Composite Nanosystem as a Potential Tool for the Local Treatment of Glioblastoma: Chitosan-coated Solid Lipid Nanoparticles Embedded in Electrospun Nanofibers. *Polymers (Basel)* **2021**, *13* (9). https://doi.org/10.3390/polym13091371.

(31) Giordano, R. C.; Ribeiro, M. P. A.; Giordano, R. L. C. Kinetics of β-Lactam Antibiotics Synthesis by Penicillin G Acylase (PGA) from the Viewpoint of the Industrial Enzymatic Reactor Optimization. *Biotechnol Adv* **2006**, *24* (1), 27–41. https://doi.org/10.1016/j.biotechadv.2005.05.003.

(32) Stoler, E.; Warner, J. C. Non-Covalent Derivatives: Cocrystals and Eutectics. *Molecules* **2015**, *20* (8), 14833–14848. https://doi.org/10.3390/molecules200814833.

(33) Sheldon, R. A. Fundamentals of Green Chemistry: Efficiency in Reaction Design. *Chem Soc Rev* **2012**, *41* (4), 1437–1451. https://doi.org/10.1039/c1cs15219j.

(34) Amrutkar, R. D.; Bhalerao, S. S.; Bhoir, A. S.; Bhusare, R. H.; Bodhare, S. S.; Borse, J. N. Role of Catalyst in Organic Synthesis. *Current Trends in Pharmacy and Pharmaceutical Chemistry* **2022**, *4* (3), 115–119. https://doi.org/10.18231/j.ctppc.2022.019.

(35) Boethling, R. S.; Sommer, E.; DiFiore, D. Designing Small Molecules for Biodegradability. *Chem Rev* **2007**, *107* (6), 2207–2227. https://doi.org/10.1021/cr050952t.

(36) Sagmeister, P.; Lebl, R.; Castillo, I.; Rehrl, J.; Kruisz, J.; Sipek, M.; Horn, M.; Sacher, S.; Cantillo, D.; Williams, J. D.; Kappe, C. O. Advanced Real-Time Process Analytics for Multistep Synthesis in Continuous Flow**. *Angewandte Chemie - International Edition* **2021**, *60* (15), 8139–8148. https://doi.org/10.1002/anie.202016007.

(37) Thompson, P. B. Acceptable Risk. *Environ Ethics* **1986**, *8* (3), 277–285. https://doi.org/10.5840/enviroethics1986836.

(38) Duvauchelle, V.; Meffre, P.; Benfodda, Z. Green Methodologies for the Synthesis of 2-Aminothiophene. *Environ Chem Lett* **2023**, *21* (1), 597–621. https://doi.org/10.1007/s10311-022-01482-1.

(39) Kharissova, O. V.; Kharisov, B. I.; González, C. M. O.; Méndez, Y. P.; López, I. *Greener Synthesis of Chemical Compounds and Materials*; 2019; Vol. 6. https://doi.org/10.1098/rsos.191378.

(40) Gharat, N. N.; Rathod, V. K. *Ultrasound-Assisted Organic Synthesis*; Elsevier Inc., 2020. https://doi.org/10.1016/B978-0-12-819540-6.00001-2.

(41) Kappe, C. O. The Use of Microwave Irradiation in Organic Synthesis. From Laboratory Curiosity to Standard Practice in Twenty Years. *ChemInform* **2006**, *37* (44), 308–312. https://doi.org/10.1002/chin.200644239.

(42) Martina, K.; Cravotto, G.; Varma, R. S. Impact of Microwaves on Organic Synthesis and Strategies toward Flow Processes and Scaling Up. *Journal of Organic Chemistry* **2021**, *86* (20), 13857–13872. https://doi.org/10.1021/acs.joc.1c00865.

(43) Albini, A.; Fagnoni, M. Photochemistry as a Green Synthetic Method. **2008**, 279–293. https://doi.org/10.1007/978-1-4020-6793-8_13.

(44) Beeler, A. B. Introduction: Photochemistry in Organic Synthesis. *Chem Rev* **2016**, *116* (17), 9629–9630. https://doi.org/10.1021/acs.chemrev.6b00378.

(45) Frontana-Uribe, B. A.; Little, R. D.; Ibanez, J. G.; Palma, A.; Vasquez-Medrano, R. Organic Electrosynthesis: A Promising Green Methodology in Organic Chemistry. *Green Chemistry* **2010**, *12* (12), 2099–2119. https://doi.org/10.1039/c0gc00382d.

(46) Zhu, C.; Ang, N. W. J.; Meyer, T. H.; Qiu, Y.; Ackermann, L. Organic Electrochemistry: Molecular Syntheses with Potential. *ACS Cent Sci* **2021**, *7* (3), 415–431. https://doi.org/10.1021/acscentsci.0c01532.

(47) Sagmeister, P.; Williams, J. D.; Hone, C. A.; Kappe, C. O. Laboratory of the Future: A Modular Flow Platform with Multiple Integrated PAT Tools for Multistep Reactions. *React Chem Eng* **2019**, *4* (9), 1571–1578. https://doi.org/10.1039/c9re00087a.

(48) Sagmeister, P.; Williams, J. D.; Oliver Kappe, C. The Rocky Road to a Digital Lab. *Chimia (Aarau)* **2023**, *77* (5), 300–306. https://doi.org/10.2533/chimia.2023.300.

(49) Zhao, W.; Chen, F.-E. One-Pot Synthesis and Its Practical Application in Pharmaceutical Industry. *Curr Org Synth* **2013**, *9* (6), 873–897. https://doi.org/10.2174/157017912803901619.

(50) Gothard, C. M.; Soh, S.; Gothard, N. A.; Kowalczyk, B.; Wei, Y.; Baytekin, B.; Grzybowski, B. A. Rewiring Chemistry: Algorithmic Discovery and Experimental Validation of One-Pot Reactions in the Network of Organic Chemistry. *Angewandte Chemie - International Edition* **2012**, *51* (32), 7922–7927. https://doi.org/10.1002/anie.201202155.

(51) Rocha, R. O.; Rodrigues, M. O.; Neto, B. A. D. Review on the Ugi Multicomponent Reaction Mechanism and the Use of Fluorescent Derivatives as Functional Chromophores. *ACS Omega* **2020**, *5* (2), 972–979. https://doi.org/10.1021/acsomega.9b03684.

(52) Neochoritis, C. G.; Zarganes-Tzitzikas, T.; Katsampoxaki-Hodgetts, K.; Dömling, A. Multicomponent Reactions: "Kinderleicht." *J Chem Educ* **2020**, *97* (10), 3739–3745. https://doi.org/10.1021/acs.jchemed.0c00290.

(53) Dömling, A.; Wang, W.; Wang, K. Chemistry and Biology of Multicomponent Reactions. *Chem Rev* **2012**, *112* (6), 3083–3135. https://doi.org/10.1021/cr100233r.

(54) Cioc, R. C.; Ruijter, E.; Orru, R. V. A. Multicomponent Reactions: Advanced Tools for Sustainable Organic Synthesis. *Green Chemistry* **2014**, *16* (6), 2958–2975. https://doi.org/10.1039/c4gc00013g.

(55) Shivam, N.; Tiwari, G.; Kumar, M.; Chauhan, A. N. S.; Erande, R. D. Recent Advances in Cascade Reactions and Their Mechanistic Insights: A Concise Strategy to Synthesize Complex Natural Products and Organic Scaffolds. *Org Biomol Chem* **2022**, 3653–3674. https://doi.org/10.1039/d2ob00452f.

(56) Bradley, D. Chemists Clean Up Synthesis With One-Pot Reactions. *Science (1979)* **1994**, *266* (October), 32–34.

(57) Nicolaou, K. C.; Edmonds, D. J.; Bulger, P. G. Cascade Reactions in Total Synthesis. *Angewandte Chemie - International Edition* **2006**, *45* (43), 7134–7186. https://doi.org/10.1002/anie.200601872.

(58) Hayashi, Y. Pot Economy and One-Pot Synthesis. *Chem Sci* **2016**, *7* (2), 866–880. https://doi.org/10.1039/c5sc02913a.

(59) Mukaiyama, T.; Ishikawa, H.; Koshino, H.; Hayashi, Y. One-Pot Synthesis of (-)-Oseltamivir and Mechanistic Insights into the Organocatalyzed Michael Reaction. *Chemistry - A European Journal* **2013**, *19* (52), 17789–17800. https://doi.org/10.1002/chem.201302371.

(60) Anne Helmenstine. *Electromagnetic Spectrum Definition and Explanation*. https://sciencenotes.org/electromagnetic-spectrum-definition-and-explanation/ (accessed 2023-10-20).

(61) Gedye, R.; Smith, F.; Westaway, K.; Ali, H.; Baldisera, L.; Laberge, L.; Rousell, J. The Use of Microwave Ovens for Rapid Organic Synthesis. *Tetrahedron Lett* **1986**, *27* (3), 279–282. https://doi.org/10.1016/S0040-4039(00)83996-9.

(62) Giguere, R. J.; Bray, T. L.; Duncan, S. M.; Majetich, G. Application of Commercial Microwave Ovens to Organic Synthesis. *Tetrahedron Lett* **1986**, *27* (41), 4945–4948. https://doi.org/10.1016/S0040-4039(00)85103-5.

(63) Seifert, R.; Wieland, T.; Mannhold, E. R. R.; Kubinyi, H.; Folkers, G.; Smith, D.; Walker, D. *Microwaves in Organic and Medicinal Chemistry*; 2005.

(64) Menéndez, J. C. Microwave Assisted Organic Synthesis. *Synthesis (Stuttg)* **2006**, *2006* (01), 186–186. https://doi.org/10.1055/s-2006-925464.

(65) Ferreira, S. E.; Rovisco, A.; Dos Santos, A.; Águas, H.; Igreja, R.; Barquinha, P.; Fortunato, E.; Martins, R. Porous ZnO Nanostructures Synthesized by Microwave Hydrothermal Method for Energy Harvesting Applications. 2021, p Nanopores. https://doi.org/10.5772/intechopen.97060.

(66) Nizamuddin, S.; Baloch, H. A.; Siddiqui, M. T. H.; Mubarak, N. M.; Tunio, M. M.; Bhutto, A. W.; Jatoi, A. S.; Griffin, G. J.; Srinivasan, M. P. An Overview of Microwave Hydrothermal Carbonization and Microwave Pyrolysis of Biomass. *Rev Environ Sci Biotechnol* **2018**, *17* (4), 813–837. https://doi.org/10.1007/s11157-018-9476-z.

(67) Hayes, B. L. *Microwave Synthesis - Chemistry at the Speed of Light*; CEM Publishing, 2002.

(68) Kappe, C. O. Microwave Dielectric Heating in Synthetic Organic Chemistry. *Chem Soc Rev* **2008**, *37* (6), 1127–1139. https://doi.org/10.1039/b803001b.

(69) de la Hoz, A.; Díaz-Ortiz, À.; Moreno, A. Microwaves in Organic Synthesis. Thermal and Non-Thermal Microwave Effects. *Chem Soc Rev* **2005**, *34* (2), 164–178. https://doi.org/10.1039/b411438h.

(70) Damm, M.; Glasnov, T. N.; Kappe, C. O. Translating High-Temperature Microwave Chemistry to Scalable Continuous Flow Processes. *Org Process Res Dev* **2010**, *14* (1), 215–224. https://doi.org/10.1021/op900297e.

(71) Kappe, C. O. The Use of Microwave Irradiation in Organic Synthesis. From Laboratory Curiosity to Standard Practice in Twenty Years. *ChemInform* **2006**, *37* (44), 308–312. https://doi.org/10.1002/chin.200644239.

(72) Kappe, C. O.; Pieber, B.; Dallinger, D. Microwave Effects in Organic Synthesis: Myth or Reality? *Angewandte Chemie - International Edition* **2013**, *52* (4), 1088–1094. https://doi.org/10.1002/anie.201204103.

(73) Kranjc, K.; Kocevar, M. Microwave-Assisted Organic Synthesis: General Considerations and Transformations of Heterocyclic Compounds. *Curr Org Chem* **2010**, *14* (10), 1050–1074. https://doi.org/10.2174/138527210791130488.

(74) Kappe, C. O. My Twenty Years in Microwave Chemistry: From Kitchen Ovens to Microwaves That Aren't Microwaves. *Chemical Record* **2019**, *19* (1), 15–39. https://doi.org/10.1002/tcr.201800045.

(75) Dallinger, D.; Kappe, C. O. Microwave-Assisted Synthesis in Water as Solvent. *Chem Rev* **2007**, *107* (6), 2563–2591. https://doi.org/10.1021/cr0509410.

(76) Xochicale-Santana, L.; Vidyasagar, C. C.; Muñoz-Flores, B. M.; Pérez, V. M. J. *Microwave Assisted Organic Syntheses (MAOS): The Green Synthetic Method*; 2021. https://doi.org/10.1016/B978-0-12-821938-6.00015-3.

(77) Leadbeater, N.; Torenius, H.; Tye, H. Microwave-Promoted Organic Synthesis Using Ionic Liquids: A Mini Review. *Comb Chem High Throughput Screen* **2012**, *7* (5), 511–528. https://doi.org/10.2174/1386207043328562.

(78) Sauvagnat, B.; Lamaty, F.; Lazaro, R.; Martinez, J. Poly(Ethylene Glycol) as Solvent and Polymer Support in the Microwave Assisted Parallel Synthesis of Aminoacid Derivatives. *Tetrahedron Lett* **2000**, *41* (33), 6371–6375. https://doi.org/10.1016/S0040-4039(00)01067-4.

(79) Loupy, A. Solvent-Free Microwave Organic Synthesis as an Efficient Procedure for Green Chemistry. *Comptes Rendus Chimie* **2004**, *7* (2), 103–112. https://doi.org/10.1016/j.crci.2003.10.015.

(80) Kappe, C. O. Controlled Microwave Heating in Modern Organic Synthesis. *Angewandte Chemie - International Edition* **2004**, *43* (46), 6250–6284. https://doi.org/10.1002/anie.200400655.

(81) Sharma, N.; Sharma, U. K.; Van der Eycken, E. V. Microwave-Assisted Organic Synthesis: Overview of Recent Applications. *Green Techniques for Organic Synthesis and Medicinal Chemistry* **2018**, 441–468. https://doi.org/10.1002/9781119288152.ch17.

(82) Larhed, M.; Moberg, C.; Hallberg, A. Microwave-Accelerated Homogeneous Catalysis in Organic Chemistry. *Acc Chem Res* **2002**, *35* (9), 717–727. https://doi.org/10.1021/ar010074v.

(83) Zhang, Y.; Lv, Z.; Zhong, H.; Zhang, M.; Zhang, T.; Zhang, W.; Li, K. Efficient Heck Cross-Coupling of 3-Iodo-Benzopyrones with Olefins under Microwave Irradiation without Phosphine. *Tetrahedron* **2012**, *68* (47), 9777–9787. https://doi.org/10.1016/j.tet.2012.09.017.

(84) Martínez, A. V.; Invernizzi, F.; Leal-Duaso, A.; Mayoral, J. A.; García, J. I. Microwave-Promoted Solventless Mizoroki-Heck Reactions Catalysed by Pd Nanoparticles Supported on Laponite Clay. *RSC Adv* **2015**, *5* (14), 10102–10109. https://doi.org/10.1039/c4ra15418e.

(85) Larhed, M.; Lindeberg, G.; Hallberg, A. Rapid Microwave-Assisted Suzuki Coupling on Solid-Phase. *Tetrahedron Lett* **1996**, *37* (45), 8219–8222. https://doi.org/10.1016/0040-4039(96)01872-2.

(86) Lei, Y.; Hu, T.; Wu, X.; Wu, Y.; Xiang, H.; Sun, H.; You, Q.; Zhang, X. Microwave-Assisted Copper- and Palladium-Catalyzed Sonogashira-Type Coupling of Aryl Bromides and Iodides with Trimethylsilylacetylene. *Tetrahedron Lett* **2016**, *57* (10), 1100–1103. https://doi.org/10.1016/j.tetlet.2016.01.088.

(87) Leadbeater, N. E.; Marco, M.; Tominack, B. J. First Examples of Transition-Metal Free Sonogashira-Type Couplings. *Org Lett* **2003**, *5* (21), 3919–3922. https://doi.org/10.1021/ol035485l.

(88) He, H.; Wu, Y. J. Copper-Catalyzed Cross-Coupling of Aryl Iodides and Aryl Acetylenes Using Microwave Heating. *Tetrahedron Lett* **2004**, *45* (16), 3237–3239. https://doi.org/10.1016/j.tetlet.2004.02.124.

(89) Pellón, R. F.; Martín, A.; Docampo, M. L.; Mesa, M. Microwave-Promoted Ullmann Condensation of 2-Aminopyridines with 2-Chlorobenzoic Acids. *Synth Commun* **2006**, *36* (12), 1715–1719. https://doi.org/10.1080/00397910600616727.

(90) Wan, Y.; Alterman, M.; Hallberg, A. Palladium-Catalyzed Amination of Aryl Bromides Using Temperature-Controlled Microwave Heating. *Synthesis (Stuttg)* **2002**, No. 11, 1597–1600. https://doi.org/10.1055/s-2002-33342.

(91) Mayo, K. G.; Nearhoof, E. H.; Kiddle, J. J. Ruthenium-Catalyzed Olefin Metathesis. **2002**.

(92) Bakhrou, N.; Lamaty, F.; Martinez, J.; Colacino, E. Ring-Closing Metathesis in Glycerol under Microwave Activation. *Tetrahedron Lett* **2010**, *51* (30), 3935–3937. https://doi.org/10.1016/j.tetlet.2010.05.101.

(93) de la Hoz, A.; Diaz-Ortis, A.; Moreno, A.; Fernando Langa. Cycloadditions under Microwave Irradiation Conditions : Methods and Applications. *European J Org Chem* **2000**, 3659–3673. https://doi.org/https://doi.org/10.1002/1099-0690(200011)2000:22<3659::AID-EJOC3659>3.0.CO;2-0.

(94) Stadler, A.; Pichler, S.; Horeis, G.; Kappe, C. O. Microwave-Enhanced Reactions under Open and Closed Vessel Conditions. A Case Study. *Tetrahedron* **2002**, *58* (16), 3177–3183. https://doi.org/10.1016/S0040-4020(02)00270-3.

(95) Hügel, H. M. Microwave Multicomponent Synthesis. *Molecules* **2009**, *14* (12), 4936–4972. https://doi.org/10.3390/molecules14124936.

(96) Santra, S.; Andreana, P. R. A One-Pot, Microwave-Influenced Synthesis of Diverse Small Molecules by Multicomponent Reaction Cascades. *Org Lett* **2007**, *9* (24), 5035–5038. https://doi.org/10.1021/ol702256t.

(97) Kappe, C. O.; Dallinger, D. Controlled Microwave Heating in Modern Organic Synthesis: Highlights from the 2004-2008 Literature. *Mol Divers* **2009**, *13* (2), 71–193. https://doi.org/10.1007/s11030-009-9138-8.

(98) Hayes, B.; Hayes, B. L. Recent Advances in Microwave- Assisted Synthesis. *Aldrichimica Acta* **2015**, *37 (2)* (January 2004), 66–76.

(99) Gronnow, M. J.; White, R. J.; Clark, J. H.; Macquarrie, D. J. Energy Efficiency in Chemical Reactions: A Comparative Study of Different Reaction Techniques. *Org Process Res Dev* **2005**, *9* (4), 516–518. https://doi.org/10.1021/op0498060.

(100) Bose, Ajay K.; Banik, Bimal K.; Lavlinskaia, Nina ; Jayaraman, Muthuswamy; Manhas, M. S. MORE Chemistry in a Microwave. *Chem. Tech.* **1997**, *26* (9), 18–23.

(101) Morschhäuser, R.; Krull, M.; Kayser, C.; Boberski, C.; Bierbaum, R.; Püschner, P. A.; Glasnov, T. N.; Kappe, C. O. Microwave-Assisted Continuous Flow Synthesis on Industrial Scale. *Green Processing and Synthesis* **2012**, *1* (3), 281–290. https://doi.org/10.1515/gps-2012-0032.

(102) Gawande, M. B.; Shelke, S. N.; Zboril, R.; Varma, R. S. Microwave-Assisted Chemistry: Synthetic Applications for Rapid Assembly of Nanomaterials and Organics. *Acc Chem Res* **2014**, *47* (4), 1338–1348. https://doi.org/10.1021/ar400309b.

(103) McQuade, D. T.; Seeberger, P. H. Applying Flow Chemistry: Methods, Materials, and Multistep Synthesis. *Journal of Organic Chemistry* **2013**, *78* (13), 6384–6389. https://doi.org/10.1021/jo400583m.

(104) Bruno, J. *Manufacturing in the 21st Century: Continuous Flow Chemistry has Arrived*. https://www.americanpharmaceuticalreview.com/Featured-Articles/169309-Manufacturing-in-the-21st-Century-Continuous-Flow-Chemistry-has-Arrived/ (accessed 2023-11-15).

(105) Hartman, R. L.; McMullen, J. P.; Jensen, K. F. Deciding Whether to Go with the Flow: Evaluating the Merits of Flow Reactors for Synthesis. *Angewandte Chemie - International Edition* **2011**, *50* (33), 7502–7519. https://doi.org/10.1002/anie.201004637.

(106) May, S. A. Flow Chemistry, Continuous Processing, and Continuous Manufacturing: A Pharmaceutical Perspective. *J Flow Chem* **2017**, *7* (3–4), 137–145. https://doi.org/10.1556/1846.2017.00029.

(107) Plutschack, M. B.; Pieber, B.; Gilmore, K.; Seeberger, P. H. The Hitchhiker's Guide to Flow Chemistry Â¥. *Chem Rev* **2017**, *117* (18), 11796–11893. https://doi.org/10.1021/acs.chemrev.7b00183.

(108) Darvas, F.; Dormán, G.; Hessel, V. *Flow Chemistry - Volume 1: Fundamentals*; Darvas, F., Dormán, G., Hessel, V., Eds.; De Gruyter, 2017. https://doi.org/10.1002/9781119403647.pubnote.

(109) Capaldo, L.; Wen, Z.; Noël, T. A Field Guide to Flow Chemistry for Synthetic Organic Chemists. *Chem Sci* **2023**, 4230–4247. https://doi.org/10.1039/d3sc00992k.

(110) Noël, T.; Su, Y.; Hessel, V. Beyond Organometallic Flow Chemistry: The Principles behind the Use of Continuous-Flow Reactors for Synthesis. *Top Organomet Chem* **2016**, *57* (2015), 1–41. https://doi.org/10.1007/3418_2015_152.

(111) Razzaq, T.; Glasnov, T. N.; Kappe, C. O. Continuous-Flow Microreactor Chemistry under High-Temperature/Pressure. *European J Org Chem* **2009**, No. 9, 1321–1325. https://doi.org/10.1002/ejoc.200900077.

(112) Malet-Sanz, L.; Susanne, F. Continuous Flow Synthesis. a Pharma Perspective. *J Med Chem* **2012**, *55* (9), 4062–4098. https://doi.org/10.1021/jm2006029.

(113) Movsisyan, M.; Delbeke, E. I. P.; Berton, J. K. E. T.; Battilocchio, C.; Ley, S. V.; Stevens, C. V. Taming Hazardous Chemistry by Continuous Flow Technology. *Chem Soc Rev* **2016**, *45* (18), 4892–4928. https://doi.org/10.1039/c5cs00902b.

(114) Harding, M. J.; Brady, S.; O'Connor, H.; Lopez-Rodriguez, R.; Edwards, M. D.; Tracy, S.; Dowling, D.; Gibson, G.; Girard, K. P.; Ferguson, S. 3D Printing of PEEK Reactors for Flow Chemistry and Continuous Chemical Processing. *React Chem Eng* **2020**, *5* (4), 728–735. https://doi.org/10.1039/c9re00408d.

(115) Prabhu, G. R. D.; Urban, P. L. Elevating Chemistry Research with a Modern Electronics Toolkit. *Chem Rev* **2020**, *120* (17), 9482–9553. https://doi.org/10.1021/acs.chemrev.0c00206.

(116) Akwi, F. M.; Watts, P. Continuous Flow Chemistry: Where Are We Now? Recent Applications, Challenges and Limitations. *Chemical Communications* **2018**, *54* (99), 13894–13928. https://doi.org/10.1039/c8cc07427e.

(117) Hartman, R. L. Managing Solids in Microreactors for the Upstream Continuous Processing of Fine Chemicals. *Org Process Res Dev* **2012**, *16* (5), 870–887. https://doi.org/10.1021/op200348t.

(118) Bassetti, B.; Hone, C. A.; Kappe, C. O. Continuous-Flow Synthesis of Δ9-Tetrahydrocannabinol and Δ8-Tetrahydrocannabinol from Cannabidiol. *Journal of Organic Chemistry* **2023**, *88* (9), 6227–6231. https://doi.org/10.1021/acs.joc.3c00300.

(119) Ganley, J. Principles of Flow Chemistry. **2018**.

(120) Ley, S. V.; Fitzpatrick, D. E.; Myers, R. M.; Battilocchio, C.; Ingham, R. J. Machine-Assisted Organic Synthesis. *Angewandte Chemie - International Edition* **2015**, *54* (35), 10122–10136. https://doi.org/10.1002/anie.201501618.

(121) Weeranoppanant, N.; Adamo, A. In-Line Purification: A Key Component to Facilitate Drug Synthesis and Process Development in Medicinal Chemistry. *ACS Med Chem Lett* **2020**, *11* (1), 9–15. https://doi.org/10.1021/acsmedchemlett.9b00491.

(122) Orehek, J.; Teslić, D.; Likozar, B. Continuous Crystallization Processes in Pharmaceutical Manufacturing: A Review. *Org Process Res Dev* **2021**, *25* (1), 16–42. https://doi.org/10.1021/acs.oprd.0c00398.

(123) Horváth, Z.; Horosanskaia, E.; Lee, J. W.; Lorenz, H.; Gilmore, K.; Seeberger, P. H.; Seidel-Morgenstern, A. Recovery of Artemisinin from a Complex Reaction Mixture Using Continuous Chromatography and Crystallization. *Org Process Res Dev* **2015**, *19* (6), 624–634. https://doi.org/10.1021/acs.oprd.5b00048.

(124) Pastre, J. C.; Browne, D. L.; Ley, S. V. Flow Chemistry Syntheses of Natural Products. *Chem Soc Rev* **2013**, *42* (23), 8849–8869. https://doi.org/10.1039/c3cs60246j.

(125) Baumann, M.; Baxendale, I. R. The Synthesis of Active Pharmaceutical Ingredients (APIs) Using Continuous Flow Chemistry. *Beilstein Journal of Organic Chemistry* **2015**, *11*, 1194–1219. https://doi.org/10.3762/bjoc.11.134.

(126) Bogdan, A. R.; Dombrowski, A. W. Emerging Trends in Flow Chemistry and Applications to the Pharmaceutical Industry. *J Med Chem* **2019**, *62* (14), 6422–6468. https://doi.org/10.1021/acs.jmedchem.8b01760.

(127) Burange, A. S.; Osman, S. M.; Luque, R. Understanding Flow Chemistry for the Production of Active Pharmaceutical Ingredients. *iScience* **2022**, *25* (3), 103892. https://doi.org/10.1016/j.isci.2022.103892.

(128) Wegner, J.; Ceylan, S.; Kirschning, A. Ten Key Issues in Modern Flow Chemistry. *Chemical Communications* **2011**, *47* (16), 4583–4592. https://doi.org/10.1039/c0cc05060a.

(129) Petersen, T. P.; Ritzén, A.; Ulven, T. A Multistep Continuous-Flow System for Rapid on-Demand Synthesis of Receptor Ligands. *Org Lett* **2009**, *11* (22), 5134–5137. https://doi.org/10.1021/ol902101c.

(130) Correia, C. A.; Gilmore, K.; McQuade, D. T.; Seeberger, P. H. A Concise Flow Synthesis of Efavirenz. *Angewandte Chemie - International Edition* **2015**, *54* (16), 4945–4948. https://doi.org/10.1002/anie.201411728.

(131) Britton, J.; Raston, C. L. Multi-Step Continuous-Flow Synthesis. *Chem Soc Rev* **2017**, *46* (5), 1250–1271. https://doi.org/10.1039/c6cs00830e.

(132) Webb, D.; Jamison, T. F. Continuous Flow Multi-Step Organic Synthesis. *Chem Sci* **2010**, *1* (6), 675–680. https://doi.org/10.1039/c0sc00381f.

(133) Ogasawara, S.; Hayashi, Y. Multistep Continuous-Flow Synthesis of (-)-Oseltamivir. *Synthesis (Germany)* **2017**, *49* (2), 424–428. https://doi.org/10.1055/s-2016-0036-1588899.

(134) Sagandira, C. R.; Mathe, F. M.; Guyo, U.; Watts, P. The Evolution of Tamiflu Synthesis, 20 Years on: Advent of Enabling Technologies the Last Piece of the Puzzle? *Tetrahedron* **2020**, *76* (January).

(135) Snead, D. R.; Jamison, T. F. A Three-Minute Synthesis and Purification of Ibuprofen: Pushing the Limits of Continuous-Flow Processing. *Angewandte Chemie - International Edition* **2015**, *54* (3), 983–987. https://doi.org/10.1002/anie.201409093.

(136) Sagmeister, P.; Ort, F. F.; Jusner, C. E.; Hebrault, D.; Tampone, T.; Buono, F. G.; Williams, J. D.; Kappe, C. O. Autonomous Multi-Step and Multi-Objective Optimization Facilitated by Real-Time Process Analytics. *Advanced Science* **2022**, *9* (10), 1–9. https://doi.org/10.1002/advs.202105547.

(137) Sagmeister, P.; Williams, J. D.; Hone, C. A.; Kappe, C. O. Laboratory of the Future: A Modular Flow Platform with Multiple Integrated PAT Tools for Multistep Reactions. *React Chem Eng* **2019**, *4* (9), 1571–1578. https://doi.org/10.1039/c9re00087a.

(138) Gioiello, A.; Piccinno, A.; Lozza, A. M.; Cerra, B. The Medicinal Chemistry in the Era of Machines and Automation: Recent Advances in Continuous Flow Technology. *J Med Chem* **2020**, *63* (13), 6624–6647. https://doi.org/10.1021/acs.jmedchem.9b01956.

(139) Grillo, G.; Cintas, P.; Colia, M.; Calcio Gaudino, E.; Cravotto, G. Process Intensification in Continuous Flow Organic Synthesis with Enabling and Hybrid Technologies. *Frontiers in Chemical Engineering* **2022**, *4* (September), 1–23. https://doi.org/10.3389/fceng.2022.966451.

(140) Cerra, B.; Carotti, A.; Passeri, D.; Sardella, R.; Moroni, G.; Di Michele, A.; MacChiarulo, A.; Pellicciari, R.; Gioiello, A. Exploiting Chemical Toolboxes for the Expedited Generation of Tetracyclic Quinolines as a Novel Class of PXR Agonists. *ACS Med Chem Lett* **2019**, *10* (4), 677–681. https://doi.org/10.1021/acsmedchemlett.8b00459.

(141) Hartman, R. L. Flow Chemistry Remains an Opportunity for Chemists and Chemical Engineers. *Curr Opin Chem Eng* **2020**, *29*, 42–50. https://doi.org/10.1016/j.coche.2020.05.002.

(142) Kannan, N.; Vakeesan, D. Solar Energy for Future World: - A Review. *Renewable and Sustainable Energy Reviews* **2016**, *62*, 1092–1105. https://doi.org/10.1016/j.rser.2016.05.022.

(143) Long, Z.; Li, Q.; Wei, T.; Zhang, G.; Ren, Z. Historical Development and Prospects of Photocatalysts for Pollutant Removal in Water. *J Hazard Mater* **2020**, *395* (January), 122599. https://doi.org/10.1016/j.jhazmat.2020.122599.

(144) Talaiekhozani, A.; Rezania, S.; Kim, K. H.; Sanaye, R.; Amani, A. M. Recent Advances in Photocatalytic Removal of Organic and Inorganic Pollutants in Air. *J Clean Prod* **2021**, *278*, 123895. https://doi.org/10.1016/j.jclepro.2020.123895.

(145) Wieder, M. E.; Hone, D. C.; Cook, M. J.; Handsley, M. M.; Gavrilovic, J.; Russell, D. A. Intracellular Photodynamic Therapy with Photosensitizer-Nanoparticle Conjugates: Cancer Therapy Using a 'Trojan Horse.' *Photochemical and Photobiological Sciences* **2006**, *5* (8), 727–734. https://doi.org/10.1039/b602830f.

(146) Chatani, S.; Kloxin, C. J.; Bowman, C. N. The Power of Light in Polymer Science: Photochemical Processes to Manipulate Polymer Formation, Structure, and Properties. *Polym Chem* **2014**, *5* (7), 2187–2201. https://doi.org/10.1039/c3py01334k.

(147) Roth, H. D. The Beginnings of Organic Photochemistry. *Angewandte Chemie International Edition in English* **1989**, *28* (9), 1193–1207. https://doi.org/10.1002/anie.198911931.

(148) *History of the department*. https://chemistry.unibo.it/en/department/presentation/history-of-the-department (accessed 2023-11-29).

(149) Ciamician, G. THE PHOTOCHEMISTRY OF TITE FUTURE. *Science (1979)* **1912**, *XXXVI*, 926.

(150) Albini, A.; Fagnoni, M. 1908: Giacomo Ciamician and the Concept of Green Chemistry. *ChemSusChem* **2008**, *1* (1–2), 63–66. https://doi.org/10.1002/cssc.200700015.

(151) Albini, A.; Fagnoni, M. Green Chemistry and Photochemistry Were Born at the Same Time. *Green Chemistry* **2004**, *6* (1), 1–6.

(152) McKendrick, K. G. *Principles and Applications of Photochemistry*; 1989; Vol. 36. https://doi.org/10.1080/09500348914551321.

(153) Schweizer, T.; Kubach, H.; Koch, T. Investigations to Characterize the Interactions of Light Radiation, Engine Operating Media and Fluorescence Tracers for the Use of Qualitative Light-Induced Fluorescence in Engine Systems. *Automotive and Engine Technology* **2021**, *6* (3–4), 275–287. https://doi.org/10.1007/s41104-021-00092-3.

(154) Albini, A.; Germani, L.; Albini, A.; Fagnoni, M. *Handbook of Synthetic Photochemistry*; WILEY, Ed.; 2010.

(155) Buglioni, L.; Raymenants, F.; Slattery, A.; Zondag, S. D. A.; Noël, T. Technological Innovations in Photochemistry for Organic Synthesis: Flow Chemistry, High-Throughput Experimentation, Scale-up, and Photoelectrochemistry. *Chem Rev* **2022**, *122* (2), 2752–2906. https://doi.org/10.1021/acs.chemrev.1c00332.

(156) Klán, P.; Wirz, J. *Photochemistry of Organic Compunds: From Concepts to Practice*; 2009.

(157) Venkatraman, R. K.; Orr-Ewing, A. J. Solvent Effects on Ultrafast Photochemical Pathways. *Acc Chem Res* **2021**, *54* (23), 4383–4394. https://doi.org/10.1021/acs.accounts.1c00549.

(158) Buglioni, L.; Raymenants, F.; Slattery, A.; Zondag, S. D. A.; Noël, T. Technological Innovations in Photochemistry for Organic Synthesis: Flow Chemistry, High-Throughput Experimentation, Scale-up, and Photoelectrochemistry. *Chem Rev* **2022**, *122* (2), 2752–2906. https://doi.org/10.1021/acs.chemrev.1c00332.

(159) By, C.; Buchi, G.; Goldman, I. M. The Intramolecular Cyclization of Carvone to Carvonecamphor. *Cyclization of Carvone to Carvonecamphor* **1957**, *79*, 4741–4748.

(160) Görner, H.; Kuhn, H. J. *Cis-Trans Photoisomerization of Stilbenes and Stilbene-Like Molecules*; 1994; Vol. 19. https://doi.org/10.1002/9780470133507.ch1.

(161) Crisenza, G. E. M.; Mazzarella, D.; Melchiorre, P. Synthetic Methods Driven by the Photoactivity of Electron Donor-Acceptor Complexes. *J Am Chem Soc* **2020**, *142* (12), 5461–5476. https://doi.org/10.1021/jacs.0c01416.

(162) Michelin, C.; Hoffmann, N. Photosensitization and Photocatalysis - Perspectives in Organic Synthesis. *ACS Catal* **2018**, *8* (12), 12046–12055. https://doi.org/10.1021/acscatal.8b03050.

(163) Shaw, M. H.; Twilton, J.; MacMillan, D. W. C. Photoredox Catalysis in Organic Chemistry. *Journal of Organic Chemistry* **2016**, *81* (16), 6898–6926. https://doi.org/10.1021/acs.joc.6b01449.

(164) Nicewicz, D. A.; Nguyen, T. M. Recent Applications of Organic Dyes as Photoredox Catalysts in Organic Synthesis. *ACS Catal* **2014**, *4* (1), 355–360. https://doi.org/10.1021/cs400956a.

(165) Yoon, T. P.; Ischay, M. A.; Du, J. Visible Light Photocatalysis as a Greener Approach to Photochemical Synthesis. *Nat Chem* **2010**, *2* (7), 527–532. https://doi.org/10.1038/nchem.687.

(166) Marzo, L.; Pagire, S. K.; Reiser, O.; König, B. Visible-Light Photocatalysis: Does It Make a Difference in Organic Synthesis? *Angewandte Chemie - International Edition* **2018**, *57* (32), 10034–10072. https://doi.org/10.1002/anie.201709766.

(167) Capaldo, L.; Ravelli, D. Hydrogen Atom Transfer (HAT): A Versatile Strategy for Substrate Activation in Photocatalyzed Organic Synthesis. *European J Org Chem* **2017**, *2017* (15), 2056–2071. https://doi.org/10.1002/ejoc.201601485.

(168) Fagnoni, M.; Dondi, D.; Ravelli, D.; Albini, A. Photocatalysis for the Formation of the C-C Bond. *Chem Rev* **2007**, *107* (6), 2725–2756. https://doi.org/10.1021/cr068352x.

(169) Nacsa, E. D.; Macmillan, D. W. C. Carbon–Carbon Bond Formation by Metallaphotoredox Catalysis. *Organic Reactions* **2019**, *100*, 471–545. https://doi.org/10.1002/0471264180.or100.08.

(170) Singh, S.; Roy, V. J.; Dagar, N.; Sen, P. P.; Roy, S. R. Photocatalysis in Dual Catalysis Systems for Carbon-Nitrogen Bond Formation. *Adv Synth Catal* **2021**, *363* (4), 937–979. https://doi.org/10.1002/adsc.202001176.

(171) Kohls, P.; Jadhav, D.; Pandey, G.; Reiser, O. Visible Light Photoredox Catalysis: Generation and Addition of N -Aryltetrahydroisoquinoline-Derived α-Amino Radicals to Michael Acceptors. *Org Lett* **2012**, *14* (3), 672–675. https://doi.org/10.1021/ol202857t.

(172) Primer, D. N.; Karakaya, I.; Tellis, J. C.; Molander, G. A. Single-Electron Transmetalation: An Enabling Technology for Secondary Alkylboron Cross-Coupling. *J Am Chem Soc* **2015**, *137* (6), 2195–2198. https://doi.org/10.1021/ja512946e.

(173) Liu, Z.; Zhong, S.; Ji, X.; Deng, G. J.; Huang, H. Photoredox Cyclization of N-Arylacrylamides for Synthesis of Dihydroquinolinones. *Org Lett* **2022**, *24* (1), 349–353. https://doi.org/10.1021/acs.orglett.1c04015.

(174) Photochemistry of Reactive Intermediates. **2007**, *1*, 2–6.

(175) Bonfield, H. E.; Mercer, K.; Diaz-Rodriguez, A.; Cook, G. C.; McKay, B. S. J.; Slade, P.; Taylor, G. M.; Ooi, W. X.; Williams, J. D.; Roberts, J. P. M.; Murphy, J. A.; Schmermund, L.; Kroutil, W.; Mielke, T.; Cartwright, J.; Grogan, G.; Edwards, L. J. The Right Light: De Novo Design of a Robust Modular Photochemical Reactor for Optimum Batch and Flow Chemistry. *ChemPhotoChem* **2020**, *4* (1), 45–51. https://doi.org/10.1002/cptc.201900203.

(176) Zhang, M.; Roth, P. Flow Photochemistry — from Microreactors to Large-Scale Processing. *Curr Opin Chem Eng* **2023**, *39*, 100897. https://doi.org/10.1016/j.coche.2023.100897.

(177) Bonfield, H. E.; Knauber, T.; Lévesque, F.; Moschetta, E. G.; Susanne, F.; Edwards, L. J. Photons as a 21st Century Reagent. *Nat Commun* **2020**, *11* (1), 2–5. https://doi.org/10.1038/s41467-019-13988-4.

(178) Rehm, T. H. Flow Photochemistry as a Tool in Organic Synthesis. *Chemistry - A European Journal* **2020**, *26* (71), 16952–16974. https://doi.org/10.1002/chem.202000381.

(179) Cambié, D.; Bottecchia, C.; Straathof, N. J. W.; Hessel, V.; Noël, T. Applications of Continuous-Flow Photochemistry in Organic Synthesis, Material Science, and Water Treatment. *Chem Rev* **2016**, *116* (17), 10276–10341. https://doi.org/10.1021/acs.chemrev.5b00707.

(180) Gisbertz, S.; Pieber, B. Heterogeneous Photocatalysis in Organic Synthesis. *ChemPhotoChem* **2020**, *4* (7), 454. https://doi.org/10.1002/cptc.202000137.

(181) Williams, J. D.; Kappe, C. O. Recent Advances toward Sustainable Flow Photochemistry. *Curr Opin Green Sustain Chem* **2020**, *25*, 100351. https://doi.org/10.1016/j.cogsc.2020.05.001.

(182) Molnár, M.; Kappe, C. O.; Ötvös, S. B. Merger of Visible Light-Driven Chiral Organocatalysis and Continuous Flow Chemistry: An Accelerated and Scalable Access into

Enantioselective α-Alkylation of Aldehydes. *Adv Synth Catal* **2023**, *365* (10), 1660–1670. https://doi.org/10.1002/adsc.202300289.

(183) Ma, X.; Zhang, W. Recent Developments in One-Pot Stepwise Synthesis (OPSS) of Small Molecules. *iScience* **2022**, *25* (9), 105005. https://doi.org/10.1016/j.isci.2022.105005.

(184) Audubert, C.; Gamboa Marin, O. J.; Lebel, H. Batch and Continuous-Flow One-Pot Processes Using Amine Diazotization to Produce Silylated Diazo Reagents. *Angewandte Chemie - International Edition* **2017**, *56* (22), 6294–6297. https://doi.org/10.1002/anie.201612235.

(185) Horikoshi, S.; Serpone, N. *RF Power Semiconductor Generator Application in Heating and Energy Utilization*; 2020. https://doi.org/10.1007/978-981-15-3548-2.

(186) Glasnov, T. N.; Kappe, C. O. Microwave-Assisted Synthesis under Continuous-Flow Conditions. *Macromol Rapid Commun* **2007**, *28* (4), 395–410. https://doi.org/10.1002/marc.200600665.

(187) Musio, B.; Mariani, F.; Śliwiński, E. P.; Kabeshov, M. A.; Odajima, H.; Ley, S. V. Combination of Enabling Technologies to Improve and Describe the Stereoselectivity of Wolff-Staudinger Cascade Reaction. *Synthesis (Germany)* **2016**, *48* (20), 3515–3526. https://doi.org/10.1055/s-0035-1562579.

(188) Colella, M.; Carlucci, C.; Luisi, R. *Supported Catalysts for Continuous Flow Synthesis*; Springer International Publishing, 2018; Vol. 376. https://doi.org/10.1007/s41061-018-0225-0.

(189) Adebar, N.; Gröger, H. Heterogeneous Catalysts "on the Move": Flow Chemistry with Fluid Immobilised (Bio)Catalysts. *European J Org Chem* **2020**, *2020* (38), 6062–6067. https://doi.org/10.1002/ejoc.202000705.

(190) Tsubogo, T.; Oyamada, H.; Kobayashi, S. Multistep Continuous-Flow Synthesis of (R)- and (S)-Rolipram Using Heterogeneous Catalysts. *Nature* **2015**, *520* (7547), 329–332. https://doi.org/10.1038/nature14343.

2 Nitroolefins as key building blocks in organic synthesis

2.1 Nitro compounds

Research in the chemistry of nitro compounds has a long history, dating back to the early 19th century, and proceeding with the elucidation of different properties of the functional group.
Nitro compounds, aliphatic or aromatic, play a significant role in synthesis, as they are crucial and versatile building blocks and synthetic intermediates for the preparation of active scaffolds that finds application in pharmaceuticals, agricultural chemicals, polymers, dyes, and explosives. Every year, millions of tons of nitro compounds are synthesized and consumed worldwide.
Their unique reactivity, electron-withdrawing nature, and ability to undergo various transformations make them valuable tools for the construction of complex organic molecules, including natural products.[1]
N-containing heterocycles are regarded as privileged structures due to their prevalence in biologically active compounds and their ability to interact with biological targets. In fact, this synthetic chameleon, as the nitro group is often referred to, can be converted into other useful functionalities, such as carbonyl, formyl, acyl, cyano, and amino groups, or it can be removed selectively.[2]
Overall, the extreme electron-withdrawing power of the nitro functionality makes it effective at acidifying geminal protons, enabling their selective deprotonation using mild bases as catalyst. The resulting anions behave as stabilized, soft carbanions, exhibiting reactivity that can be harnessed in various transformations, including the Henry reaction and Michael additions.[3]
Among nitro compounds, nitroarenes surely had a major role in chemistry development, as precursor of aromatic amines, but the interest towards aliphatic nitro compounds has progressively grown over the years.
Nowadays, the attention is focused on the development of new selective and safe synthetic methods for their preparation, the control of their reactivity and stereochemistry, with an eye on the use of more compatible solvents and reduction of waste production, in line with the Twelve Principle of Green Chemistry.

2.1.1 Aliphatic nitro compounds: important syntheses and reactivity

Aliphatic nitro compounds represent a valuable and versatile class in organic synthesis. For this reason, a number of approaches have been developed to access their synthesis.

Nitroalkanes
Generally, nitroalkanes can be synthesized upon direct nitration of aliphatic hydrocarbons, activated hydrocarbons via anionic intermediates, alkenes and ketones; nitration of alkyl halides or alcohol derivatives (mesylates or tosylates) using metal nitrites; and conversion from other functionalities, such as carbonyls, amines, oximes, azides, etc.

The introduction of nitro group via direct nitration is a widely used and powerful transformation for aromatic compounds, whereas saturated non-activated aliphatic hydrocarbons are usually inert

towards conventional nitrating agents under ambient conditions. For this reason, the nitration of alkanes is typically carried out using harsh methodologies that involve the use of excess nitrogen dioxide or nitric acid at elevated temperatures ranging from 250 to 450 °C. These conditions are required to induce thermal alkane C-H bond scission, generating alkyl radicals. However, this process often leads to undesired cleavage of the alkane's carbon-carbon (C-C) skeleton, resulting in poor selectivity for the desired nitroalkane products and formation of byproducts. In the last two decades, several groups focused on the development of new processes, such as the use of nitrogen dioxide or nitric acid and N-hydroxyphthalimide (NHPI) as catalyst in the presence of O_2 under mild conditions proposed by Ishi et al,[4,5] and a vanadium-substituted Keggin-type phosphomolybdates-catalized method developed by Yamaguchi et al. for the nitration of alkanes and alkylbenzenes using nitric acid in acetic acid.[6] More recently, Peng et al.[7] presented a selective C-H nitration using nontoxic and inexpensive metal nitrate [$Fe(NO_3)_3 \cdot 9H_2O$], serving as both precursor catalyst and nitro source, even though more studies need to be done to increase the product's yield and to expand the substrate scope.

One of the most important methods for the preparation of aliphatic nitro compounds is the nitration of alkyl halides with metal nitrites. To this scope, silver, potassium or sodium nitrites are frequently used in Victor-Meyer reaction ($AgNO_2$)[8] and Kornblum reaction (KNO_2, $NaNO_2$, **Scheme 2.1**),[9,10] respectively.

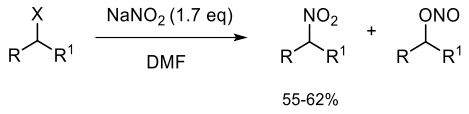

Scheme 2.1 Kornblum nitroalkanes preparation from alkyl halides and sodium nitrite

Kornblum's work allowed the synthesis of a variety of primary and secondary nitroalkanes, obtained in good yield at room temperature. Alkylnitrites were identified as the most abundant by-products, but the use of DMF as solvent was able to enhance sodium nitrite solubility and to minimize further possible side reactions.

Advancement toward more efficient and sustainable processes were made over the years, and in 2004 Ballini *et al.*[11,12] presented a variation of the Victor-Meyer reaction for the conversion of aliphatic and benzylic halides into the correspond nitro compounds in aqueous medium in short reaction times and under mild conditions, thus allowing the preservation of other functionalities (**Scheme 2.2, Example a**).

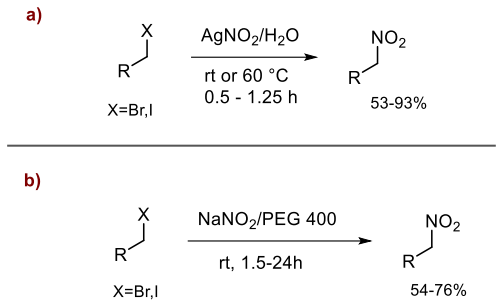

Scheme 2.2 Sustainable methods for the preparation of nitroalkanes

Important improvements were documented few years later by the same group,[13] with the chemoselective synthesis of primary nitroalkanes in good yield, using sodium nitrite in polyethylene glycol (PEG 400)[14] as green solvent at room temperature (**Scheme 2.2, Example b**).

Other interesting methods include the nucleophilic displacement of tosylates and mesylates, thus expanding the chemical space for nitroalkane synthesis to readily available alcohols. Products can be obtained in two steps, with the conversion from tosylated (or mesylated) intermediate proceeding with commercially available tetrabutyl ammonium nitrite (Bu_4NNO_2) in toluene at room temperature, in less than 3 hours (**Scheme 2.3**).[15]

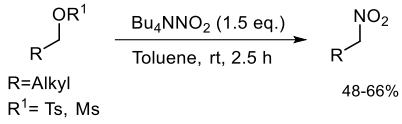

Scheme 2.3 Direct conversion of tosylates/mesylates into nitroalkanes

Valuable alternatives for the synthesis of are represented by the oxidation of primary amines. To serve this scope, various reagents including ozone, $NaMnO_4$, $KMnO_4$, peracetic acid, meta-chloroperbenzoic acid (MCPBA) and dimethyldioxirane can be employed. In this context, a pioneering example was provided by Keinan et al.[16] with the ozonation at low temperature upon absorption of amines on dry silica, that provided nitroalkanes in 65-70% yield. This paved the way for the development of recent continuous flow procedures (**Figure 2.1**),[17–19] able to safely handle unstable and explosive ozonides and peroxides that can be generated within the process.

Other significant methodologies involve the conversion of carbonyl into nitro compounds (retro Nef reaction), achieved upon oxidation of oximes,[20,21] and oxidation of azides.[22] A new sustainable method has been recently presented by Chu et al,[23] involving a Titanium-Silicate 1 (TS-1) catalyzed oxidation of oximes and a new tandem oxidation of ketones with H_2O_2 and NH_3, with some encouraging preliminary results on the feasibility of the process.

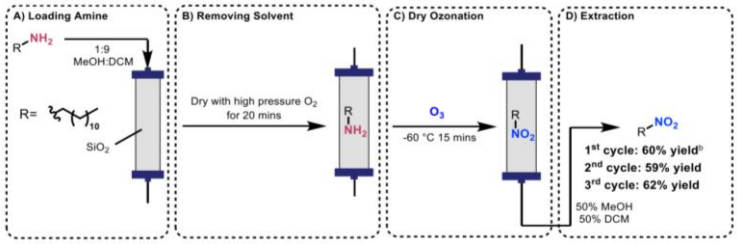

Figure 2.1 Example of recent ozonation flow procedure, adaptation of Keinan synthesis, by Skrotzki et al. Figure taken from ref. [19]

The electron-withdrawing effect due to the presence of the nitro group confers to primary and secondary nitroalkanes characteristic capability to generate stabilized carbanions, specifically nitronate anions, under basic conditions. This nitronate anions are commonly employed as nucleophiles, leading to the formation of both C-C single bonds and C=C double bonds, through Henry and Michael reactions, that will be discussed in the next sections.[24,25] Moreover, the versatility of nitroalkanes extends to their ability to undergo various transformations, allowing for the conversion of the nitro group into different functional groups, [1,26] such as amines,[27] oximes,[28,29] nitriles,[30] and carbonyl derivatives, [31] or removed upon denitration (**Scheme 2.4**).[32] As a result, the obtained adducts can serve as strategic substrate for a variety of purposes, from the synthesis of substituted nitroalkanes to more complex molecular structures. This broad range of transformations provides wide opportunities for the synthesis of diverse compounds.[33]

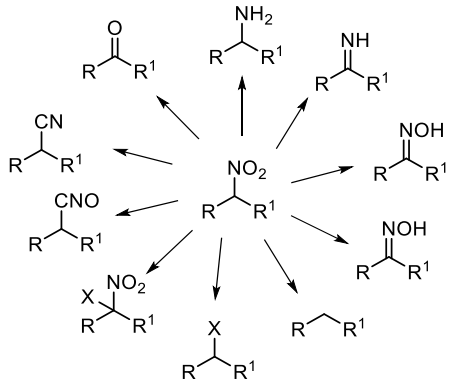

Scheme 2.4 Nitro group conversion into different funtionalities

Nitroalkenes

Nitroolefins are generally prepared following two main methods: by direct nitration of a preformed double bond (**Scheme 2.5, example a**), or by elimination of suitable leaving groups at either α or β positions to the nitro functionality of a molecule, such as a *β*-nitroalcohol, after a nitro-aldol reaction

between a carbonyl compound and nitroalkane, i.e. Henry reaction (**Scheme 2.5**, **example b**).[34] The latter, one of the most adopted strategies for their synthesis, will be also discussed in the following sections, dedicated to some particular class of nitroalkenes, namely *β*-nitroenones (2.2.1) and *β*-nitroacrylates (2.1.4).

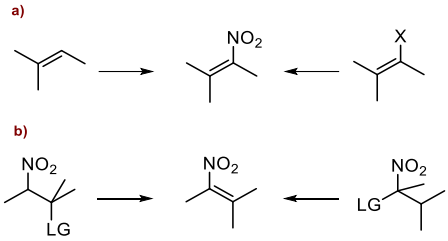

Scheme 2.5 Main approaches for the synthesis of nitroolefins

Direct nitration is a well-established and effective, but quite challenging methodology. Many progresses have been done in the development of new nitrating agents, but poor stereoselectivity and group tolerance still represents the main drawback.

Earlier approaches used nitrogen oxides, in particular nitrogen monoxide (NO),[35,36] however, they bearded several disadvantages, such as difficult handling and severe toxicity. In 2010, an iron mediated nitration reaction was proposed by Taniguchi and coworkes, enabling the synthesis of the desired nitroolefins via elimination of the formed halo-nitro compounds intermediate. The method involved the radical addition of NO_2, generated in situ through thermal decomposition of $Fe(NO_3)_3 \cdot 9H_2O$ (**Scheme 2.6**).

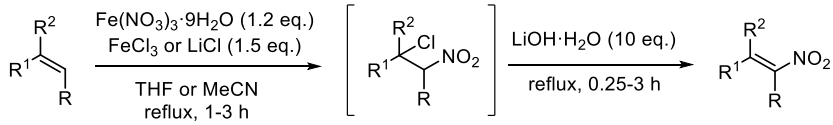

Scheme 2.6 Synthesis of nitroolefins using $Fe(NO_3)_3 \cdot 9H_2O$

Important contributions to the field was provided by Maiti and researchers, with the development of several protocols.[37,38] Among them, two significant ones: an efficient and stereoselective nitration of mono-, di-, trisubstitued olefins in high yields and exclusively in (*E*) configuration, obtained using silver nitrite ($AgNO_2$) and 2,2,6,6-tetramethyl-piperidine-1-oxyl (TEMPO), with an extended substrate scope and great functional groups tolerance (**Scheme 2.7, Example** a);[39,40] and a more sustainable, stereoselective metal-free procedure, exploiting tert-butyl nitrite (*t*-BuONO) and TEMPO conducted in the presence of air, applicable to a broad range of olefins (**Scheme 2.7, Example b**).[41]

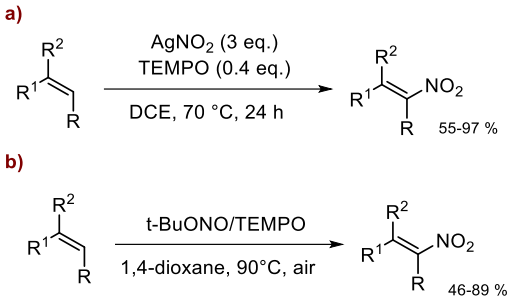

Scheme 2.7 Selective approaches for the formation of nitroolefins

A more recent contribution was provided by Reddy and Corey, for the nitration of cycloalkenes,[42] afforded by the in-situ generation of triflyl nitrate.

Other approaches include the nitrodecarboxylation of aromatic *a,β*-unsaturated carboxylic acids, exploiting their large availability and variability, inhert safety and easy storage of these substrate,[43] and the nitration of arylboronic acids.

As anticipated, nitro-aldol condensation (Henry reaction) is one of the most widely used approach for the formation of nitroolefins. It involves a reaction between a carbonyl compound and a nitroalkane, in the presence of a basic catalyst, generally under mild conditions. Once the *β*-nitro alcohol is formed it can undergo dehydration to afford nitroalkenes, when an acidic α-proton is available (**Scheme 2.8**).

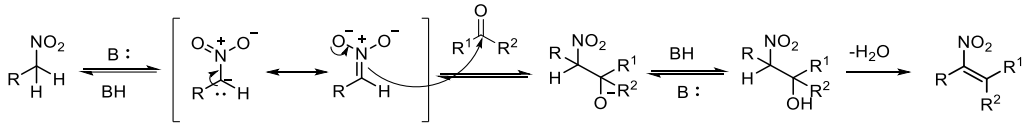

Scheme 2.8 General mechanism of Henry reaction

The reaction includes two steps, but when aromatic aldehydes are used with nitroalkanes, the result is the straightforward formation of the product, since the elimination of water is driven by the formation of conjugated double bond. Whereas, reactions with aliphatic aldehydes and subsequent dehydration can be carried out under different conditions,[2] in homogeneous and heterogeneous systems, protic and aprotic solvents and solventless conditions, and in combination with advanced enabling technologies, depending on factors such as the type of functionality present, the solubility of the reactants, and the ease of nitronate generation.[25]

In fact, since its first appearance in 1895,[44] many protocols have been envisaged. Initially, the preferred catalysts for facilitating nitroaldol reactions were typically alkoxide or hydroxide derivatives employed in alcoholic or aqueous solvent systems. In the case of structurally simple substrates, ammonia and various amines have also proven to be effective in nitroaldol condensation, leading to the formation of nitroolefins (**Scheme 2.9, Examples a-b**). Tertiary amines are capable of promoting the formation of β-nitroalcohols, however, for reaction of higher nitroalkanes with both

aldehydes and ketones, better results are achieved by employing stronger bases such as 1,1,3,3-tetramethylguanidine (TMG) and 1,8-Diazabicyclo[5.4.0]undec-7-ene (DBU) (**Scheme 2.9, Example c**).

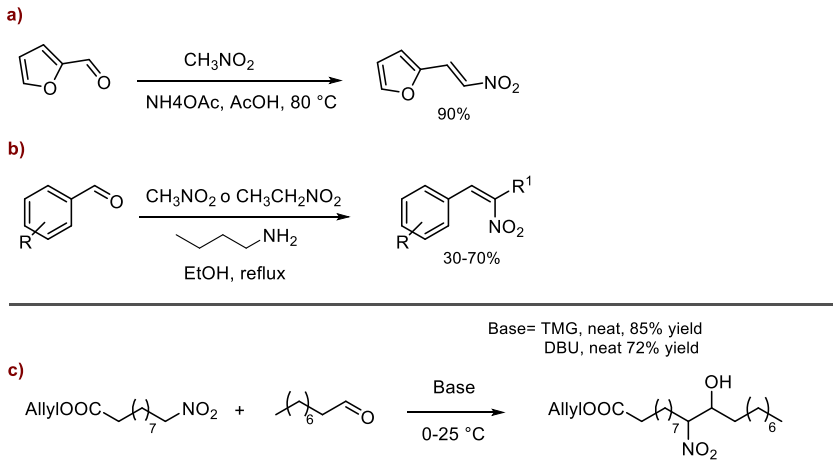

Scheme 2.9 a) aldol condensation of furfural using ammonium acetate for the production of natural alkaloids,[45] b) synthesis of arylnitroalkenes promoted by n-butylamine,[46,47] c) Henry reaction promoted by TMG or DBU

Over the years, many solid supported reagents (SSR) have been investigated by Ballini and researchers, in order to achieve more environmentally sustainable transformations, with particular attention on solvents employment, and catalysts recovery and reuse. Furthermore, the use of solid supported species reduces the subsequent reactions work-ups to simple filtration. This is particularly useful in this case, in order to avoid acidification usually need in homogeneous systems, and further possible undesired Nef reaction.[48] Few examples are reported in **Scheme 2.10**, regarding the usage, in all case without solvent, of commercial and inexpensive Amberlyst® A21,[49] N,N-diethylpropylamine on amorphous silica (KG-60-NEt_2),[50] and Si-carbonate [silica trimethylammonium carbonate; Si-TMS$(CO_3^{-2})_{0.5}$].[51] The reactions required mild conditions and afforted the desired *β*-nitroalcohols, respectively in 70-90%, 75-94%and 58-87% yield.

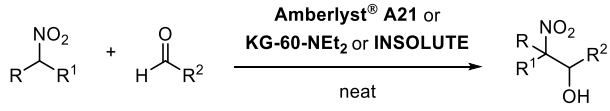

Scheme 2.10 Solid supported Henry reactions

Other interesting solid supported system were proposed by Rokhum's research group,[52] in particular one using polymer supported DMAP (10 mol%),[53] and leading to products formation in high yield at room temperature, with the possibility to recycle the catalyst up to 5 times. The same group recently proposed the use of biowaste derived Musa acuminata (banana) peel ash (MAPA) as

heterogeneous catalyst, [54] able to provide a variety of *β*-nitroalcohols in excellent yield within 15-30 minutes.
Also, the use of fluoride anion has been explored to this scope, both as free potassium fluoride in alcoholic solvent,[55] and supported on alumina.[56]

The subsequent dehydration to afford nitroolefins can be carried out exploiting different reagents, such as dicyclohexylcarbodiimide, trifluoracetic anhydride with thiethylamine,[57] basic alumina,[58] mesyl chloride with triethylamine (**Scheme 2.11**).[59,60]

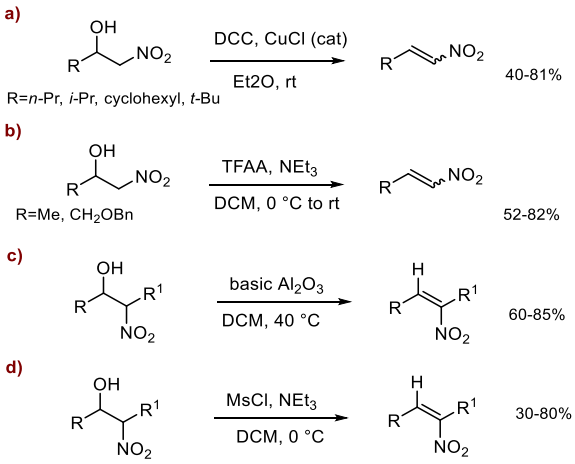

Scheme 2.11 Principal methods for β-nitroalcohol dehydration

Nitroolefins exhibit high versatility and remarkable reactivity, primarily attributed to the electron-withdrawing nature of the nitro group. The presence of the nitro group directly attached to an olefinic carbon atom creates an electron-deficient double bond, which acts as a highly reactive Michael acceptor capable of undergoing addition reactions with various nucleophiles.[2,24]
Nitroalkens compounds play a crucial role in the construction of new carbon-carbon bond, as extremely reactive species in pivotal processes, such as Diels–Alder cycloaddition,[61] Morita–Baylis–Hillman reaction,[62] and Stetter reaction,[63] making them valuable intermediates in the synthesis of important heterocyclic systems and biologically active molecules (**Scheme 2.12**).[64] The unique feature of nitroolefins, allowing for the introduction of additional functionalities directly linked to the double bond or at specific key positions, greatly enhances their synthetic utility. This capability enables the efficient synthesis of complex molecular structures in a one-pot manner and/or under mild reaction conditions. The versatility and control offered by these transformations facilitate the development of efficient and streamlined synthetic routes to diverse and functionally-rich compounds.

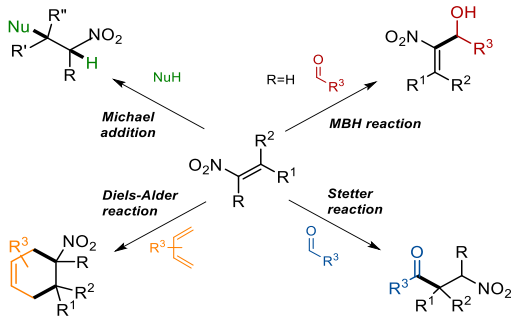

Scheme 2.12 Some synthetic application of β-nitroolefins

2.1.2 *β*-nitroenones

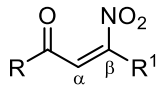

Figure 2.2 General structure of a β-nitroenone

β-nitroenones (**Figure 2.2**) are particular subclass of nitroolefins that over the last years have proven to be valuable and versatile building block for a variety of highly functionalized materials.
The resonance structures reported below (**Scheme 2.13**) put in evidence the presence of two possible nucleophilic centers and three electrophilic ones.

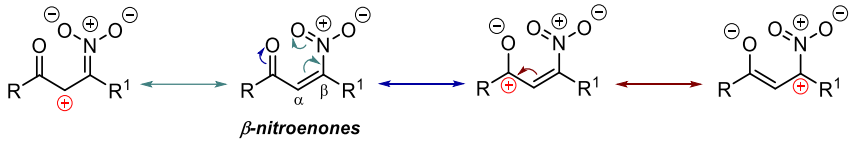

Scheme 2.13 Resonance structures of β-nitroenones

Generally, when a nucleophile species is present, the first attack preferentially occurs on the α position, thanks to the enhanced electron withdrawing character of the nitro group in respect to the ketone. Moreover, when employing a di-nucleophilic compound, it becomes possible to exploit an additional electrophilic center to achieve ring closure (**Scheme 2.14**). In fact, they have been extensively utilized for the synthesis of various heterocyclic systems.

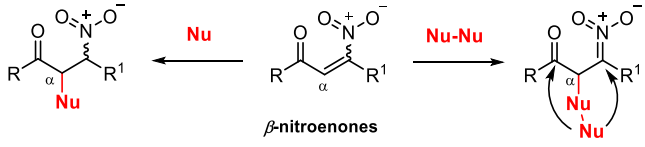

Scheme 2.14 Nucleophilic and di-nucleophilic attack on β-nitroenones

β-nitroenones can be smoothly prepared by a three-step synthetic pathway, starting from an alkyl or aryl glyoxal and a nitroalkane. These compounds undergo a Henry addition (**Scheme 2.15, Step 1**), and the outcoming nitro-alcohol product is subsequently treated with acetic anhydride and an acidic promoter to provide an acetylated intermediate (**Scheme 2.15, Step 2**). The last step is an acetic acid elimination, which occurs under basic conditions (**Scheme 2.15, Step 3**), to produce the targeted *β*-nitroenone.

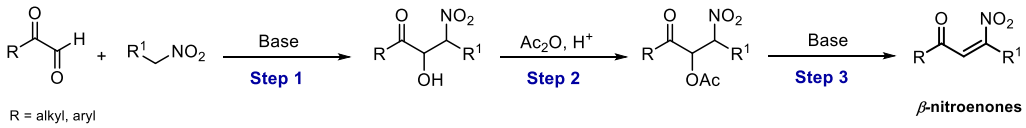

Scheme 2.15 Preparation of *β*-nitroenones

For what concerns their applicability, they have been proficiently used for the asymmetric derivatization of indoles and pyrroles,[65] and for the formation of skipped dienes in a enantioselective olefination-elimination reaction sequence, when in combination with aldehydes.[66] They can also be subjected to nucleophilic addition for the preparation of *β*-nitroketones,[67] and they can be involved in the α-alkenylation of *β*-ketoesters,[68] thanks to the reverse reactivity of the α-carbon provided by the presence of the nitro group.

Furthermore, they have been exploited by our research group to yield 1,4 diketones,[69] which are useful precursor of heterocyclic systems, with the retainment of the multipotent nitro functionality, and to obtain functionalized *β*-nitroketones by a chemoselective reduction of the double bond.[70] Additionally, they have proven to be effective starting materials, with α-functionalized ketones, for the preparation of substituted furans,[71] pivotal scaffold of many bioactive compounds.

Recently, a new reactivity of these compounds has been discovered by our team, when treating them with metal allylating agents. In this case, the carbonyl group is involved in the reaction, leading to the formation of the corresponding homoallylic alcohols. Moreover, a subsequent dehydration can give access to a conjugated nitrotriene system.[72]

It is important to underline that many of these recent works focus their attention not only to the production of the targeted compounds, but also to the employment of green methodologies, such as one-pot processes, sustainable solvents or neat conditions, and heterogeneous catalysis.

As we will discuss below, they are also valuable precursor of *β*-nitro-*β,γ*-unsaturated ketones, that were profitably applied in two of the project presented in this thesis work, i.e. in **Chapter 2.2** and **2.3**.

2.1.3 *β*-nitro-*β,γ*-unsaturated ketones

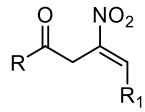

Figure 2.3 General structure of β-nitro-β,γ-unsaturated ketones

β-nitro-*β,γ*-unsaturated ketones (**Figure 2.3**) constitute a special subclass of nitroolefins, and for this reason they can undergo to the characteristic reactions of these compounds and, additionally, the presence of the ketone group opens new space for further functionalization.

Unfortunately, there are not many synthetic procedures for their synthesis, all marked by poor versatility and limited substrate scope. The methods reported in the literature include the elimination of hydrobromic acid from γ-brominated *β*-nitroketones,[73,74] Morita-Baylis-Hillman (MBH) coupling between nitroolefins and dicarbonyl compounds,[75] or via nitration of allenyl ketones.[76]

Though, in recent years, our research group has developed an efficient synthesis of *β*-nitro-*β,γ*-unsaturated ketones by isomerization of *β*-nitroenones, exploiting MW irradiation.[77] An example of the synthesis, with optimized conditions, is provided in **Scheme 2.16**.

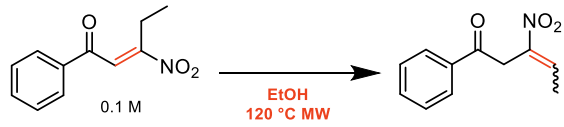

Scheme 2.16 Synthesis of β-nitro-β,γ-unsaturated ketones starting from β-nitroenones

When irradiating a solution of the starting material, an isomerization from *a,β* to *β,γ* occurs. This transformation is achieved with enhanced product yield and better diastereoselectivity when performed using alcoholic solvents.

More recently, a visible-light driven isomerization of *β*-nitroenones to the respective *β*-nitro-*β,γ*-enones has been documented.[78]

β-nitro-*β,γ*-unsaturated ketones reactivity is currently subject of explorations and represents an important topic of this thesis work. In fact, this interesting class of compounds has already proven to be valuable for the synthesis of bioactive heterocyclic systems and relevant frameworks present in many drugs, such as pyrroles,[77] carbazoles (**Chapter 2.2**),[79] and conjugated dienones (**Chapter 2.3**).[80] Anew, *β*-nitro-*β,γ*-unsaturated ketones were exploited by our research group for the synthesis of substituted pyridazines,[81] in a one-pot two-step procedure.

2.1.4 *β*-nitroacrylates

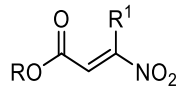

Figure 2.4 General structure of *β*-nitroacrylates

Similarly to *β*-nitroenones, *β*-nitroacrylates (**Figure 2.4**) constitutes a highly reactive class of electron-poor alkenes. The molecular framework in the structure offers several opportunities in term reactivity and further manipulation and functionalization, due to the presence of both nucleophilic and electrophilic centers. The presence of both functionalities, ester and nitro, on the compound enhances its ability to act as an exceptional Micheal acceptor, while the carboxylic group remains unreactive.

Generally, they are obtained by direct nitration of acrylic esters with different nitrating agents, or by dehydration of the corresponding nitro alcohols.
The latter is the most practical one, as the nitro alcohols can be obtained either by radical nitration of acrylates using ceric ammonium nitrate (CAN) and $NaNO_2$, or by Henry reaction starting from a nitroalkane and a glyoxalates, employing Amberlyst® A21 in EtOAc at room temperature (**Scheme 2.17**).

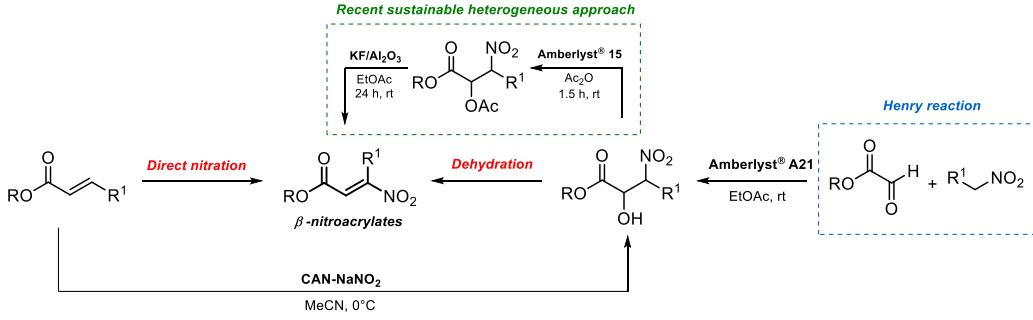

Scheme 2.17 Procedures for the preparation of β-nitroacrylates

Nitro-alcohols intermediates can be efficiently converted into the target *β*-nitroacrylates using a two steps sustainable procedure of recent discover, that involves heterogeneneous catalysts (i.e., Amberlyst® 15 and KF/Al_2O_3),[82] solventless and mild conditions,[83] thus avoiding the low temperature and toxic reagents required by McMurry procedure, commonly used for the scope.[59] The method provide *β*-nitroacrylates in excellent yield on the overall process (92-99%), and diasteroselectivity (E:Z>96:4).

The attractive chemistry of these compounds has been profoundly explored during the last decades, leading to their employment for the construction of a different range of heterocycles,[84,85] drug molecules,[86] as well as highly functionalized species,[87,88,89] useful for further transformation and

manipulation (**Scheme 2.18**). Generally, the development of these processes always tried to involve green protocols, such as one-pot reactions,[90] continuous flow synthesis,[91] supported systems,[92] photochemical transformations,[93] neat conditions or sustainable solvents,[94,95] or a combination of all these methodologies.[96,97]

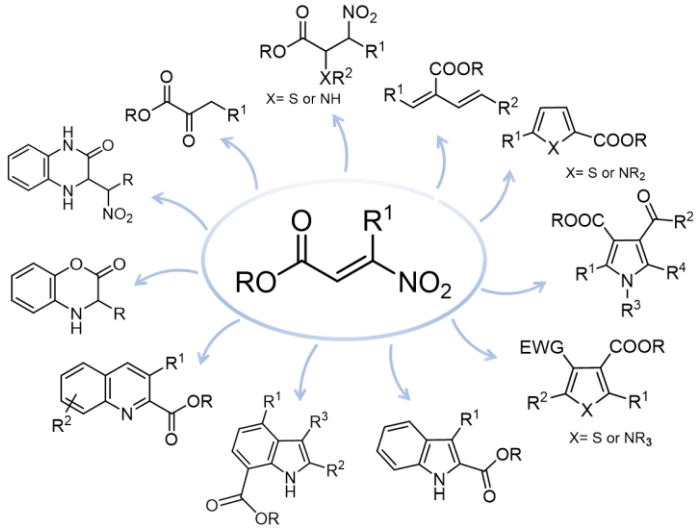

Scheme 2.18 β-nitroacrylates as building block for the synthesis of polyfunctionalized molecules

In my thesis work, *β*-nitroacrylates were profitably used to explore their reactivities under photochemical conditions, with a development of a process for their hydroalkylation both in batch and flow (**Chapter 2.4**).[98]

2.2 Thesis work: One-pot synthesis of polysubstituted carbazoles

The results presented in this section are adapted from:

A New and Effective One-Pot Synthesis of Polysubstituted Carbazoles Starting from β-Nitro-β,γ-Unsaturated-Ketones and Indoles, Lupidi, G., Bassetti, B., Ballini, R., Petrini, M., Palmieri, A., *Asian J. Org. Chem.* **2021**, *10*, 1–5

2.2.1 Introduction

Carbazole alkaloids (**1**) have been extensively studied and are characterized by a polycyclic nitrogen-containing system consisting of two fused benzene rings and a central pyrrole unit, with the nitrogen atom showing extensive electron delocalization. Carbazole alkaloids are naturally occurring compounds that are primarily found in plants, fungi, and marine organisms. These compounds are highly significant due to their diverse range of applications (**Figure 2.5**). They exhibit a multitude of biological activities, including anti-tuberculosis, anti-viral,[99] anti-inflammatory, anti-cancer, and anti-bacterial properties.[100] Additionally, the carbazole scaffold finds applications in material sciences, particularly as dyes and conductive polymers. They have been employed as transistors, enabling the development of electronic devices with improved performance. Moreover, among other applications, these polymers have been used in the creation of smart windows and light-emitting diodes and solar cells.

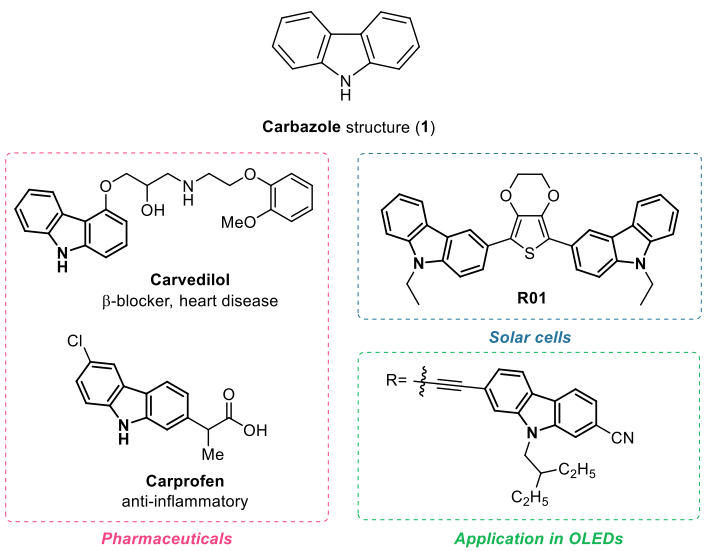

Figure 2.5 Carbazoles application in different fields

The literature has seen a growing number of studies focusing on expanding the synthetic toolbox for accessing carbazole derivatives with diverse chemical functionalities, due to their versatility. In fact, in recent years, there has been a notable interest in developing efficient and selective synthetic strategies. These methods often involve the functionalization of different positions on a pre-existing carbazole scaffold, allowing for the introduction of various substituents or functional groups, but regioselectivity problems occurs frequently and only simple substituents can be introduced. Another approach is the use simple building blocks to achieve the formation of complex polysubstituted carbazole structures. In this case, the limited availability of substrate with suitable substituted carbon backbone can greatly influence the feasibility and success of the synthetic approach.

Based on this, numerous approaches were developed by leveraging electron-rich heteroaromatic **indole** core, as readily accessible starting materials.[101] Moreover, the possibility offered by a post-synthetic modification on the reactive C-2 and C-3 positions of the indole ring, significantly broaden the number of accessible carbazoles derivatives.

Examples of this approach are provided in Scheme 2.19. In the first case, Verma and co-workers (**Scheme 2.19, Example a**)[102] obtained substituted carbazoles in good yields after three regioselective successive oxidative Heck reaction, and subsequent cyclization, starting from alkenes and non-protected indoles. In the second case, the regioselective formation of carbazoles was achieved by Wang et al.[103] (**Scheme 2.19, Example b**) through a NBS-catalyzed intermolecular annulation of acetyl indoles with alkynes, conducted under mild conditions. A recent strategy, envisaged by Deng et al.,[104] involve a metal-free three component one-pot synthesis of substituted carbazoles, starting from indoles, aromatic ketones, and electron deficient alkenes (**Scheme 2.19, Example c**). Different functional groups on the alkene determines the formation of different di/tri-substituted carbazoles, with an ester group transfer phenomenon from C-1 to C-2 in one case, and the target formation upon decarboxylation in the second. Carbazoles products were obtained in good yield, regioselectivity, and group tolerance, but long reaction time are required.

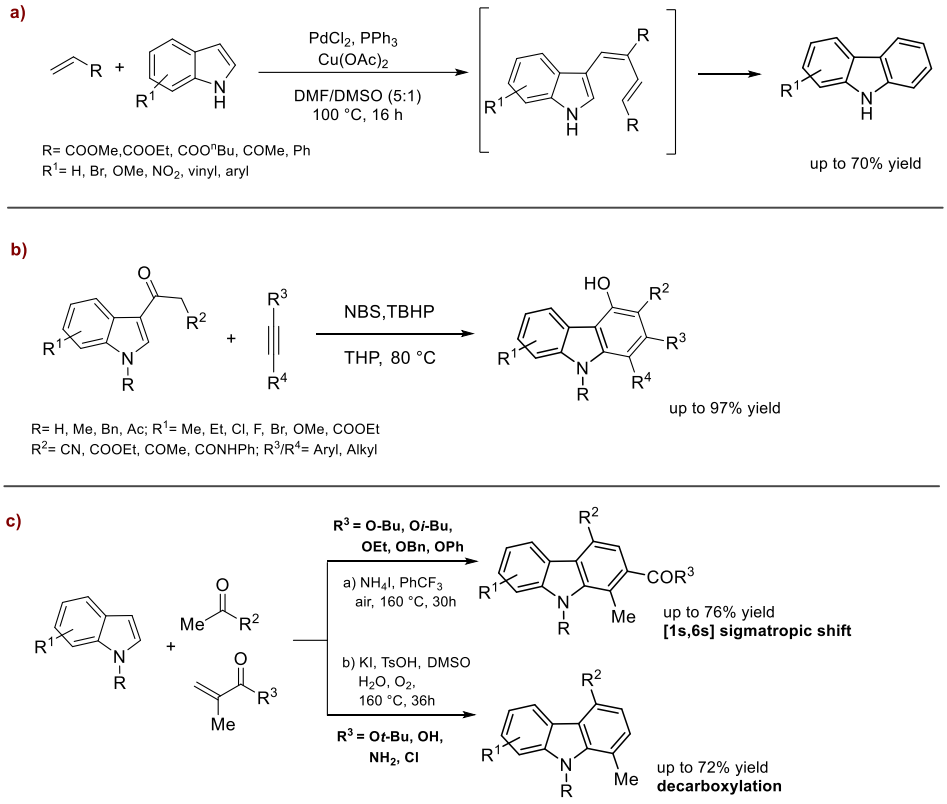

Scheme 2.19 Examples of carbazoles synthetic approaches from indoles

Polyfunctionalized nitroolefins, specifically *β*-nitroacrylates and *β*-nitroenones, have emerged as valuable building blocks in the synthesis of structurally diverse homo- and heteroaromatic substituted systems, offering a versatile and efficient route to access structurally diverse compounds with tailored properties and potential applications in various fields.

In this context, and in continuation with our work on the reactivity of nitroolefins, the use of *β*-nitro-*β,γ*-unsaturated ketones (**2**), recently proved to be effective for the synthesis of polysubstituted pyrroles (**Scheme 2.20**).[105]

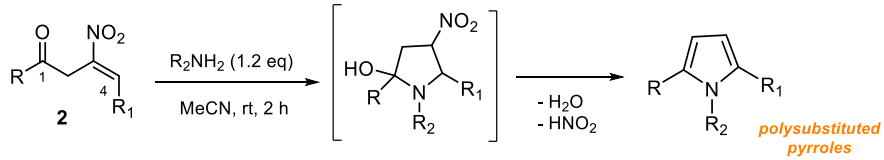

Scheme 2.20 Synthesis of polysubstituted carbazoles from β-nitro-β,γ-unsaturated ketones

The presence of the two electrophilic centers in 1,4 postitions makes these compounds a source of 1,3 diene synthons, and the aromatization potential of the formed intermediate, by elimination of

HNO_2 and H_2O, offers strategic opportunities for the construction of complex molecules with desired functionalities.

With this knowledge in our hands, the application of this subclass of functionalized nitroolefins, in combination with indoles (**3**) provided access to the multipotent carbazoles scaffold, in a one-pot regioselective synthesis (**Scheme 2.21**).

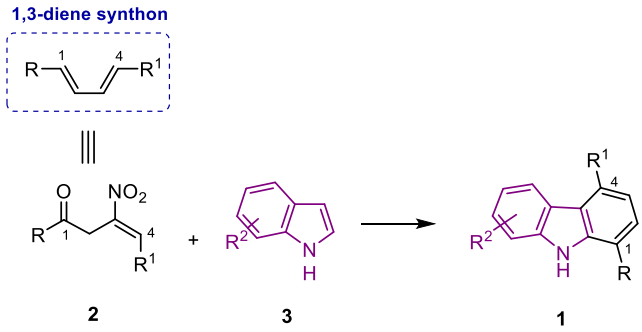

Scheme 2.21 Synthesis of polysubstituted carbazoles

2.2.2 Results and discussion

The one-pot protocol for synthesizing the title compound **1** involves a two sequential steps, as explained in the proposed mechanism reported in **Scheme 2.22**. In the first one, a Friedel-Craft reaction takes place between *β*-nitro-*β,γ*-unsaturated ketones **2** and indole **3**, leading to the formation of intermediate **4**. In the second step of the reaction sequence, a domino intramolecular Friedel-Crafts cyclization and aromatization process occurs, resulting in the formation of a new ring, namely the final product **1**.

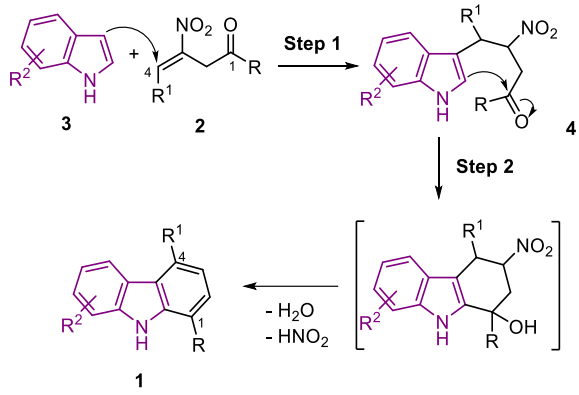

Scheme 2.22 One-pot preparation of carbazoles

With the aim of finding the optimal conditions for the synthesis we started investigating the two steps separately.

Firstly, we selected the two starting materials, nitroolefins **2a** and indole **3a**, as model compounds for the investigation of the first step. The initial attempt was performed using basic alumina under solvent-free conditions (neat) at 60 °C (**Scheme 2.23, conditions a**), previously applied by our research group for the addition of nitroalkenes to indole core structures.[106,107]

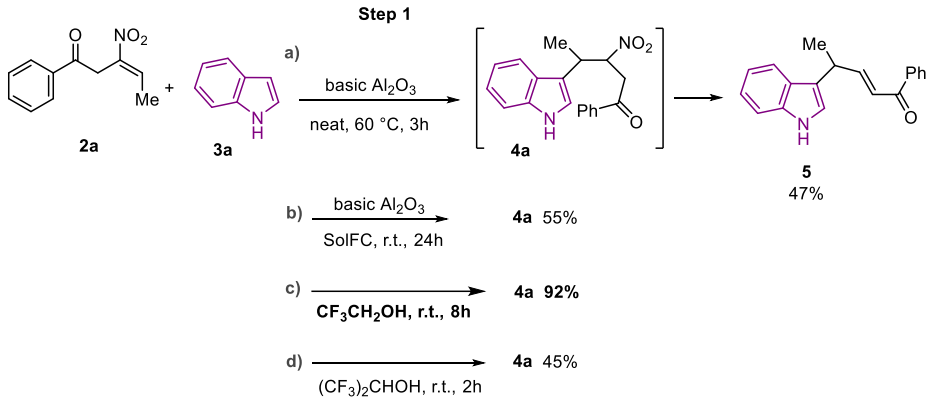

Scheme 2.23 First step investigations

Despite the reaction's overall effectiveness, it was observed that the intermediate **4a** exhibited instability under the given conditions. Consequently, a direct isolation of the unsaturated ketone **5** was achieved, in 47% yield. Unfortunately, the E-configuration of the double bond displayed by compound **5** was not suitable for the subsequent cyclization (Step 2), highlighting the importance of achieving the desired stereochemistry in in the earlier stages of the reaction sequence.

The reaction was repeated at room temperature (**Scheme 2.23, conditions b**), and this time the desired intermediate **4a** was obtained in 55% after 24 hours, with observation of unreacted starting materials. However, even when the amount of basic alumina employed was modified, no notable improvements in the reaction were observed.

Hence, drawing inspiration from an article published by Crousse et al.,[108] which discusses the use of fluorinated solvents to enhance the Friedel-Crafts reaction between indoles and nitroalkenes, we decided to investigate their applicability to our specific process. In particular, we tested 2,2,2-trifluoroethanol (TFE) and hexafluoro-2-propanol (HFIP). In the first case, the reaction underwent completion in 8 hours, resulting in a 92% yield of compound **4a** (**Scheme 2.23, conditions c**). On the other hand, when HFIP was used as solvent, the substrates were consumed within two hours, but the giving only **4a** in 45% yield. Additionally, a complex mixture of inseparable by-products was detected (**Scheme 2.23, conditions d**).

By using fluorinated solvents in the process, we likely created an environment that promoted the reactivity of nitroolefins, thus leading to the observed regioselectivity.

The successful outcome achieved with TFE in Step 1 prompted us to shift our attention toward the conversion of compound **4a** into the titled target **1a** (**Step 2**), as summarized in (**Table 2.1**).

To achieve our goal, and based on our previous investigation regarding cyclization process facilitated by Amberlyst® 15,[101,109] we proceeded by directly adding this heterogeneous acid catalyst to the TFE solution obtained during Step 1.

Table 2.1 Second step optimization

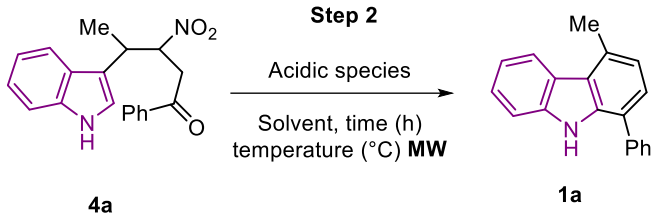

4a **1a**

Entry	Acidic species	g/mmol	Solvent	T [°C] MW	t [h]	3a yield [%]
1	Amberlyst® 15	1	TFE	90	2	-
2	Amberlyst® 15	1	EtOH	90	4	54
3	Amberlyst® 15	1	*i*-PrOH	90	4	60
4	Amberlyst® 15	1	2-MeTHF	90	3	63
5	Amberlyst® 15	1	EtOAc	90	4	36
6	Amberlyst® 15	1	MeCN	90	4	18
7	Amberlyst® 15	1	DCM	90	4	19
8	Amberlyst® 15	1	Toluene	90	4	26
9	Amberlyst® 15	1.2	2-MeTHF	90	3	68
10	Amberlyst® 15	1.4	2-MeTHF	90	3	67
11	**Amberlyst® 15**	**1.2**	**2-MeTHF**	**100**	**3**	**75**
12	Amberlyst® 15	1.2	2-MeTHF	110	3	73
13	*p*-TSOH·H_2O	0.29	2-MeTHF	100	3	57
14	Acidic Al_2O_3	1.2	2-MeTHF	100	3	Traces
15	Mont. K10	1.2	2-MeTHF	100	3	19
16	Zeolite HSZ-320	1.2	2-MeTHF	100	3	11
17	-		2-MeTHF	100	3	-

Unfortunately, the reaction at room temperature proved to be ineffective, and upon warming the reaction mixture at 90 °C with microwave irradiation a mixture of degradation by-products was obtained, instead of the desired carbazole **1a** (**Table 2.1, Entry 1**).

Our reaction conditions screening proceeded initially with the search of other possible solvents, and to this scope TFE was removed under vacuum, and replaced with alternative reaction media (**Table 2.1, Entries 2-8**). Then, the attention was focused on the amount of the acidic species and on the reaction temperature (**Table 2.1, Entries 9-12**).

Among the solvents tested, 2-MeTHF exhibited superior performance in promoting the desired transformation of compound **4a** into carbazole **1a**. In particular, the best result was obtained at 100°C with microwave irradiation, in the presence of 1.2 g/mmol of Amberlyst® 15 as catalyst, and with a reaction time of 3 hours, yielding carbazole **1a** in 75% (**Table 2.1, Entry 11**).

When exploring the use of other acidic species, only *p*-toluenesulfonic acid (*p*-TSOH·H_2O, **Table 2.1, Entry 13**) exhibited acceptable but worst results compared to Amberlyst® 15, while acidic alumina (Acidic Al_2O_3, **Table 2.1, Entry 14**) provided the unsaturated ketone **5** as main product. When using montmorillonite K10 (Mont. K10) and zeolite HSZ-320 the formation of product **1a** was observed in traces or in very low yield (**Table 2.1, Entries 15-16**), with the presence of unreacted adduct **4a** (75%).
Finally, the total absence of any acidic species resulted in no conversion at all of compound **4a** into carbazole **1a** (**Table 2.1, Entry 17**), underscoring the critical role of acid catalyst in promoting the desired transformation, indicating that its presence is essential for initiating and driving the cyclization and aromatization process.
In addition, we also explored the direct conversion of compounds **2a** and **3a** into carbazole **1a**, under the optimized reaction conditions established for Step 2. However, the results obtained were not favorable, with an ineffective conversion observed at room temperature, and a negligible yield of 9% when performing the reaction at 100 °C, indicating that the solvent change is of primary importance for the process to be successful.

Afterwards, the generality of our protocol under optimized conditions for the two coupled steps was proven using a variety of nitroolefins **2** and indoles **3** on a 1 mmol scale, providing in all cases the isolation of the products **1a-m** from good to very good yield (55-78 %, **Scheme 2.24**). To further validate the scalability of the reaction, the conversion of compound **4a** into carbazole **1a** was also repeated on a 2 mmol scale, with a comparable result of 73% to the 75% yield obtained on the 1 mmol scale.
The ability to react of various indoles, included 7-alkylindoles, broadens the substrate scope and applicability of our reaction conditions. For what concerns electrophilic nitroolefins **1**, they can bear terminal unsaturation or alkyl groups at the nitroalkene moiety (R^1=H, alkyl). However, while our reaction conditions support different aryl groups (R^2 = aryl), when alkyl frameworks are present in the ketone moiety (R = alkyl) our reaction conditions have shown limited effectiveness (**Scheme 2.24**).
While acknowledging the limitations concerning alkyl substituent, our procedure allows the efficient one-pot synthesis of a structurally significant array of 1,4-disubstitued carbazoles, starting from easily accessible starting materials such as indoles and β-nitro-β,γ-unsaturated ketones.
By employing sustainable solvents such as TFE and 2-MeTHF in the respective reaction steps, and implementing a solid-supported catalyst (i.e. Amberlyst® 15), that minimize the materials and energy consumption, and wastes generated by aqueous work-ups, the protocol demonstrates a commitment to green chemistry principles. Moreover, the one-pot protocol allows for the efficient synthesis of the title compounds, avoiding the need for separate reaction steps or isolation of intermediates, providing a streamlined pathway to access the desired compounds in a single synthetic operation.

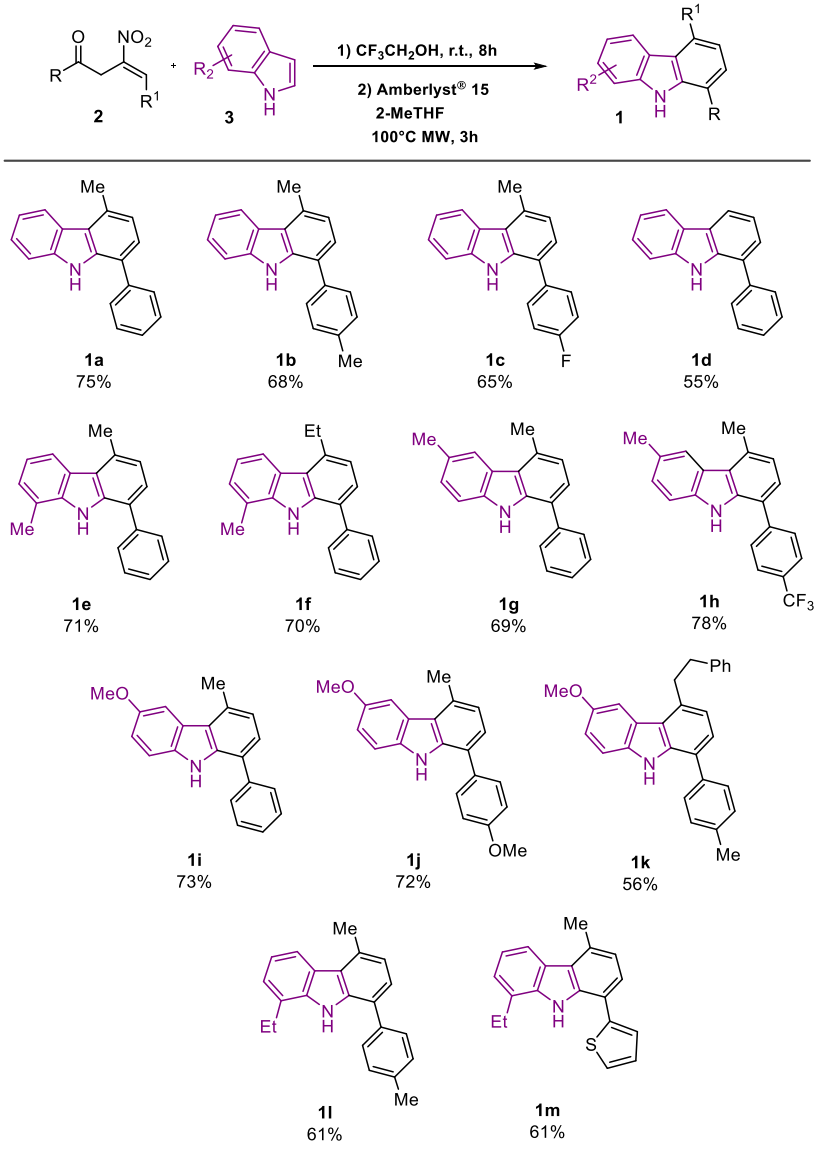

Scheme 2.24 Carbazoles substrate scope

2.2.3 Experimental section

General procedure for the synthesis of carbazoles 1a-m

A trifluoroethanolic solution (4 mL) of the proper indole **3** (1.2 mmol) and nitroolefin **2** (1 mmol) was stirred, in a 20 mL microwave vial, at room temperature for 8 hours. Subsequently, the solvent was removed under vacuum and the residue intermediate **4** was resolubilized in 2-MeTHF (10 mL), treated with Amberlyst 15 (1.2 g) and irradiated by means of a Biotage® Initiator at 100°C for 3 hours. Finally, Amberlyst 15 was filtered off and washed with EtOAc (20 mL), the solvent was evaporated under reduced pressure and the crude product **1** was purified by flash column chromatography (hexane:ethylacetate = 95:5).

Spectroscopic data 1a-m

Compound **1a**
Yield 75% (193 mg). White solid, **m.p.** = 94-96°C. **IR** (cm^{-1}, neat): 701, 724, 1247, 1318, 1453, 1580, 3429. **^{1}H-NMR** ($CDCl_3$, 400MHz) δ: 2.95 (s, 3H), 7.11-7.14 (m, 1H), 7.25-7.31 (m, 1H), 7.37 (d, *J* = 7.4Hz, 1H), 7.41-7.46 (m, 3H), 7.54-7.58 (m, 2H), 7.67-7.70 (m, 2H), 8.24 (d, *J* = 7.9Hz, 1H), 8.37 (bs, 1H). **^{13}C-NMR** ($CDCl_3$, 100MHz) δ: 21.0, 110.7, 119.7, 121.6, 122.3, 122.9, 124.4, 125.6, 125.8, 127.6, 128.7, 129.5, 132.9, 137.4, 139.4, 139.7. **GC-MS** (70eV): *m/z*: 257 ([M^+], 100), 241 (16), 180 (10), 127 (14). **Anal. Calcd. for C_{19} H_{15}N** (257.12): C, 88.68; H, 5.88; N, 5.44. **Found**: C, 88.63; H, 5.91; N, 5.46.

Compound **1b**
Yield 68% (184 mg). White solid, **m.p.** = 107-109°C. **IR** (cm^{-1}, neat): 503, 736, 800, 1251, 1318, 1378, 1457, 1501, 1584, 1600, 3029, 3053, 3413, 3433. **^{1}H-NMR** ($CDCl_3$, 400MHz) δ: 2.50 (s, 3H), 2.96 (s, 3H), 7.14 (d, *J* = 7.4Hz, 1H), 7.29-7.32 (m, 1H), 7.36-7.40 (m, 3H), 7.44-7.46 (m, 2H), 7.59-7.61 (m, 2H), 8.26 (d, *J* =7.9Hz, 1H), 8.37 (bs, 1H). **^{13}C-NMR** ($CDCl_3$, 100MHz) δ: 21.0, 21.5, 110.7, 119.7, 121.6, 122.3, 122.9, 124.5, 125.5, 125.7, 128.6, 130.2, 132.7, 136.5, 137.4, 139.7. **GC-MS** (70eV): *m/z*: 271 ([M^+], 100), 254 (17), 127 (10). **Anal. Calcd. for $C_{20}$$H_{17}$N** (271.13): C, 88.52; H, 6.31; N, 5.16. **Found**: C, 88.56; H, 6.28; N, 5.11.

Compound **1c**
Yield 65% (179 mg). Pale yellow solid, **m.p.** = 129-132°C. **IR** (cm^{-1}, neat): 731, 812, 836, 1160, 1208, 1458, 1495, 1596, 3050, 3459. **^{1}H-NMR** ($CDCl_3$, 400MHz) δ: 2.94 (s, 3H), 7.12 (d, *J* = 7.4Hz, 1H), 7.21-7.33 (m, 4H), 7.44 (d, *J* = 3.9Hz, 2H), 7.60-7.66 (m, 2H), 8.24 (d, *J* = 8.4Hz, 2H). **^{13}C-NMR** ($CDCl_3$, 100MHz) δ: 21.0, 110.8, 116.3, 116.5, 119.9, 121.7, 121.9, 122.4, 122.9, 124.4, 125.7, 125.8, 130.2, 130.3, 133.1, 135.3, 135.4, 137.4, 139.7, 161.2, 163.7. **GC-MS** (70eV): *m/z*: 275 ([M^+], 100), 259 (11), 180 (6), 137 (7). **Anal. Calcd. for $C_{19}$$H_{14}$FN** (275.33): C, 82.89; H, 5.13; N, 5.09. **Found**: C, 82.93; H, 5.10; N, 5.07.

Compound **1d**
Yield 55% (134 mg). Yellow solid, **m.p.** = 126-128°C. **IR** (cm^{-1}, neat): 701, 752, 1057, 231, 1322, 1410, 1435, 1505, 2907, 2990, 3061, 3437. **^{1}H-NMR** ($CDCl_3$, 400MHz) δ: 7.26-7.30 (m, 1H), 7.36 (t, *J* = 7.6Hz, 1H), 7.41-7.49 (m, 4H), 7.58 (t, *J* = 7.6Hz, 2H), 7.72 (d, *J* = 7.1Hz, 2H), 8.10-8.15 (m, 2H), 8.33 (bs, 1H). **^{13}C-NMR** ($CDCl_3$, 100MHz) δ: 110.9, 119.7, 119.8, 120.2, 120.7, 123.8, 124.0, 125.3, 126.0, 26.2, 127.8, 128.6, 129.5, 137.5, 139.3, 139.7. **GC-MS** (70eV): *m/z*: 243 ([M^+], 100), 120 (13). **Anal. Calcd. For C_{18} H_{13}N** (243.10): C, 88.86; H, 5.39; N, 5.76. **Found**: C, 88.91; H, 5.42; N, 5.79.

Compound **1e**

Yield 71% (192 mg). Pale yellow solid, **m.p.** = 105-109 °C. **IR** (cm^{-1}, neat): 701, 748, 788, 1065, 1235, 133, 1382, 1437, 1489, 1580, 3053, 3453. **^{1}H-NMR** ($CDCl_3$, 400MHz) δ: 2.56 (s, 3H), 2.95 (s, 3H), 7.12-7.14 (m, 1H), 7.20-7.28 (m, 2H), 7.36 (d, *J* = 7.4Hz, 1H), 7.45-7.49 (m, 1H), 7.59 (t, *J* = 7.6Hz, 2H), 7.72-7.74 (m, 2H), 8.10 (d, *J* = 7.6Hz, 1H), 8.22 (bs, 1H). **^{13}C-NMR** ($CDCl_3$, 100MHz) δ: 17.2, 21.0, 119.8, 119.9, 120.6, 121.7, 123.0, 123.9, 125.8, 126.2, 127.6, 128.6, 129.6, 133.0, 137.2, 139.0, 139.6. **GC-MS** (70eV): *m/z* : 271 ([M$^+$], 100), 254 (17), 194 (4), 127 (10). **Anal. Calcd. for $C_{20}H_{17}N$** (271.13): C, 88.52; H, 6.31; N, 5.16. **Found**: C, 88.56; H, 6.34; N, 5.19.

Compound **1f**

Yield 70% (200 mg). Pale yellow sticky oil. **IR** (cm^{-1}, neat): 574, 705, 760, 800, 1247, 1299, 1394, 1473, 1520, 1580, 3025, 3437. **^{1}H-NMR** ($CDCl_3$, 400MHz) δ: 1.56 (t, *J* = 7.5Hz, 3H), 2.61 (s, 3H), 3.36 (q, *J* = 7.5Hz, 2H), 7.17 (d, *J* = 7.5Hz, 1H), 7.26-7.29 (m, 1H), 7.33-7.35 (m, 1H), 7.40 (d, *J* = 7.5Hz, 1H), 7.43-7.48 (m, 1H), 7.56-7.60 (m, 2H), 7.70-7.73 (m, 2H), 8.02 (s, 1H), 8.30 (bs, 1H). **^{13}C-NMR** ($CDCl_3$,100MHz) δ: 14.4, 22.0, 27.5, 110.4, 119.5, 121.5, 122.9, 123.0, 124.0, 125.8, 126.9, 127.6, 128.7, 129.0, 129.5, 137.9, 138.0, 139.2, 139.5. **GC-MS** (70eV): *m/z*: 285 ([M$^+$], 100), 270 (90), 254 (23). **Anal. Calcd. for $C_{21}H_{19}N$** (285.15): C, 88.38; H, 6.71; N, 4.91. **Found**: C, 88.42; H, 6.74; N, 4.94.

Compound **1g**

Yield 69% (187 mg). White solid, **m.p.** = 166-169°C. **IR** (cm^{-1}, neat): 573, 703, 762, 802, 1019, 1054, 1251, 1299, 1393, 1441, 1472, 1519, 1583, 1602, 3026, 3057, 2440. **^{1}H-NMR** ($CDCl_3$, 400MHz) δ: 2.58 (s, 3H), 2.94 (s, 3H), 7.09-7.11 (m, 1H), 7.25-7.27 (m, 1H), 7.32-7.35(m, 2H), 7.42-7.46 (m, 1H), 7.56 (t, *J* = 7.7Hz, 2H), 7.67-7.70 (m, 2H), 8.02 (m, 1H), 8.21 (bs, 1H). **^{13}C-NMR** ($CDCl_3$, 100MHz) δ: 21.1, 21.9, 110.3, 121.4, 122.2, 122.8, 122.9, 124.6, 125.6, 126.9, 127.5, 128.7, 128.9, 129.5, 132.9, 137.78, 137.9, 139.5. **GC-MS** (70eV): *m/z* : 271 ([M$^+$], 100), 254 (17), 127 (10). **Anal. Calcd. for $C_{20}H_{17}N$** (271.13): C, 88.52; H, 6.31; N, 5.16. **Found**: C, 88.49; H, 6.34; N, 5.12.

Compound **1h**

Yield 78% (265 mg). Yellow solid, **m.p.** = 147-149°C. **IR** (cm^{-1}, neat): 566, 797, 1070, 1102, 1122, 1163, 1321, 1476, 1613, 3042, 3444, 3484. **^{1}H-NMR** ($CDCl_3$, 400MHz) δ: 2.56 (s, 3H), 2.93 (s, 3H), 7.10 (d, *J* = 7.4Hz, 1H), 7.22-7.27 (m, 1H), 7.29-7.35 (m, 2H), 7.79 (s, 4H), 8.00 (s, 1H), 8.18 (bs, 1H). **^{13}C-NMR** ($CDCl_3$, 100MHz) δ: 21.1, 21.9, 110.4, 121.3, 121.6, 122.5, 122.9, 123.1, 124.5, 125.7, 126.3, 126.4, 127.1, 128.9, 129.2, 133.9, 137.5, 137.9, 143.2. **GC-MS** (70eV): *m/z* : 339 ([M$^+$], 100), 324 (10), 268 (9), 254 (9). **Anal. Calcd. for $C_{21}H_{16}F_3N$** (339.36): C, 74.33; H, 4.75; N, 4.13. **Found**: C, 74.37; H, 4.78; N, 4.9.

Compound **1i**

Yield 73% (210 mg). Pale yellow sticky oil. **IR** (cm^{-1}, neat): 705, 760, 808, 1033, 1168, 1211, 1283, 1295, 1473, 1520, 1584, 3029, 3057, 3358, 3429. **^{1}H-NMR** ($CDCl_3$, 400MHz) δ: 2.94 (s, 3H), 3.96 (s, 3H), 7.08-7.11 (m, 2H), 7.33-7.35 (m, 2H), 7.41-7.45 (m, 1H), 7.54-7.57 (m, 2H), 7.68-7.70 (m, 2H), 7.76 (d, *J* = 2.5Hz, 1H), 8.23 (bs, 1H). **^{13}C-NMR** ($CDCl_3$, 100MHz) δ: 21.0, 56.4, 106.7, 111.2, 114.0, 121.3, 122.4, 123.0, 124.9, 125.8, 127.6, 128.7, 129.5, 132.9, 134.7, 138.3, 139.4, 154.0. **GC-MS** (70eV): *m/z* : 287 ([M$^+$], 100), 272 (88), 244 (17), 230 (9), 121 (9). **Anal. Calcd. for $C_{20}H_{17}NO$** (287.13): C, 83.59; H, 5.96; N, 4.87. **Found**: C, 83.63; H, 5.99; N, 4.90.

Compound **1j**

Yield 72% (228 mg). White solid, **m.p.** = 138-140°C. **IR** (cm^{-1}, neat): 514, 796, 867, 1026, 1033, 1168, 1208, 1235, 1295, 1437, 1469, 1501, 1572, 1600, 3002, 3342. **^{1}H-NMR** ($CDCl_3$, 400MHz) δ: 2.95 (s, 3H), 3.90 (s, 3H), 3.97 (s, 3H), 7.07-7.12 (m, 4H), 7.30-7.35 (m, 2H), 7.61 (d, *J* = 8.6Hz, 2H), 7.76 (d, *J* = 2.1 Hz, 1H), 8.25 (bs, 1H). **^{13}C-NMR** ($CDCl_3$, 100MHz) δ: 20.9, 55.6, 56.5, 106.7, 111.2,

114.0, 114.9, 121.2, 122.3, 122.8, 125.0, 125.7. 129.7, 131.8, 132.4, 134.7, 138.4, 154.0, 159.2. **GC-MS** (70eV): *m/z*: 317 ([M+], 100), 302 (69), 286 (3), 258 (7), 230 (7). **Anal. Calcd. for $C_{21}H_{19}NO_2$** (317.14): C, 79.47; H, 6.03; N, 4.41. **Found**: C, 79.51; H, 6.04; N, 4.38.

Compound **1k**
Yield 56% (219 mg). Pale yellow oil. **IR** (cm^{-1}, neat): 701, 728, 804, 1033, 1208, 1295, 1481, 1501, 1580, 3025, 3358, 3433. **^{1}H-NMR** ($CDCl_3$, 400MHz) δ: 2.48 (s, 3H), 3.20-3.24 (m,2H), 3.56-3.61 (m, 2H), 3.91 (s, 3H), 7.09-7.12 (m, 2H), 7.27-7.30 (m, 1H), 7.34-7.42 (m, 8H), 7.59-7.61 (m, 2H), 7.74 (d, *J* = 2.4Hz, 1H), 8.28 (bs, 1H). **^{13}C-NMR** ($CDCl_3$, 100MHz) δ: 21.5, 36.3, 36.6, 56.3, 106.3, 111.4, 114.4, 120.5, 121.6, 123.4, 124.1, 125.8, 126.3, 128.5, 128.7, 128.8, 130.2, 134.7, 136.4, 136.5, 137.4, 138.7, 142.2, 154.1. **GC-MS** (70eV): *m/z*: 391 ([M+], 30), 300 (100), 257 (15). **Anal. Calcd. for $C_{28}H_{25}NO$** (391.19): C, 85.90; H, 6.44; N, 3.58. **Found**: C, 85.94; H, 6.47; N, 3.61.

Compound **1l**
Yield 61% (182 mg). White solid, **m.p.** = 154-156°C **IR** (cm^{-1}, neat): 518, 750, 806, 1074, 1236, 1314, 1378, 1425, 1504, 1579, 3022, 3053, 3459, 3475. **^{1}H-NMR** ($CDCl_3$, 400MHz) δ: 1.40 (t, *J* = 7.6Hz, 3H), 2.49 (s, 3H), 2.90-2.92 (m, 2H), 2.93 (s, 3H) 7.10-7.12 (m, 1H), 7.23-7.30 (m, 2H), 7.33 (d, *J* = 7.4Hz, 1H), 7.40 (d, *J* = 7.8Hz, 2H), 7.61 (d, *J* = 8.0Hz, 2H), 8.10 (d, *J* = 7.6Hz, 1H), 8.24 (bs, 1H). **^{13}C-NMR** ($CDCl_3$,100MHz) δ: 13.9, 21.0, 21.5, 24.3, 120.0, 120.5, 121.6, 122.9, 124.1, 125.6, 125.9, 128.4, 130.3, 132.7, 136.6, 137.3, 138.2. **GC-MS** (70eV): *m/z*: 299 ([M+], 100), 284 (62), 268 (17), 254 (7). **Anal. Calcd. for $C_{22}H_{21}N$** (299.16): C, 88.25; H, 7.07; N, 4.68. **Found**: C, 88.29; H, 7.11; N, 4.71.

Compound **1m**
Yield 66% (192 mg). White solid, **m.p.** = 126-128°C. **IR** (cm^{-1}, neat): 681, 732, 800, 851, 1069, 1231, 1299, 1386, 1421, 1493, 1580, 1608, 3061, 3449. **^{1}H-NMR** ($CDCl_3$,400MHz) δ: 1.47 (t, *J* = 7.6Hz, 3H), 2.94 (s, 3H), 2.99 (q, *J* = 7.6Hz, 2H), 7.09-7.11 (m, 1H), 7.26-7.35 (m, 3H), 7.44-7.46 (m, 2H), 7.51 (d, *J* = 7.5Hz, 1H), 8.11 (d, *J* = 7.7 Hz, 1H) 8.55 (bs, 1H). **^{13}C-NMR** ($CDCl_3$ 100MHz) δ: 14.0, 21.0, 24.4, 115.8, 120.3, 120.6, 121.7, 123.2, 124.0, 124.4, 124.6, 125.0, 125.5, 126.1, 128.4, 133.6, 136.8, 138.3, 141.7. **GC-MS** (70eV): *m/z*: 291 ([M+], 100), 276 (72), 261 (12), 228 (7). **Anal. Calcd. for $C_{19}H_{17}NS$** (291.10): C, 78.31; H, 5.88; N, 4.81; S, 11.00. **Found**: C, 78.35; H, 5.91; N, 4.78; S, 10.97.

Spectroscopic data of compounds 4a and 5

Compound **4a**.
Yellow solid, **m.p.** = 166-169°C. **IR** (cm^{-1}, neat): 542, 693, 740, 863, 1014, 1239, 1330, 1378, 1449, 1540, 1687, 2914, 3061, 3406. **^{1}H-NMR** ($CDCl_3$, 400MHz) δ: 1.49 (d, *J* = 7.2Hz, 3H), 3.06 (dd, *J* = 18.3, 2.5Hz, 1H), 3.97 (dd, *J* = 18.3, 10.6Hz, 1H), 4.07-4.13 (m, 1H), 5.61-5.65 (m, 1H), 7.10 (d, *J* = 2.4Hz, 1H), 7.18-7.26 (m, 2H), 7.36-7.44 (m, 3H), 7.53-7.57 (m, 1H), 7.77 (d, *J* = 7.8Hz, 1H), 7.84-7.87 (m, 2H), 8.21 (bs, 1H). **^{13}C-NMR** ($CDCl_3$, 100MHz) δ: 14.9, 34.9, 36.4, 86.1, 111.8, 115.6, 118.9, 120.4, 122.0, 123.0, 126.3, 128.3, 128.9, 133.9, 136.2, 136.6, 196.0. **GC-MS** (70eV): *m/z*: 275 ([M+], 100), 258 (32), 230 (6), 170 (93), 154 (25), 128 (13), 105 (99), 77 (55). **Anal. Calcd. for $C_{19}H_{18}N_2O_3$** (322.13): C, 70.79; H, 5.63; N, 8.69. **Found**: C, 70.75; H, 5.62; N, 8.66.

Compound **5**.
Dark yellow sticky oil. **IR** (cm^{-1}, neat): 693, 740, 1006, 1101, 1212, 1259, 1283, 1338, 1417, 1449, 1612, 1663, 2867, 2930, 2966, 3057, 3410. **^{1}H-NMR** ($CDCl_3$, 400MHz) δ: 1.60 (d, *J* = 7.0Hz, 3H), 4.00-4.12 (m, 1H), 6.89-6.93 (m, 1H), 7.04 (d, *J* = 2.4Hz, 1H), 7.12 (t, *J* = 7.5Hz, 1H), 7.19-7.30 (m, 2H), 7.37-7.45 (m, 3H), 7.51-7.55 (m, 1H), 7.62 (d, *J* = 7.9Hz, 1H), 7.86-7.88 (m, 2H), 8.12 (bs, 1H). **^{13}C-NMR** ($CDCl_3$, 100MHz) δ: 20.1, 34.4, 111.5, 118.5, 119.4, 119.7, 121.0, 122.4, 124.6, 126.7, 128.7, 128.8, 132.8, 136.7, 138.2, 153.5, 191.7. **GC-MS** (70eV): *m/z*: 275 ([M+], 100), 258 (31), 170

(100), 143 (21), 105 (90), 77 (45). **Anal. Calcd. for $C_{19}H_{17}NO$** (275.13): C, 82.88; H, 6.22; N, 5.09. **Found**: C, 82.83; H, 6.25; N, 5.10.

NMR Spectra of the described compounds can be found at: doi.org/10.1002/ajoc.202100342

2.3 Thesis work: One-pot synthesis of (*E,E*)-conjugated dienones

The results presented in this section are adapted from:

Fast, Mild and Diastereoselective Conversion of *β*-Nitro-*β,γ*-Unsaturated-Ketones into Conjugated (*E,E*)-Dienones, Bassetti, B., Ballini, R., Petrini, M., Palmieri, A., *Adv. Synth. Catal.* **2023**, *365*, 13 –16

2.3.1 Introduction

The importance and impact of *β*-nitro-*β,γ*-unsaturated ketones has been already discussed in the previous chapters, as they constitute a versatile class of electron-poor alkenes. These compounds serve as versatile intermediates in the synthesis of diverse heterocyclic systems, which are important structural motifs found in many natural products and pharmaceutical compounds, and they can be exploited for the preparation of highly functionalized molecules.
In this context, their reactivity has been subject of recent interest for our research group and our investigations has led to the employment of these compounds for the synthesis of polysubstituted pyrroles[77] and carbazoles.[79]

Recently, when focusing our attention on the addition of diethylmalonate on model nitroolefin **2a**, we were quite surprised to find out that applying some particular conditions the reaction did not lead to the formation of the expected addition-elimination adduct **6a**. The presence of a new species was detected in the reaction mixture, and further NMR characterization reveal that the structure corresponded to the conjugated dienones **7a** (**Scheme 2.25**).

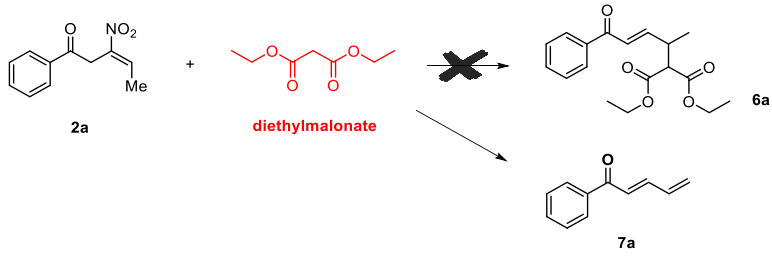

Scheme 2.25 Addition of diethylmalonate to β-nitro-β,γ-unsaturated ketones

Conjugated dienones play a critical role in organic and medicinal chemistry as they represent a fundamental molecular architecture found in many drugs and natural products (**Figure 2.6**).[110] The presence of this structural motif provides a versatile scaffold for the synthesis of complex molecules and contributes to the biological activity and therapeutic potential of these compounds. The use and exploration of these molecules in synthetic field have significant implications for the development of

novel pharmaceuticals and bioactive compounds, such as monoamino oxidase B inhibitors MK1-MK15.[111]

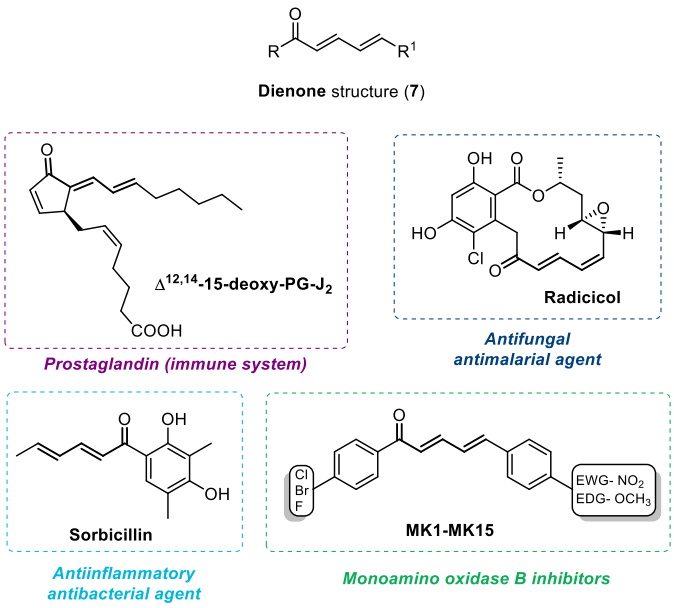

Figure 2.6 Applications of conjugated dienone derivatives

Their characteristic feature is also present in the natural unsaturated prostaglandin $\Delta^{12,14}$-15-deoxy-PG-J_2 and in other related compounds and analogues, which are studied as anticancer agents.[112] Conjugated dienone framework is present in the resorcylic acid lactone Radicicol,[113] an antifungal antibiotics which is involved in the regulation of many cellular processes, and whose derivatives seems to exhibit antitumoral activity.[114,115] The same antibacterial agent Sorbicillin and his derivatives,[116,117] which are investigated for different applications,[118] contain this interesting feature. Furthermore, conjugated dienones can be also found as component in foods,[119] such as in oat groat,[120,121] and infusions.[122]

Traditionally, target compounds **7** have been synthesized using well-established methods such as the Wittig-Horner reaction (**Scheme 2.26, Example a**), as reported by Paulsen et al;[123] Cadierno documented the synthesis of dienones starting from propargylic alcohol, that undergoes a ruthenium catalyzed Meyer-Schuster rearrangement and a subsequent Knoevenagel condensation with hexafluoropentanedione (**Scheme 2.26, Example b**), providing the product upon treatment with an excess of K_2CO_3;[124] and, to a lesser extent, by Claisen rearrangement, as reported by Giovannini et al.[125], that obtain the desired product starting from functionalized γ-hydroxyvinyl sulfones, after a DBU-promoted elimination of benzebsulfinic acid from 3-phenylsulfonyl ester derivatives (**Scheme 2.26, Example c**). However, it is worth noting that these approaches often suffer from limitations due to their requirement for harsh reaction conditions, which can be detrimental to the presence of

sensitive functional groups, thereby reducing the substrate scope and potentially affecting the stereochemistry of the final products.

Attempts have been made to address these limitations with the development of new strategies, which has brought advancements in the synthesis of conjugated dienones. However, these protocols introduce their own challenges, including the reliance on precious and toxic metals (such as Pd, Ru, Rh, Ir) as catalysts and the requirement for complex starting molecules.[126,127] In this sense, one example is provided by Pan et al.[128] with the synthesis of conjugated (*E,E*)-dienones from palladium-catalyzed γ,δ-dehydrogenation of enones under oxygen atmosphere (**Scheme 2.26, Example d**).

Balancing the benefits and drawbacks of these new methodologies is crucial to ensure sustainable, efficient, and practical approaches.

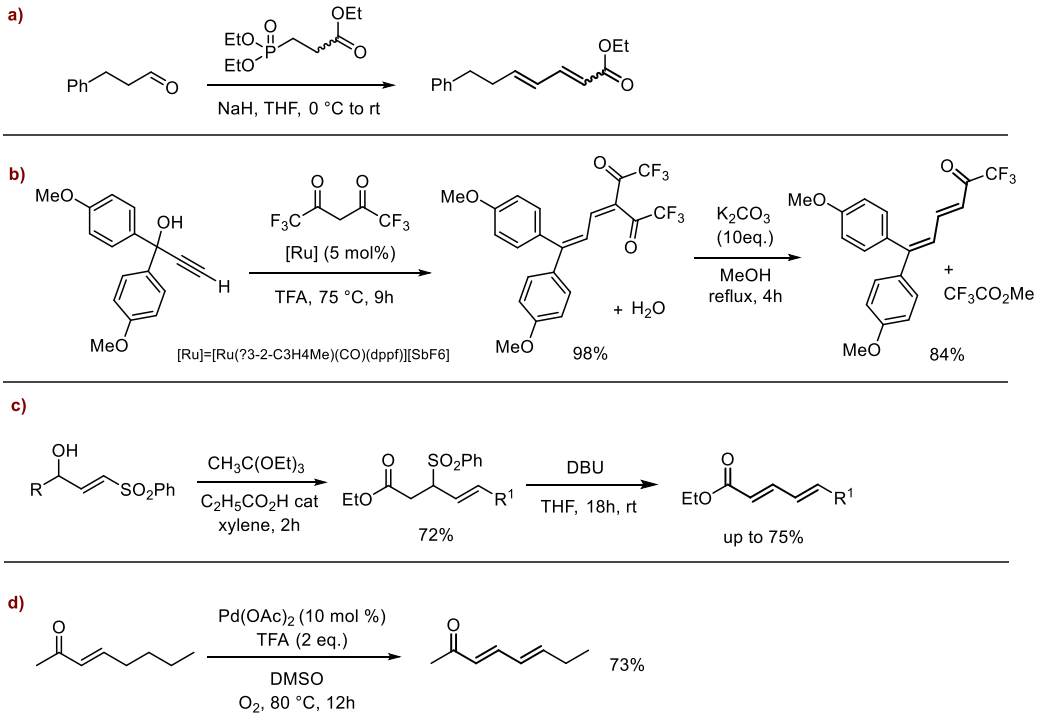

Scheme 2.26 Synthetic procedures for the synthesis of conjugated dienones

2.3.2 Results and discussion

Excited and motivated by our serendipitous discovery, we started investigating the required conditions for the conversion of β-nitro-β,γ-unsaturated ketone **2a** into compound **7a**, that was initially obtained, in presence of diethylmalonate, using of carbonate on silica and 2-MeTHF as solvent, at room temperature. The effectiveness of the reaction was confirmed when the product was isolated even if diethylmalonate was omitted from the experiment, but only in 38% yield. Besides, a complex mixture of inseparable byproducts was detected.

To optimize the reaction conditions for the synthesis of our target, we focused on **2a** as the model substrate and conducted a series of preliminary trials on a 0.5 mmol scale. The screening aimed to evaluate extensively the conversion considering various variables, such as temperature, base, acidic species, solvent, concentration, and stoichiometry (**Table 2.2**).

After the results obtained using carbonate on silica, that seemed to be too reactive, we decided to investigate the conversion conducing the trials in 2-methyltetrahydrofuran (0.05 M) and using K_2CO_3 (1.5 eq.) and silica (0.7 g), respectively as base and source of proton (**Table 2.2, Entry 2**).

Table 2.2 Optimization studies

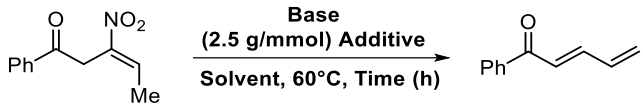

2a **7a**

Entry	Base [eq.]	Additive[a]	Solvent [M]	T [°C]	t [h]	Yield 7a [%][b]
1	Carbonate on Silica [2]	-	2-MeTHF [0.05]	rt	4.5	38
2	K_2CO_3 [1.5]	Silica	2-MeTHF [0.05]	rt	120	42
3	K_2CO_3 [1.5]	-	2-MeTHF [0.05]	rt	120	-
4	-	Silica	2-MeTHF [0.05]	rt	120	-
5	K_2CO_3 [1.5]	Silica	2-MeTHF [0.05]	40	35	46
6	K_2CO_3 [1.5]	Silica	2-MeTHF [0.05]	60	19	52
7	K_2CO_3 [2]	Silica	2-MeTHF [0.05]	60	8	60
8	K_2CO_3 [3]	Silica	2-MeTHF [0.05]	60	8	53
9	K_2CO_3 [2]	Silica [0.35]	2-MeTHF [0.05]	60	12	34
10	KF/Alumina [2]	-	2-MeTHF [0.05]	60	2	Degr.
11	SiO_2-$(CH_2)_2NEt_2$ [2]	-	2-MeTHF [0.05]	60	24	-
12	K_2CO_3 [2]	Silica	MeCN [0.05]	60	5	64
13	K_2CO_3 [2]	Silica	EtOAc [0.05]	60	5	51
14	K_2CO_3 [2]	Silica	Dioxane [0.05]	60	5	43
15	Cs_2CO_3 [2]	Silica	MeCN [0.05]	60	1.5	49
16	K_3PO_4 [2]	Silica	MeCN [0.05]	60	3	52
17	KF [2]	Silica	MeCN [0.05]	60	7.5	48
18	K_2CO_3 [2]	Silica	MeCN [0.1]	60	5	58
19	K_2CO_3 [2]	Silica	MeCN [0.025]	60	5	73
20	K_2CO_3 [2]	Silica	MeCN [0.00125]	60	5	70
21	K_2CO_3 [2]	Mont. K10	MeCN [0.025]	60	7.5	32
22	K_2CO_3 [2]	Amberlyst® 15	MeCN [0.025]	60	7	27
23	K_2CO_3[2]	Acidic alumina	MeCN [0.025]	60	7.5	9

[a] 0.7 g unless otherwise indicated

[b] Yield of pure isolated product

To further confirm the importance of both reagents we conducted two experiments in the absence of the one and the other (**Table 2.2, Entries 3-4**), that resulted in no product formation at all.

When we tried to increase the temperature (**Table 2.2, Entries 5-6**) a better yield of **7a** was obtained, reaching its best outcome when 2 equivalent of potassium carbonate were used at 60 °C, with a 60% yield in 8 hours (**Table 2.2, Entry 7**). Any attempts to further increase the equivalents of K_2CO_3 or to reduce the amount of silica (**Table 2.2, Entries 8-9**), had detrimental consequences.

Later, we screened other solid supported species, such as KF on alumina and triethylamine on silica, which could be potentially used both as base and proton source (**Table 2.2, Entries 10-11**). Potassium fluoride on basic alumina was ineffective in promoting the reaction at room temperature, but led to the total degradation of the substrate at 60 °C. On the other hand, triethylamine on silica resulted completely ineffective even at 60 °C.
Successively, we focused our attention on the solvents (**Table 2.2, Entries 12-14**), and encouraged by the 64% yield of **7a** obtained with MeCN in 5 hours (**Table 2.2, Entry 12**) we tested other bases, namely Cs_2CO_3, K_3PO_4 and KF (**Table 2.2, Etries 15-17**), but no reaction improvement was observed. Finally, an examination of possible reaction concentrations (**Table 2.2, Entries 18-20**) led to the isolation of **7a** in 73% yield, when performing the trial in a 0.025 M solution of **2a** in MeCN at 60 °C (**Table 2.2, Entry 19**).
In the end, other acids (Montmorillonite K10, Amberlyst® 15 and acidic alumina) were examined (**Table 2.2, Entries 20-23**), but also in these cases no yield improvement was possible.

As consequence of our optimization screening, we explored the general applicability of our protocol, testing a variety of *β*-nitro-*β,γ*-unsaturated ketones (**2aa–al**) under the optimized reaction conditions (**Scheme 2.27**). In all cases, the desired conjugated dienones **7aa–al** were obtained with good yields, ranging from 61% to 71%. Notably, our synthesis confirmed to be stereoselective, as the conjugated dienones were all isolated in the *E,E* configuration.
Another significant advantage of our optimized, mild and metal-free reaction conditions was the preservation of key functionalities that can be important for further manipulations. Functional groups such as ether, ester, cyano, trifluoromethyl groups, as well as unconjugated double bonds and chlorine atoms, remained intact during the reaction. In addition, instead of resorting to conventional wasteful aqueous treatments, our method involves a straightforward filtration and evaporation step, improving the efficiency of the synthetic process and also minimizing material and waste generation, making the overall procedure more sustainable.
We also successfully demonstrated the scalability of our procedure by performing the model reaction on a 5 mmol scale, obtaining compound **7a** in 72% yield.

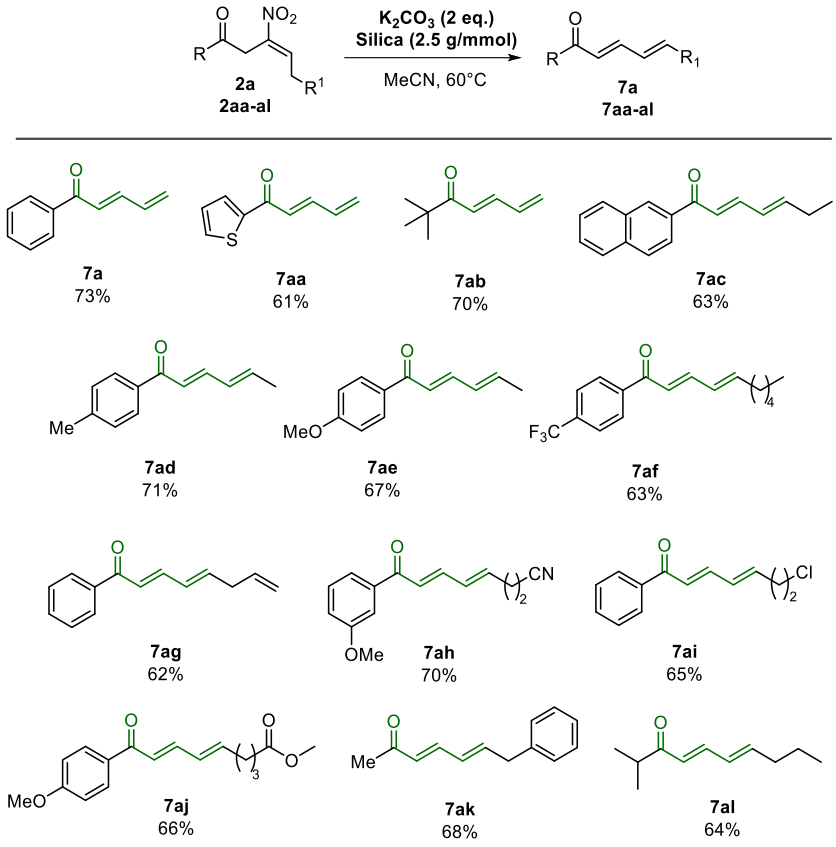

Scheme 2.27 Substrate scope demonstration

Overall, we proposed a reaction mechanism for the transformation, suggesting that the synthesis of dienones **7** involves an initial deprotonation of **2** in the δ allylic position to form the nitronate anion **A**. This is followed by protonation of the generated nitronic acid intermediate **B** that provide β-nitroketone **C**. Lastly, base-assisted elimination of nitrous acid from **C** leads to the formation of dienones **7**.[129] **Scheme 2.28** provides a visual representation of this plausible reaction mechanism.

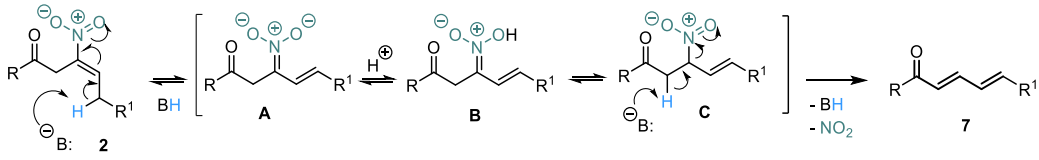

Scheme 2.28 Proposed reaction mechanism

2.3.3 Experimental section

General procedure for the synthesis of conjugated dienones 7a and 7aa-al

A solution of β-nitro-β,γ-unsaturated ketone **2** (0.5 mmol) in MeCN (20 mL) was treated with K_2CO_3 (1 mmol) and silica (1.2 g), and stirred at 60°C for the appropriate time. Then, the reaction mixture was filtered through a Gooch funnel (G2) washing the solid residue with fresh ethyl acetate (20 mL). Finally, the filtrate was concentrated under reduced pressure to give the crude product **7**, which was purified by flash column chromatography (hexane:ethyl acetate = 95:5).

Spectroscopic data of compounds 7a and 7aa-al

Compound 7a
Yield 73% (58 mg). Pale yellow oil. **IR** (cm^{-1}, neat): 663, 686, 705, 783, 1008, 1017, 1219, 1272, 1447, 1586, 1612, 1663. **^{1}H-NMR** ($CDCl_3$, 400MHz) δ: 5.59 (ddd, 1H, *J* = 10.0, 1.3, 0.7 Hz), 5.72 (ddd, 1H, *J* = 16.9, 1.4, 0.7 Hz), 6.53-6.65 (m, 1H), 6.99 (dd, 1H, *J* = 15.1, 0.7 Hz), 7.33-7.46 (m, 1H), 7.48 (dd, 2H, J = 7.4, 0.9 Hz), 7.53-7.59 (m, 1H), 7.94 (dd, 2H, *J* = 8.3, 1.3 Hz). **^{13}C-NMR** ($CDCl_3$, 100MHz) δ: 126.2, 126.9, 128.4, 128.6, 132.8, 135.4, 137.9, 144.7, 190.7. **GC-MS** (70eV): *m/z :* 158 (M^+, 100), 157 (38), 129 (61), 115 (29), 105 (62), 81 (25), 77 (64), 54 (32), 51 (37). **Anal. Calcd. For $C_{11}H_{10}O$** (158.20): C, 83.52; H, 6.37. **Found**: C, 83.56; H, 6.40.

Compound 7aa
Yield 61% (50 mg). Yellow oil. **IR** (cm^{-1}, neat): 717, 775, 860, 1005, 1275, 1409, 1514, 1584, 1607, 1648. **^{1}H-NMR** ($CDCl_3$, 400MHz) δ: 5.60 (ddd, 1H, *J* = 9.9, 1.3, 0.6 Hz), 5.73 (ddd, 1H, *J* = 16.9, 1.3, 0.6 Hz), 6.52-6.64 (m, 1H), 6.89 (d, 1H, *J* = 15.0 Hz), 7.15 (dd, 1H, *J* = 4.9, 3.8 Hz), 7.43 (dd, 1H, *J* = 15.0, 11.1 Hz), 7.66 (dd, 1H, *J* = 4.9, 1.1 Hz), 7.77 (dd, 1H, *J* = 3.8, 1.1 Hz). **^{13}C-NMR** ($CDCl_3$, 100MHz) δ: 125.7, 127.1, 128.2, 131.8, 133.9, 135.1, 144.0, 145.3, 182.3. **GC-MS** (70eV): *m/z :* 164 (M^+, 100), 135 (96), 111 (93), 91 (24), 53 (33), 39 (35). **Anal. Calcd. For C_9H_8OS** (164.22): C, 65.82; H, 4.91; S, 19.52. **Found**: C, 65.87; H, 4.88; S, 19.55.

Compound 7ab
Yield 70% (48 mg). Pale yellow oil. **IR** (cm^{-1}, neat): 1203, 1600, 1626, 1660. **^{1}H-NMR** ($CDCl_3$, 400MHz) δ: 1.15 (s, 9H), 5.51 (ddd, 1H, *J* = 10.0, 1.4, 0.7 Hz), 5.64 (ddd, 1H, *J* = 16.9, 1.3, 0.7 Hz), 6.40-6.51 (m, 1H), 6.57 (d, 1H, *J* = 15.0 Hz), 7.20-7.29 (m, 1H). **^{13}C-NMR** ($CDCl_3$, 100MHz) δ: 26.2, 43.0, 124.9, 126.2, 135.2, 142.9, 204.6. **GC-MS** (70eV): *m/z :* 138 (M^+, 2), 110 (58), 95 (18), 81 (100), 57 (65), 53 (55), 41 (39), 29 (14). **Anal. Calcd. For $C_9H_{14}O$** (138.21): C, 78.21; H, 10.21. Found: C, 78.16; H, 10.18.

Compound 7ac
Yield 63% (74 mg). Pale yellow oil. **IR** (cm^{-1}, neat): 472, 751, 997, 1122, 1461, 1586, 1625, 1656. **^{1}H-NMR** ($CDCl_3$, 400MHz) δ: 1.12 (t, 3H, *J* = 7.5 Hz), 2.23-2.34 (m, 2H), 6.28-6.44 (m, 2H), 7.09 (d, 1H, *J* = 15.1 Hz), 7.52 (dd, 1H, *J* = 15.0, 10.0 Hz), 7.54-7.63 (m, 2H), 7.87-7.94 (m, 2H), 7.98 (d, 1H, *J* = 8.0 Hz), 8.07 (dd, 1H, *J* = 8.6, 1.7 Hz), 8.48 (s, 1H). **^{13}C-NMR** ($CDCl_3$, 100MHz) δ: 12.9, 26.3, 123.7, 124.5, 126.7, 127.8, 128.2, 128.3, 128.4, 129.5, 129.7, 132.6, 135.4, 135.7, 145.4, 147.8, 190.6. **GC-MS** (70eV): *m/z :* 236 (M^+, 39), 207 (100), 179 (22), 155 (12), 127 (40). **Anal. Calcd. For $C_{17}H_{16}O$** (236.31): C, 86.40; H, 6.82. **Found**: C, 86.45; H, 6.85.

Compound 7ad

Yield 71% (65 mg). White solid, **m.p.** = 64-66°C. **IR** (cm^{-1}, neat): 782, 999, 1258, 1340, 1580, 1607, 1625, 1653. **^{1}H-NMR** ($CDCl_3$, 400MHz) δ: 1.89 (dd, 3H, *J* = 6.4, 0.6 Hz), 2.41 (s, 3H), 6.19-6.39 (m, 2H), 6.87 (d, 1H, *J* = 15.1 Hz), 7.26 (d, 2H, *J* = 7.9 Hz), 7.39 (dd, 1H, *J* = 15.0, 10.2 Hz), 7.85 (d, 2H, *J* = 8.1 Hz). **^{13}C-NMR** ($CDCl_3$, 100MHz) δ: 18.9, 21.6, 123.3, 128.5, 129.2, 130.6, 135.7, 140.8, 143.3, 144.8, 190.4. **GC-MS** (70eV): *m/z :* 186 (M^+, 36), 171 (100), 143 (20), 128 (21), 119 (20), 91 (29), 65 (21), 39 (11). **Anal. Calcd. For $C_{13}H_{14}O$** (186.25): C, 83.83; H, 7.58. **Found**: C, 83.78; H, 7.55.

Compound 7ae

Yield 67% (68 mg). White solid, **m.p.** = 74-76°C. **IR** (cm^{-1}, neat): 610, 793, 840, 1005, 1250, 1344, 1582, 1601, 1627, 1652. **^{1}H-NMR** ($CDCl_3$, 400MHz) δ: 1.89 (d, 3H, *J* = 6.2 Hz), 3.86 (s, 3H), 6.18-6.38 (m, 2H), 6.88 (d, 1H, *J* = 15.4 Hz), 6.94 (d, 2H, *J* = 9.0 Hz), 7.39 (dd, 1H, *J* = 15.0, 10.4 Hz), 7.95 (d, 2H, *J* = 9.0 Hz). **^{13}C-NMR** ($CDCl_3$, 100MHz) δ: 18.9, 55.5, 113.7, 123.1, 130.6, 131.2, 140.5, 144.4, 163.2, 189.1. **GC-MS** (70eV): *m/z :* 202 (M^+, 64), 187 (100), 159 (22), 135 (43), 92 (19), 77 (25). **Anal. Calcd. For $C_{13}H_{14}O_2$** (202.25): C, 77.20; H, 6.98. **Found**: C, 77.24; H, 7.01.

Compund 7af

Yield 63% (93 mg). Pale yellow oil. **IR** (cm^{-1}, neat): 1065, 1128, 1109, 1319, 1590, 1627, 1665. **^{1}H-NMR** ($CDCl_3$, 400MHz) δ: 0.90 (t, 3H, *J* = 6.9 Hz), 1.26-1.36 (m, 4H), 1.41-1.51 (m, 2H), 2.23 (q, 2H, *J* = 6.8 Hz), 6.29-6.34 (m, 2H), 6.84 (d, 1H, *J* = 15.1 Hz), 7.38-7.46 (m, 1H), 7.73 (d, 2H, *J* = 8.2 Hz), 8.01 (d, 2H, *J* = 8.2Hz). **^{13}C-NMR** ($CDCl_3$, 100MHz) δ: 14.0, 22.5, 28.3, 31.4, 32.3, 123.0, 125.5 (q, *J* = 3.8 Hz), 128.6, 128.9, 133.7 (q, J = 32.8 Hz), 141.1, 146.7, 148.0, 190.0. **GC-MS** (70eV): *m/z:* 296 (M^+, 6), 277 (5), 225 (100), 173 (32), 145 (28), 81 (8), 41 (7). **Anal. Calcd. For $C_{17}H_{19}F_3O$** (296.33): C, 68.90; H, 6.46. **Found**: C, 68.94; H, 6.49.

Compound 7ag

Yield 62% (61 mg). Pale yellow oil. **IR** (cm^{-1}, neat): 694, 731, 1000, 1275, 1350, 1590, 1626, 1662. **^{1}H-NMR** ($CDCl_3$, 400MHz) δ: 2.97 (dt, 2H, *J* = 6.3, 0.9 Hz), 5.06-5.14 (m, 2H), 5.79-5.91 (m, 1H), 6.20-6.41 (m, 2H), 6.91 (d, 1H, *J* = 15.1 Hz), 7.38-7.50 (m, 3H), 7.53-7.58 (m, 1H), 7.94 (dd, 2H, *J* = 8.4, 1.3 Hz). **^{13}C-NMR** ($CDCl_3$, 100MHz) δ: 37.1, 116.6, 124.2, 128.4, 128.5, 129.9, 132.6, 134.9, 138.2, 143.0, 144.9, 190.8. **GC-MS** (70eV): *m/z :* 198 (M^+, 12), 157(100), 144 (13), 128 (17), 115 (11), 105 (76), 91 (18), 77 (69), 51 (19), 39 (11). **Anal. Calcd. For $C_{14}H_{14}O$** (198.26): C, 84.81; H, 7.12. **Found**: C, 84.86; H, 7.08.

Compound 7ah

Yield 70% (84 mg). Yellow oil. **IR** (cm^{-1}, neat): 777, 1001, 1025, 1269, 1429, 1580, 1630, 1662, 2246. **^{1}H-NMR** ($CDCl_3$, 400MHz) δ: 2.46-2.60 (m, 4H), 3.85 (s, 3H), 6.12-6.23 (m, 1H), 6.43 (dd, 1H, *J* = 15.2, 10.9 Hz), 6.94 (d, 1H, *J* = 15.1 Hz), 7.10 (ddd, 1H, *J* = 8.2, 2.6, 0.4 Hz), 7.32-7.41 (m, 2H), 7.44-7.53 (m, 2H). **^{13}C-NMR** ($CDCl_3$, 100MHz) δ: 16.9, 28.7, 55.5, 112.7, 118.7, 119.4, 120.9, 125.7, 129.6, 131.7, 139.2, 139.3, 143.5, 159.9, 190.2. **GC-MS** (70eV): *m/z :* 241 (M^+, 41), 201 (30), 187 (100), 159 (17), 135 (24), 107 (17), 77 (25). **Anal. Calcd. For $C_{15}H_{15}NO_2$** (241.29): C, 74.67; H, 6.27; N, 5.81. **Found**: C, 74.72; H, 6.30; N, 5.78.

Compound 7ai

Yield 65% (72 mg). Yellow solid, **m.p.** = 35-37°C. **IR** (cm^{-1}, neat): 666, 686, 1001, 1257, 1447, 1574, 1585, 1625, 1659. **^{1}H-NMR** ($CDCl_3$, 400MHz) δ: 2.68 (dq, 2H, *J* = 6.8, 1.2 Hz), 3.61 (t, 2H, *J* = 6.8 Hz), 6.16-6.25 (m, 1H), 6.37-6.46 (m, 1H), 6.94 (d, 1H, *J* = 15.1 Hz), 7.39 (dd, 1H, *J* = 15.1, 10.9 Hz), 7.43-7.50 (m, 2H), 7.52-7.58 (m, 1H), 7.93 (dd, 2H, *J* = 8.4, 1.3 Hz). **^{13}C-NMR** ($CDCl_3$, 100MHz) δ: 36.0, 43.1, 125.0, 128.4, 128.6, 131.7, 132.7, 138.1, 140.1, 144.1, 190.7. **GC-MS** (70eV): *m/z :* 220 (M+, 10), 171 (8), 157 (100), 128 (15), 105 (20), 77 (32), 51 (13). **Anal. Calcd. For $C_{13}H_{13}ClO$** (220.70): C, 70.75; H, 5.94. **Found**: C, 70.79; H, 5.91.

Compound 7aj

Yield 66% (95 mg). White solid, **m.p.** = 71-73°C. **IR** (cm^{-1}, neat): 838, 999, 1017, 1168, 1238, 1254, 1583, 1599, 1625, 1652, 1727. **^{1}H-NMR** ($CDCl_3$, 400MHz) δ: 1.73-1.85 (m, 2H), 2.24 (q, 2H, *J* = 7.1 Hz), 2.34 (t, 2H, *J* = 7.4 Hz), 3.66 (s, 3H), 3.86 (s, 3H), 6.12-6.21 (m, 1H), 6.32 (dd, 1H, *J* = 15.2, 10.9 Hz), 6.90 (d, 1H, *J* = 15.0 Hz), 6.94 (d, 2H, *J* = 8.9 Hz), 7.37 (dd, 1H, *J* = 15.0, 10.8 Hz), 7.94 (d, 2H, *J* = 8.9 Hz). **^{13}C-NMR** ($CDCl_3$, 100MHz) δ: 24.0, 32.5, 33.5, 51.9, 55.8, 114.4, 124.5, 130.7, 131.4, 131.8, 144.7, 144.8, 164.2, 174.7, 190.1. **GC-MS** (70eV): *m/z :* 288 (M^+, 14), 187 (93), 135 (100), 77 (26). **Anal. Calcd. For $C_{17}H_{20}O_4$** (288.34): C, 70.81; H, 6.99. **Found**: C, 70.85; H, 7.03.

Compound 7ak

Yield 68% (63 mg). Yellow oil. **IR** (cm^{-1}, neat): 698,995,1254, 1360, 1494, 1594, 1630, 1665, 1687. **^{1}H-NMR** ($CDCl_3$, 400MHz) δ: 2.26 (s, 3H), 3.52 (d, 2H, *J* = 6.6 Hz), 6.09 (d, 1H, *J* = 15.7 Hz), 6.14-6.36 (m, 2H), 7.12 (dd, 1H, *J* = 15.6, 10.4 Hz), 7.14-7.35 (m, 5H). **^{13}C-NMR** ($CDCl_3$, 100MHz) δ: 27.2, 39.4, 126.5, 128.7, 129.6, 129.8, 138.7, 143.2, 143.4, 198.7. **GC-MS** (70eV): *m/z :* 186 (M^+, 28), 143 (69), 128 (81), 115 (38), 95 (100), 91 (27), 82 (36), 65 (18), 43 (29). **Anal. Calcd. For $C_{13}H_{14}O$** (186.25): C, 83.83; H, 7.58. **Found**: C, 83.79; H, 7.55.

Compound 7al

Yield 64% (53 mg). Clear oil. **IR** (cm^{-1}, neat): 999, 1207, 1466, 1595, 1633, 1664, 1687. **^{1}H-NMR** ($CDCl_3$, 400MHz) δ: 0.91 (t, 3H, *J* = 7.4 Hz), 1.11 (dd, 6H, *J* = 6.9 Hz), 1.39-1.52 (m, 2H), 2.10-2.19 (m, 2H), 2.74-2.87 (m, 1H), 6.08-6.24 (m, 3H), 7.13-7.24 (m, 1H). **^{13}C-NMR** ($CDCl_3$, 100MHz) δ: 13.7, 18.5, 21.9, 35.1, 38.8, 126.0, 129.0, 142.9, 145.5, 204.4. **GC-MS** (70eV): *m/z :* 166 (M^+, 12), 123 (100), 95 (39), 81 (54), 67 (15), 53 (18), 41 (14). **Anal. Calcd. For $C_{11}H_{18}O$** (166.26): C, 79.46; H, 10.91. **Found**: C, 79.51; H, 10.94.

NMR Spectra of the described compounds can be found at:

https://doi.org/10.1002/adsc.202201151

2.4 Thesis work: Photocatalyzed hydroalkylation of nitroolefins in batch and flow

The results presented in this section are adapted from:

More Chips to Nitroolefins: Decatungstate Photocatalysed Hydroalkylation Under Batch and Flow Conditions, Jorea, A., Bassetti, B., Gervasoni, K., Protti, S., Palmieri, A., Ravelli, D., *Adv. Synth. Catal.* **2023**, *365*, 1 – 7

2.4.1 Introduction

In photochemical reactions, radicals can be formed through two fundamental approaches. The first one relies on a substrate containing directly exciting functional groups or chromophores, where light absorption leads to the formation of a radical intermediate. The second approach involves the use of a light-absorbing catalyst (photocatalyst, **PC**), where electron or hydrogen atom transfer occurs between the catalyst and an organic molecule, upon excitation. Generally, both approaches require suitable functional groups in the starting materials to guide the reaction pathway and facilitate the desired photochemical transformations.

Photocatalysis relies on the ability of transition metal complexes,[130] usually polypyridyl complexes of rhutenium and iridium, or organocatalysts, such as aromatic ketones, quinones, heterocycles and dyes,[131] to engage different possible pathways when excited (**PC***)[132]:

- single electron transfer (SET), interacting with a SD, a sacrificial electron donor
- single electron transfer (SET), interacting with an AD, a sacrificial electron acceptor generating a reducing or oxidizing catalyst toward the desired substrate
- direct energy transfer, generating an electronically excited substrate ***S**
- proton-coupled electron transfer (PCET)
- hydrogen atom transfer (HAT), generally considered a subclass of PCET, and that can be either direct or indirect

In fact, HAT can be defined as a process in which there is a concerted movement of a proton and an electron (H• ≡ H+ +e−), that share the starting and final orbitals, between to substrates in a single kinetic step.[133]

Direct hydrogen atom transfer (**Scheme 2.29**) is achieved by using a selected photocatalyst, which upon excitation (**PC*** = **X**• = hydrogen abstractor), is responsible for substrate activation by extraction of an hydrogen from a donor (R-**H**), thus generating a radical **R***. Hydrogen-catalyst radical •**PC-H** is formed consequentially. The final product can be generated after hydrogen back-

donation (back-HAT step) from **•PC-H** or through a sequential electron/proton transfer (ET/PT) mechanism toward a chemical species **Y** (already present or transiently formed within the process), regenerating the **PC**.

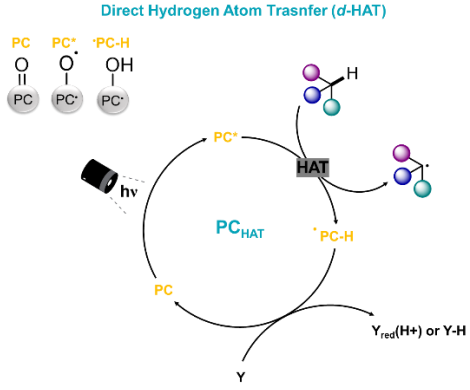

Scheme 2.29 Direct Hydrogen Atom Transfer cycle

Notably, hydrogen atom transfer (HAT) plays a crucial role in a wide range of chemical reactions, including hydrocarbon combustion, aerobic oxidations, and various atmospheric phenomena.[133]
HAT represent one of the most interesting strategy for aliphatic C-H bond's activation, known to be an "unfunctional group", that generally relies on the use of activating or directing groups.[134] The are different factors to take into account when operating the selective HAT-based C−H functionalization, such as: (1) the bond strength of the C-H bond that needs to be cleaved – generally the lower is the bond dissociation energy the more stable is the generated radical, (2) hyperconjugation and conjugation, (3) the strain release associated to the cleavage, (4) steric hindrance, (5) the proximity of polar functionalities as well as the polarity discrepancy between the hydrogen abstractor and character of the C−H bond, (6) the presence of electron-donating functionalities whose non-bonding electrons can activate C-H through hyperconjugation, (7) stereoelectronic effect of possible heteroatoms; of course also the presence of solvents or additive that could act as hydrogen bond donor or acceptor has to be considered.[135]
It is of primary importance the accurate selection of the hydrogen abrstractor that will be photochemically generated, considering that the newly formed X−H bond has to be stronger than the C−H that needs to be cleaved.
The majority of the HAT photocatalysts (PC_{HAT}) exhibit a common structural motif, which is the presence of an oxo group (Z=O). In the reactive excited state, this oxo group acquires a distinct O-centered radical character, that closely resembles electrophilic alkoxyl radicals, which have a strong capability to abstract hydrogen atoms from C-H bonds. Generally, they can be classified on the base of the X-element that carries the oxo moiety, that can be a carbonyl derivatives, which includes simple aromatic ketones and aldehydes, α-diketones, α-ketoacids, and (anthra)quinones, or inorganic ones, such as the decatungstate anion $[W_{10}O_{32}]^{4-}$ (Z = W) and the uranyl cation $[UO_2]^{2+}$ (Z = U).[136]

Among these, decatungstate anion $(W_{10}O_{32})^{4-}$ has emerged as promising PC_{HAT} for the generation of carbon-centered radicals thanks to his high photocatalytic activity,[137] and it is usually employed as tetrabutylammonium salt (TBADT: tetrabutylammonium decatungstate, $(n\text{Bu}_4\text{N})_4[W_{10}O_{32}]$) (**Figure 2.7**).[138] This catalyst is part of the polyoxometalates (POMs) family which are molecular metal oxide anions, characterized by the presence of three or more metal centers in their high oxidation state.[139]

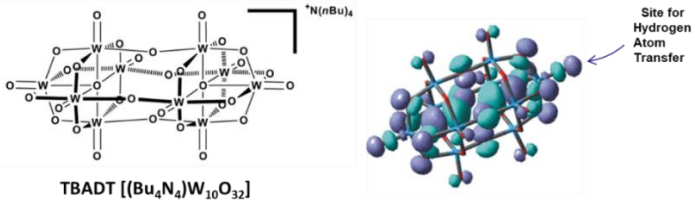

Figure 2.7 Tetrabutylammonium decatungstate structure; 3D image taken from ref.[139]

Among its advantages, such as high reactivity and selectivity, TBADT can be prepared in a single step from inexpensive precursors. For these reasons, it has been widely used over the years and applied for different C−H functionalizations.[136,140–144]

As photocatalytic strategies have gained significant attention, the reactivity of nitro compounds has been explored only to a limited extent. For what concerns nitroalkenes, the attention has been mainly focused on their role as traps for generated radical intermediates, and primarily restricted to β-nitrostyrene derivatives.[145] In these derivatives, the loss of the nitro group ($-NO_2$) in a quantitative manner leads to an *ipso*-substitution process (**Scheme 2.30**). However, this approach has proven to be successful in the synthesis of various synthetic targets, including stilbenes,[146] chalcones,[147] vinyl thiocyanates,[148] trifluoromethyl alkenes,[149] as well as in the alkenylation of cyclic ethers and unactivated alkenes.[150,151]

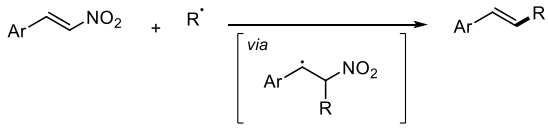

Scheme 2.30 Radical mediated ipso-substitution on nitroolefins

Until now, the retention of the nitro group in the final product has been reported only in a few specific cases. For example, in the photocatalyzed alkylation of indoles, using chromium-complexes and rose Bengal (**Scheme 2.31**),[152] and in the preparation of Diels-Alder adducts (only one reported example where the nitro group is retained).[153]

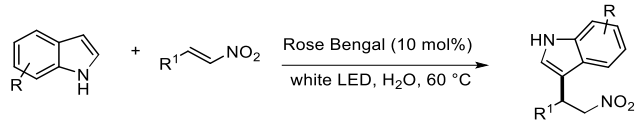

Scheme 2.31 Friedel–Craft alkylation of indoles with nitroalkenes in presence of Rose Bengal

2.4.2 Results and discussion

In order to start our investigation, we selected (*E*)-1-nitrooct-1-ene **8a** and 2,2-dimethyl-1,3-dioxolane **9a**, the hydrogen atom donor, as model reactants for the formation of product **10** (**Scheme 2.32**). To establish the reaction conditions, we initially adapted methodologies that had been previously employed favourably for the functionalization of C-H bonds in oxygenated heterocycles (**Table 2.3**).[143,154]

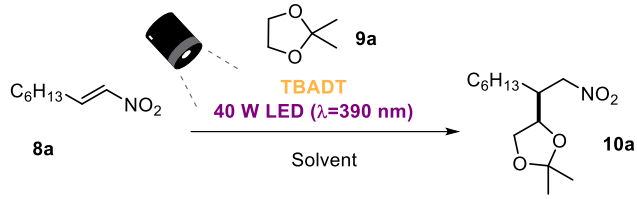

Scheme 2.32 General reaction scheme for the hydroalkylation of nitroolefins

The selection of the correct wavelength, at which subsequently conduct our studies, was empirically established by examination of the UV-Vis spectra of the catalyst, and compared to the absorption of some selected nitroolefins of our interest (**8a**, **c**, **d**). In fact, the excitation of the decatungstate anion calls for the use of a light source emitting around 390 nm, wherein the employed nitroolefins may absorb as well. As reported in **Figure 2.8**, compounds **8 a**, **d** exhibit only a modest absorption at wavelengths >300 nm, thus not hampering photocatalyst excitation and the formation of hydroalylated products **10**. On the other hand, the UV-Vis spectrum of *β*-nitrostyrene **8c** features an intense absorption in the near UV range tailing at wavelengths >380 nm, suggesting the prevention of photocatalyst excitation.

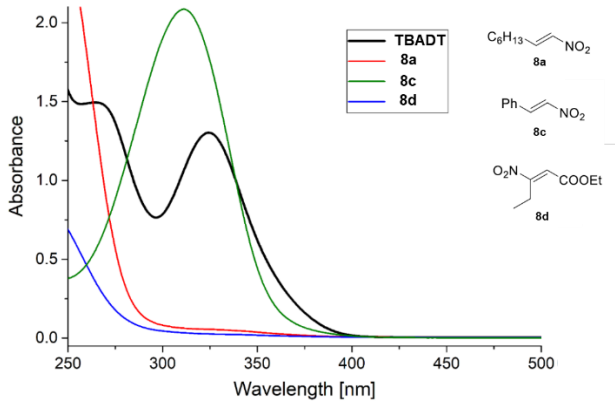

Figure 2.8 UV-Vis spectra of 10^{-4} M MeCN solutions of nitroalkenes 8a, 8c and 8d, along with TBADT

The optimization was performed in a Pyrex vessel containing (E)-1-nitrooct-1-ene **8a** (5 mmol), in presence of 5 equivalent of **9a** and the catalyst TBADT in 2 mol%, using MeCN as solvent (5 mL).[135] The reaction mixture was subjected to irradiation using a 390 nm LED lamp with a power of 40 W for a reaction time of 6 hours, keeping the temperature of 0 °C using an ice bath. Under these conditions the desired adduct **10a** (mixture of diastereoisomers) was obtained with a 83% yield, as determined by gas chromatography (GC) analysis.

Table 2.3 Optimization of β-nitroalkenes hydroalkylation

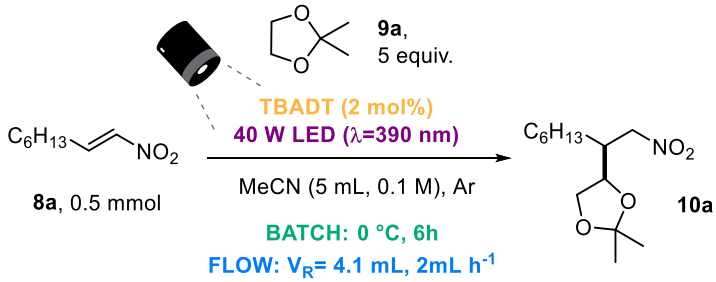

Entry	Variations from standard conditions	10a [GC yield]
1	none	83%
2	room temperature	39%
3	λ = 390 nm (50% power)	41%
4	λ = 427 nm	37%
5	λ = 456 nm	n.d.
6	TBADT omitted	n.d.
7	in the dark	n.d.
8	TEMPO (1 eq) as additive	Traces
9	flow conditions, rt	90%
10	flow conditions, 0 °C	89%

A subsequent screening of possible variables was performed to optimize the reaction performance. In particular, when the reaction was conducted a room temperature (**Table 2.3, Entry 2**), the product was formed but with a significant decrease in term of yield.
When the power of the 390 nm LED lamp was reduced to 50% of its maximum level, or when lamps emitting light at less energetic wavelengths (specifically, 427 nm and 456 nm lamps with a power of 40 W) were employed, it had a negative impact on the outcome of the reaction. This is evidenced by the results observed in **Table 2.3 Entries 3-5** of the experimental table, where the yield of the desired product was lower compared to the original conditions, with 50% of unreacted starting material **8a** detected in the first case (**Table 2.3, Entry 3**).
Necessary control experiments were also performed, thus demonstrating that both the presence of light and the catalyst are mandatory for the formation of **10a** (**Table 2.3, Entries 6-7**).
Conducting the reaction with the addition of 1 equivalent of 2,2,6,6-tetramethylpyrrolidine-N-oxyl (TEMPO) as co-catalyst to the reaction mixture resulted in the formation of only traces amount of the desired product **10a** (**Table 2.3, Entry 8**), thus providing important insights and confirmation on the possible radical pathway of the reaction.

In fact, GC-analysis of the same reaction mixture reported in Entry 8 compared to control analysis of reference compounds (nitroalkene **8a**, product **10a** and TEMPO) and a mixture containing only the H-dornor **9a** with TBADT and TEMPO, demonstrated that the additive seemed to completely shut down the formation of product **10a**. In particular, significant amount of unreacted **8a** was detected and an additional peak was present, while no product peak was observed in the mixture. The new one had the same retention time of the peak found when subjecting the mixture of **9a**, catalyst and TEMPO, to GC measurements. A subsequent evaluation of mass spectra of TEMPO and of the new unknown species showed several common peaks, attributable both to the additive skeleton and to **9a**, possibly derived from the formation of the TEMPO adduct of the 2,2-dimethyl-1,3 dioxolan-4-yl radical.
Therefore, the proposed reaction mechanism is the one reported by **Scheme 2.33**.

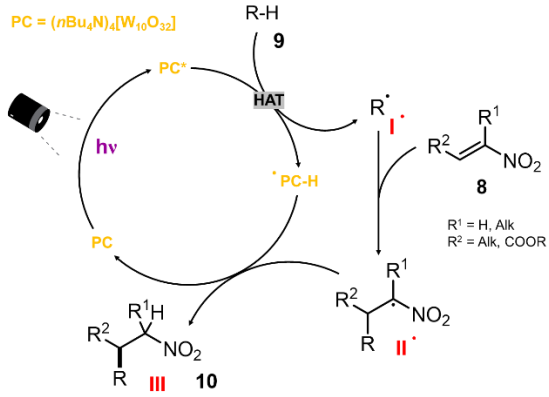

Scheme 2.33 Proposed reaction mechanism

Photoexcited TBADT is responsible for the aliphatic C-H bond-cleavage of the hydrogen donor **9**. Then, the photogenerated alkyl radical intermediate **I•** is intercepted by the nitroolefin **8** leading to the formation of radical adduct **II•** , through conjugate addition. Finally, the formation of the final hydroalkylated product **III** (compound **10**) is coupled with the recovery of the photocatalyst via a back-HAT step.

Then, going back to the experimentation, we transitioned to flow conditions, using a 3D-printed reactor made of polypropylene, already successfully exploited for the hydrofunctionalization of alkenoic acids under TBADT-photocatalyzed conditions.[155] We applied this reactor design to our current study, aiming to improve the reaction efficiency and control. By circulating the reaction mixture using a syringe pump at a flow rate of 2 mL h^{-1} (corresponding to a residence time of 2 hours and 3 min), the desired product **10a** was obtained with a high yield of approximately 90%. Significantly, this was achieved regardless of the temperature used, as indicated in **Table 2.3 Entries 9-10**.

After determining the optimal reaction conditions, we proceeded with the actual isolation of the nitroalkane product **10a** on a 0.5 mmol scale, thus validating the one obtained by GC analysis both in batch (81%) and flow conditions (89%). As expected, the product was isolated as a mixture of diastereoisomers, with a ratio of almost 1:1. We also exploited flow conditions to perform the model reaction between **8a** and **9a** on a larger scale of 2 mmol. In this case, the reaction was conducted at room temperature for ease of operation, and **10a** was isolated in 91% yield.

Subsequently, we evaluated the reaction scope by exploring the applicability of the established conditions to a range of substrates nitroolefins and hydrogen donor (**Scheme 2.34**).

A modification in the substitution pattern on the 1,3-dioxolane ring resulted in a distinct outcome in terms of regioselectivity. Thus, in the case of 2-methyl-1,3-dioxolane **9b**, its functionalization resulted in the clean formation of product **10b** with a yield of 52% using batch conditions (20% at room temperature), exclusively targeting the acetal position. On the other hand, the use of 1,3- dioxolane **9c**, with consequent presence of more reactive sites, yielded a mixture of regioisomers **10c** and **10c'** in a ratio of 2.5:1, considering the higher reactivity of position 2.

Successively, we explored the reactivity of 1,3-benzodioxole **9d** (1.5 equiv. in this case) and tetrahydrofuran **9e** under optimized conditions, which yielded both adducts **10e** and **10f** in 69%.

Functionalization of the 6-membered oxygenated ring of 1,4-dioxane **9f** and tetrahydropyran **9g** resulted in the formation of products **10f** and **10g** with yields of 45% and 61% respectively. In the latter case, the reaction occurred at room temperature under irradiation in only 1 hour.

Conversely, the modification of the 4-membered ring of oxetane **9h** presented greater challenges, and the resulting adduct **10h** could only be isolated with a yield of 48% when exploiting flow conditions.

We then explored the possibility of using substrates that contained various heteroatoms. As a result, tetrahydrothiophene **9i** readily underwent a smooth reaction with 1a, leading to the formation of product **10i** with an isolated yield of 54%. Additionally, *N,N*-dimethyl formamide **9j** and *N,N*-

dimethyl acetamide **9k** yielded adducts **10j** and **10k**, through selective functionalization at the α-to-*N* methyl group, with yields of 72% and 69% respectively.[140]

Unfortunately, when adopting *N*-Boc pyrrolidine as substrate a sluggish reaction was observed and, for this reason, data was not reported.

Cycloalkanes were also found to be suitable substrates, as demonstrated by the successful functionalization of cyclohexane **9l** and cyclooctane **9m**, resulting in the formation of the corresponding products with an isolated yield of 50% in both cases.

Lastly, we investigated the impact of introducing an aromatic substituent on the nitroalkene structure. As a result, the reactivity of (*E*)-(4-nitrobut-3-en-1-yl)benzene **8b** was retained, allowing for the formation of compound **10n** in a good yield, through hydroalkylation with the model H-donor **9a**. Conversely, when *β*-nitrostyrene **8c** was reacted with **9a**, it resulted in the formation of a complex mixture. In fact, when it was measured, compound **8c** featured an intense absorption in the near UV range tailing at wavelengths >380 nm, thus preventing photocatalyst excitation.

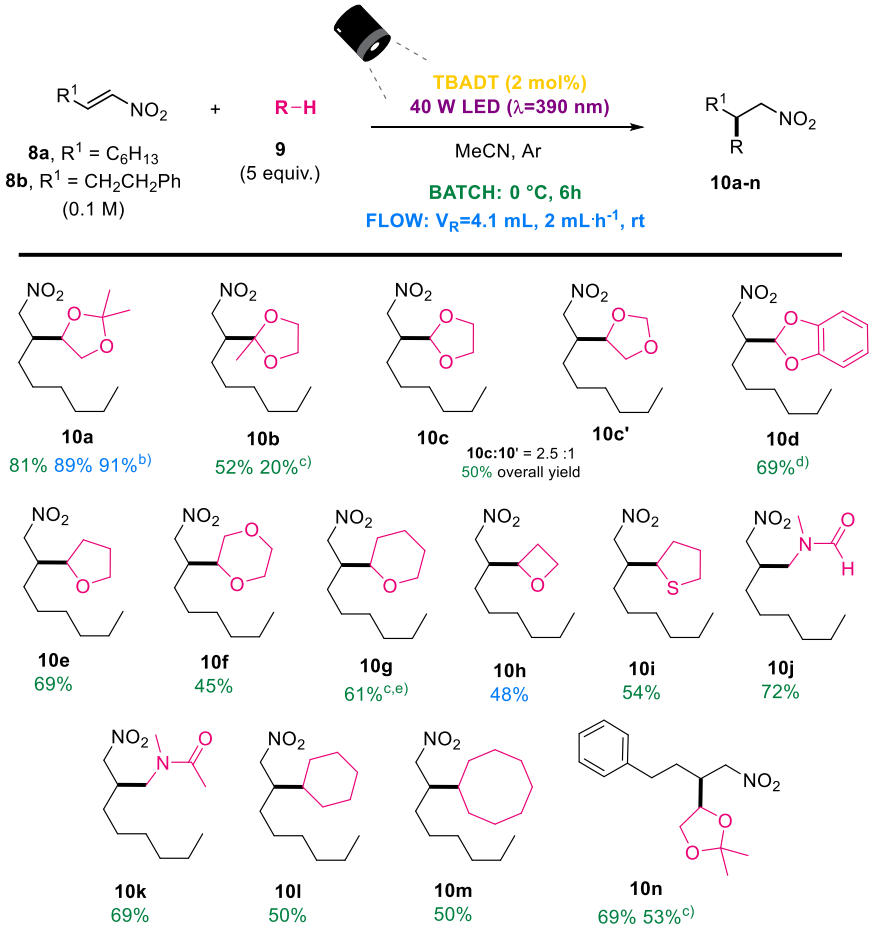

[a] Isolated yields for reactions performed under batch or flow conditions on a 0.5 mmol scale.
[b] Reaction performed on a 2 mmol scale.
[c] Reaction performed at room temperature.
[d] 1.5 equiv. of 1,3-benzodioxole 2 d were used.
[e] Reaction mixture irradiated for 1 h.

Scheme 2.34 Photocatalyzed hydroalkylation of β-nitroalkenes

To further demonstrate the versatility of the procedure under flow conditions, and its applicability in the synthesis of highly functionalized materials, we expanded the photoalkylation investigations to (*E*)-*β*-nitroacrylates, knowing that they have already shown remarkable reactivity upon direct photoirradiation, leading to the corresponding (*Z*)-stereoisomers.[93]

To this scope, we selected *β*-nitroacrylate **8d** as model substrate for our experiments, in the presence of hydrogen-donor 1,3-benzodioxole **9d** (only 1.3 equiv. were sufficient in this case), for the preparation of hydroalkylated product **10o** (**Table 2.4**).
As temperature can significantly influence the reaction profile and final yield of the desired products we transitioned from using the 3D-printed reactor to Syrris Asia modular flow apparatus

(**Experimental section, Figure 2.9** and **2.10**), which can provide enhanced flexibility and fine control over reaction parameters, such as temperature. In fact, the system can easily and stably operates within a broad range of temperature, -40 °C and +80 °C, under irradiation conditions. The flow set-up consisted of 54W LED irradiation system, composed by 4 LED modules (λ=385 nm) positioned in an alternated fashion with "blaks" modules (the system can support max. 8 LED lamps). Moreover, the light can be set at different intensity levels.

Table 2.4 Optimization of *β*-nitroacrylates hydroalkylation

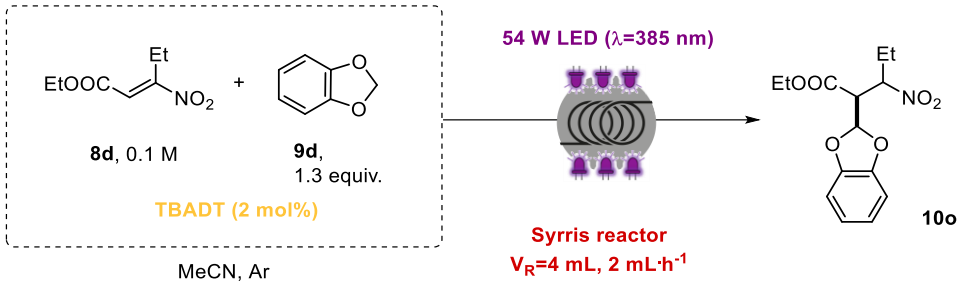

Entry	T [°C]	Light intensity (% power)	10o [yield][b]
1	20	50	48
2	5	50	50
3[c)]	5	50	40
4	-10	50	53
5	-10	100	49
6	-10	25	61
7	-10	15	35
8	-20	25	43

[a)] Reaction conditions: an Ar-bubbled MeCN solution (5 mL)
[b)] Isolated yield
[c)] Reaction carried out under stop-flow conditions.

Initially, the reaction was carried out at 20 °C while maintaining a 2 mL · h^{-1} flow rate, using the LED lamps at their half power. With these conditions, expected product **10o** was obtained in 48% yield (**Table 2.4, Entry 1**), while a decrease to 5 °C resulted in a slight improvement, yielding **10o** in 50% (**Table 2.4, Entry 2**). Operating in "stop-flow" conditions, at the same temperature, led to a consistent yield diminishing (**Table 2.4, Entry 3**).

Encouraging results (53%) were obtained when setting the temperature to -10 °C (**Entry 2.4**), enabling us to proceed on the evaluation of lamps power's impact on the reaction outcome (**Table 2.4, Entries 4-7**). Light intensity of 25% guaranteed the best performance, leading to the formation of products **10o** in 61% yield (**Entry 6**), any further decrease was found detrimental to the process efficiency, as well as a conducting the reaction using 100% of power.

Conversely of what detected from simple nitroalkenes, temperature variation shows a limited effect on the reaction outcome under flow conditions, probably due to the shortened reaction time required for the conversion (around 2 hours vs 6 hours) limiting the possibility of the product to undergo

undesired decomposition pathways. In any case, we can state that working at low temperature seems to be convenient for our reaction for guaranteeing good products yield, in particular when working with *β*-nitroacrylates.
Furthermore, we conducted the model reaction on a larger scale of 2 mmol scale, achieving a comparable yield of product (62%, 366 mg) to that obtained on 0.5 mmol, thus proving again the scalability of our process with different nitroolefins.

Subsequently, the optimized procedure was employed for the synthesis of a variety of α-(1,3-benzodioxolan-2-yl) β-nitro esters **10p-u** on a 0.5 mmol scale (**Scheme 2.35**). The application of the protocol to different substrates bearing different substituents allowed the synthesis of all the hydroalkylated products in good yield, with further expansion of the substrate scope.

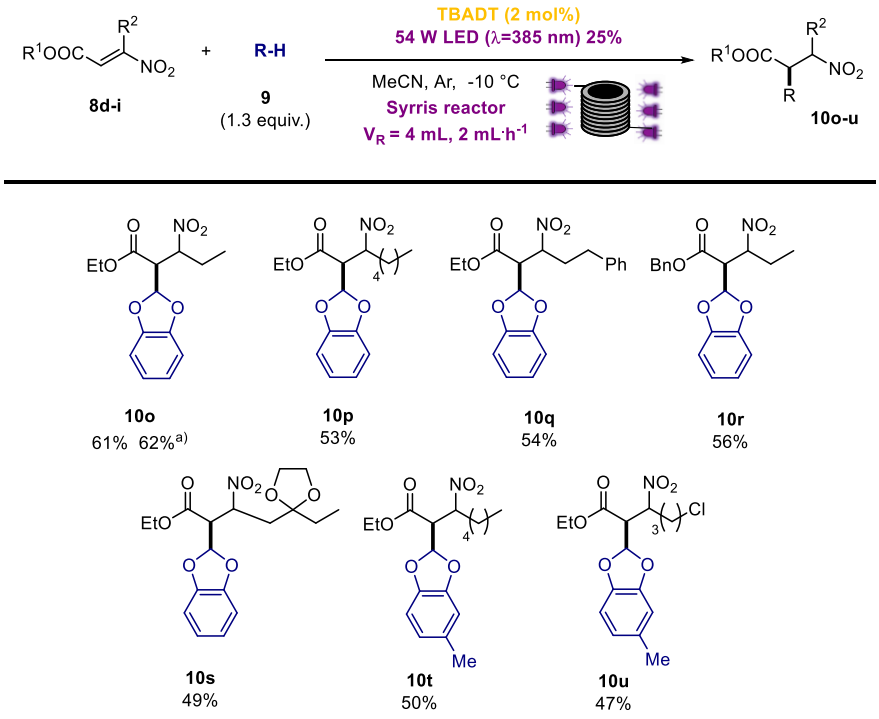

Scheme 2.35 Photocatalyzed hydroalkylation of (E)-β-nitroacrylates

Notably, not even the presence of a 1,3-dioxolane ring on olefin **8h** alter the reactivity, allowing to prepare also compound **10s** in a good yield. Comparable results were obtained when employing 5-methyl-1,3-benzodioxole 9n as the H-donor, leading to the isolation of the desired products **10t** and **10u** in 50% and 47% yield, respectively.
The successful implementation of the approach highlights the distinctive characteristics of the TBADT photocatalyst, which effectively retains the multipotent nitro group upon irradiation.

2.4.3 Experimental section

General procedure A (batch conditions) for the synthesis of 10a-n

A solution of nitroalkene **8** (0.5 mmol, 0.1 M), hydrogen donor **9** (0.75-2.5 mmol, 0.15-0.5 M; 1.5-5 equiv.) and TBADT (2 mol%, 2 mM) in 5 mL of MeCN was poured in a Pyrex vessel, deaerated (by nitrogen bubbling for 10 minutes) and irradiated for 6 hours at 0°C using at 390 nm LED lamp (Kessil PR-160L, 40 W, Figure XX). The progress of the reaction was monitored by GC-FID and, upon completion. Then, the mixture was poured into a round-bottom flask, concentrated under reduced pressure to give the crude product **10**, which was purified by flash column chromatography (cyclohexane:ethyl acetate).

General procedure B (flow conditions in 3D-printed reactor) for the synthesis of 10a-n

A solution of nitroalkene **8** (0.5 mmol, 0.1 M), hydrogen donor **9** (0.75-2.5 mmol, 0.15-0.5 M; 1.5-5 equiv.) and TBADT (2 mol%, 2 mM) in 5 mL of MeCN was deaerated (by nitrogen bubbling for 10 minutes) and charged into a coiled tubing reservoir (PTFE, internal diameter: 1 mm). The reaction mixture was then flown through the channels of a 3D-printed reactor by means of a syringe pump using a flow rate of 2 mL·h^{-1} upon irradiation with a 390 nm LED lamp by applying fan cooling to keep temperature below 30 °C (**Figure 2.9**). The progress of the reaction was monitored by GC-FID and, upon completion. Then, the mixture was poured into a round-bottom flask, concentrated under reduced pressure to give the crude product **10**, which was purified by flash column chromatography (cyclohexane:ethyl acetate).

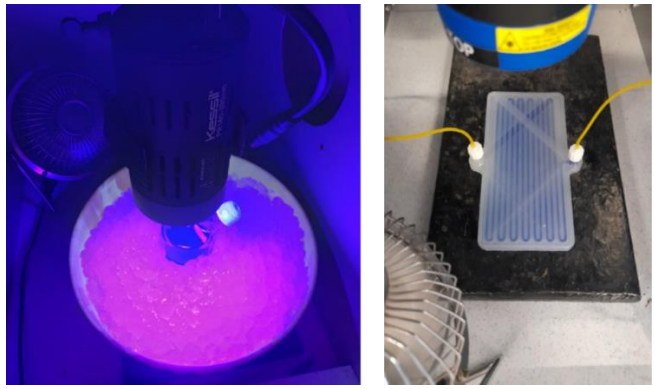

Figure 2.9 Batch (left) a 3D printed flow set-up (right)

General procedure C (flow conditions using Syrris apparatus) for the synthesis of 10o-u

A solution of nitroacrylate **8** (0.5 mmol, 0.1 M), hydrogen donor **9** (0.65 mmol, 0.13 M; 1.3 equiv.) and TBADT (2 mol%, 2 mM) in 5 mL of MeCN was deaerated (by nitrogen bubbling for 10 minutes) and charged into the Asia Reagent Injector equipped with a simple loop of 5 mL (PTFE, internal diameter: 0.5 mm). The reaction mixture was then flown, using MeCN as carrier solvent, with a flow rate of 2 mL·h^{-1} through a 4 mL PTFE coil reactor maintained at -10°C by means of the Asia Cryo

Controller and irradiated at 385 nm by the Asia Photochemistry Reactor equipped with 4 LED modules and setting the power at 25% (**Figure 2.10**). The irradiated solution was collected in a 25 mL round bottom flask, concentrated under reduced pressure to give the crude product **10**, which was purified by flash column chromatography (cyclohexane:ethyl acetate = 8:2).

For more details on the apparatus used, see: https://www.syrris.com/families/asia-lab-scale-flow-chemistry/

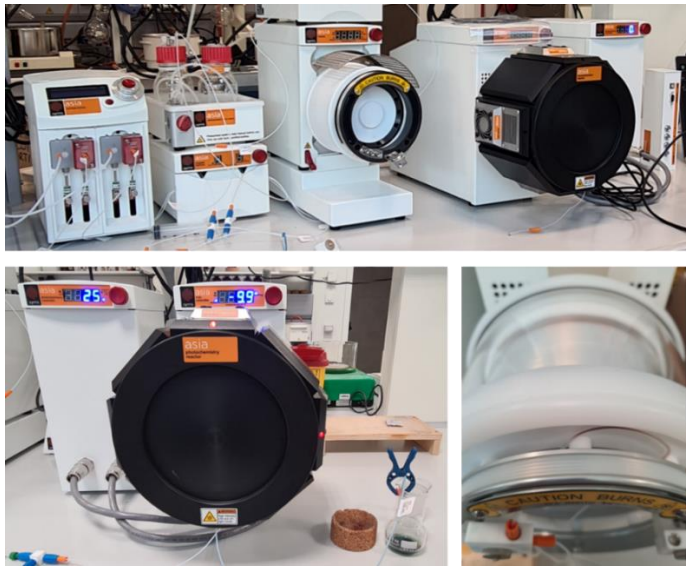

Figure 2.10 Asia Syrris equipment and flow set-up for β-nitroacrylates hydroalkylation

Spectroscopic data and specifics of compounds 10a-u

Compound 10a
Prepared according to general procedures A and B. Flash column chromatography cyclohexane:ethyl acetate = 8:2. **10a** 1.4:1 mixture of diastereoisomers *ca.*; A: **Yield** 81% (105 mg); B: **Yield** 89% (115 mg). Yellowish oil. The reaction also performed on a 2 mmol scale according to general procedure B: **Yield** 91% (471 mg).
^{1}H NMR (300 MHz, Acetone-d_6, mixture of diastereoisomers) δ: 4.73–4.44 (m, 4H), 4.29–4.01 (m, 4H), 3.75–3.72 (m, 2H), 2.60–2.50 (m, 1H), 2.42–2.31 (m, 1H), 1.45–1.25 (m, 32H), 0.99–0.77 (m, 6H); **^{13}C NMR** (75 MHz, Acetone-d_6, mixture of diastereoisomers) δ: 109.8, 109.6, 77.6, 77.5, 77.2, 76.8, 68.7, 66.7, 42.4, 40.9, 32.5, 32.5, 30.2, 29.9, 29.1, 27.5, 27.1, 26.8, 26.6, 25.6, 25.3, 23.4, 14.5. **Anal. Calcd. for $C_{13}H_{25}NO_4$**: C, 60.21; H, 9.72; N, 5.40. **Found**: C, 60.2; H, 9.6; N, 5.4.

Compound 10b
Prepared according to general procedure A. Flash column chromatography cyclohexane:ethyl acetate from 100:0 to 95:5. **Yield** 52% (64 mg). Yellowish oil. When the reaction was performed according to general procedure A at room temperature, product **3b** was isolated in 20% yield.
^{1}H NMR (300 MHz, Acetone-d_6) δ: 4.53 (dd, J = 13.3, 7.4 Hz, 1H), 4.37 (dd, J = 13.3, 5.2 Hz, 1H), 3.97-3.85 (m, 4H), 2.68–2.54 (m, 1H), 1.72–1.57 (m, 1H), 1.53-1.17 (m, 12H), 0.90 (t, J = 6.5 Hz,

3H); **^{13}C NMR** (75 MHz, Acetone-d_6) δ: 111.2, 76.7, 65.6, 65.3, 46.4, 32.5, 30.2, 29.1, 28.1, 23.4, 21.4, 14.4. **Anal. Calcd. for $C_{12}H_{23}NO_4$**: C, 58.75; H, 9.45; N, 5.71. **Found**: C, 58.6; H, 9.5; N, 5.7.

Compound 10c and 10c'

Prepared according to general procedure A. Flash column chromatography cyclohexane:ethyl acetate from 100:0 to 90:10. **10c** and **10c'** (**10c'**; *ca.* 1:1 mixture of diastereoisomers) in a ratio **10c:10c'** = 2.5:1 **Overall yield** 50% (58 mg). Yellowish oil.

^{1}H NMR (300 MHz, $CDCl_3$, major regioisomer **10c**) δ: 4.90 (d, *J* = 3.2 Hz, 1H), 4.60–4.48 (m, 1H), 4.24 (dd, *J* = 12.8, 6.2 Hz, 1H), 4.00–3.88 (m, 4H), 2.69–2.51 (m, 1H), 1.39–1.20 (m, 10H), 0.88 (t, *J* = 7.1 Hz, 3H). **^{1}H NMR** (300 MHz, $CDCl_3$, minor regioisomer **10c'**, mixture of diastereoisomers) δ: 5.02 (d, *J* = 19.2 Hz, 2H), 4.79 (d, *J* = 14.8 Hz, 2H), 4.55–4.39 (m, 4H), 4.16–4.09 (m, 2H), 4.04–3.96 (m, 2H), 3.74–3.58 (m, 2H), 1.53–1.45 (m, 2H), 1.39–1.20 (m, 20H), 0.88 (t, *J* = 7.1 Hz, 6H). **^{13}C NMR** (75 MHz, $CDCl_3$, from the mixture) δ: 104.1, 95.6, 95.3, 76.5, 76.4, 76.3, 75.8, 74.8, 68.7, 66.5, 65.3, 65.3, 64.7, 41.2, 40.9, 40.2, 31.7, 31.7, 29.4, 29.4, 29.2, 28.2, 27.9, 26.9, 26.8, 26.3, 22.7, 14.2.

Compound 10d

Prepared according to general procedure A. Flash column chromatography cyclohexane:ethyl acetate 8:2. **Yield** 40% (56 mg). Yellowish oil.

^{1}H NMR (300 MHz, Acetone-d_6) δ: 6.84 (s, 4H), 6.26 (d, *J* = 4.1 Hz, 1H), 4.74 (dd, *J* = 13.6, 6.8 Hz, 1H), 4.63 (dd, *J* = 13.6, 5.7 Hz, 1H), 3.00–2.85 (m, 1H), 1.81–1.62 (m, 1H), 1.61–1.43 (m, 3H), 1.40–1.23 (m, 6H), 0.88 (t, *J* = 6.4 Hz, 3H); **^{13}C NMR** (75 MHz, Acetone-d_6) δ 148.3, 122.8, 112.0, 109.5, 74.9, 42.5, 32.4, 30.1, 27.7, 27.2, 23.3, 14.4. **Anal. Calcd. for $C_{15}H_{21}NO_4$**: C, 64.50; H, 7.58; N, 5.01. **Found**: C, 64.5; H, 7.5; N, 5.0.

Compound 10e

Prepared according to general procedure A. Flash column chromatography cyclohexane:ethyl acetate 8:2. **3e** *ca.* 2:1 mixture of diastereoisomers. **Yield** 69% (79 mg). Yellowish oil.

^{1}H NMR (300 MHz, Acetone-d_6, mixture of diastereoisomers) δ: 4.68–4.38 (m, 4H), 3.94–3.52 (m, 6H), 2.55–2.44 (m, 1H), 2.28–2.19 (m, 1H), 2.14–1.75 (m, 4H), 1.70–1.53 (m, 2H), 1.50–1.23 (m, 22H), 0.88 (t, *J* = 6.7 Hz, 6H); **^{13}C NMR** (75 MHz, Acetone-d_6 mixture of diastereoisomers) δ: 80.8, 80.2, 78.0, 77.6, 68.6, 68.4, 43.7, 42.5, 32.6, 32.5, 30.7, 30.4, 30.3, 30.1, 29.6, 28.2, 27.6, 27.1, 26.7, 26.6, 23.4, 14.5. **Anal. Calcd. for $C_{12}H_{23}NO_3$**: C, 62.85; H, 10.11; N, 6.11. **Found**: C, 62.9; H, 10.0; N, 6.1.

Compound 10f

Prepared according to general procedure A. Flash column chromatography cyclohexane:ethyl acetate 8:2. **10f** *ca.* 1.3:1 mixture of diastereoisomers; Yield 45% (55 mg). Yellowish oil.

^{1}H NMR (300 MHz, Acetone-d_6, mixture of diastereoisomers) δ: 4.73–4.55 (m, 2H), 4.47 (dd, *J* = 13.1, 6.8 Hz, 2H), 3.88–3.27 (m, 14H), 2.45–2.33 (m, 1H), 2.30–2.19 (m, 1H), 1.60–1.21 (m, 20H), 0.89 (t, *J* = 7.0 Hz, 6H); **^{13}C NMR** (75 MHz, Acetone-d_6, mixture of diastereoisomers) δ: 77.3, 76.9, 76.6, 76.4, 70.2, 68.9, 68.1, 68.0, 67.2, 67.1, 40.6, 40.3, 32.5, 32.2, 30.2, 29.3, 28.3, 27.8, 27.1, 23.4, 14.5. **Anal. Calcd. for $C_{12}H_{23}NO_4$**: C, 58.75; H, 9.45; N, 5.71. **Found**: C, 58.6; H, 9.5; N, 5.7.

Compound 10g

Prepared according to general procedure A, except for the reaction temperature (rt conditions adopted) and irradiation time (1h has been used). Flash column chromatography cyclohexane:ethyl acetate = 85:15. **3g** *ca.* 1.3:1 mixture of diastereoisomers; **Yield** 61% (74 mg). Yellowish oil.

^{1}H NMR (300 MHz, Acetone-d_6, mixture of diastereoisomers) δ: 4.69–4.57 (m, 2H), 4.48–4.36 (m, 2H), 3.95–3.85 (m, 2H), 3.46–3.21 (m, 4H), 2.36–2.25 (m, 1H), 2.25–2.17 (m, 1H), 1.90–1.81 (m, 2H), 1.61–1.42 (m, 10H), 1.42–1.20 (m, 20H), 0.88 (t, *J* = 5.9 Hz, 6H); **^{13}C NMR** (75 MHz, Acetone-

d_6, mixture of diastereoisomers) δ: 78.8, 78.4, 77.9, 77.5, 69.4, 69.3, 43.9, 43.5, 32.6, 30.3, 29.5, 28.4, 28.3, 28.0, 27.2, 27.0, 26.9, 24.4, 24.4, 23.4, 14.5. **Anal. Calcd. for $C_{13}H_{25}NO_3$**: C, 64.16; H, 10.36; N, 5.76. **Found**: C, 64.2; H, 10.4; N, 5.7.

Compound 10h

Prepared according to general procedure B. Flash column chromatography cyclohexane:ethyl acetate = 8:2. **10h** *ca.* 1:1 mixture of diastereoisomers; **Yield** 48% (52 mg). Yellowish oil.

^{1}H NMR (300 MHz, Acetone-d_6, mixture of diastereoisomers) δ: 4.93–4.18 (m, 10H), 2.87–2.42 (m, 6H), 1.59–1.17 (m, 20H), 0.88 (t, *J* = 5.9 Hz, 6H). **^{13}C NMR** (75 MHz, Acetone-d_6, mixture of diastereoisomers) δ: 83.0, 82.9, 76.5, 76.3, 68.5, 68.4, 45.4, 44.1, 32.5, 32.5, 30.4, 30.3, 28.0, 28.0, 27.3, 27.2, 27.2, 25.3, 23.4, 14.5. **Anal. Calcd. for $C_{11}H_{21}NO_3$**: C, 61.37; H, 9.83; N, 6.51. **Found**: C, 61.3; H, 9.9; N, 6.5.

Compound 10i

Prepared according to general procedure A. Flash column chromatography cyclohexane:ethyl acetate = 8:2. Yield 54% (66 mg). Yellowish oil.

^{1}H NMR (300 MHz, Acetone-d_6) δ: 4.71 (dd, *J* = 13.3, 7.3 Hz, 1H), 4.54 (dd, *J* = 13.2, 5.3 Hz, 1H), 3.57-3.47 (m, 1H), 2.85–2.76 (m, 2H), 2.40–2.28 (m, 1H), 2.24–2.11 (m, 2H), 1.91–1.74 (m, 1H), 1.62–1.45 (m, 3H), 1.36–1.23 (m, 8H), 0.87 (t, *J* = 6.3 Hz, 3H); **^{13}C NMR** (75 MHz, Acetone-d_6) δ: 78.8, 51.7, 43.9, 34.6, 32.6, 32.5, 32.3, 32.0, 30.3, 27.0, 23.4, 14.5. **Anal. Calcd. for $C_{12}H_{23}NO_2S$**: C, 58.74; H, 9.45; N, 5.71. **Found**: C, 58.7; H, 9.5; N, 5.8.

Compound 10j

Prepared according to general procedure A. Flash column chromatography cyclohexan:ethyl acetate gradient from 5:5 to 0:10. **Yield** 72% (83 mg). Yellowish oil.

^{1}H NMR (400 MHz, Acetone-d_6, mixture of rotamers) δ 8.05 (s, 1H), 8.03 (s, 1H), 4.60–4.41 (m, 4H), 3.47–3.27 (m, 4H), 3.01 (s, 3H), 2.82 (s, 3H), 2.64–2.55 (m, 2H), 1.45–1.24 (m, 20H), 0.88 (t, *J* = 6.9 Hz, 6H); **^{13}C NMR** (100 MHz, Acetone-d_6, mixture of rotamers) δ 164.0, 163.5, 78.6, 77.9, 51.8, 46.4, 36.4, 35.1, 31.5, 31.4, 30.7, 30.2, 30.1, 26.9, 26.9, 23.3, 23.1, 14.4. **Anal. Calcd. for $C_{11}H_{22}N_2O_3$**: C, 57.37; H, 9.63; N, 12.16. **Found**: C, 57.4; H, 9.6; N, 12.1.

Compound 10k

Prepared according to general procedure A. Flash column chromatography cyclohexane:ethyl acetate gradient from 5:5 to 0:10. **Yield** 69% (84 mg). Yellowish oil.

^{1}H NMR (300 MHz, Acetone-d_6, mixture of rotamers) δ: 4.65–4.34 (m, 4H), 3.62–3.42 (m, 2H), 3.29–3.19 (m, 2H), 3.07 (s, 3H), 2.86 (s, 3H), 2.66–2.53 (m, 2H), 2.04 (s, 3H), 2.02 (s, 3H), 1.44–1.26 (m, 20H), 0.89 (t, *J* = 7.0 Hz, 6H); **^{13}C NMR** (75 MHz, Acetone-d_6, mixture of rotamers) δ 171.5, 170.6, 78.9, 78.2, 53.1, 49.8, 37.6, 37.3, 37.0, 33.5, 32.5, 30.8, 30.3, 27.2, 27.0, 23.4, 22.0, 21.7, 14.5. **Anal. Calcd. for $C_{12}H_{24}N_2O_3$**: C, 58.99; H, 9.90; N, 11.47. **Found**: C, 59.0; H, 9.9; N, 11.5.

Compound 10l

Prepared according to the general procedure A. Flash column chromatography cyclohexane:ethyl acetate = 8:2. **Yield** 50% (61 mg). Yellowish oil.

^{1}H NMR (300 MHz, $CDCl_3$) δ: 4.38 (dd, *J* = 12.0, 6.6 Hz, 1H), 4.24 (dd, *J* = 12.0, 7.4 Hz, 1H), 2.18–2.03 (m, 1H), 1.83–1.57 (m, 4H), 1.52–0.97 (m, 17H), 0.89 (t, *J* = 6.9 Hz, 3H); **^{13}C NMR** (75 MHz, $CDCl_3$) δ: 78.1, 43.1, 39.0, 31.8, 29.7, 29.5, 29.5, 28.8, 27.1, 26.7, 26.7, 26.6, 22.7, 14.2. **Anal. Calcd. for $C_{14}H_{27}N$**: C, 69.67; H, 11.28; N, 5.80. **Found**: C, 69.8; H, 11.1; N, 5.8.

Compound 10m

Prepared according to general procedure A. Flash column chromatography cyclohexane:ethyl acetate = 8:2. **Yield** 50% (67 mg). Yellowish oil.

^{1}H NMR (300 MHz, Acetone-d_6) δ: 4.56–4.48 (m, 1H), 4.45–4.36 (m, 1H), 2.18–2.09 (m, 1H), 1.94–1.19 (m, 25H), 0.89 (t, *J* = 6.6 Hz, 3H); **^{13}C NMR** (75 MHz, Acetone-d_6) δ: 79.2, 46.1, 38.6, 32.6, 31.1, 31.0, 30.3, 29.6, 28.2, 27.7, 27.4, 27.3, 27.2, 27.2, 23.5, 14.5. **Anal. Calcd. For $C_{16}H_{31}NO_2$**: C, 71.33; H, 11.60; N, 5.20. **Found**: C, 71.4; H, 11.5; N, 5.2.

Compound 10n

Prepared according to general procedure A. Flash column chromatography cyclohexane:ethyl acetate = 8:2. **10n** *ca.* 1:1 mixture of diastereoisomers; **Yield** 69% (96 mg). Yellowish oil. Reaction performed according to general procedure A at room temperature: **Yield** 53%.

^{1}H NMR (300 MHz, Acetone-d_6, mixture of diastereoisomers) δ: 7.38–7.12 (m, 10H), 4.79–4.52 (m, 4H), 4.34–3.97 (m, 4H), 3.79–3.63 (m, 2H), 2.84–2.36 (m, 6H), 1.92–1.62 (m, 4H), 1.33 (s, 3H), 1.30 (s, 3H), 1.28 (s, 6H); **^{13}C NMR** (75 MHz, Acetone-d_6, mixture of diastereoisomers) δ: 142.9, 142.9, 129.6, 129.6, 129.5, 127.2, 77.6, 77.2, 76.9, 68.8, 66.9, 42.2, 40.7, 33.9, 33.5, 32.2, 31.2, 30.5, 27.0, 26.8, 25.8, 25.5. **Anal. Calcd. for $C_{15}H_{21}NO_4$**: C, 64.50; H, 7.58; N, 5.01. **Found**: C, 64.6; H, 7.5; N, 4.9.

Compound 10o

Prepared according to general procedure C. **10o** 60:40 mixture of diastereoisomers; **Yield** 61% (90 mg). Yellowish oil. Reaction performed also on a 2 mmol scale (procedure C): **Yield** 62% (366 mg).

^{1}H NMR (400 MHz, $CDCl_3$, mixture of diastereoisomers) δ: 6.80-6.85 (m, 4H), 6.42 (d, *J* = 5.0 Hz, 0.4H), 6.37 (d, *J* = 6.1 Hz, 0.6H), 4.96-5.03 (m, 0.4H), 4.81-4.89 (m, 0.6H), 4.15-4.24 (m, 2H), 3.65 (dd, *J* = 8.7, 6.1 Hz, 0.6H), 3.55 (dd, *J* = 7.2, 5.0, Hz, 0.4H), 2.00-2.17 (m, 1.20H), 1.78-1.92 (m, 0.80H), 1.18-1.27 (m, 3H), 0.96-1.03 (m, 3H); **^{13}C NMR** (100 MHz, $CDCl_3$, mixture of diastereoisomers) δ: 167.2, 166.9, 146.5, 146.3, 122.2, 122.1, 109.0, 108.9, 108.0, 107.6, 86.2, 86.1, 62.1, 62.0, 53.1, 51.7, 24.9, 24.8, 13.9, 13.8, 10.1, 9.9. **Anal. Calcd. for $C_{14}H_{17}NO_6$**: C, 56.95; H, 5.80; N, 4.74. **Found**: C, 56.99; H, 5.77; N, 4.71.

Compound 10p

Prepared according to general procedure C. **10p** 75:25 mixture of diastereoisomers; Yield 53% (89 mg). Yellowish oil.

^{1}H NMR (400 MHz, $CDCl_3$, mixture of diastereoisomers) δ: 6.74-6.92 (m, 4H), 6.45 (d, *J* = 5.0 Hz, 0.25H), 6.39 (d, *J* = 6.1 Hz, 0.75H), 5.00-5.11 (m, 0.25H), 4.84-4.98 (m, 0.75H), 4.09-4.31 (m, 2H), 3.66 (dd, *J* = 8.5, 6.1 Hz, 0.75H), 3.55 (dd, *J* = 7.0, 5.0 Hz, 0.25H), 1.94-2.17 (m, 1.5H), 1.64-1.83 (m, 0.5H), 1.14-1.44 (m, 9H), 0.76-0.98 (m, 3H); **^{13}C NMR** (100 MHz, $CDCl_3$, mixture of diastereoisomers) δ: 167.2, 167.0, 146.5, 146.3, 122.3, 122.2, 109.1, 109.0, 108.0, 107.7, 84.9, 84.8, 62.1, 53.3, 52.1, 31.4, 31.2, 30.9, 30.8, 25.2, 25.1, 22.2, 14.0, 13.9. **Anal. Calcd. for $C_{17}H_{23}NO_6$**: C, 60.52; H, 6.87; N, 4.15. **Found**: C, 60.56; H, 6.91; N, 4.18.

Compound 10q

Prepared according to general procedure C. **10q** 60:40 mixture of diastereoisomers; **Yield** 54% (100 mg). Yellowish oil.

^{1}H NMR (400 MHz, $CDCl_3$, mixture of diastereoisomers) δ: 7.23-7.33 (m, 3H), 7.12-7.16 (m, 2H), 6.81-6.87 (m, 4H), 6.45 (dd, *J* = 5.1, 1.0 Hz, 0.25H), 6.38 (dd, *J* = 4.1, 2.0 Hz, 0.75H), 5.03-5.08 (m, 0.25H), 4.91-4.97 (m, 0.75H), 4.14-4.25 (m, 2H), 3.68-3.71 (m, 0.75H), 3.57-3.60 (m, 0.25H), 2.71-2.78 (m, 1.25H), 2.56-2.66 (m, 0.75H), 2.38-2.48 (m, 1.25H), 2.06-2.15 (m, 0.75H), 1.18-1.25 (m, 3H); **^{13}C NMR** (100 MHz, $CDCl_3$, mixture of diastereoisomers) δ: 167.1, 166.8, 146.4, 146.3, 139.2, 139.1, 128.7, 128.4, 126.7, 126.6, 122.3, 122.2, 109.1, 109.0, 107.9, 107.7, 84.1, 83.9, 62.2, 62.1, 53.1, 52.0,

33.0, 32.9, 31.8, 31.9, 13.7, 13.8. **Anal. Calcd. for $C_{20}H_{21}NO_6$**: C, 64.68; H, 5.70; N, 3.77. **Found**: C, 64.73; H, 5.73; N, 3.80.

Compound 10r

Prepared according to general procedure C. **10r** 75:25 mixture of diastereoisomers; **Yield** 56% (100 mg). Yellowish oil.

^{1}H NMR (400 MHz, $CDCl_3$, mixture of diastereoisomers) δ: 7.27-7.40 (m, 5H), 6.78-6.86 (m, 4H), 6.42 (d, *J* = 5.0 Hz, 0.25H), 6.39 (d, *J* = 6.1 Hz, 0.75H), 5.14-5.22 (m, 2H), 4.99-5.06 (m, 0.25H), 4.80-4.92 (m, 0.75H), 3.73 (dd, *J* = 8.8, 6.1 Hz, 0.75H), 3.64 (dd, *J* = 7.4, 5.0 Hz, 0.25H), 2.09-2.16 (m, 0.5H), 1.96-2.04 (m, 0.75H), 1.73-1.85 (m, 0.75H), 1.00 (t, J = 7.4 Hz, 0.75H), 0.95 (t, *J* = 7.3 Hz, 2.25H); **^{13}C NMR** (100 MHz, $CDCl_3$, mixture of diastereoisomers) δ: 167.2, 166.8, 146.3, 146.2, 134.7, 134.6, 128.7, 128.6, 128.5, 128.4, 122.3, 122.2, 109.1, 109.0, 108.0, 107.5, 86.2, 86.0, 67.9, 67.8, 53.1, 51.6, 25.0, 24.9, 10.1, 9.9. **Anal. Calcd. for $C_{19}H_{19}NO_6$**: C, 63.86; H, 5.36; N, 3.92. **Found**: C, 63.90; H, 5.32; N, 3.89.

Compound 10s

Prepared according to general procedure C. **10s** 75:25 mixture of diastereoisomers; Yield 49% (93 mg). Yellowish oil.

^{1}H NMR (400 MHz, $CDCl_3$, mixture of diastereoisomers) δ : 6.80-6.86 (m, 4H), 6.50 (d, *J* = 6.3 Hz, 0.25H), 6.36 (d, *J* = 6.2 Hz, 0.75H), 5.17-5.23 (m, 0.25H), 5.09-5.16 (m, 0.75H), 4.04-4.29 (m, 2H), 3.86-3.98 (m, 4H), 3.47-3.53 (m, 1H), 2.74-2.83 (m, 1H), 2.49 (dd, *J* = 15.6, 4.1 Hz, 0.25H), 2.17 (dd, *J* = 15.7, 1.7 Hz, 0.75H), 1.33 (br s, 3H), 1.21-1.26 (m, 3H); **^{13}C NMR** (100 MHz, $CDCl_3$, mixture of diastereoisomers) δ: 167.1, 167.0, 146.4, 146.3, 122.2, 122.1, 109.1, 109.0, 107.9, 107.8, 107.6, 107.5, 80.4, 80.1, 64.9, 64.8, 64.7, 64.6, 62.1, 62.0, 53.2, 52.8, 39.1, 38.9, 24.1, 24.0, 13.9. **Anal. Calcd. for $C_{17}H_{21}NO_8$**: C, 55.58; H, 5.76; N, 3.81. **Found**: C, 55.63; H, 5.80; N, 3.84.

Compound 10t

Prepared according to general procedure C. **10t** 75:25 mixture of diastereoisomers; Yield 50 % (88 mg). Yellowish oil.

^{1}H NMR (400 MHz, $CDCl_3$, mixture of diastereoisomers) δ: 6.58-6.74 (m, 3H), 6.40 (dd, *J* = 5.0, 0.9 Hz, 0.25H), 6.34 (dd, *J* = 6.2, 0.6 Hz, 0.75H), 5.00-5.07 (m, 0.25H), 4.86-4.94 (m, 0.75H), 4.17-4.25 (m, 2H), 3.60-3.65 (m, 0.75H), 3.49-3.54 (m, 0.25H), 2.27 (s, 0.75H), 2.26 (s, 2.25H), 1.98-2.13 (m, 1.25H), 1.69-1.79 (m, 0.75H), 1.19-1.35 (m, 9H), 0.84-0.91 (m, 3H); **^{13}C NMR** (100 MHz, $CDCl_3$, mixture of diastereoisomers) δ: 167.3, 167.0, 146.6, 146.3, 144.4, 144.1, 132.2, 132.0, 122.1, 122.0, 108.9, 108.8, 108.5, 108.4, 108.1, 107.7, 84.9, 84.8, 62.1, 53.2, 53.1, 52.0, 31.4, 31.2, 31.1, 30.9, 30.8, 25.2, 25.1, 22.2, 21.2, 21.1, 13.9, 13.8. **Anal. Calcd. for $C_{18}H_{25}NO_6$**: C, 61.52; H, 7.17; N, 3.99. **Found**: C, 61.48; H, 7.14; N, 3.96.

Compound 10u

Prepared according to general procedure C. **10u** 65:35 mixture of diastereoisomers; **Yield** 47% (84 mg). Yellowish oil.

^{1}H NMR (400 MHz, $CDCl_3$, mixture of diastereoisomers) δ: 6.60-6.73 (m, 3H), 6.42 (dd, *J* = 4.9, 0.35H), 6.37 (d, *J* = 6.0 Hz, 0.65H), 5.03-5.11 (m, 0.35H), 4.86-4.97 (m, 0.65H), 4.15-4.27 (m, 2H), 3.68 (dd, *J* = 8.2, 6.0 Hz, 0.65H), 3.49-3.59 (m, 2.35H), 2.27 (s, 1.05H), 2.26 (s, 1.95H), 2.13-2.32 (m, 1.35H), 1.99-2.11 (m, 0.65H), 1.72-1.96 (m, 2H), 1.20-1.29 (m, 3H); **^{13}C NMR** (100 MHz, $CDCl_3$, mixture of diastereoisomers): δ 167.1, 166.8, 146.5, 146.3, 144.3, 132.3, 132.2, 122.2, 122.1, 110.0, 109.9, 108.5, 108.4, 107.9, 107.6, 84.0, 62.3, 53.1, 53.0, 51.9, 43.5, 43.4, 28.5, 28.4, 21.2, 21.1, 14.0, 13.9. **Anal. Calcd. for $C_{16}H_{20}ClNO_6$**: C, 53.71; H, 5.63; N, 3.91. **Found**: C, 53.75; H, 5.60; N, 3.88.

NMR Spectra of the described compounds can be found at:
https://doi.org/10.1002/adsc.202201314

2.5 References

(1) Ballini, R.; Palmieri, A. *Nitroalkanes - Synthesis, Reactivity, Applications*; WILEY-VCH, 2021.

(2) Ono, Noboru. *The Nitro Group in Organic Synthesis*; Wiley-VCH, 2001.

(3) Zard, S. Z. Some Aspects of the Chemistry of Nitro Compounds. *Helv Chim Acta* **2012**, *95* (10), 1730–1757. https://doi.org/10.1002/hlca.201200324.

(4) Sakaguchi, S.; Nishiwaki, Y.; Kitamura, T.; Ishii, Y. Efficient Catalytic Alkane Nitration with NO2 under Air Assisted by N-Hydroxyphthalimide. *Angewandte Chemie - International Edition* **2001**, *40* (1), 222–224. https://doi.org/10.1002/1521-3773(20010105)40:1<222::AID-ANIE222>3.0.CO;2-W.

(5) Nishiwaki, Y.; Sakaguchi, S.; Ishii, Y. An Efficient Nitration of Light Alkanes and the Alkyl Side-Chain of Aromatic Compounds with Nitrogen Dioxide and Nitric Acid Catalyzed by N-Hydroxyphthalimide. *Journal of Organic Chemistry* **2002**, *67* (16), 5663–5668. https://doi.org/10.1021/jo025632d.

(6) Shinachi, S.; Yahiro, H.; Yamaguchi, K.; Mizuno, N. Nitration of Alkanes with Nitric Acid by Vanadium-Substituted Polyoxometalates. *Chemistry - A European Journal* **2004**, *10* (24), 6489–6496. https://doi.org/10.1002/chem.200400049.

(7) Peng, L.; Peng, H.; Li, N.; Zhong, W.; Mao, L.; You, K.; Yin, D. Facile Access to Nitroalkanes: Nitration of Alkanes by Selective C[Sbnd]H Nitration Using Metal Nitrate, Catalyzed by in-Situ Generated Metal Oxide. *Catal Commun* **2020**, *142*. https://doi.org/10.1016/j.catcom.2020.106035.

(8) Meyer, V.; Stüber, O. Ueber Die Nitroverbindungen Der Fettreihe. *Chem. Ber.* **1872**, 203. https://doi.org/https://doi.org/10.1002/cber.187200501121.

(9) Kornblum, N.; Smiley, R. A.; Blackwood, R. K.; Iffland, D. C.; Taub, B. The Mechanism of the Reaction of Silver Nitrite with Alkyl Halides. The Contrasting Reactions of Silver and Alkali Metal Salts with Alkyl Halides. The Alkylation of Ambident Anions. *J. Am. Chem. Soc.* **1955**, *77*, 6269.

(10) Kornblum, N.; Larson, H. O.; Blackwood, R. K.; Mooberry, D. D.; Oliveto, E. P.; Graham, G. E. A New Method for the Synthesis of Aliphatic Nitro Compounds. *J. Am. Chem. Soc.* **1956**, *78*, 1497–1501.

(11) Ballini, R.; Barboni, L.; Fringuelli, F.; Palmieri, A.; Pizzo, F.; Vaccaro, L. Recent Developments on the Chemistry of Aliphatic Nitro Compounds under Aqueous Medium. *Green Chemistry* **2007**, *9* (8), 823–883. https://doi.org/10.1039/b702334k.

(12) Ballini, R.; Barboni, L.; Giarlo, G. Nitroalkanes in Aqueous Medium as an Efficient and Eco-Friendly Source for the One-Pot Synthesis of 1,4-Diketones, 1,4-Diols, δ-Nitroalkanols, and Hydroxytetrahydrofurans. *Journal of Organic Chemistry* **2003**, *68* (23), 9173–9176. https://doi.org/10.1021/jo0351163.

(13) Ballini, R.; Barboni, L.; Palmieri, A. Improved Chemoselective, Ecofriendly Conditions for the Conversion of Primary Alkyl Halides into Nitroalkanes under PEG400. *Green Chemistry* **2008**, *10* (9), 1004–1006. https://doi.org/10.1039/b805985c.

(14) Sheldon, R. A. Green Solvents for Sustainable Organic Synthesis: State of the Art. *Green Chemistry* **2005**, *7* (5), 267–278. https://doi.org/10.1039/b418069k.

(15) Palmieri, A.; Gabrielli, S.; Ballini, R. Easy and Direct Conversion of Tosylates and Mesylates into Nitroalkanes. *Beilstein Journal of Organic Chemistry* **2013**, *9*, 533–536. https://doi.org/10.3762/bjoc.9.58.

(16) Keinan, E.; Mazur, Y. Dry Ozonation of Amines. Conversion of Primary Amines to Nitro Compounds. *J. Org. Chem.* **1977**, *42* (5), 844.

(17) Irfan, M.; Glasnov, T. N.; Kappe, C. O. Continuous Flow Ozonolysis in a Laboratory Scale Reactor. *Org Lett* **2011**, *13* (5), 984–987. https://doi.org/10.1021/ol102984h.

(18) McPake, C. B.; Murray, C. B.; Sandford, G. Sequential Continuous Flow Processes for the Oxidation of Amines and Azides by Using HOF·MeCN. *ChemSusChem* **2012**, *5* (2), 312–319. https://doi.org/10.1002/cssc.201100423.

(19) Skrotzki, E. A.; Vandavasi, J. K.; Newman, S. G. Ozone-Mediated Amine Oxidation and Beyond: A Solvent-Free, Flow-Chemistry Approach. *Journal of Organic Chemistry* **2021**, *86* (20), 14169–14176. https://doi.org/10.1021/acs.joc.1c00768.

(20) Emmons, W. D.; Pagano, A. S. Peroxytrifluoracetic Acid. The Oxidation of Oxymes to Nitroparaffins. *J. Am. Chem. Soc.* **1955**, *77* (17), 4557–4559.

(21) Olah, G. A.; Ramaiah, P.; Lee, C.-S.; Prakash, G. K. S. Convinient Oxidation of Oximes to Nitro Compounds with Sodium Perborate in Glacial Acetic Acid. *Synlett* **1992**, 337–339.

(22) Rozen, S.; Carmeli, M. From Azides to Nitro Compounds in a Few Seconds Using HOF·CH3CN. *J Am Chem Soc* **2003**, *125* (27), 8118–8119. https://doi.org/10.1021/ja035616d.

(23) Chu, Q.; He, G.; Xi, Y.; Wang, P.; Yu, H.; Liu, R.; Zhu, H. Green Synthesis of Low-Carbon Chain Nitroalkanes via a Novel Tandem Reaction of Ketones Catalyzed by TS-1. *Catal Commun* **2018**, *108*, 46–50. https://doi.org/10.1016/j.catcom.2018.01.022.

(24) Ballini, R.; Bosica, G.; Fiorini, D.; Palmieri, A.; Petrini, M. Conjugate Additions of Nitroalkanes to Electron-Poor Alkenes: Recent Results. *Chem Rev* **2005**, *105* (3), 933–971. https://doi.org/10.1021/cr040602r.

(25) Luzzio, F. A. The Henry Reaction: Recent Examples. *Tetrahedron* **2001**, *57*, 915–945.

(26) Rosini, G.; Ballini, R. Functionized Nitroalkanes as Useful Reagents for Alkyl Anion Synthon. *Synthesis (Stuttg)* **1988**, 833.

(27) Orlandi, M.; Brenna, D.; Harms, R.; Jost, S.; Benaglia, M. Recent Developments in the Reduction of Aromatic and Aliphatic Nitro Compounds to Amines. *Org Process Res Dev* **2018**, *22* (4), 430–445. https://doi.org/10.1021/acs.oprd.6b00205.

(28) Cai, S.; Zhang, S.; Zhao, Y.; Wang, D. Z. New Approach to Oximes through Reduction of Nitro Compounds Enabled by Visible Light Photoredox Catalysis. *Org Lett* **2013**, *15* (11), 2660–2663. https://doi.org/10.1021/ol4009443.

(29) Wang, K.; Qian, X.; Cui, J. One Step from Nitro to Oxime: A Convenient Preparation of Unsaturated Oximes by the Reduction of the Corresponding Vinylnitro Compounds. *Tetrahedron* **2009**, *65* (50), 10377–10382. https://doi.org/10.1016/j.tet.2009.10.042.

(30) Kaim, L. El; Gacon, A. A New Conversion of Primary Nitro Compounds into Nitriles. *Tetrahedron Lett* **1997**, *38* (19), 3391–3394.

(31) Ballini, R.; Petrini, M. Recent Synthetic Developments in the Nitro to Carbonyl Conversion (Nef Reaction). *Tetrahedron* **2004**, *60* (5), 1017–1047. https://doi.org/10.1016/j.tet.2003.11.016.

(32) Valachová, D.; Marčeková, M.; Caletková, O.; Kolarovič, A.; Jakubec, P. The Last Fortress of Tin's Tyranny – Protodenitration of Nitroalkanes. *European J Org Chem* **2023**, *26* (13). https://doi.org/10.1002/ejoc.202201341.

(33) Romney, D. K.; Sarai, N. S.; Arnold, F. H. Nitroalkanes as Versatile Nucleophiles for Enzymatic Synthesis of Noncanonical Amino Acids. *ACS Catal* **2019**, *9* (9), 8726–8730. https://doi.org/10.1021/acscatal.9b02089.

(34) Yan, G.; Borah, A. J.; Wang, L. Recent Advances in the Synthesis of Nitroolefin Compounds. *Org Biomol Chem* **2014**, *12* (32), 6049–6058. https://doi.org/10.1039/c4ob00573b.

(35) Mukaiyama, T.; Hata, E.; Yamada, T. Convenient and Simple Preparation of Nitroolefins Nitration of Olefins with Nitric Oxide. *Chem Lett* **1995**, *24* (7), 505–506.

(36) Jovel, I.; Prateeptongkum, S.; Jackstell, R.; Vogl, N.; Weckbecker, C.; Beller, M. A Selective and Practical Synthesis of Nitroolefins. *Adv Synth Catal* **2008**, *350* (16), 2493–2497. https://doi.org/10.1002/adsc.200800509.

(37) Naveen, T.; Maity, S.; Sharma, U.; Maiti, D. A Predictably Selective Nitration of Olefin with Fe(NO3) 3 and TEMPO. *Journal of Organic Chemistry* **2013**, *78* (12), 5949–5954. https://doi.org/10.1021/jo400598p.

(38) Paul, N.; Maity, S.; Panja, S.; Maiti, D. Recent Advances in the Nitration of Olefins. *Chemical Record* **2021**, *21* (10), 2896–2908. https://doi.org/10.1002/tcr.202100217.

(39) Maity, S.; Manna, S.; Rana, S.; Naveen, T.; Mallick, A.; Maiti, D. Efficient and Stereoselective Nitration of Mono- and Disubstituted Olefins with AgNO2 and TEMPO. *J Am Chem Soc* **2013**, *135* (9), 3355–3358. https://doi.org/10.1021/ja311942e.

(40) Maity, S.; Naveen, T.; Sharma, U.; Maiti, D. Efficient and Stereoselective Nitration of Olefins with AgNO2 and TEMPO. *Synlett* **2014**, *25* (5), 603–607. https://doi.org/10.1055/s-0033-1340467.

(41) Maity, S.; Naveen, T.; Sharma, U.; Maiti, D. Stereoselective Nitration of Olefins with TBuONO and TEMPO: Direct Access to Nitroolefins under Metal-Free Conditions. *Org Lett* **2013**, *15* (13), 3384–3387. https://doi.org/10.1021/ol401426p.

(42) Reddy, G. S.; Corey, E. J. A Useful Method for the Conversion of Olefins to Nitro Olefins. *Org Lett* **2021**, *23* (9), 3399–3402. https://doi.org/10.1021/acs.orglett.1c00868.

(43) Majedi, S.; Majedi, S.; Behmagham, F. Chemical Review and Letters Recent Advances in Decarboxylative Nitration of Carboxylic Acids. *Chem Rev Lett* **2019**, *2*, 187–192.

(44) Wisniak, J. Louis Henry: The Henry Reaction and Other Organic Syntheses. **2018**.

(45) Gao, S.; Tu, Y. Q.; Hu, X.; Wang, S.; Hua, R.; Jiang, Y.; Zhao, Y.; Fan, X.; Zhang, S. General and Efficient Strategy for Erythrinan and Homoerythrinan Alkaloids: Syntheses of (±)-3-Demethoxyerythratidinone and (±)- Erysotramidine. *Org Lett* **2006**, *8* (11), 2373–2376. https://doi.org/10.1021/ol0607185.

(46) Celano, L.; Carabio, C.; Frache, R.; Cataldo, N.; Cerecetto, H.; González, M.; Thomson, L. Arylnitroalkenes as Scavengers of Macrophage-Generated Oxidants. *Eur J Med Chem* **2014**, *74*, 31–40. https://doi.org/10.1016/j.ejmech.2013.12.029.

(47) Hock, K. J.; Grimmer, J.; Göbel, D.; Gasaya, G. G. T.; Roos, J.; Maucher, I. V.; Kühn, B.; Fettel, J.; Maier, T. J.; Manolikakes, G. Modular Regiospecific Synthesis of Nitrated Fatty Acids. *Synthesis (Germany)* **2017**, *49* (3), 615–636. https://doi.org/10.1055/s-0036-1588314.

(48) Akutu, K.; Kabashima, H.; Seki, T.; Hattori, H. Nitroaldol Reaction over Solid Base Catalysts. *Appl Catal A Gen* **2003**, *247* (1), 65–74. https://doi.org/10.1016/S0926-860X(03)00124-8.

(49) Ballini, R.; Bosica, G.; Forconi, P. Nitroaldol (Henry) Reaction Catalyzed by Amberlyst A-21 as a Far Superior Heterogeneous Catalyst. *Tetrahedron* **1996**, *52* (5), 1677–1684.

(50) Ballini, R.; Bosica, G.; Livi, D.; Palmieri, A.; Maggi, R.; Sartori, G. Use of Heterogeneous Catalyst KG-60-NEt2 in Michael and Henry Reactions Involving Nitroalkanes. *Tetrahedron Lett* **2003**, *44* (11), 2271–2273. https://doi.org/10.1016/S0040-4039(03)00274-0.

(51) Ballini, R.; Bosica, G.; Palmieri, A.; Pizzo, F.; Vaccaro, L. Isolute® Si-Carbonate Catalyzes the Nitronate Addition to Both Aldehydes and Electron-Poor Alkenes under Solvent-Free Conditions. *Green Chemistry* **2008**, *10* (5), 541–554. https://doi.org/10.1039/b719477c.

(52) Rokhum, S. L.; Bez, G. One-Pot Solid Phase Synthesis of (E)-Nitroalkenes. *Tetrahedron Lett* **2013**, *54* (40), 5500–5504. https://doi.org/10.1016/j.tetlet.2013.07.146.

(53) Das, D.; Pathak, G.; Rokhum, L. Polymer Supported DMAP: An Easily Recyclable Organocatalyst for Highly Atom-Economical Henry Reaction under Solvent-Free Conditions. *RSC Adv* **2016**, *6* (106), 104154–104163. https://doi.org/10.1039/c6ra23696k.

(54) Rajkumari, K.; Das, D.; Pathak, G.; Rokhum, L. Waste-to-Useful: A Biowaste-Derived Heterogeneous Catalyst for a Green and Sustainable Henry Reaction. *New Journal of Chemistry* **2019**, *43* (5), 2134–2140. https://doi.org/10.1039/c8nj05029e.

(55) Pandey, G.; Bagul, T. D.; Sahoo, A. K. [3 + 2] Cycloaddition of Nonstabilized Azomethine Ylides. 7. Stereoselective Synthesis of Epibatidine and Analogues. *J Org Chem* **1998**, *63* (3), 760–768.

(56) Mélot, J.-M.; Texier-Boullet, F.; Foucaud, A. PREPARATION AND OXIDATION OF Alfa-NITRO ALCOHOLS WITH SUPPORTED REAGENTS. *Tetrahedron Lett* **1986**, *27* (4), 493–496.

(57) Lucet, D.; Sabelle, S.; Kostelitz, O.; Le Gall, T.; Mioskowski, C. Enantioselective Synthesis of α-Amino Acids and Monosubstituted 1,2- Diamines by Conjugate Addition of 4-Phenyl-2-Oxazolidinone to Nitroalkenes. *European J Org Chem* **1999**, 2583–2591. https://doi.org/10.1002/(sici)1099-0690(199910)1999:10<2583::aid-ejoc2583>3.0.co;2-e.

(58) Ballini, R.; Castagnani, R.; Petrini, M. Chemoselective Synthesis of Functionalized Nitroalkenes. *J. Org. Chem.* **1992**, *57*, 2160–2162.

(59) Melton, J.; Mc Murry, J. E. A New Method for the Dehydration of Nitro Alcohols. *J. Org. Chem* **1975**, *40* (14), 2138–2139.

(60) Heinrich, D. M.; Youte, J. J.; Denny, W. A.; Tercel, M. A New Enantioselective Approach to the Core Structure of Hypoxia Selective Prodrugs Related to the Duocarmycins. *Tetrahedron Lett* **2011**, *52* (51), 7000–7003. https://doi.org/10.1016/j.tetlet.2011.10.105.

(61) Jia, Z. J.; Zhou, Q.; Zhou, Q. Q.; Chen, P. Q.; Chen, Y. C. Exo-Selective Asymmetric Diels-Alder Reaction of 2,4-Dienals and Nitroalkenes by Trienamine Catalysis. *Angewandte Chemie - International Edition* **2011**, *50* (37), 8638–8641. https://doi.org/10.1002/anie.201102013.

(62) Basavaiah, D.; Reddy, B. S.; Badsara, S. S. Recent Contributions from the Baylis - Hillman Reaction to Organic Chemistry. *Chem Rev* **2010**, *110* (9), 5447–5674. https://doi.org/10.1021/cr900291g.

(63) DiRocco, D. A.; Oberg, K. M.; Dalton, D. M.; Rovis, T. Catalytic Asymmetric Intermolecular Stetter Reaction of Heterocyclic Aldehydes with Nitroalkenes: Backbone Fluorination Improves Selectivity. *J Am Chem Soc* **2009**, *131* (31), 10872–10874. https://doi.org/10.1021/ja904375q.

(64) Halimehjani, A. Z.; Namboothiri, I. N. N.; Hooshmand, S. E. Part I: Nitroalkenes in the Synthesis of Heterocyclic Compounds. *RSC Adv* **2014**, *4* (89), 48022–48084. https://doi.org/10.1039/c4ra08828j.

(65) Arai, T.; Awata, A.; Wasai, M.; Yokoyama, N.; Masu, H. Catalytic Asymmetric Friedel-Crafts/Protonation of Nitroalkenes and N-Heteroaromatics. *Journal of Organic Chemistry* **2011**, *76* (13), 5450–5456. https://doi.org/10.1021/jo200546a.

(66) Li, Y.; Ibsen, L.; Jørgensen, K. A. Formal Asymmetric α-Alkenylation of Aldehydes and the Synthetic Application toward Forming α-Exo-Methylene-γ-Butyrolactones and Skipped Dienes. *Org Lett* **2017**, *19* (5), 1200–1203. https://doi.org/10.1021/acs.orglett.7b00254.

(67) Dell'Aera, M.; Perna, F. M.; Vitale, P.; Altomare, A.; Palmieri, A.; Lewis,]; Maddock, C. H.; Bole, L. J.; Kennedy, A. R.; Hevia, E.; Capriati, V. Boosting Conjugate Addition to Nitroolefins Using Lithium Tetraorganozincates: Synthetic Strategies and Structural Insights. *Chem.Eur.J* **2020**, *26*, 8742–8748. https://doi.org/doi.org/10.1002/chem.202001294.

(68) Choudhury, A. R.; Manna, M. S.; Mukherjee, S. Nitro-Enabled Catalytic Enantioselective Formal: Umpolung Alkenylation of β-Ketoesters. *Chem Sci* **2017**, *8* (9), 6686–6690. https://doi.org/10.1039/c7sc02232h.

(69) Palmieri, A.; Gabrielli, S.; Sampaolesi, S.; Ballini, R. A New Synthesis of Polyfunctionalized 2-Alkyl-1,4-Diketones. *Synlett* **2015**, *26* (9), 1207–1212. https://doi.org/10.1055/s-0034-1380500.

(70) Gabrielli, S.; Chiurchiù, E.; Sampaolesi, S.; Ballini, R.; Palmieri, A. Synthesis of β-Nitro Ketones by Chemoselective Reduction of β-Nitro Enones under Solid Heterogeneous Catalysis. *Synthesis (Germany)* **2017**, *49* (13), 2980–2984. https://doi.org/10.1055/s-0036-1588993.

(71) Chiurchiù, E.; Gabrielli, S.; Ballini, R.; Palmieri, A. A New Valuable Synthesis of Polyfunctionalized Furans Starting from β-Nitroenones and Active Methylene Compounds. *Molecules* **2019**, *24* (24). https://doi.org/10.3390/molecules24244575.

(72) Yuan, L.; Kachalova, L.; Khan, M. E. I.; Ballini, R.; Petrini, M.; Palmieri, A. Overcoming the Usual Reactivity of β-Nitroenones: Synthesis of Polyfunctionalized Homoallylic Alcohols and Conjugated

Nitrotriene Systems. *Journal of Organic Chemistry* **2023**, *88* (7), 4770–4777. https://doi.org/10.1021/acs.joc.2c02669.

(73) Smith, L. I.; Kelly, R. E. Cyclopropanes. XI. Pyrones from Nitrocyclopropyl Ketones. *J. Am. Chem. Soc.* **1952**, *74* (13), 3305–3309.

(74) Smith, L. I.; Holly, E. D. Cyclopropanes. XVII. 1-p-Bromobenzoyl-2-Nitro-3-Phenylcyclopropane: Action of Acidic Reagents. *J. Am. Chem. Soc.* **1956**, *78* (7), 1475–1480.

(75) Deb, I.; Shanbhag, P.; Mobin, S. M.; Namboothiri, I. N. N. Morita-Baylis-Hillman Reactions between Conjugated Nitroalkenes or Nitrodienes and Carbonyl Compounds. *European J Org Chem* **2009**, No. 24, 4091–4101. https://doi.org/10.1002/ejoc.200900475.

(76) Miao, M.; Luo, Y.; Xu, H.; Jin, M.; Chen, Z.; Xu, J.; Ren, H. Strain-Promoted Nitration of 3-Cyclopropylideneprop-2-En-1-Ones and the Application for the Synthesis of Pyrroles. *Journal of Organic Chemistry* **2017**, *82* (23), 12224–12237. https://doi.org/10.1021/acs.joc.7b02087.

(77) Chiurchiù, E.; Xhafa, S.; Ballini, R.; Maestri, G.; Protti, S.; Palmieri, A. Diastereoselective Isomerization of (E)-β-Nitroenones into β-Nitro-β,γ-Unsaturated Ketones under Microwave Conditions. *Adv Synth Catal* **2020**, *362* (21), 4680–4686. https://doi.org/10.1002/adsc.202000747.

(78) Raviola, C.; Carrera, C.; Serra, M.; Palmieri, A.; Lupidi, G.; Maestri, G.; Protti, S. Visible-Light-Driven Competitive Stereo- and Regioisomerization of (E)-β-Nitroenones. *ChemPhotoChem* **2021**, *5* (9), 871–875. https://doi.org/10.1002/cptc.202100081.

(79) Lupidi, G.; Bassetti, B.; Ballini, R.; Petrini, M.; Palmieri, A. A New and Effective One-Pot Synthesis of Polysubstituted Carbazoles Starting from β-Nitro-β,γ-Unsaturated-Ketones and Indoles. *Asian J Org Chem* **2021**, *10* (9), 2334–2337. https://doi.org/10.1002/ajoc.202100342.

(80) Bassetti, B.; Ballini, R.; Petrini, M.; Palmieri, A. Diastereoselective Conversion of β-Nitro-β,γ-Unsaturated Ketones into Conjugated (E,E)-Dienones. *Adv Synth Catal* **2023**, *365* (1), 13–16. https://doi.org/10.1002/adsc.202201151.

(81) Khan, M. E. I.; Yuan, L.; Petrini, M.; Palmieri, A. A New One-Pot Synthesis of 3,6-Disubstituted Pyridazines Starting from β-Nitro-β,γ-Unsaturated Ketones. *Synthesis (Stuttg)* **2023**, *55* (19), 3204–3208.

(82) Palmieri, A.; Gabrielli, S.; Ballini, R. Low Impact Synthesis of β-Nitroacrylates under Fully Heterogeneous Conditions. *Green Chemistry* **2013**, *15* (9), 2344–2348. https://doi.org/10.1039/c3gc40936h.

(83) Gabrielli, S.; Chiurchiù, E.; Palmieri, A. β-Nitroacrylates: A Versatile and Growing Class of Functionalized Nitroalkenes. *Adv Synth Catal* **2019**, *361* (4), 630–653. https://doi.org/10.1002/adsc.201800709.

(84) Ballini, R.; Gabrielli, S.; Palmieri, A. β-Nitroacrylates as an Emerging, Versatile Class of Functionalized Nitroalkenes for the Synthesis of a Variety of Chemicals. *Curr Org Chem* **2010**, *14*, 65–83.

(85) Gabrielli, S.; Palmieri, A.; Panmand, D. S.; Lanari, D.; Vaccaro, L.; Ballini, R. β-Nitroacrylates as Key Starting Materials for the One-Pot Synthesis of Densely Functionalized Penta-Substituted Anilines. *Tetrahedron* **2012**, *68* (39), 8231–8235. https://doi.org/10.1016/j.tet.2012.07.065.

(86) Ishikawa, H.; Suzuki, T.; Orita, H.; Uchimaru, T.; Hayashi, Y. High-Yielding Synthesis of the Anti-Influenza Neuraminidase Inhibitor (-)-Oseltamivir by Two "One-Pot" Sequences. *Chemistry - A European Journal* **2010**, *16* (42), 12616–12626. https://doi.org/10.1002/chem.201001108.

(87) Palmieri, A.; Gabrielli, S.; Ballini, R. Michael Reaction of Nitroalkanes with β-Nitroacrylates under a Solid Promoter: Advanced Regio-and Diastereoselective Synthesis of Nitro-Functionalized Bβ-Unsaturated Esters and 1,3-Butadiene-2-Carboxylates. *Adv Synth Catal* **2010**, *352* (9), 1485–1492. https://doi.org/10.1002/adsc.201000142.

(88) Lewandowska, E. Nucleophilic α-Addition to β-Nitroacrylates: Application to the Synthesis of α-Thioacrylates. *Tetrahedron* **2006**, *62* (20), 4879–4883. https://doi.org/10.1016/j.tet.2006.03.015.

(89) Massolo, E.; Benaglia, M.; Annunziata, R.; Palmieri, A.; Celentano, G.; Forni, A. Stereoselective Synthesis of Functionalized Chiral 2- Nitrocyclohexanecarboxylic Esters via Catalytic Dienamine Addition to β-Substituted β-Nitroacrylates. *Adv Synth Catal* **2014**, *356* (2–3), 493–500. https://doi.org/10.1002/adsc.201301074.

(90) Palmieri, A.; Gabrielli, S.; Lanari, D.; Vaccaro, L.; Ballini, R. A New One-Pot Synthesis of Polysubstituted Indoles from Pyrroles and β-Nitroacrylates. *Adv Synth Catal* **2011**, *353* (9), 1425–1428. https://doi.org/10.1002/adsc.201000965.

(91) Palmieri, A.; Ley, S. V.; Polyzos, A.; Ladlow, M.; Baxendale, I. R. Continuous Flow Based Catch and Release Protocol for the Synthesis of α-Ketoesters. *Beilstein Journal of Organic Chemistry* **2009**, *5*. https://doi.org/10.3762/bjoc.5.23.

(92) Gabrielli, S.; Ciabattoni, L.; Sampaolesi Susanna; Ballini Roberto; Palmieri Alessandro. A New Fully Heterogeneous Synthesis of Pyrrole-2-Acetic Acid. *RCS Advances* **2016**, *6*, 44341–44344. https://doi.org/https://doi.org/10.1039/C6RA05348C.

(93) Khan, M. E. I.; Di Terlizzi, L.; Protti, S.; Palmieri, A. Visible-Light-Driven Photocatalyst-Free Preparation of (Z) β-Nitroacrylate Isomers. *European J Org Chem* **2022**, *2022* (26). https://doi.org/10.1002/ejoc.202200635.

(94) Ballini, R.; Bazán, N. A.; Bosica, G.; Palmieri, A. Uncatalyzed, Anti-Michael Addition of Amines to β-Nitroacrylates: Practical, Eco-Friendly Synthesis of β-Nitro-α-Amino Esters. *Tetrahedron Lett* **2008**, *49* (24), 3865–3867. https://doi.org/10.1016/j.tetlet.2008.04.076.

(95) Palmieri, A.; Gabrielli, S.; Cimarelli, C.; Ballini, R. Fast, Mild, Eco-Friendly Synthesis of Polyfunctionalized Pyrroles from β-Nitroacrylates and β-Enaminones. *Green Chemistry* **2011**, *13* (12), 3333–3336. https://doi.org/10.1039/c1gc16012e.

(96) Chiurchiù, E.; Patehebieke, Y.; Gabrielli, S.; Ballini, R.; Palmieri, A. β-Nitroacrylates as Starting Materials of Thiophene-2-Carboxylates Under Continuous Flow Conditions. *Adv Synth Catal* **2019**, *361* (9), 2042–2047. https://doi.org/10.1002/adsc.201801660.

(97) Ballini, R.; Gabrielli, S.; Palmieri, A. β-Nitroacrylates as Precursors of Tetrasubstituted Furans in a One-Pot Process and under Acidic Solvent-Free Conditions. *Synlett* **2010**, No. 16, 2468–2470. https://doi.org/10.1055/s-0030-1258031.

(98) Jorea, A.; Bassetti, B.; Gervasoni, K.; Protti, S.; Palmieri, A.; Ravelli, D. More Chips to Nitroolefins: Decatungstate Photocatalysed Hydroalkylation Under Batch and Flow Conditions. *Adv Synth Catal* **2023**, *365* (5), 722–727. https://doi.org/10.1002/adsc.202201314.

(99) Caruso, A.; Ceramella, J.; Iacopetta, D.; Saturnino, C.; Mauro, M. V.; Bruno, R.; Aquaro, S.; Sinicropi, M. S. Carbazole Derivatives as Antiviral Agents: An Overview. *Molecules* **2019**, *24* (10).

(100) Patil, S. A.; Patil, S. A.; Ble-González, E. A.; Isbel, S. R.; Hampton, S. M.; Bugarin, A. Carbazole Derivatives as Potential Antimicrobial Agents. *Molecules* **2022**, *27* (19). https://doi.org/10.3390/molecules27196575.

(101) Aggarwal, T.; Sushmita; Verma, A. K. Recent Advances in the Synthesis of Carbazoles from Indoles. *Org Biomol Chem* **2019**, *17* (36), 8330–8342. https://doi.org/10.1039/c9ob01381d.

(102) Verma, A. K.; Danodia, A. K.; Saunthwal, R. K.; Patel, M.; Choudhary, D. Palladium-Catalyzed Triple Successive C-H Functionalization: Direct Synthesis of Functionalized Carbazoles from Indoles. *Org Lett* **2015**, *17* (15), 3658–3661. https://doi.org/10.1021/acs.orglett.5b01476.

(103) Wang, H.; Wang, Z.; Wang, Y. L.; Zhou, R. R.; Wu, G. C.; Yin, S. Y.; Yan, X.; Wang, B. N-Bromosuccinimide (NBS)-Catalyzed C-H Bond Functionalization: An Annulation of Alkynes with Electron Withdrawing Group (EWG)-Substituted Acetyl Indoles for the Synthesis of Carbazoles. *Org Lett* **2017**, *19* (22), 6140–6143. https://doi.org/10.1021/acs.orglett.7b03021.

(104) Chen, S.; Jiang, P.; Wang, P.; Pei, Y.; Huang, H.; Xiao, F.; Deng, G. J. Three-Component Cascade Synthesis of Carbazoles through [1s,6s] Sigmatropic Shift under Metal-Free Conditions. *Journal of Organic Chemistry* **2019**, *84* (6), 3121–3131. https://doi.org/10.1021/acs.joc.8b02994.

(105) Chiurchiù, E.; Xhafa, S.; Ballini, R.; Maestri, G.; Protti, S.; Palmieri, A. Diastereoselective Isomerization of (E)-β-Nitroenones into β-Nitro-β,γ-Unsaturated Ketones under Microwave Conditions. *Adv Synth Catal* **2020**, *362* (21), 4680–4686. https://doi.org/10.1002/adsc.202000747.

(106) Ballini, R.; Clemente, R. R.; Palmieri, A.; Petrini, M. Conjugate Addition of Indoles to Nitroalkenes Promoted by Basic Alumina in Solventless Conditions. *Adv Synth Catal* **2006**, *348* (1–2), 191–196. https://doi.org/10.1002/adsc.200505339.

(107) Ballini, R.; Gabrielli, S.; Palmieri, A.; Petrini, M. Improved Preparation of Alkyl 2-(3-Indolyl)-3-Nitroalkanoates under Fully Heterogeneous Conditions: Stereoselective Synthesis of Alkyl (E)-2-(3-Indolyl)-2-Alkenoates. *Tetrahedron* **2008**, *64* (23), 5435–5441. https://doi.org/10.1016/j.tet.2008.04.014.

(108) Tang, R. J.; Milcent, T.; Crousse, B. Friedel-Crafts Alkylation Reaction with Fluorinated Alcohols as Hydrogen-Bond Donors and Solvents. *RSC Adv* **2018**, *8* (19), 10314–10317. https://doi.org/10.1039/c8ra01397g.

(109) Gabrielli, S.; Panmand, D.; Ballini, R.; Palmieri, A. β-Nitroacrylates: New Key Precursors of Indole-2-Carboxylates via Fischer Indole Synthesis. *Applied Sciences* **2019**, *9* (5168). https://doi.org/10.3390/app9235168.

(110) Burghart-Stoll, H.; Brückner, R. Total Syntheses of the Gregatins A-D and Aspertetronin A: Structure Revisions of These Compounds and of Aspertetronin B, Together with Plausible Structure Revisions of Gregatin E, Cyclogregatin, Graminin A, the Penicilliols A and B, and the Huaspenones A and B. *European J Org Chem* **2012**, No. 21, 3978–4017. https://doi.org/10.1002/ejoc.201200207.

(111) Mathew, B.; Oh, J. M.; Abdelgawad, M. A.; Khames, A.; Ghoneim, M. M.; Kumar, S.; Nath, L. R.; Sudevan, S. T.; Parambi, D. G. T.; Agoni, C.; Soliman, M. E. S.; Kim, H. Conjugated Dienones from Differently Substituted Cinnamaldehyde as Highly Potent Monoamine Oxidase-B Inhibitors:

Synthesis, Biochemistry, and Computational Chemistry. *ACS Omega* **2022**, *7* (9), 8184–8197. https://doi.org/10.1021/acsomega.2c00397.

(112) Iqbal, M.; Evans, P. Conjugate Addition-Peterson Olefination Reactions: Expedient Routes to Cross Conjugated Dienones. *Tetrahedron Lett* **2003**, *44* (30), 5741–5745. https://doi.org/10.1016/S0040-4039(03)01297-8.

(113) Bräse, S.; Encinas, A.; Keck, J.; Nising, C. F. Chemistry and Biology of Mycotoxins and Related Fungal Metabolites. *Chem Rev* **2009**, *109* (9), 3903–3990. https://doi.org/10.1021/cr050001f.

(114) Soga, S.; Shiotsu, Y.; Akinaga, S.; Sharma, S. V. Development of Radicicol Analogues. *Curr Cancer Drug Targets* **2003**, *3*, 359–369.

(115) Chalapareddy, S.; Bhattacharyya, M. K.; Mishra, S.; Bhattacharyya, S. Radicicol Confers Mid-Schizont Arrest by Inhibiting Mitochondrial Replication in Plasmodium Falciparum. *Antimicrob Agents Chemother* **2014**, *58* (8), 4341–4352. https://doi.org/10.1128/AAC.02519-13.

(116) Trifonov, L. S.; Ben, J. H.; Piewo, R.; Dreiding, A. S. ISOLATION AND STRUCTURE ELUCIDATION OF THREE METABOLITES FROM VERTICILLIUM INTERTEXTUM: SORBICILLIN, DIHYDROSORBICILLIN AND BISVERTINOQUINOL. *Tetrahedron* **1983**, *39* (24), 4243–4256.

(117) Meng, J.; Wang, X.; Xu, D.; Fu, X.; Zhang, X.; Lai, D.; Zhou, L.; Zhang, G. Sorbicillinoids from Fungi and Their Bioactivities. *Molecules* **2016**, *21* (715). https://doi.org/10.3390/molecules21060715.

(118) Meng, J.; Gu, G.; Dang, P.; Zhang, X.; Wang, W.; Dai, J.; Liu, Y.; Lai, D.; Zhou, L. Sorbicillinoids from the Fungus Ustilaginoidea Virens and Their Phytotoxic, Cytotoxic, and Antimicrobial Activities. *Front Chem* **2019**, *7* (435). https://doi.org/10.3389/fchem.2019.00435.

(119) Greenberg, M. J. Characterization of Meat and Bone Meal Flavor Volatiles. *J. Agric. Food Chem.* **1981**, *29*, 1276–1280.

(120) Heydanek, M. G.; Mcgorrin, R. J. Gas Chromatography-Mass Spectroscopy Investigations on the Flavor Chemistry of Oat Groats. *J. Agric. Food. Chem.* **1981**, *29*, 950–954.

(121) Heydanek, M. G.; McGorrin, R. J. Gas Chromatography-Mass Spectroscopy Identification of Volatiles from Rancid Groats. *J. Agric. Food. Chem.* **1981**, *29*, 1093–1095.

(122) Habu, T.; Flath, R. A.; Richard Mon, T.; Morton, J. F.; Col-lectanea, M. Volatile Components of Rooibos Tea (Aspalathus Linearis). *J. Agric. Food Chem.* **1985**, *33*, 249–254.

(123) Poulsen, P. H.; Vergura, S.; Monleón, A.; Jørgensen, D. K. B.; Jørgensen, K. A. Controlling Asymmetric Remote and Cascade 1,3-Dipolar Cycloaddition Reactions by Organocatalysis. *J Am Chem Soc* **2016**, *138* (20), 6412–6415. https://doi.org/10.1021/jacs.6b03546.

(124) Cadierno, V. (E)-1,1,1-Trifluoro-6,6-Bis(4-Methoxyphenyl)Hexa-3,5-Dien-2-One. *Molbank* **2020**, *2020* (1). https://doi.org/10.3390/M1120.

(125) Giovannini, R.; Marcantoni, E.; Petrini, M. Claisen Rearrangement of γ-Hydroxyvinyl Sulfones via Ketene Acetal Derivatives. A New Entry to Functionalized (2E,4E)-Alkadienoic Esters. *Tetrahedron Lett* **1998**, *39*, 5827–5830.

(126) Keck, D.; Muller, T.; Bräse, S. A Stereoselective Suzuki Cross-Coupling Strategy for the Synthesis of Ethyl-Substituted Conjugated Dienoic Esters and Conjugated Dienones. *Synlett* **2006**, No. 20, 3457–3460. https://doi.org/10.1055/s-2006-958406.

(127) Huang, Y.-Z.; Mo, X.-S. Conjugated Polyenic Tellurides As Novel Building Blocks: A Facile and Novel Stereoselective Preparation of Conjugated Polyenic Ketones. *Tetrahedron Lett* **1998**, *39*, 1945–1948.

(128) Pan, G. F.; Zhang, X. L.; Zhu, X. Q.; Guo, R. L.; Wang, Y. Q. Synthesis of (E,E)-Dienones and (E,E)-Dienals via Palladium-Catalyzed γ,δ-Dehydrogenation of Enones and Enals. *iScience* **2019**, *20*, 229–236. https://doi.org/10.1016/j.isci.2019.09.027.

(129) Ballini, R.; Palmieri, A. Formation of Carbon-Carbon Double Bonds: Recent Developments via Nitrous Acid Elimination (NAE) from Aliphatic Nitro Compounds. *Adv Synth Catal* **2019**, *361* (22), 5070–5097. https://doi.org/10.1002/adsc.201900563.

(130) Twilton, J.; Le, C. C.; Zhang, P.; Shaw, M. H.; Evans, R. W.; MacMillan, D. W. C. The Merger of Transition Metal and Photocatalysis. *Nat Rev Chem* **2017**, *1*. https://doi.org/10.1038/s41570-017-0052.

(131) Ravelli, D.; Fagnoni, M.; Albini, A. Photoorganocatalysis. What For? *Chem Soc Rev* **2013**, *42* (1), 97–113. https://doi.org/10.1039/c2cs35250h.

(132) Srivastava, V.; Singh, P. K.; Singh, P. P. Recent Advances of Visible-Light Photocatalysis in the Functionalization of Organic Compounds. *Journal of Photochemistry and Photobiology C: Photochemistry Reviews* **2022**, *50* (100488). https://doi.org/10.1016/j.jphotochemrev.2022.100488.

(133) Capaldo, L.; Ravelli, D. Hydrogen Atom Transfer (HAT): A Versatile Strategy for Substrate Activation in Photocatalyzed Organic Synthesis. *European J Org Chem* **2017**, *2017* (15), 2056–2071. https://doi.org/10.1002/ejoc.201601485.

(134) Hartwig, J. F.; Larsen, M. A. Undirected, Homogeneous C-H Bond Functionalization: Challenges and Opportunities. *ACS Cent Sci* **2016**, *2* (5), 281–292. https://doi.org/10.1021/acscentsci.6b00032.

(135) Capaldo, L.; Ravelli, D.; Fagnoni, M. Direct Photocatalyzed Hydrogen Atom Transfer (HAT) for Aliphatic C-H Bonds Elaboration. *Chem Rev* **2022**, *122* (2), 1875–1924. https://doi.org/10.1021/acs.chemrev.1c00263.

(136) Fagnoni, M.; Dondi, D.; Ravelli, D.; Albini, A. Photocatalysis for the Formation of the C-C Bond. *Chem Rev* **2007**, *107* (6), 2725–2756. https://doi.org/10.1021/cr068352x.

(137) Cao, H.; Tang, X.; Tang, H.; Yuan, Y.; Wu, J. Photoinduced Intermolecular Hydrogen Atom Transfer Reactions in Organic Synthesis. *Chem Catalysis* **2021**, *1* (3), 523–598. https://doi.org/10.1016/j.checat.2021.04.008.

(138) Tzirakis, M. D.; Lykakis, I. N.; Orfanopoulos, M. Decatungstate as an Efficient Photocatalyst in Organic Chemistry. *Chem Soc Rev* **2009**, *38* (9), 2609–2621. https://doi.org/10.1039/b812100c.

(139) Waele, V. De; Poizat, O.; Fagnoni, M.; Bagno, A.; Ravelli, D. Unraveling the Key Features of the Reactive State of Decatungstate Anion in Hydrogen Atom Transfer (HAT) Photocatalysis. *ACS Catal* **2016**, *6* (10), 7174–7182. https://doi.org/10.1021/acscatal.6b01984.

(140) Angioni, S.; Ravelli, D.; Emma, D.; Dondi, D.; Fagnoni, M.; Albini, A. Tetrabutylammonium Decatungstate (Chemo)Selective Photocatalyzed, Radical C-H Functionalization in Amides. *Adv Synth Catal* **2008**, *350* (14–15), 2209–2214. https://doi.org/10.1002/adsc.200800378.

(141) Protti, S.; Fagnoni, M.; Ravelli, D. Photocatalytic C-H Activation by Hydrogen-Atom Transfer in Synthesis. *ChemCatChem* **2015**, *7* (10), 1516–1523. https://doi.org/10.1002/cctc.201500125.

(142) Ravelli, D.; Protti, S.; Fagnoni, M. Decatungstate Anion for Photocatalyzed "Window Ledge" Reactions. *Acc Chem Res* **2016**, *49* (10), 2232–2242. https://doi.org/10.1021/acs.accounts.6b00339.

(143) Raviola, C.; Ravelli, D. Efficiency and Selectivity Aspects in the C-H Functionalization of Aliphatic Oxygen Heterocycles by Photocatalytic Hydrogen Atom Transfer. *Synlett* **2019**, *30* (7), 803–809. https://doi.org/10.1055/s-0037-1612079.

(144) Cruise, A.; Baumann, M. TBADT-Mediated C-C Bond Formation Exploiting Aryl Aldehydes in a Photochemical Flow Reactor. *ChemCatChem* **2023**, *15* (2). https://doi.org/10.1002/cctc.202201328.

(145) Huang, J.; Ding, F.; Rojsitthisak, P.; He, F. S.; Wu, J. Recent Advances in Nitro-Involved Radical Reactions. *Organic Chemistry Frontiers* **2020**, *7* (18), 2873–2898. https://doi.org/10.1039/d0qo00563k.

(146) Zhang, N.; Quan, Z. J.; Zhang, Z.; Da, Y. X.; Wang, X. C. Synthesis of Stilbene Derivatives via Visible-Light-Induced Cross-Coupling of Aryl Diazonium Salts with Nitroalkenes Using-NO2 as a Leaving Group. *Chemical Communications* **2016**, *52* (99), 14234–14237. https://doi.org/10.1039/c6cc08182g.

(147) Tripathi, S.; Kapoor, R.; Yadav, L. D. S. Visible Light Activated Radical Denitrative Benzoylation of β-Nitrostyrenes: A Photocatalytic Approach to Chalcones. *Adv Synth Catal* **2018**, *360* (7), 1407–1413. https://doi.org/10.1002/adsc.201701559.

(148) Kapoor, R.; Chawla, R.; Yadav, L. D. S. Denitrative Thiocyanation of β-Nitrostyrenes through Visible Light Photoredox Catalysis: An Easy Access to (E)-Vinyl Thiocyanates. *Tetrahedron Lett* **2020**, *61* (46). https://doi.org/10.1016/j.tetlet.2020.152505.

(149) Midya, S. P.; Rana, J.; Abraham, T.; Aswin, B.; Balaraman, E. Metal-Free Radical Trifluoromethylation of β-Nitroalkenes through Visible-Light Photoredox Catalysis. *Chemical Communications* **2017**, *53* (50), 6760–6763. https://doi.org/10.1039/c7cc02589k.

(150) Zhang, M.; Yang, L.; Yang, H.; An, G.; Li, G. Visible Light Mediated C(Sp3)-H Alkenylation of Cyclic Ethers Enabled by Aryl Ketone. *ChemCatChem* **2019**, *11* (6), 1606–1609. https://doi.org/10.1002/cctc.201802079.

(151) Kulthe, A. D.; Mainkar, P. S.; Akondi, S. M. Intermolecular Trifluoromethyl-Alkenylation of Alkenes Enabled by Metal-Free Photoredox Catalysis. *Chemical Communications* **2021**, *57* (45), 5582–5585. https://doi.org/10.1039/d1cc01806j.

(152) Yu, Z. Y.; Zhao, J. N.; Yang, F.; Tang, X. F.; Wu, Y. F.; Ma, C. F.; Song, B.; Yun, L.; Meng, Q. W. Rose Bengal as Photocatalyst: Visible Light-Mediated Friedel-Crafts Alkylation of Indoles with Nitroalkenes in Water. *RSC Adv* **2020**, *10* (8), 4825–4831. https://doi.org/10.1039/c9ra09227g.

(153) Stevenson, S. M.; Higgins, R. F.; Shores, M. P.; Ferreira, E. M. Chromium Photocatalysis: Accessing Structural Complements to Diels-Alder Adducts with Electron-Deficient Dienophiles. *Chem Sci* **2016**, *8* (1), 654–660. https://doi.org/10.1039/c6sc03303b.

(154) Ravelli, D.; Albini, A.; Fagnoni, M. Smooth Photocatalytic Preparation of 2-Substituted 1,3-Benzodioxoles. *Chemistry - A European Journal* **2011**, *17* (2), 572–579. https://doi.org/10.1002/chem.201002546.

(155) Jorea, A.; Ravelli, D.; Romarowski, R. M.; Marconi, S.; Auricchio, F.; Fagnoni, M. Photocatalyzed Functionalization of Alkenoic Acids in 3D-Printed Reactors. *ChemSusChem* **2022**, *15* (17). https://doi.org/10.1002/cssc.202200898.

3 Bioactive natural products in organic synthesis

3.1 Natural products in organic synthesis

Natural products can be defined as all substances that are produced by any living organism in the entire world, such as, bacteria, fungi and plants, which means something unambiguously wide and measureless.

However, to somehow narrow the field to organic chemistry and synthesis, natural products often refer to organic compounds that are isolated from various natural sources, as main or, more frequently, as secondary metabolites.[1] These latter, in particular, are organic compounds that are not directly involved in the growth, development, or reproduction of the organism that is producing them, serving various ecological functions such as defence against predators, competition for resources, or communication. Usually, they can be generated by other reaction pathways and be present just in traces.[2]
The interest in these compounds arises and it is often related to their applications and effects on human sphere, either in pharmacotherapy (especially for cancer and infectious diseases),[3–6] cosmetic,[7] or as foods and supplements,[8] to cite some.
The first challenges consist in their isolation from the natural source,[9] followed by the characterization and definition of the properties and potential activity towards different systems. Subsequent steps can be devoted to access them, in considerable amount, through total or semi-synthesis, which can be more than arduous, but also crucial.[10] This is due and resides in the intrinsic structural complexity of natural derivatives. Moreover, once obtained, further modification to the structure, or late-stage modifications, can provide an array of useful analogues, with the possibility to enhance the activity, solubility or bioavailability, or reduce the toxicity.[11] Natural sources provide an incredible starting point for conducting fundamental research on potential bioactive compounds that can be further developed for commercial purposes, particularly as lead compounds in drug discovery,[12–14] but also in other fields, such as agriculture.[15]

It is well documented how the pharmaceutical industry has shown a progressively decreased interest in drug development from natural sources in the 21st century, probably due to the many challenges derived from supply chain, costs of extraction and purification, regulatory affairs and seasonal variability.[16,17] Moreover, natural sources are not infinite, and climate change with related instability is a looming threat for their use and investigation, whatever the purpure might be. In this context, the possibility to envisage a synthetic process for these enigmatic natural compounds appears to be of paramount importance.[18]

Numerous drugs, about 35% of the one at our disposal on the marked every year, have natural origin,[19] and if we consider that less than 10% of world's total biodiversity has been currently evaluated for potential biological activity,[20] this can give an idea of what their actual impact is now, and what it could be also in the future. Few examples are documented in **Figure 3.1**.
Avermectin B1a is the most potent anthelmintic in the avermectins family, antiparasitic agents isolated from *Streptomyces avermitilis* in the 1970s.[21] This macrolactone's first synthesis was envisaged

more than a decade later by Hanessian and coworkers,[22] but the search for new efficient and straightforward synthetic routes never stopped. In 2016 a protocol, based on the fragmentation of the molecule into two distinct segments (north and south) with a final glycosylation, leaded to the total synthesis of Avermectin B1a.[23]

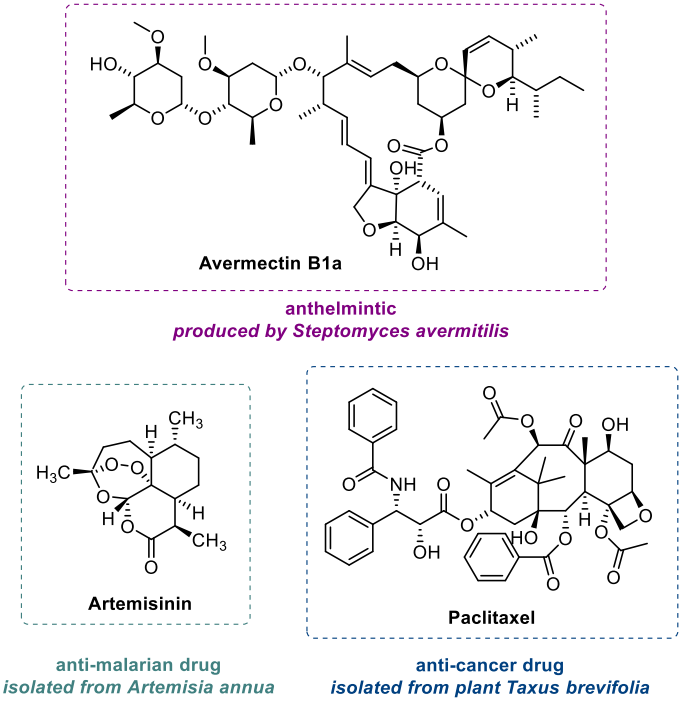

Figure 3.1 Examples of natural drug molecules

Artemisinin is sesquiterpene lactone, which is an organic compound characterized by the presence of an endoperoxide bridge within the structure, essential for its ability to effectively target and eradicate the malaria parasite.[24] Its mysterious discovery dates back to the years of the Vietnam War, in which a lot of soldiers lost their lives also due to the contraction of the disease. The war actually boosted the research for treatments, and through the screening of the traditional Chinese pharmacopoeia, scientists were able to identify over ten plants that exhibited promising antimalarial activities. Among these, *Artemisia annua* (known as qinghao) was particularly noteworthy.[25] This has contributed to further research and the development of effective treatments for malaria, untill the introduction of artemisinin-based combinatory therapies (ACTs).[26] Although various routes for the total synthesis have been reported,[27–30] the current reliance on the natural plant as source highlights the complexities involved in achieving a consistent and cost-effective production of artemisinin, mostly on large scale.

Paclitaxel, also called Taxol®, is a well-known drug, established treatment in several different types of tumor, such as breast, ovarian and lung cancer,[31] firstly isolated from *Taxus brevifolia*. By interfering

with these activities, paclitaxel prevents proper cellular functioning and induces cell death (cytotoxic effects).[32]

Paclitaxel is one of the most active compounds within the taxanes family, but its low concentration in the yew trees (about 0.02%) and limited availability of the natural sources, delayed the landing on the market.[32,33] Major advancements were obtained with the identification and isolation of the key precursor 10-deacetylbaccatin III (10-DAB) in the more common european *Taxus baccata*.[34–36] Notwithstanding, researchers still focused on the possible total synthesis of these compounds starting from more accessible starting materials, an attention that never faded away. Great contribution in this sense were provided by Holton and Nicolau and their respective groups, with the first total syntheses ever published,[37–40] and few years later by Danishefsky and coworkers,[41] followed by Mohira et. al.[42] More recent examples testify the continuous search for alternative routes to access the molecule,[43–46] as summarized by **Figure 3.2**.[46]

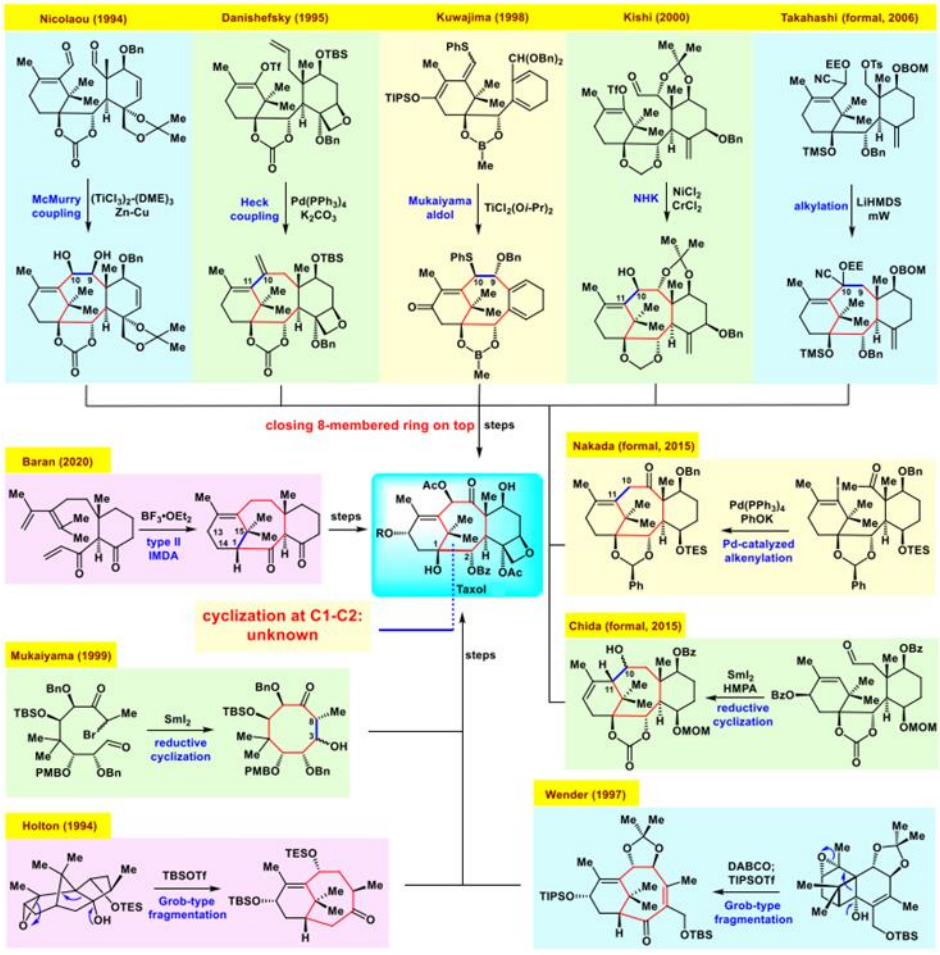

Figure 3.2 Summary of synthetic routes to access Paclitaxel. Figure taken from ref.[46]

While the scientific advancements have demonstrated the feasibility of synthesizing paclitaxel through total synthesis, the challenges associated with low yields of intermediates and the numerous synthetic steps limit its practical application on an industrial scale. Therefore, alternative strategies such as semi-synthesis, which involves modifying naturally derived precursors, or utilizing more efficient extraction methods from natural sources, are currently favoured.[32]
Currently, the anticancer is still produced mainly by semi-synthetic procedure from 10-DAB,[47] which is also an intermediate in the synthesis another potent antineoplastic drug, namely Docetaxel, thus responding to the growing demands of these molecules. Furthermore, a standardized method guarantees controlled production with higher purity grade of the API.[48]

The report of these few examples, with their challenges and perspectives, aimed to reflect the complexity derived from the synthesis of important natural products that, however, have great impact on the pharmaceutical field for the treatment of several major conditions.

During my PhD, I had the occasion of work on the synthesis of different natural products and their metabolites,[49–51] with the possibility of exploiting enabling techniques to achieve the purpose. In particular, within this thesis work two examples are reported, namely the preparation of flavonoid Luteoloside starting from the more accessible Luteolin (**Chapter 3.2**),[49] and the selective conversion of Cannabidiol (CBD) into Δ^9-THC and Δ^8-THC, using continuous flow chemistry **(Chapter 3.4)**.[50]

3.2 Thesis work: Synthetic approach for the preparation of Luteoloside

The results presented in this section are adapted from:

A Practical and Efficient Conversion of Luteolin into Luteoloside, Bassetti, B., Ballini, R., Ciceri, D., Allegrini, P., Palmieri, A., *Synthesis* **2021**, *53*, 4075-4078

3.2.1 Introduction

Flavonoids are a significant class of natural products that are widely present throughout the plant kingdom, mainly as secondary metabolites.[52,53] They are characterized by a phenylbenzopyran backbone structure (**Figure 3.3**) that is predominantly functionalized with hydroxy or O-derivatized groups, resulting in a polyphenolic structure.[54] Due to their widespread presence in various fruits, such as apples, cherries, oranges, and strawberries, and vegetables, including broccoli, berries, and onions, flavonoids are regarded as important components of the human diet.[55,56]

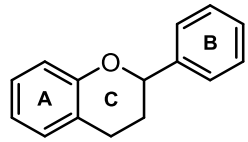

Figure 3.3 General structure of flavonoids

Furthermore, due to their demonstrated wide range of biological effects, such as anti-inflammatory,[57] antioxidant,[58] antimicrobial,[59] and anticarcinogenic activities,[60] flavonoids have garnered significant attention from academic researchers and have piqued the interest of the supplement and pharmaceutical industries. The broad spectra of biological properties have made them a subject of extensive study and have prompted exploration for potential therapeutic applications.[61,62]

Among flavonoids, luteolin (**11**, **Figure 3.4**) holds significant biomedical relevance, second only to quercetin (**Figure 3.4**). Luteolin has shown potential in various areas such as inflammation, cancer, obesity, and dermatology.[63,64] It shares a common feature with quercetin, which is a catechol functionalization on ring B. The main difference between the two compounds lies in the presence of an additional hydroxyl group at position C-3 in quercetin. This slight structural variation between luteolin and quercetin accounts for their distinct properties and potential applications in different biomedical contexts.[65]

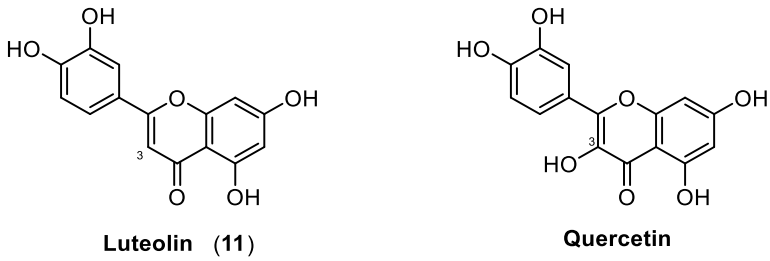

Figure 3.4 Luteolin and quercetin structures

Despite sharing a similar flavonoid core structure, luteolin and quercetin differ in the native glycosidic forms they possess. In luteolin, glycosylation predominantly occurs at the 7-hydroxyl position, resulting in the formation of the 7-O-glucoside (also known as luteoloside or cynaroside, **12** , **Figure 3.5**). On the other hand, quercetin undergoes glycosylation primarily at the 3-hydroxyl position,[66] leading to the formation of the 3-O-rutinoside (also known as rutin, **Figure 3.5**). Both of these glycosides are naturally occurring and have widespread distribution in nature.

However, it is important to note that while rutin is readily isolated and commercially available,[67] the isolation of luteolin glycosides, such as cynaroside, is less common. As a result, rutin is more readily accessible for various applications and research purposes compared to luteolin glycoside.[68]

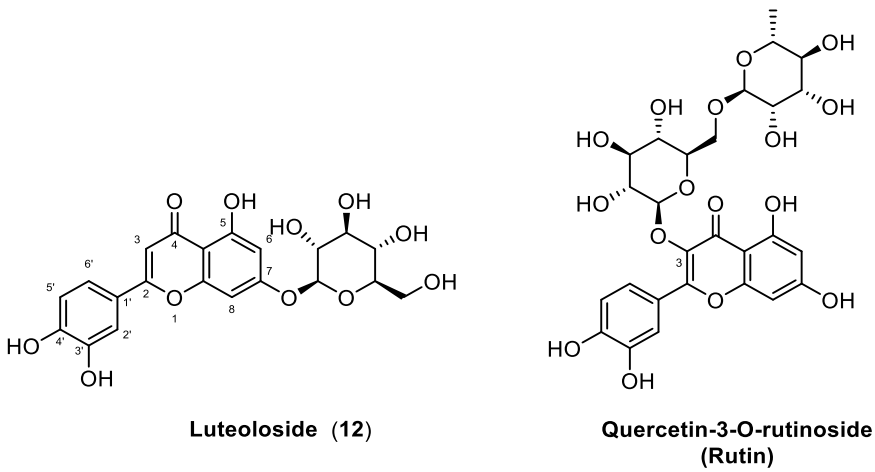

Figure 3.5 Luteoloside and Rutin structures

In contrast, the isolation of luteoloside from its primary natural sources, such as artichoke (*Cynara scolimus* L.), weld (*Reseda luteola* L.), and Japanese honeysuckle (*Lonicera japonica* Thumb), presents challenges due to its lower overall concentration compared to sources of rutin.[69] Additionally, the purification process of luteoloside is further complicated by the presence of analogues or structurally similar compounds that coexist in these sources. These factors make the isolation and purification of luteoloside more complex and potentially less efficient. As reported in **Figure 3.6**, its isolation

from *Cynara scolymus* L., require a long and tedious procedure with number of liquid-liquid extractions, with consequent employment of large amount of solvents, filtrations, oven drying, and also column chromatography purification.

Nevertheless, luteoloside is getting more and more attention in research field, and many recent articles can be found in literature, documenting a variety of activities, exerting an important role in respiratory, cardiovascular and central nervous systems.[70]
Luteoloside exhibits diverse pharmacological effects, including antioxidant,[71] anti-inflammatory,[72,73] antimicrobial,[74] and anticancer.[75,76]

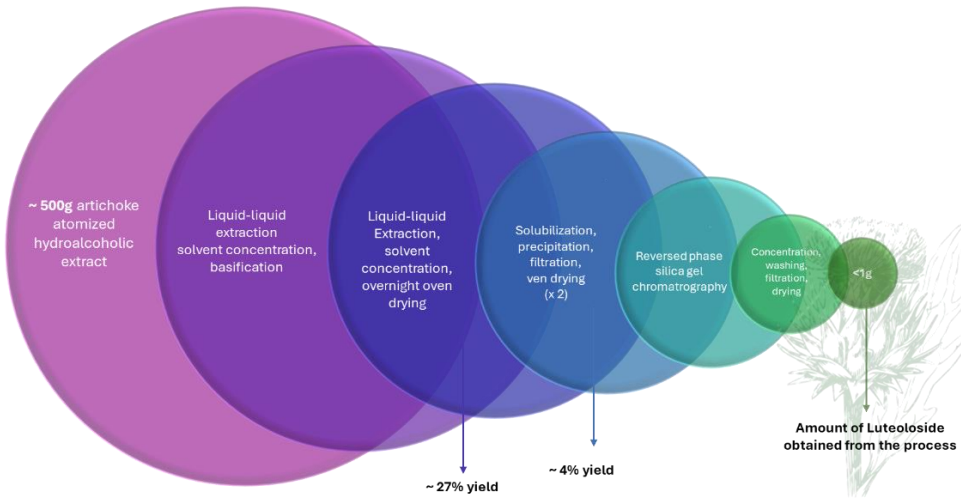

Figure 3.6 Example of extraction process of Luteoloside, performed by Indena Spa

In vitro studies have shed light on specific cellular and molecular mechanisms associated with this compound, however, further investigations are necessary to precisely elucidate its mechanisms, considering its versatile nature. As well as pharmacokinetic and toxicological studies to determine the absorption, availability, and metabolism of luteoloside.[70] Still, these preliminary results open up new possibility for the application of this compound, that could be enhanced with a specific methodology for its synthesis.

For these same reasons, a valuable alternative to overcome the extraction and purification issues can be provided by the synthetic approach. However, only few protocols are reported in the literature, such as the one proposed by Lee et a. (**Scheme 3.1**), [77] starting from benzyl protected luteolin in the catechol moiety, which however suffers from a low overall yield (22%).

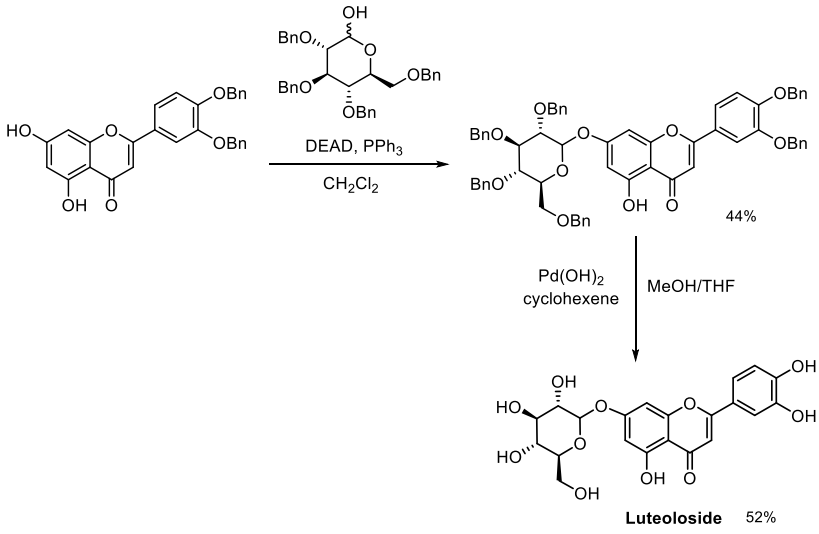

Scheme 3.1 Lee et al. approach for the synthesis of Luteoloside

3.2.2 Results and discussion

Based on previous experimentations focused on the synthesis and derivatization of heterocyclic systems,[78–80] and of biologically active natural compounds,[81,82] made by our research group, we started our investigation towards a more efficient method for the conversion of luteolin into luteoloside. The aim was to provide an improved approach that allows larger-scale production, which is crucial for conducting in vivo bioactivity studies. Additionally, it facilitates the generation of analytical standards that can be used for quantification purposes in food and medicinal plants, thereby enhancing the purification efficiency of luteoloside.

- **Step 1**

We began our study by exploring the protection of luteolin's catechol functionality (**Step 1, Table 3.1**). Preliminary trials were performed using α,α-dichlorodiphenylmethane (1.5-1.6 eq.) in diphenyl ether and at a temperature of 165-175 °C (**Table 1.3, Entries 1-2**), after a literature research.[83,84] In the first case, diphenylmethylene ketal derivative **13** was obtained after 2.5 hours in 51% yield, after a long work-up and purification. Using the second procedure, with a slightly enhanced temperature of 175 °C but shorter reaction time, the product was isolated in 41%.

A further increase in temperature to 185 °C, which is difficult to achieve, control and maintain in conventional batch synthesis, especially for long reaction time, led to a slightly increased product yield (57%, **Table 3.1, Entry 2**). Therefore, to increase the efficiency of the conversion,

we switched from conventional heating to microwave irradiation (see **Chapter 1.3** for a general overview of this enabling technology).

Table 3.1 Investigation on the protection of luteolin's catechol moiety

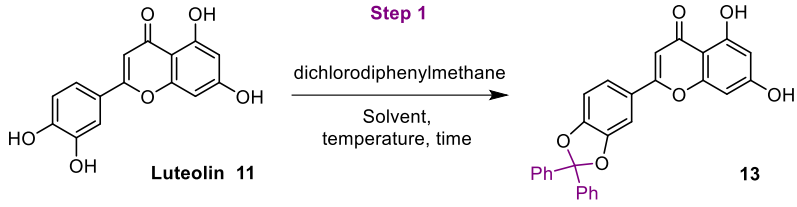

Entry	Solvent	T [°C]	Warming	time [h]	13 [Yield %]
1	PhOPh	165	Conventional heating	2.5	51
2	PhOPh	175	Conventional heating	0.5	41
3	PhOPh	185	Conventional heating	3	57
4	PhOPh	185	MW	2	82
5	PhOPh	175	MW	2	75
6	**1,4-Dioxane**	**185**	**MW**	**2**	**87**
7	CPME	185	MW	-	-
8	2Me-THF	185	MW	-	-

By means of this technique, which bear the flexibility to work under pressure, we were able to expand the range of solvents that could be used in the process. In fact, this allowed us to explore the effects of different ethereal solvents on the synthesis of intermediate **13**, and optimize the reaction conditions. The transfer of batch conditions to MW had the outcome of leading to the isolation of the product in 82% after 2 hours (**Table 1.3, Entry 4**), providing also a cleaner reaction profile, as visible on TLC plates, by reduction of byproducts. A decrease in temperature to 175 °C provided 75% of yield (**Tabe 1.3, Entry 5**). The best yield, 87%, was obtained by conducing the reaction in 1,4-dioxane at 185 °C (the reaction proceeded at 85– 90 W, generating 9 bar of pressure, **Table 1.3, Entry 6**). The use of less polar solvents, such as cyclopentyl methyl ether (CPME) and 2-methyltetrahydrofuran (2-MeTHF) failed in the warming up to 185 °C (**Table 1.3, Entries 7-8**).[85]

- **Step 2**

Subsequently, we adopted a strategy, inspired by the results obtained by Saha for similar substrates,[86] for the glycosylation. Initially, we conducted the reaction using α-D-glucose pentaacetate under Lewis acid conditions, specifically employing $BF_3 \cdot OEt_2$; however it resulted to be completely ineffective. Then, we decided to change approach and to use 1-bromo-α-D-glucose tetraacetate (**16**) as the glycosyl donor, in the presence of tetrabutylammonium bromide (TBAB), K_2CO_3, and chloroform,

motivated by the results obtained by Wang when applying this methodology for the derivatization of 4'-O-benzylapigenin. Under these reaction conditions, we were able to successfully isolate product **14**, in a very good yield of 80% (**Scheme 3.2**).

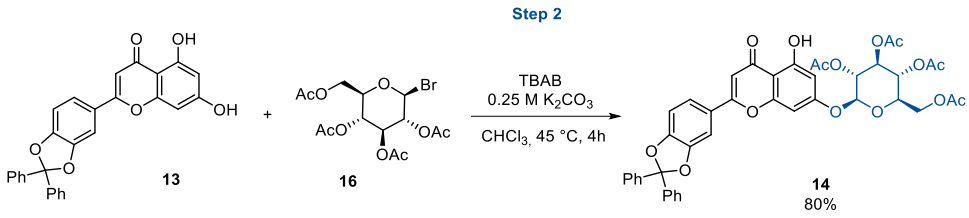

Scheme 3.2 Synthetic approach for the preparation of compound 14

The following steps were necessary for the deprotection of the ketal moiety and for the deacetylation, to provide the final product luteoloside 12.

- **Step 3**

Our primary focus was directed towards the removal of the diphenylmethylene ketal moiety. In this context, hydrogenolysis emerged as the most effective approach.[87–89]

Notably, we achieved a yield of 75% for compound **15** by employing 10% Pd/C (350 mg/mmol) as a catalyst, hydrogen gas (H_2) at 2 atm, and a solvent mixture of ethanol and 1,4-dioxane (S**cheme 3.3**).

The addition of 1,4-dioxane in the solvent mixture played a crucial role in enhancing the solubility of compound 14 and, consequently, improving the overall reaction efficiency. In fact, when the same reaction was performed without 1,4-dioxane, it resulted in incomplete conversion and a lower yield of 58% for compound **15**.

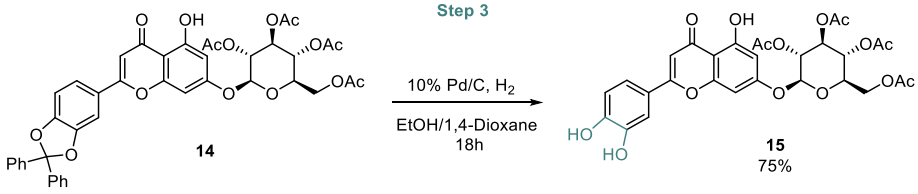

Scheme 3.3 Deprotection of the ketal moiety

- **Step 4**

Finally, we focused on the deacetylation of compound **15** to obtain the desired luteoloside **12**. For this purpose, we successfully applied the conditions established by Kondo and Oyama for similar flavonoids.[90] Specifically, the hydrolysis reaction was carried out using sodium methoxide in a solution of methanol and chloroform in a 2:1 ratio. As a result, compound **12** was isolated with a yield of 76% (**Scheme 3.4**).

We also explored an alternative approach by attempting the reaction reaction using a 2 M solution of ammonia in methanol. However, this attempt did not lead to any improvement in the yield of the desired product. Instead, the yield obtained was 66%, which was slightly lower compared to the yield achieved with the sodium methoxide/methanol-chloroform system.

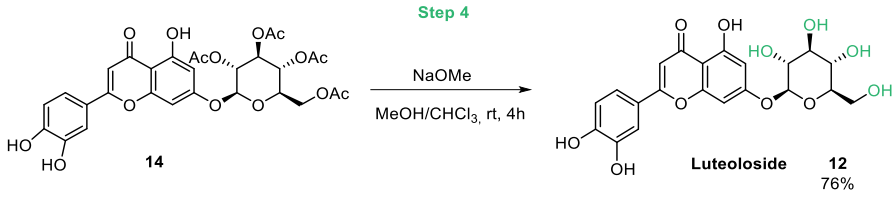

Scheme 3.4 Final deacetylation step

To briefly summarize, our final protocol was based on four synthetic steps (**Scheme 3.5**): the protection of the 3' and 4' hydroxyl groups using α,α-dichlorodiphenylmethane (**Step 1**), the 7-O-glycosylation using 1-bromo-α-D-glucose tetraacetate (**Step 2**), the cleavage of the diphenylmethylene ketal moiety (**Step 3**), and the final hydrolysis of the four acetal esters to provide **12** (**Step 4**).

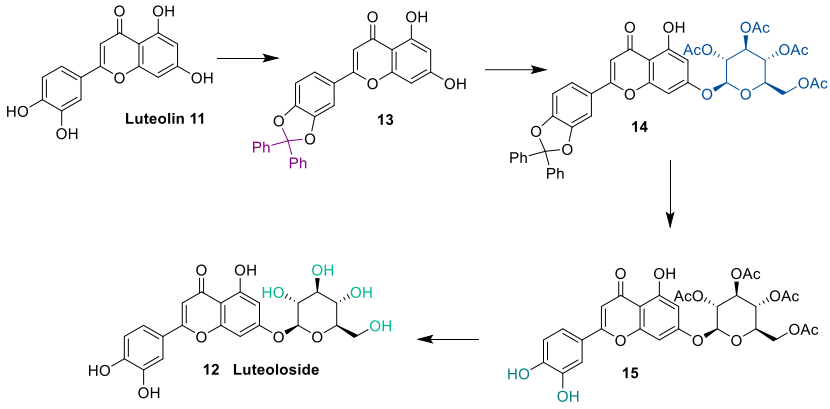

Scheme 3.5 Synthetic procedure for the preparation of luteoloside

This synthetic approach allows for the efficient conversion of luteolin into luteoloside, achieving a 40% overall yield.

By employing this novel method, we aim to address the challenges associated with the isolation and purification of luteoloside from natural sources. The developed approach not only enables a more scalable production of luteoloside but also provides analytical standards that can be utilized for accurate quantification in various applications. The enhanced purification efficiency achieved through this method opens up new possibilities for exploring the bioactivity and potential therapeutic applications of luteoloside.

3.2.3 Experimental section

Procedure for compound 13

A solution of luteolin (**11**; 0.572 g, 2 mmol) and α,α-dichlorodiphenylmethane (0.711 g, 3 mmol) in 1,4-dioxane (16 mL) was irradiated using Biotage Initiator at 185 °C for 2 h. Then, the reaction mixture was transferred to a beaker and treated with PE (50 mL) to favor the precipitation of the crude compound **13**. The precipitate was collected by filtration on a Büchner funnel under vacuum and purified by flash column chromatography on silica gel (hexane:EtOAc = 7:3, R_f = 0.32).

Yield: 87% (0.784 g); Yellow solid; **mp**: 209–211 °C; **IR** (cm^{-1}, neat): 3070, 1648, 1596, 1485, 1378, 1338, 1251, 1168, 1017, 839, 697, 641 cm^{-1}. **^{1}H-NMR** (DMSO-d_6, 400MHz) δ: 12.85 (s, 1 H), 10.88 (br s, 1 H), 7.77 (d, *J* = 1.7 Hz, 1 H), 7.69 (dd, *J* = 8.3, 1.8 Hz, 1 H), 7.56–7.49 (m, 4 H), 7.48–7.40 (m, 6 H), 7.21 (d, *J* = 8.3 Hz, 1 H), 6.88 (s, 1 H), 6.50 (d, *J* = 2.1 Hz, 1 H), 6.17 (d, *J* = 2.1 Hz, 1 H). **^{13}C-NMR** (DMSO-d_6, 100 MHz): δ: 182.5, 165.0, 163.4, 162.1, 158.0, 150.2, 147.9, 139.8, 130.3, 129.4, 126.5, 125.7, 122.9, 118.2, 109.9, 107.5, 104.9, 104.5, 99.6, 94.8. **Anal. Calcd for $C_{28}H_{18}O_6$** (450.45): C, 74.66; H, 4.03. **Found**: C, 74.71;H, 4.06.

Procedure for compound 14

A 0.25 M aq. solution of K_2CO_3 (16 mL) was added to a $CHCl_3$ (50 mL) mixture of **13** (0.9 g, 2 mmol), TBAB (0.322 g, 1 mmol), and 1-bromo-α-D-glucose tetraacetate **16** (1.645 g, 4 mmol). The resulting mixture was stirred at 45 °C for 5 h, then the solution was left to cool down to r.t. The two layers were separated by means of a separatory funnel and the aqueous layer was extracted with $CHCl_3$ (3 × 30 mL). The com- bined organic layers were dried (Na_2SO_4), filtered, and evaporated un- der reduced pressure to give the crude product **14**, which was purified by chromatography on silica gel (PE:EtOAc = 7:3, R_f = 0.29).

Yield: 80% (1.249 g); pale yellow solid; **mp**: 115–117 °C. **IR** (cm^{-1}, neat): 3087, 1747, 1655, 1608, 1490, 1445, 1212, 1173, 1038, 1014, 820, 697, 598 cm^{-1}. **^{1}H-NMR** ($CDCl_3$, 400 MHz): δ: 12.78 (s, 1 H), 7.60–7.54 (m, 4 H), 7.45 (dd, *J* = 8.2, 1.9 Hz, 1 H), 7.42–7.36 (m, 7 H), 6.99 (d, *J* = 8.2 Hz, 1 H), 6.57 (d, *J* = 2.2 Hz, 1 H), 6.55 (s, 1 H), 6.43 (d, *J* = 2.2 Hz, 1 H), 5.35–5.27 (m, 2 H), 5.19–5.13 (m, 2 H), 4.29 (dd, *J* = 12.3, 5.9 Hz, 1 H), 4.20 (dd, *J* = 12.3, 2.4 Hz, 1 H), 3.98–3.89 (m, 1 H), 2.10 (s, 3 H), 2.07 (s, 3 H), 2.06 (s, 3 H), 2.04 (s, 3 H). **^{13}C-NMR** ($CDCl_3$, 100 MHz): δ: 182.7, 170.9, 170.4, 169.7, 169.5, 164.4, 162.5, 162.2, 157.5, 150.8, 148.4, 139.7, 129.7, 128.7, 126.4, 125.2, 122.0, 118.7, 109.2, 107.1, 106.9, 105.1, 100.0, 98.4, 95.7, 72.8, 72.6, 71.1, 68.4, 62.1, 20.9, 20.8. **Anal. Calcd for $C_{42}H_{36}O_{15}$** (780.74): C, 64.61; H, 4.65. **Found**: C, 64.56; H, 4.61.

Procedure for compound 15

In a Parr reactor, compound **14** (1.171 g, 1.5 mmol) was dissolved in a EtOH/1,4-dioxane mixture (9:1, 350 mL) and 10% Pd/C (0.525 g) was added. The suspension was hydrogenated (2 atm) at r.t. and under stirring for 24 h. Then the catalyst was removed by filtration through a silica gel pad and washed with EtOAc (100 mL). Finally, after the evaporation of the solvent under vacuum, the crude product **15** was purified by flash column chromatography on silica gel ($CHCl_3$:MeOH = 98:2,

R_f = 0.25).

Yield: 75% (0.694 g); yellow solid; **mp:** 193–195 °C. **IR** (cm^{-1}, neat): 3497, 1747, 1660, 1596, 1493, 1366, 1212, 1176, 1038, 839, 756, 602 cm^{-1}. **^{1}H-NMR** (DMSO-d_6, 400 MHz) δ: 13.04 (br s, 1 H), 9.68 (br s, 2 H), 7.47–7.35 (m, 2 H), 6.88 (d, J = 8.3 Hz, 1 H), 6.76 (s, 1 H), 6.74 (d, J = 2.1 Hz, 1 H), 6.43 (d, J = 2.1 Hz, 1 H), 5.75 (d, J = 8.0 Hz, 1 H), 5.39 (t, J = 9.5 Hz, 1 H), 5.12–5.05 (m, 1 H), 5.00 (t, J = 9.5 Hz, 1 H), 4.36–4.28 (m, 1 H), 4.21–4.14 (m, 1 H), 4.12–4.06 (m, 1 H), 2.02–1.99 (m, 19 H), 1.96 (s, 3 H). **^{13}C-NMR** (DMSO-*d*6, 100 MHz) δ: 182.6, 170.6, 170.3, 170.1, 169.8, 165.3, 162.2, 162.1, 157.5, 150.7, 146.5, 121.9, 119.9, 116.6, 114.3, 106.6, 103.9, 99.9, 97.5, 95.7, 72.5, 71.8, 71.1, 68.6, 62.4, 21.1, 21.0, 20.9. **Anal. Calcd for $C_{21}H_{20}O_{11}$** (448.38): C, 56.25; H, 4.50. **Found:** C, 56.29; H, 4.53.

Procedure for compound 12 (Luteoloside)

To a solution of **15** (0.616 g, 1 mmol) in a mixture of MeOH/$CHCl_3$ (2:1, 30 mL) was added NaOMe (6 mmol, 0.324 g) at rt. After stirring for 4 h, the reaction mixture was neutralized with Dowex 50W- 8X(H^+), filtered, and evaporated under vacuum to give the crude luteoloside (**12**), which was purified by flash column chromatography on silica gel ($CHCl_3$:MeOH = 8:2, R_f = 0.35).

Yield: 76% (0.341 g); yellow solid; **mp**: 260–262 °C. **IR** (cm^{-1}, neat): 3287, 1655, 1592, 1493, 1255, 1172, 1061, 1026, 839 cm^{-1}. **^{1}H-NMR** (DMSO-d_6, 400 MHz): δ: 13.00 (br s, 1 H), 7.47–7.41 (m, 2 H), 6.91 (d, J = 8.3 Hz, 1 H), 6.80 (d, J = 2.1 Hz, 1 H), 6.76 (s, 1 H), 6.45 (d, J = 2.1 Hz, 1 H), 5.09 (d, J = 7.5 Hz, 1 H), 3.75–3.68 (m, 1 H), 3.52–3.42 (m, 2 H), 3.35–3.24 (m, 2 H), 3.21–3.15 (m, 1 H). **^{13}C-NMR** (DMSO-*d*6, 100 MHz): δ: 182.6, 165.2, 163.6, 161.8, 157.6, 150.7, 146.5, 122.0, 119.9, 116.6, 114.2, 106.0, 103.8, 100.5, 100.2, 95.4, 77.8, 77.1, 73.8, 70.2, 61.3. **Anal. Calcd for $C_{21}H_{20}O_{11}$** (448.38): C, 56.25; H, 4.50. **Found**: C, 56.29; H, 4.53.

NMR Spectra of the described compounds can be found at:
https://doi.org/10.1055/a-1531-2385

3.3 Thesis work: Continuous flow synthesis of Δ^9-THC and Δ^8-THC from Cannabidiol

The results presented in this section are adapted from:

Continuous-Flow Synthesis of Δ^9-Tetrahydrocannabinol and Δ^8-Tetrahydrocannabinol from Cannabidiol, B. Bassetti, C. A. Hone, C. O. Kappe, *J. Org. Chem.* **2023**, 88, 9, 6227–6231

3.3.1 Introduction

Cannabis is an important plant, indigenous to Central Asia and the Indian subcontinent, which has been used for a variety of applications since the ancient times.[91] It was firstly exploited as a source of textile fibers, but also to make paper, ropes, clothes, oils and as a medicine.[92]
Nowadays this plant has seen a renewal of interest precisely for its multi-purpose applications, with particular attention from the pharmaceutical and construction fields. Indeed, bioplastic and concrete-like materials can be made out from its stem tissues. [93,94]

From a botanical standpoint, generally three different species of hemp are described: *Cannabis sativa*, *Cannabis indica* and *C. ruderalis*. Each of these present different characteristics, such as height, size, leaflets, colour.[95] Hence, Cannabis is a complex plant, counting over 500 chemical entities of which the most representative class is composed by phytocannabinoids, i.e. merotherpenes with a very differentiated number of effects.[96]
Among them, Δ^9-tetrahydrocannabinol (**Δ^9-THC**), the primary psychoactive constituent of Cannabis, tetrahydrocannabinolic acid (**THCA**), cannabinol (**CBN**), cannabidiol (**CBD**), the primary non-psychotropic active compound, cannabidiolic acid (**CBDA**) and cannabigerolic acid (**CBGA**), the biosynthetic precursor of both THCA and CBDA (**Scheme 3.6**).[97]
In fact, phytocannabinoids are biosynthesized in the acid form in plant tissues; then, under the action of heat and light, they undergo decarboxylation. Usually, they accumulate in the secretory cavity of the glandular trichomes, which are found in most aerial parts of the plants, but they have also been detected in low quantity in seeds, roots and the pollen.[98] More generally, the concentration of these compounds depends on tissue type, age, variety, growth conditions, like nutrition, humidity, light level, harvest time and storage conditions.[99]

Most of the biological properties ascribed to cannabinoids rely on their interactions with the endocannabinoid system, in which two main receptors have been identified: cannabinoid receptor 1 (CB1) and cannabinoid receptor 2 (CB2).[100]

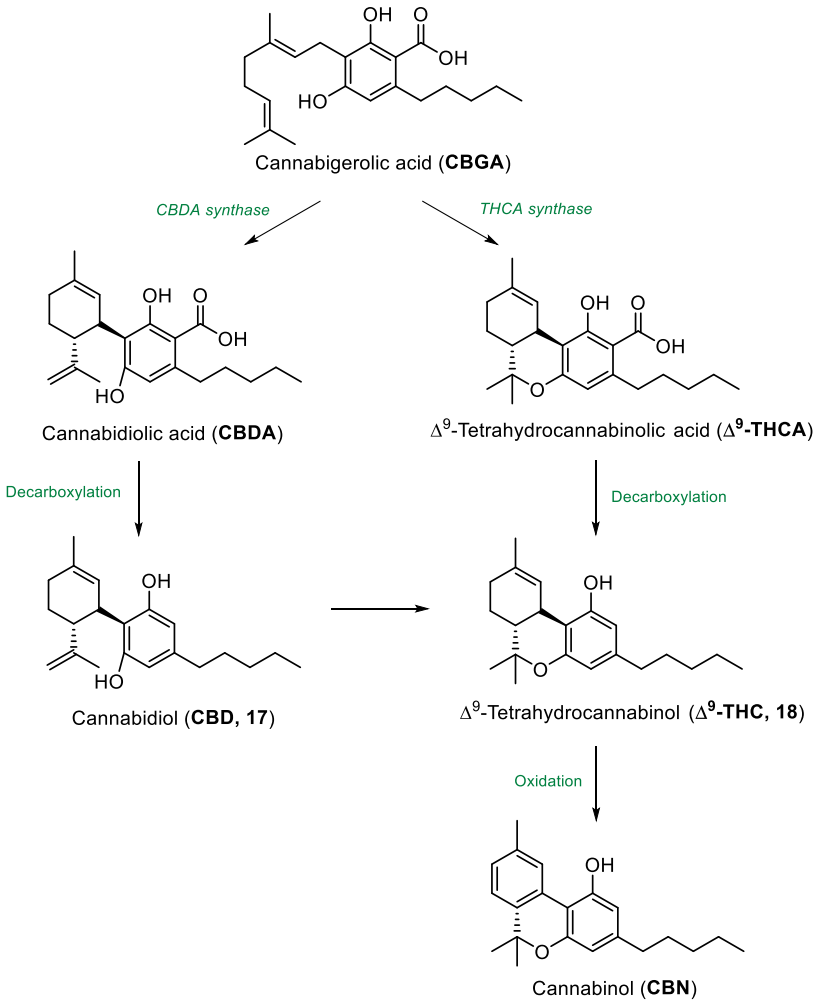

Scheme 3.6 Principal phytocannabinoids

CB1 receptors are widely distributed throughout the central nervous system (CNS) and the peripheral nervous system (PNS), affecting fundamental functions such as, memory, emotion, cognition, and movement.[101] Moreover, they are found in regions involved in the modulation of nociceptive transmission and pain perception. CB2 receptors are located peripherally and are thought to have immunomodulatory effects and to regulate the cytokines activity, but they are also present in the gastrointestinal system.[102,103]

Among phytocannabinoids, **Δ^9-THC**, is a partial agonist of both CB1 and CB2 receptors, but has higher affinity for the CB1 receptor, which appears to mediate its psychoactive properties. Besides these, Δ^9-THC exerts its action through other receptors and exhibits potent anti-inflammatory, anti-cancer, analgesic, [104] muscle relaxant, neuro-antioxidative and antispasmodic activities,[105] and in the prevention of nausea. [106] Nevertheless, his application in current pharmacology is limited by its important side effects, which include anxiety, cholinergic deficits, and immunosuppression and by

its narrow therapeutic index.[92] A combination with CBD, which seems to have very low affinity with CB receptors and to play a protective role, could be able to mitigate some of these adverse reactions, like the anxiogenic and psychotic effects.[107,108]

Under acidic conditions, Δ9-THC isomerizes to its thermodynamically more stable double bond isomer, **Δ8-THC** (**Figure 3.7**). Δ8-THC displays milder psychoactive effects when compared to Δ9-THC but shows comparable efficacy *in vitro* and *in vivo*.[109] Although being less abundant in natural cannabis than Δ9-THC, recently there has been growing interest (and concerns) towards this compound.[110–112] Further clinical pharmacology studies will be essential for a comprehensive understanding of Δ8-THC's pharmacokinetics and pharmacodynamics, as well as its distinct characteristics compared to Δ9-THC.[113]

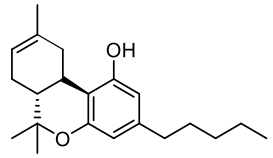

Δ8-Tetrahydrocannabinol (**Δ8-THC, 19**)

Figure 3.7 Δ8-tetrahydrocannabinol structure

Cannabidiol (CBD), is the most important phytocannabinoid after Δ9-THC.
CBD, the second major compound present in *C. sativa*, displays many characteristics and activities that differ from its cyclized counterpart Δ9-THC.[98] For this reason, intensive studies have been performed in order to clarify its pharmacological effects and its mechanism.[114]
The main difference between CBD and Δ9-THC, is that the first one does not exhibit a psychotropic activity, as well as significantly reduced and generally mild side effects.[115] CBD lack of action seems to be accountable for a very low affinity to cannabinoid receptors, due to a difference in the conformation adopted by the two compounds while interacting with the binding site.[116] One of the more accounted and described effect of Cannabidiol is the anticonvulsant one.[117] It is a potential therapeutic agent also for the treatment of chronic pain,[118] neurodegenerative diseases,[119] schizophrenia,[120,121] and affective disorders. It has also anxiolytic, anti-inflammatory and immunomodulatory properties.[122]

At the moment there are a few approved drugs derived from Cannabis. *Dronabinol* (Δ9-THC), in the isomer (-)-trans, an oral preparation, to treat severe nausea and vomiting caused by chemotherapy and HIV/AIDS-induced anorexia.[123] *Nabilone*, marketed as Cesamet™ in 2006, is a synthetic cannabinoid with the same therapeutical use and for neuropathic pain.[124] A cannabis standardized combination of Δ9-THC/CBD, namely *Nabiximols* (Sativex®), was approved in 2010 as a botanical drug in the United Kingdom. The U.S. Food and Drug Admininstration approved, in 2018, *Epidiolex*, a cannabidiol (CBD) oral solution for the treatment of seizures associated with two rare and sever form of epilepsy.[125]

Extraction procedures are a well-established method to obtain cannabinoids,[126,127] but the increasing interest and demand in these compounds, and also in their metabolites (present in lower amount in the extracts) and derivatives,[128,129] made the search for synthetic strategies of primary importance.
Though many studies have been focused on the synthesis of CBD, there are a number of synthetic strategies to access Δ^9-THC, for which different chiral pool terpenoids and asymmetric chemo- and biocatalytic approaches were explored.[130]
The first stereospecific synthesis of (-)-Δ^9-trans-THC (**18**) was published by Mechoulam et al. in 1967 (**Scheme 3.7**). The synthesis involves the condensation of olivetol and (S)-cis-verbenol in the presence of a Lewis acid (*p*TSA or BF_3), resulting in the formation of (-)-Δ^8-trans-THC (**19**). To convert compound **19** to compound **18**, it is treated with hydrochloric acid and zinc chloride as catalyst, and finally with sodium hydride.

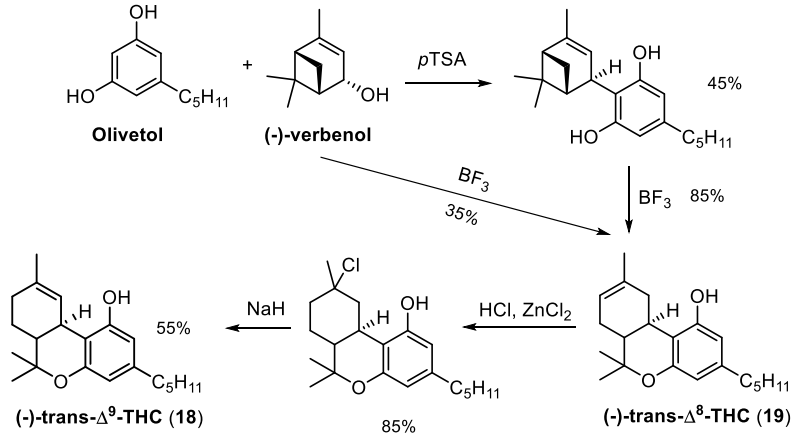

Scheme 3.7 First Δ^9-THC synthesis by Mechoulam, Braun and Gaoni

Few years later, Razdan et al. reported a one-step reaction from (+)-*trans-p*-mentha-2,8-dien-1-ol and olivetol in the presence of $BF_3 \cdot OEt_2$ and $MgSO_4$ to afford Δ^9-THC (**18**) in 31% yield after column chromatography (**Scheme 3.8, a**), while Petrzilka and co-workers exploited the same terpenoid to achieve the stereoselective synthesis of Δ^8-THC (**19**), via formation of (−)-*trans*-CBD (**18**) upon electrophilic aromatic substitution, subsequent cyclization to Δ^9-THC, and final isomerization to the more stable isomer **19**, using pTSA (**Scheme 3.8, b**).

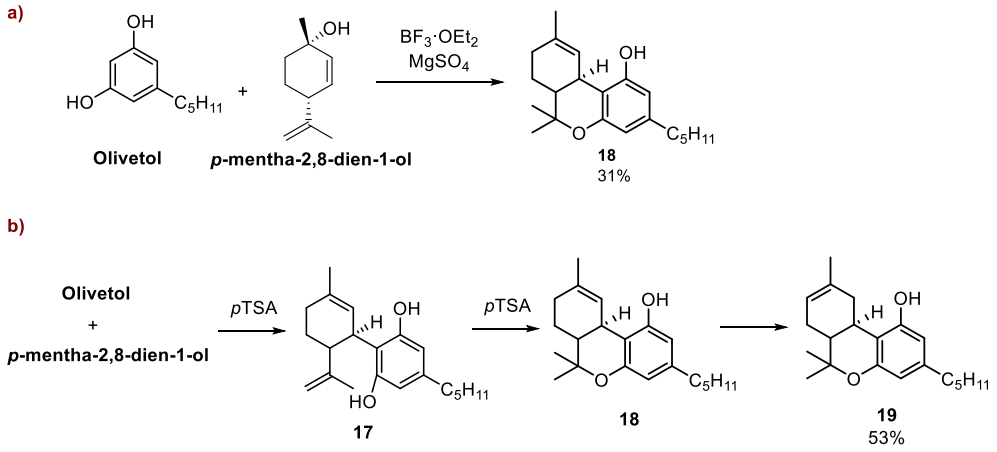

Scheme 3.8 Stategies for the preparation of Δ^9-THC and Δ^8-THC

This method is still commonly used, since it is a straightforward approach to obtain **18**, in a single step. Recent methods have utilized asymmetric catalysis or auxiliaries for the stereospecific preparation of THC analogs.[131–133] Nevertheless, considering scalability, the use of chiral pool feedstocks is still favoured, despite the fact that they provide low to moderate selectivity to a particular THC product.

In this context, the utilization of flow technologies for the synthesis of THC analogs has received attention,[134–137] enabling precise control over reaction parameters and offering several advantages in terms of efficiency, selectivity and further scalability (see **Chapter 1.4** for more insights on Flow Chemistry).[138]

Among these, Antoniotti and co-workers reported a flow synthesis using supported species (Au nanoparticles and Ti-doped montmorillonite) under O_2 atmosphere, that leads to the formation of *orto*-THC derivatives, unfortunately with relatively poor selectivity (**Scheme 3.9, a**).[134] More recently, Rutjes and co-workers envisaged a continuous-flow synthesis methods starting from (+)-*trans*-*p*-mentha-2,8-dien-1-ol and (−)-verbenol and using both homogeneous and heterogeneous Lewis acids, but this afforded **19** and **18** in low isolated yields, 17% and 30%, respectively (**Scheme 3.9, b**).[137]

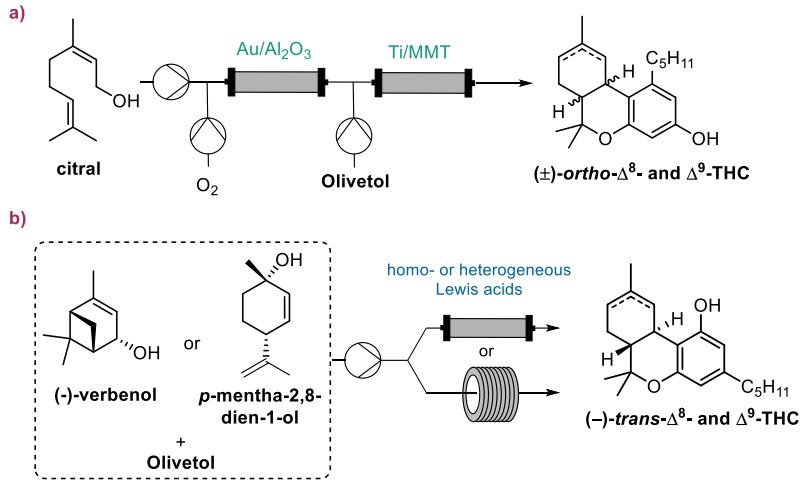

Scheme 3.9 Antoniotti (a) and Rutjes (b) flow strategies for the synthesis of tetrahydrocannabinoids

One effective strategy for the formation of Δ^9-THC (**18**) and Δ^8-THC (**19**) involves the intramolecular cyclization of CBD (**17**) through acidic catalysis (**Scheme 3.10**).[139]

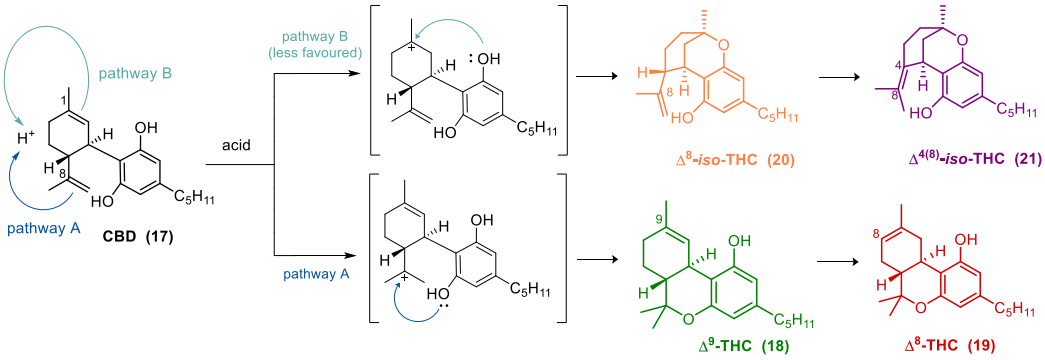

Scheme 3.10 Reaction pathways for acidic cyclization of CBD

This can lead to two main pathways either via the activation of the Δ^8 double bond to form Δ^9-THC (**19**) or the Δ^1 double bond (generally less favoured) resulting in Δ^8-*iso*-THC (**20**). In this context, measuring the distribution of the reaction components at a single time end point in different conditions has proven to be an interesting approach,[140] especially as both Δ^9-THC and Δ^8-*iso*-THC can overreact to more thermodynamically stable products, namely Δ^8-THC (**19**) and (Δ^4)^8-*iso*-THC (**21**) respectively.

The reaction of CBD in the presence of thermal and acidic conditions has been the subject of contrasting results in the literature. The acid-catalyzed cyclization process is highly dependent on various reaction parameters, including the specific acid species employed, reaction temperature, and reaction time. Therefore, careful optimization and selection of appropriate reaction conditions are necessary to achieve the desired cyclization and product formation.

With this in mind, we started our study by collecting time profile data in batch under different acidic conditions and then used this knowledge to develop continuous-flow protocols for the selective synthesis of Δ⁹-THC (**18**) and Δ⁸-THC (**19**).

3.3.2 Results and discussion: batch investigation

Initially, the influence of different Lewis and Bronsted acids on conversion and selectivity towards compound **18** and **19** was investigated (**Scheme 3.11** and **Table 3.2**). Since our objective was obtaining a high conversion of CBD while minimizing the formation of undesired products (Δ⁸-*iso*-THC, (Δ⁴)⁸-*iso*-THC and CBN), a thorough understanding of the reaction kinetics was required, particularly how it is influenced by the choice of acid species.

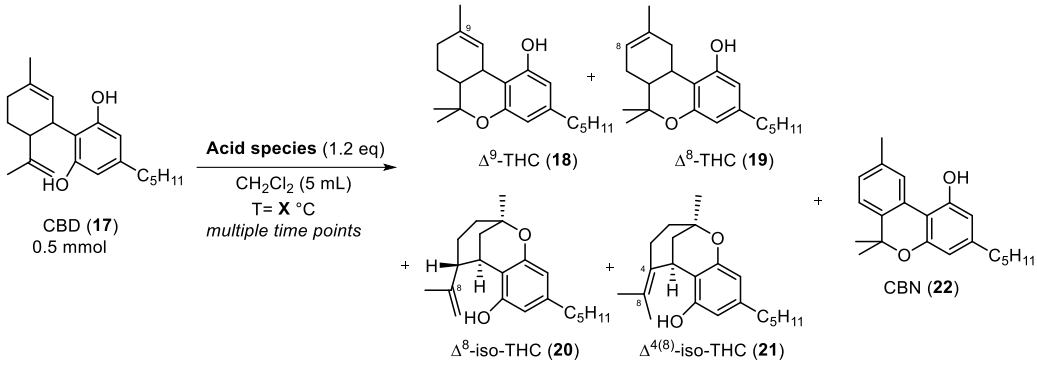

Scheme 3.11 General reaction scheme for CBD cyclization

A reaction network consisting of four first-order rate-limiting steps based on the cannabinoid species was analyzed using kinetic fitting software Compunetis. The simultaneous fitting of the rate constants to the experimental data allowed for a detailed understanding of the reaction kinetics and provided insights into the relative importance of each step in the process (**Scheme 3.12**).

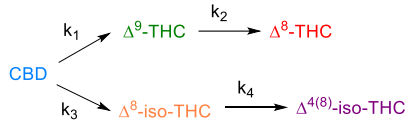

Scheme 3.12 Model structure for the kinetic fitting

In order to investigate the conversion, and based on literature research,[135,139] we set some parameters and operating actions, such as the solvent (CH_2Cl_2), the equivalent of the acid (1.2) temperature (generally -10 °C, 0 °C and rt), and the sequential sampling of the reaction to monitor the conversion e possible side-products formation over time. All the experiments were conducted using 0.5 mmol of CBD **17** (**Table 3.2**).

As boron trifluoride etherate ($BF_3 \cdot OEt_2$) is a commonly used acid for the preparation of Δ^9-THC from CBD, we started our studies using this acid. The best conversion was obtained performing the reaction at -10 °C, and it gave 98% conversion of CBD and 85% selectivity of **18** within 2 h (**Entry 1**). The reaction rate displayed a 5-fold increase at 0 °C when compared to −10 °C ($k_{1,0\ °C}/k_{1,-10\ °C} = 5.09$), providing 83% selectivity within 30 min at 0 °C (**Table 3.2, Entry 2**; kintic is shown **Figure 3.8, a**).

The overreaction of Δ^9-THC to the more thermodynamically stable Δ^8-THC isomer was very slow, with 1% selectivity. The main side product was Δ^8-*iso*-THC, with a slight increase observed at 0 °C (entry 2). Interestingly, when switching to toluene (PhMe) as solvent, a higher formation of Δ8-*iso*-THC (**20**) was favored (**Table 3.2, Entry 3**), and after 22 h, the overreaction product, $(\Delta^4)^8$-*iso*-HC (**21**), resulted in 32% selectivity (**Table 3.2, Entry 4**; **Figure 3.8, b**). This is particularly relevant for possible further investigations, since the *iso*-THC compounds have received less attention compared to the other cannabinoids.[141]

Table 3.2 Lewis acid batch screening of CBD (**17**) cyclization

Entry	Acid	T [°C]	time	conv. **17**[a]	sel. **18**[a]	sel. **19**[a]	sel. **20**[a]	sel. **21**[a]
1	$BF_3 \cdot OEt_2$	−10	2 h	98	85	1	14	-
2	$BF_3 \cdot OEt_2$	0	30 min	>99	83	1	16	-
3[b]	$BF_3 \cdot OEt_2$	0	7 h	>99	30	21	45	4
4[b]	$BF_3 \cdot OEt_2$	0	22 h	>99	1	54	7	32
5	$In(OTf)_3$	−10	4 h	94	80	11	10	-
6	$In(OTf)_3$	0	30 min	88	81	9	10	-
7	$Sc(OTf)_3$	0	30 h	83	92	5	4	-
8	$Sc(OTf)_3$	rt	3 h	98	81	13	6	-
9	TMSOTf	−10	2 min	97	81	13	5	-
10	TMSOTf	−10	1 h	>99	2	90	2	5
11	TMSCl	rt	48 h	63	83	3	14	-
12	$TiCl_4$	−10	2 min	>99	11	43	2	2
13	$AlCl_3$	−10	2 min	>99	87	2	3	-

[a]Determined by GC-FID peak area percent. Percent of product with respect to all peaks except the substrate
[b]Reaction was performed in PhMe as solvent.

We next investigated the influence of metal triflates, specifically of $In(OTf)_3$ and $Sc(OTf)_3$. It was observed that $In(OTf)_3$ exhibited moderate reactivity, resulting in 94% conversion of **17** and 80% selectivity towards **18** within 4 hours at a temperature of -10 °C (**Table 3.2, Entry 5**). At 0 °C the reaction rate was increased, but with comparable results in term of selectivity (**Table 3.2, Entry 6**). On the other hand, $Sc(OTf)_3$ required a higher temperature to promote the reaction, leading to 83% conversion only after 30 hours (**Table 3.2, Entry 7**) and achieving a similar selectivity towards Δ^9-THC when working at 0 °C (**Table 3.2, Entry 8**).

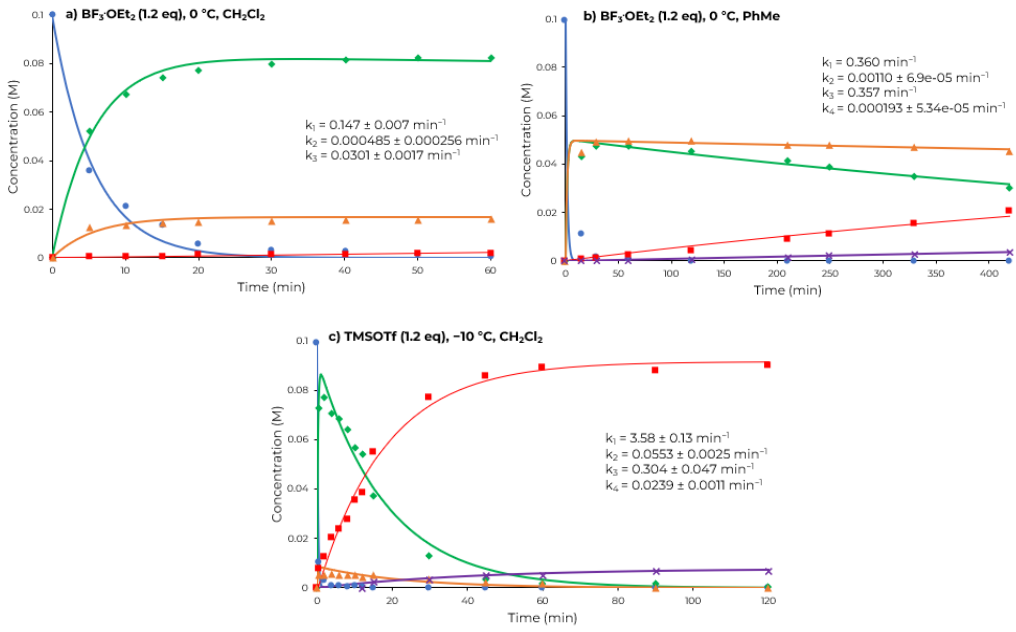

Figure 3.8 Kinetic fitting and reaction profiles under different Lewis acidic conditions

Subsequently, we examined the use of trimethylsilyltrifluoromethanesulfonate (TMSOTf), which caused a rapid reaction rate (**Figure 3.8, c**), with 97% conversion of CBD **17** and 81% selectivity of Δ^9-THC **18** within 2 min of reaction time (**Table 3.2, Entry 9**). By continuous collecting of the reaction, TMSOTf afforded 90% selectivity of Δ^8-THC **19** after 60 min, and the overreaction of Δ^8-*iso*-THC **20** to $(\Delta^4)^8$-*iso*-THC **21** was also observed (**Table 3.2, Entry 10**), providing further understanding of the reaction selectivity.

Trimethylsilyl chloride (TMSCl) was also expored but it displayed a slow reaction rate, with only 63% conversion and 83% selectivity toward Δ^9-THC after 48 h at room temperature (**Table 3.2, Entry 11**). The use of titanium chloride ($TiCl_4$) resulted in a fast reaction rate with >99% conversion within 2 min, but leaded to a complex impurity profile (**Entry 12**).

Interestingly, the use of anhydrous aluminum trichloride ($AlCl_3$) at −10 °C afforded full conversion of **17**, with 87% selectivity of **18**. Moreover, low amounts of Δ^8-THC and Δ^8-*iso*-THC were detected also after 15 min of reaction (**Entry 13**). The observed result was intriguing also do to the absence of previous reports utilizing this acid for the synthesis of Δ^9-THC from CBD.

Next, we proceeded to assess the effects exerted by Brønsted acids. In particular, we examined *p*-toluene sulfonic acid (*p*TSA), camphorsulfonic acid (CSA), trifluoroacetic acid (TFA) and chlorosulfuric acid (HSO3Cl). The first needed 0 °C for activation, with 51% conversion of **17** and 80% selectivity of Δ^9-THC after 30 h (**Table3.3, Entry 1**). Incomplete conversion (93%) was obtained at room temperature, with a selectivity of 68% and 28% for Δ^9-THC **18** and Δ^8-THC **19**, respectively (**Entry 2**). In the case of CSA, the use of low temperatures (−10 °C to rt) gave very low conversion and reaction rate. Under reflux conditions, it provided 81% conversion of **17** and 67%

selectivity of Δ^9-THC were (**Table 3.3, Entry 3**). We decided to do some trials exploiting microwave irradiation, however, after some investigation concerning acid equivalents, time and temperature, the product distribution between Δ^9-THC and Δ^8-THC could not be improved (**Table 3.3, Entries 4-6**). At a temperature of -10 °C, TFA demonstrated good selectivity towards **18** but provided only a 16% conversion of compound 17 after 6 hours (**Table 3.3, Entry 7**). Lowering the temperature to 0 °C improved the reaction rate, but it led to the formation of a mixture of products (**Entry 8**). On the other hand, when HSO_3Cl was employed as a reagent, the reaction proceeded rapidly even at -10 °C, resulting in an 84% selectivity toward Δ^8-THC **19** within 10 minutes.
No overreaction of Δ^8-*iso*-THC (**20**) to form $(\Delta^4)^8$-*iso*-THC (**21**) was observed in the presence of Brønsted acids.

Table 3.3 Brønsted acid batch screening of CBD (**17**) cyclization

Entry	Acid	T [°C]	time	conv. **17**[a]	sel. **18**[a]	sel. **19**[a]	sel. **20**[a]
1	*p*TSA	0	30 h	51	80	8	8
2	*p*TSA	rt	1.5 h	93	68	28	2
3	CSA	40	3 h	81	67	30	4
4	CSA	65 [MW]	45 min	49	80	16	4
5[b]	CSA	90 [MW]	15 min	81	59	37	4
6[b]	CSA	110 [MW]	10 min	96	23	74	3
7	TFA	−10	6 h	16	94	6	-
8	TFA	0	3 h	88	77	17	6
9	HSO_3Cl	−10	10 min	94	7	84	4

[a]Determined by GC-FID peak area percent. Percent of product with respect to all peaks except the substrate.
[b]Experiments were performed using 1.5 eq of acid.

Later, we expanded the studies to supported acid reagents (**Table 3.4**), as they have the potential benefit of a simplest work-up by means of just a filtration, since the product is in a separate phase to the acid, assuming no leaching occurs in flow conditions.[142,143]
The activity of polymer-bound *p*TSA was investigated and found to be superior to that of *p*TSA. At a temperature of -10 °C, *p*TSA on polymer allowed a 73% conversion of compound **17** after 27 hours. However, like standard pTSA, we obtained a mixture of products. Although higher temperatures increased the reaction rate, they did not favor the production of Δ^9-THC over other possible products (**Table 3.4, Entries 1-2**).
Due to the promising results with $Sc(OTf)_3$, scandium on polymer was attempted, but only trace amounts (<1%) of Δ^9-THC were observed (data not reported).
We also investigated silica-propylsulfonic acid (**Table 3.4, Entries 3-4**), Amberlyst® 15 (**Table 3.4, Entries 5-6**), and Nafion™ NR50 (data not reported), but all resulted in a mixture of products. In particular, the latter, at room temperature still resulted in incomplete conversion (81%) even after 8 days, probably due to the relatively small surface area of the solid Nafion NR50.

When employing Montmorillonite K10 (MK10) at room temperature the reaction proceeded with 98% conversion of **17** and high selectivity (84%) of Δ^9-THC **18** after 5 h (**Table 3.4, Entry 8**). Whereas uncomplete conversion was observed at 0 °C (**Table 3.4, Entry 7**).

The promising results obtained using $BF_3{\cdot}OEt_2$ as reagent (**Table 3.2**) led us to investigate the reaction using commercially available silica-supported boron trifluoride (Si-BF_3) and synthesized polyvinylpyrrolidone-supported boron trifluoride (PVP-BF_3). Unfortunately, the rate using Si-BF_3 was substantially slower and less selective compared to its homogenous counterparts and, after 6 h at 0 °C, 98% conversion of **17** and 65% selectivity of Δ^9-THC were obtained (**Table 3.4, Entries 6-7**). In this case, an extra peak in the GC chromatogram was observed at 12.1 min retention time, which was then assigned to the aromatized oxidation product, cannabinol (CBN, **22**). Generally, the same trend detected when using homogeneous $BF_3{\cdot}OEt_2$ was observed, with the formation of more Δ^8-*iso*-THC at higher temperatures (**Table 3.4, Entries 6-8**). Interestingly, the reaction rate could be significantly increased by operating at room temperature with no drop in selectivity toward Δ9-THC **18** (**Entry 8**). On the other hand, when using PVP-BF_3, a high yield of Δ^9-THC could be obtained but only after a prolonged reaction time (156h) at room temperature (**Table 3.4, Entry 9**). When conducing the reaction at 40 °C, 99% conversion of **17** and 89% selectivity of Δ^9-THC **18** were achieved after 6 h, which, although lower in reactivity, is similar to the selectivity achieved using $BF_3{\cdot}OEt_2$.

Table 3.4 Results for the measured responses from the supported acid screening

Entry	Acid (loading)[b]	T [°C]	time	conv. **17**[a]	sel. **18**[a]	sel. **19**[a]	sel. **20**[a]
1	*p*-TSA on polymer	−10	27 h	73	70	12	10
2	*p*-TSA on polymer	rt	45 min	87	55	32	10
3	Si-propylsulfonic acid (983 mg)	−10	6 h	25	88	4	-
4	Si-propylsulfonic acid (983 mg)	0	4 h	85	68	13	7
5	Amberlyst® 15	0	6 h	69	72	12	9
6	Amberlyst® 15	rt	2 h	88	55	31	9
7	Mont. K10	0	4 h	89	12	-	-
8	Mont. K10	rt	5 h	98	84	3	8
6	Si-BF_3	−10	4 h	92	68	1	12
7	Si-BF_3	0	6 h	98	65	4	14
8	Si-BF_3	rt	10 min	95	72	3	20
9	PVP-BF_3 (400 mg)	rt	156 h	>99	89	4	7
10	PVP-BF_3 (400 mg)	40	6 h	99	84	3	13

[a]Determined by GC-FID peak area percent. Percent of product with respect to all peaks except the substrate.

[b]0.2 g, unless otherwise indicated

No overreaction of Δ^8-*iso*-THC (**20**) to form (Δ^4)^8-*iso*-THC (**21**) was observed.

Among the acids evaluated during the batch screening, we identified five as the most promising:

- MK10,
- PVP-BF_3,
- $BF_3 \cdot Et_2O$
- TMSOTf
- $AlCl_3$

Using these reagents we proceeded a flow screening, with the objective of developing a protocol that provided high selectivity toward either Δ^9-THC and Δ^8-THC within a short residence time in a reproducible and scalable manner.

Among the many advantages of continuous flow, the adoption of this technology in this reaction can allow to maintain isothermal conditions from when the reagents are in contact with each other in the stream to the outlet, avoiding the challenge of the careful addition of the acid that is needed in a batch protocol. As the products "flows" trough the reaction coil or packed bed, its contact with the reagents is minimized, thus avoiding possible over-reaction and side products formation.

3.3.3 Results and discussion: continuous flow investigation

For what concerns the solid supported acids selected (MK10 and PVP-BF_3), the flow configuration was constituted of a single syringe pump that was used for the introduction of the substrate **17** (CBD) in CH_2Cl_2, which then flowed through a packed bed reactor filled with the supported acid catalyst, contained within a column cartridge (**Scheme 3.13, a**).

A two-feed continuous flow setup was used for the other acids and consisted of syringe pumps, one for the introduction of **17** and a second pump for the introduction of the acid solution. Then, the two feeds were combined within a tee-piece before entering the reactor coil (**Scheme 3.13, b**).

For both configurations the timing of the quench was achieved by introducing the effluent into a vessel containing $NaHCO_3$ in a semibatch manner.

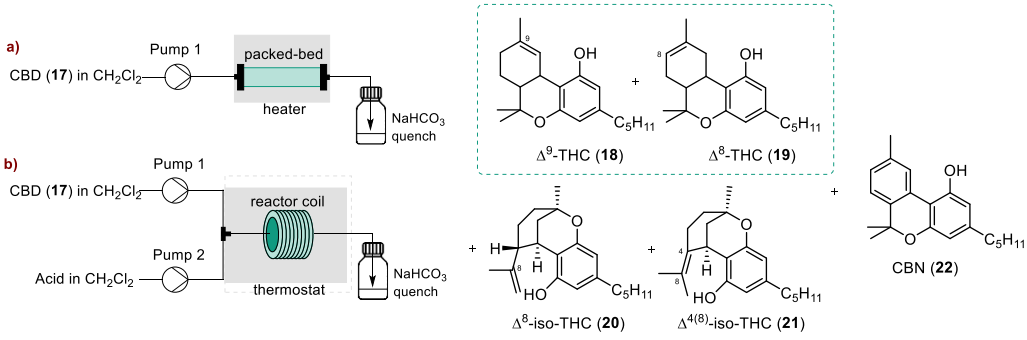

Scheme 3.13 Flow configurations: a)supported acids, b)two-feed flow, with possible products of the reaction

Promising outcomes were observed when employing MK10 in a flow system. At room temperature, a yield of 81% of Δ^9-THC was achieved within a short time span of 2 minutes (**Table 3.5, Entry 1**).

However, when fractionating the outlet and subsequently packing the column with fresh MK10, the system's performance varied throughout the duration of the experiment, leading to different results (**Table 3.5, Entry 2**). The same outcome resulted when performing twice the reaction and reusing the clay, with 1.5 min as residence time (**Entry 3-4**).

Our findings align with previous observations made by other researchers regarding the possible inconsistent performance of commercial MK10, that could be attributed to the availability of acid sites, which depends on the packing of the clay material. Additionally, the water content within the clay has the potential to influence the overall performance of the system.

Table 3.5 Flow experiments using Montmorillonite K10

Entry	Acid [mg]	t_{res} [min]	conv. **17**[a]	sel. **18**[a]	sel. **19**[a]	sel. **20**[a]
1	405	2	99	80	7	13
2[b]	405	2	91	86	2	12
3	405	1.5	94	86	2	12
4[c]	405	1.5	99	80	8	12

Experiments were performed using 0.1 M solution of CBD (**17**).

[a] Determined by GC-FID peak area percent. Percent of product with respect to all peaks except the substrate.

[b] Entry 1 repeated, but using fresh clay.

[c] Entry 3 repeated.

A consistent reactor performance was not achieved also when performing experiments using PVP-BF_3. In this case, when the collected fractions were analyzed by GC they showed that the conversion of **17** and yield of Δ^9-THC **18** displayed a linear decrease over the duration of the runs (**Table 3.6, Figure 3.9**). This curious trend was confirmed by repeating the experiment (data not reported).

Table 3.6 PVP-BF_3 flow experiment

Entry	Acid [mg]	t_{res} [min]	T [°C]	**17**[a]	**18**[a]	**19**[a]	**20**[a]
1	500	7	40	12-40	50-71.5	1.5-7	7.5-11.5

Experiment was performed using 0.1 M solution of CBD (**17**).

[a] Determined by GC-FID peak area percent. Percent of product with respect to all peaks except the substrate.

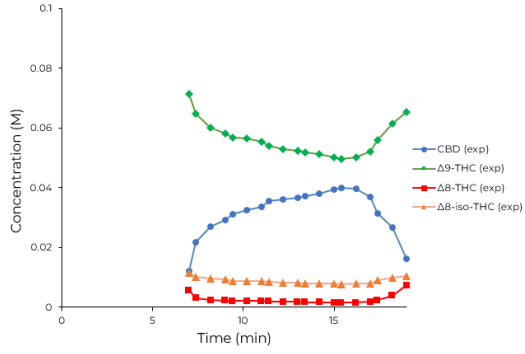

Figure 3.9 PVP-BF_3, reaction profile over time

As the supported acid catalysts did not show sufficient stability, probably due to deactivation of solid acids which limited their synthetic applicability to the scope, we continued our investigation exploring the use of $BF_3 \cdot OEt_2$ in flow conditions, encouraged by the possibility of minimizing pathway B, thus reducing the formation of Δ^8-*iso*-THC (**20**) observed in batch.
However, $BF_3 \cdot OEt_2$ afforded Δ^9-THC **19** and Δ^8-*iso*-THC **20** in 83% and 15% selectivity, respectively, within 15 min of residence time at 10 °C, confirming the data previously obtained. Further investigations could not decrease the high amounts of Δ8-*iso*-THC formed.

In the case of TMSOTf, the batch results showed how a precise control over reaction time was necessary to maintain control over the selectivity toward Δ^9-THC, due to the rapid overreaction to its more stable isomer Δ^8-THC **19** (**Table 3.2, Entries 9-10**). Notwithstanding, also when decreasing the equivalents of acid (**Table 3.7, Entries 2-4**), the use of more diluted solution of the substrate CBD **17** (**Entries 5-7**) and even operating at lower temperatures (**Entries 6-7**) led to a good selectivity of **18** with residence time within 1.5 min.
On the other hand, we did identify that a selective synthesis of Δ^8-THC could be achieved in a 2 min residence time (**Table 3.7, Entry 1**). After a short optimization (**Table 3.7, Entries 8-14**), we were able to obtain the total conversion of **17**, providing 91% selectivity towards **19** (87% assay NMR yield) by operating at room temperature, using 1.2 equivalent of the acid (**Table 3.7, Entry 14**).

Table 3.7 TMSOTf investigation in flow conditions

Entry	CBD (17) [M]	Acid eq.	T [°C]	t_{res} [min]	conv. **17**[a]	sel. **18**[a]	sel. **19**[a]	sel. **20**[a]	sel. **21**[a]
1	0.2	1.2	−10	2	95	3	94	1	-
2	0.2	0.6	−10	1	93	74	18	5	-
3	0.1	0.1	−10	1	31	90	3	6	-
4	0.1	0.5	−10	1	90	84	7	6	-
5	0.05	0.5	−10	1	>99	81	14	5	-
6	0.05	0.5	−20	1	88	88	5	5	-
7	0.05	0.5	−20	1.5	97	86	9	5	-
8	0.2	1.2	0	4	97	19	75	4	-
9	0.2	1.2	0	8	>99	3	89	2	6
10	0.2	1.2	25	2	>99	2	91	1	5
11	0.2	1.2	25	4	>99	2	89	1	6
12	0.2	1.5	25	2	>99	2	89	0	6
13	0.2	2	30	2	>99	2	88	1	6
14	**0.2**	**1.2**	**25**	**2**	**>99**	**2**	**91**	**1**	**5**

[a] Determined by GC-FID peak area percent. Percent of product with respect to all peaks except the substrate.

The last acid that needed to be tested, after our preliminary batch screening, was $AlCl_3$. However, we knew that we would need to optimize the equivalents (i.e. 1.2) to avoid solubility issues in flow.
In fact, $AlCl_3$ was not completely soluble in our reaction conditions, and frequent clogging caused pump blockage when performing the first experiments in flow.

Thus, we performed a further batch optimization (**Table 3.8**). Several parameters, such as reaction time, temperature, the use of alternative solvents (**Table 3.8, Entries 3-4**), and equivalents of the acid, were investigated. In particular, we were able to efficiently combine a reduction of the equivalents to a higher reaction temperature (**Table 3.8, Entries 5-8**), that could also positively enhance the solubility of the acid. Good performance was achieved using 0.2 equiv of $AlCl_3$ at room temperature, with a 98% conversion of CBD **17** and 92% selectivity toward Δ^9-THC **18** (**Table 3.8, Entry 8, Figure 3.10**).

Table 3.8 AlCl3 further batch optimization

Entry	acid eq.	solvent	T [°C]	time [min]	conv. **17**[a]	sel. **18**[a]	sel. **19**[a]	sel. **20**[a]
1	1.2	CH_2Cl_2	−10	15	>99	88	3	3
2	1.2	CH_2Cl_2	−10	10	>99	86	8	3
3	1.2	PhMe	−10	20	>99	78	5	8
4	1.2	PhMe/Et_2O	−10	60	>99	81	4	14
5	0.5	CH_2Cl_2	0	15	>99	89	4	4
6	0.1	CH_2Cl_2	0	120	93	95	2	3
7	0.1	CH_2Cl_2	rt	30	90	92	3	4
8	**0.2**	**CH_2Cl_2**	**rt**	**25**	**98**	**92**	**4**	**4**

General conditions: All experiments were performed using 0.5 mmol of **17** in 5 mL of solvent.
[a]) Determined by GC-FID peak area percent. Percent of product with respect to all peaks except the substrate. No overreaction of Δ^8-*iso*-THC (**20**) to form (Δ^4)^8-*iso*-THC (**21**) was observed.

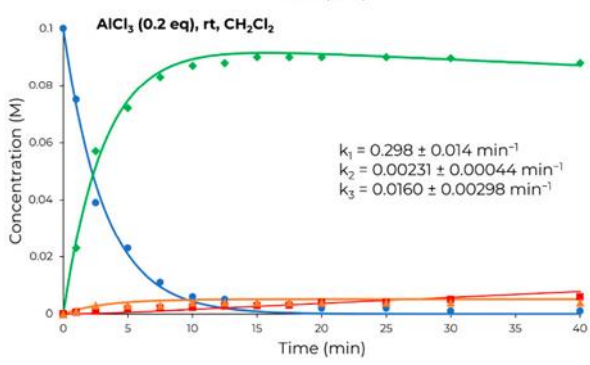

Figure 3.10 $AlCl_3$ reaction profile of the reaction reported in Table 3.7, Entry 8

Finally, we were able to perform an optimization using promising $AlCl_3$ in flow conditions (**Table 3.9**). To this aim, a peristaltic pump was used for the $AlCl_3$ feed, as it can handle suspensions, thus avoiding possible clogging of the tubings.

In the first trials (**Table 3.9, Entries 1-3**) incomplete conversion of CBD was observed, but an intermediate residence time of 18 min and a progressive increase of the temperature to 37 °C (both feeds of the substrate and acids were warmed at the same temperature of the coil) leaded to 99% conversion of **17** with a 92% selectivity towards our title target Δ^9-THC **18**, as showed in **Entry 7** of **Table 3.9**.

Table 3.9 $AlCl_3$ flow opitimization

Entry	T [°C]	t_{res} [min]	conv. **17**[a]	sel. **18**[a]	sel. **19**[a]	sel. **20** [a]
1	20	16.66	90	93	2	4
2	25	16.66	95	92	3	5
3	25	20	87	93	2	5
4	25	18	97	91	3	6
5	30	18	99	90	3	7
6	35	18	97	92	3	5
7	**37**	**18**	**99**	**92**	**4**	**4**

General conditions: All experiments were performed using 0.2 M feed solution of CBD (**17**) and 0.04 M feed solution of $AlCl_3$.
[a]Determined by GC-FID peak area percent. Percent of product with respect to all peaks except the substrate.

3.3.4 Results and discussion: long runs for Δ^9-THC and Δ^8-THC

Finally, the robustness of our protocols were demonstrated by a long run experiments for both Δ^9-THC and Δ^8-THC using $AlCl_3$ and TMSOTf, respectively.

For what concerns Δ^9-THC, the experiment was conducted applying conditions reported in **Table 3.9**, **Entry 7**, and the reaction was performed over a total operation time of 6 hours, corresponding to a 13.3 mmol scale. The system operated consistently for the duration of the run. A >99% conversion of **17** and 92% selectivity of **Δ^9-THC 18** (90% assay NMR yield) were observed for the combined fractions with no relevant fluctuation (**Table 3.10**, **Figure 3.11**).
Finally, after filtration and removal of the solvent, **18** was obtained in 97% isolated yield, that corresponds to a throughput of 1.02 g/h.

Table 3.10 Measured responses for the Δ^9-THC (**18**) long run, determined by GC-FID peak area percent

Vial	Fractionated time interval [min]	**17**[a]	**18**[a]	**19**[a]	**20**[a]
1	18-28	1.2	91.6	2.4	4.7
2	28-38	1.2	91.8	2.1	4.9
3	38-48	1.1	91.7	2.1	5.0
4	48-78	0.9	91.9	2.0	5.0
5	78-108	1.0	91.9	2.1	5.0
6	108-138	1.0	92.0	1.9	5.1
7	138-168	1.0	91.5	2.0	5.1
8	168-198	0.8	91.6	1.9	5.1
9	198-228	0.9	91.6	2.0	5.0
10	228-258	0.7	91.9	2.0	4.9
11	258-268	0.7	91.9	2.0	4.9
Average		**1.0**	**91.8**	**2.1**	**5.0**

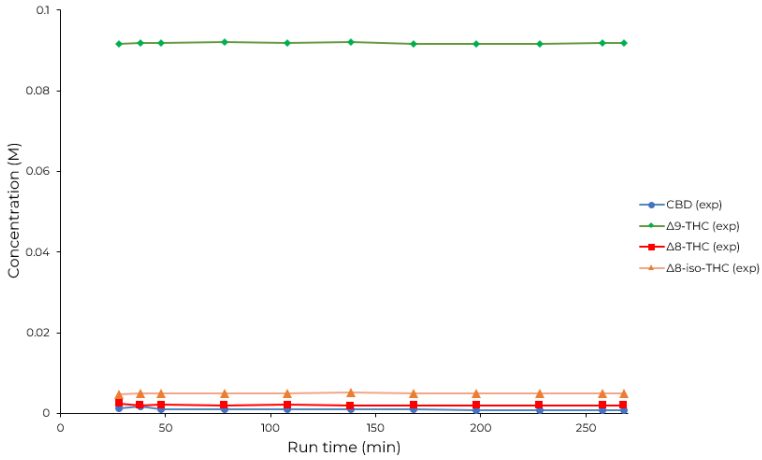

Figure 3.11 Concentration of the different components over the duration of the Δ^9-THC (**18**) long run

We also performed a 4.77 mmol scale experiment for the preparation of Δ^8-THC, conducted for a run time of 24 min. Again, the system performed in a stable manner, as showed in **Table 3.11** and in **Figure 3.12**, with the complete conversion of CBD and overall 90.5% selectivity of Δ^8-THC **19**. The product was isolated in 98% yield after filtration and removal of the solvent.

Table 3.11 Preparative-scale Experiment to Prepare Δ^8-THC

Vial	Fractionated time interval [min]	17[a]	18[a]	19[a]	20[a]	21[a]
1	2-3	-	2.1	90.8	-	4.3
2	3-4	-	2.2	89.8	-	4.7
3	4-5	-	2.2	90.2	-	4.7
4	5-7	-	1.9	90.7	--	4.4
5	7-9	-	2.0	90.2	-	4.5
6	9-11	-	2	90.1	-	4.5
7	11-13	-	2.1	90.5	-	4.5
8	13-15	-	1.9	90.9	-	4.4
9	15-17	-	1.9	90.8		4.5
10	17-19	-	1.9	91	-	4.4
11	19-21	-	2.0	90.2	-	4.6
12	21-22	-	2.2	90.0	-	4.3
13	22-23	-	1.9	90.9	-	4.1
14	23-24	-	2.1	91.2	0.3	4.3
Average		**-**	**2.0**	**90.5**	**0.0**	**4.5**

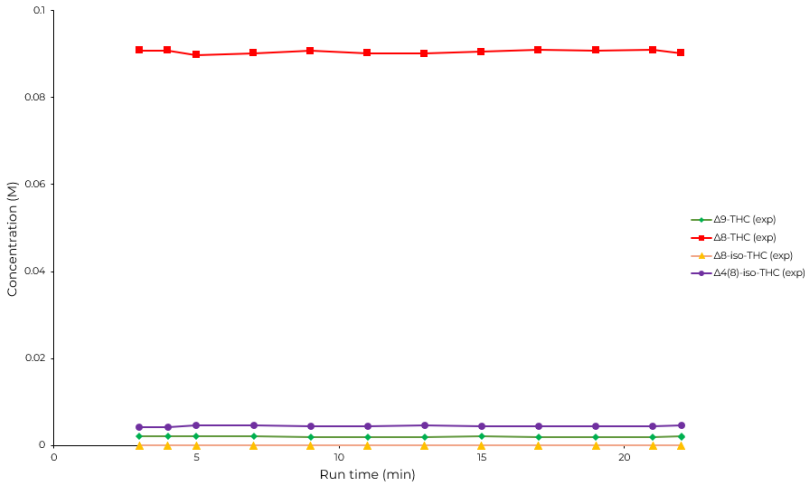

Figure 3.12 Concentration of the different components over time for the preparation of Δ^8-THC

Continuous flow protocols enabled the efficient selective synthesis of Δ^9-THC and Δ^8-THC from CBD in high product yields, overcoming complex mixtures of products, that are challenging to purify, usually obtained with traditional synthetic methods. Flow techniques, allowing the precise control of reaction parameters, with significantly enhancement in product selectivity and reaction performance, could be applied for the synthesis of other THC analogues.

3.3.5 Experimental section

General batch procedure

Substrate **17** (0.157 g, 0.500 mmol) was dissolved in anhydrous dichloromethane (5 mL, 0.1 M). The reaction was maintained at the desired temperature and the solution was stirred (minimum 500 rpm) using a magnetic stirrer. Then the acid (1.2 eq) was added and the reaction was profiled over time. Aliquots were taken from the reaction and added to a saturated solution of $NaHCO_3$ to quench the reaction. Then an aliquot was taken for analysis: 25 µL reaction mixture was diluted in 985 µL dichloromethane and analyzed by GC analysis.

General Flow Configurations (**Figure 3.13**)

For pumping feed solutions, syringe pumps (Syrris Asia) equipped with syringes appropriate for the desired flow rate were used. All of the pumps were used with check valves (Upchurch, CV-3321) and internal pressure sensors. The pressure limit of the pumps was set to 20 bar. Above this pressure and the pumps would turn-off automatically for safety reasons. The syringe pumps were calibrated by pumping for a specified time and checking the mass balance. All pumps were found to dose within ± 2%. Standard PFA tubing (0.8 mm or 1.6 mm i.d.), PTFE or PEEK fittings and T-pieces were used in the flow setups. The reactor coil was cut to length depending on the desired volume required. The reactor coil was kept at the desired temperature (−20 to 40 °C) by placing it inside the heating fluid which was maintained at a constant temperature using a thermostat (Huber Ministat 230).

- **Montmorillonite K10 / PVP-BF_3**

Montmorillonite K10 or PVP-BF_3 was packed into a column (Omnifit) and then placed on the heater module (Syrris Asia) to perform the reaction at the desired temperature.

- **$AlCl_3$**

For pumping light suspensions, i.e., in the case of $AlCl_3$, a peristaltic pump (Vapourtec SF-10) was used. Above this pressure and the pump would turn-off automatically for safety reasons.

Long run for Δ^9-THC

We performed a long run for the preparation of Δ^9-THC (**18**) using the optimized conditions shown in **Table 3.9**, **Entry 7**, to assess the robustness of our protocol.

Before/after experiment: Before running the reactions, the system was flushed with technical grade dichloromethane for 10 min. After the experiments, the setup was rinsed with dichloromethane and then the system was stored under isopropanol.

Feed preparation: Feed solutions were prepared in volumetric flasks. *Substrate feed preparation:* Cannabidiol (**17**) (6.28 g, 20.0 mmol) was dissolved in anhydrous dichloromethane (100 mL, 0.2 M). *Acid feed preparation:* Aluminium trichloride ($AlCl_3$) (1.06 g, 8 mmol) was dissolved in anhydrous dichloromethane (200 mL, 0.04 M).

Flow reaction protocol: The system was operated for a total of 268 min (from start-up to collecting the final fraction), which corresponded to the processing 4.20 g (13.3 mmol) of CBD (**17**). The feed

solution of $AlCl_3$ (0.04 M) in CH_2Cl_2 was introduced using a peristaltic pump (Vapourtec SF-10). The $AlCl_3$ feed solution was stirred at 37 °C for the duration of the experimental run. CBD (0.2 M) in CH_2Cl_2 was introduced using a syringe pump (Syrris Asia). The substrate solution was pumped at a flow rate of 0.278 mL/min and the $AlCl_3$ solution was pumped at a flow rate of 0.278 mL/min, giving a residence time of 18 min. A simple T-piece was used to mix the two feeds prior to the reactor. The reactor coil (10 mL internal volume) was submerged in the thermostat heating solution (EtOH) to control the temperature, which was set at 37 °C. The outlet stream was fractionated into stirred vials containing $NaHCO_3$ in CH_2Cl_2. Sample collection was started once color was observed at the end of the reactor (after 18 min). The reaction outlet was collected in 10 mL vials containing a quench ($NaHCO_3$ in CH_2Cl_2) and a stirring bar, the first 30 min (1 vial every 10 min), then in 20 mL vials for the central 3.5 h (1 vial every 30 min), and again in a 10 mL vial for the last ten minutes. Eleven fractions were collected and analyzed on the GC-FID (Table S10). 1,2-dichloro-4-nitrobenzene was used as internal standard to measure the NMR assay yield, which was determined to be 90% (value based on the average of three separate NMR samples). The collected fractionated vials were combined, filtered and then solvent was removed under reduced pressure (the rotary evaporator bath was maintained at 35 °C) to obtain **18** (4.07 g, 12.9 mmol, 97% yield) as a yellow oil.

(−)-*trans*-Δ⁹-Tetrahydrocannabinol (Δ⁹-THC, 18)

Yellow oil. **^{1}H NMR** (300 MHz, $CDCl_3$) δ 6.33 (s, 1H), 6.30 (d, J = 1.2 Hz, 1H), 6.16 (d, J = 1.3 Hz, 1H), 4.81 (s, 1H), 3.26-3.19 (m, 1H), 2.46 (dt, J = 7.4, 2.2 Hz, 2H), 2.23-2.16 (m, 2H), 1.97-1.89 (m, 1H), 1.74-1.65 (m, 4H), 1.58 (m, 2H), 1.47-1.40 (m, 4H), 1.37-1.27 (m, 4H), 1.12 (s, 3H), 0.90 (t, J = 6.9 Hz, 3H). **^{13}C{^{1}H} NMR** (75 MHz, $CDCl_3$): δ 154.7, 154.2, 142.8, 134.4, 123.7, 110.1, 109.1, 107.5, 45.8, 35.5, 33.6, 31.5, 31.2, 30.6, 27.6, 25.0, 23.4, 22.5, 19.3, 14.0. **GC-MS** analysis: m/z 314 confirmed

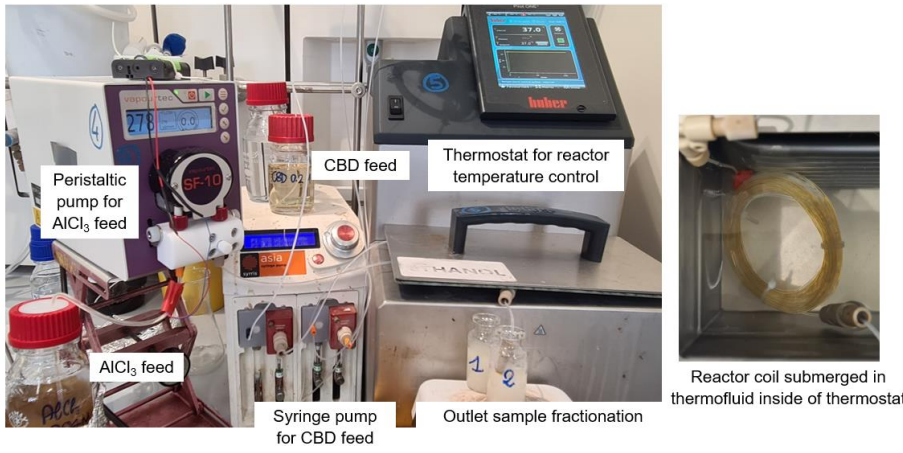

Figure 3.13 Labelled image of continuous-flow setup for the preparation of Δ⁹-THC

Preparative-scale experiment for Δ⁸-THC

We performed an experiment for the preparation of Δ⁸-THC (**19**) using the optimized conditions shown in **Table 3.7**, **Entry 14**, to assess the robustness of our protocol.

Before/after experiment: Before running the reactions, the system was flushed with technical grade dichloromethane for 10 min. After the experiments, the setup was rinsed with dichloromethane and then the system was stored under isopropanol.

Feed preparation: Feed solutions were prepared in volumetric flasks. *Substrate feed preparation:* Cannabidiol (**17**) (1.51 g, 4.80 mmol) was dissolved in anhydrous dichloromethane (24 mL, 0.2 M). *Reagent feed preparation:* Trimethylsilyl trifluoromethanesulfonate (TMSOTf) (1.28 g, 1.05 mL, 5.76 mmol) was dissolved in anhydrous dichloromethane (24 mL, 0.24 M).

Flow reaction protocol: The system was operated for a total of 24 min (from start-up to collecting the final fraction). The two feed solutions were introduced at the same flow rate using syringe pumps (Syrris Asia). The combined flow rate was 2.25 mL/min. A simple T-piece was used to mix the two feeds prior to the reactor. The reactor coil (4.5 mL internal volume) was submerged in the thermostat heating solution (EtOH) to control the temperature, which was set at 25°C. The reaction outlet was collected in 10 mL vials containing a quench ($NaHCO_3$ in CH_2Cl_2) and a stirring bar, for the first 3 min (1 vial every 1 min), then in 10 mL vials for the central 16 min (1 vial every 2 min), and again in a 4 mL vial for the last three min. Fourteen fractions were collected and analyzed on the GC-FID. 1,2-dichloro-4-nitrobenzene was used as internal standard to measure the NMR assay yield, which was determined to be 87% (value based on the average of three separate NMR samples). The collected fractionated vials were combined, filtered and then solvent was removed under reduced pressure (the rotary evaporator bath was maintained at 35 °C) to obtain **19** (1.48 g, 4.71 mmol, 98% yield) as a red oil.

(–)-*trans*-Δ^8-Tetrahydrocannabinol (Δ^8-THC, 19)

Red oil. **^{1}H NMR** (300 MHz, $CDCl_3$) δ 6.30 (s, 1H), 6.13 (brs, 1H), 5.45 (m, 1H), 3.22 (dd, J = 15.7, 3.1 Hz, 1H), 2.72 (td, J = 10.8, 4.7 Hz, 1H), 2.46 (td, J = 7.5, 3.3 Hz, 2H), 2.20-2.13 (m, 1H), 1.91-1.79 (m, 2H), 1.73 (s, 3H), 1.62-1.55 (m, 2H), 1.41 (s, 3H), 1.38-1.29 (m, 5H), 1.14 (s, 3H), 0.91 (t, J = 6.9 Hz, 3H). 1,2-dichloro-4-nitrobenzene was used as internal standard to assess the purity of the yellow oil which was measured to be 87% (value based on the average of three separate NMR samples). **^{13}C{^{1}H} NMR** (75 MHz, $CDCl_3$): δ 154.9, 154.7, 142.7, 134.7, 119.3, 110.5, 110.2, 107.6, 77.6, 44.9, 36.0, 35.5, 31.6, 30.6, 27.9, 27.6, 23.5, 22.5, 18.5, 14.0. GC-MS analysis: m/z 314 confirmed.

Kinetic fitting

The fitting of the rate constants for the rate limiting steps was performed using a software package called Compunetics (v3.1.1) (https://compunetics.net/). The software automatically adjusted the rate constant values based to improve the model fit to the experimental data. The sum of squared error (SSE) difference between the ordinary differential equation (ODE) curves and the experimental data were minimized to arrive at the final estimated rate constant values. The errors on fitted rate constant values are absolute errors, whereby this is the maximum possible error in the ODE based on fittings of each permutation of the ±2.5% relative error specified concentration for each of the species fitted. Moreover, the maximum variance was determined from the original fitting, and reported as the absolute error in the parameter fit. If a rate constant displayed no sensitivity to the

fit then it was removed. The model structure which was fitted to the reaction profiles is shown in Scheme S2. The four rate limiting steps were simultaneously fitted for the reaction profile. The reactions were fitted as first order. In the case of the batch reaction with MK10 and Si-BF_3 an additional rate-limiting step, k_5, Δ^9-THC (**19**) to CBN (**22**) was also fitted.

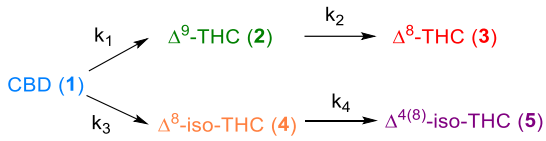

NMR Spectra of the described compounds and additional information can be found at: https://doi.org/10.1021/acs.joc.3c00300

3.4 References

(1) Starmans, D. A. J.; Nijhuis, H. H. Extraction of Secondary Metabolites from Plant Material: A Review. *Trends Food Sci Technol* **1996**, *7*, 192–197.

(2) Crozier, Alan.; Clifford, M. N. (Michael N.); Ashihara, Hiroshi. *Plant Secondary Metabolites : Occurrence, Structure and Role in the Human Diet*; Blackwell Pub, 2006.

(3) Veeresham, C. Natural Products Derived from Plants as a Source of Drugs. *Adv Pharm Technol Res* **2012**, *3* (4), 200–201. https://doi.org/10.4103/2231-4040.104709.

(4) Borris, R. P. Natural Products Research: Perspectives from a Major Pharmaceutical Company. *J. Ethnopharmacol.* **1996**, *51*, 29–38.

(5) Mushtaq, S.; Abbasi, B. H.; Uzair, B.; Abbasi, R. Natural Products as Reservoirs of Novel Therapeutic Agents. *EXCLI J* **2018**, *17*, 420–451. https://doi.org/10.17179/excli2018-1174.

(6) Newman, D. J.; Cragg, G. M. Natural Products as Sources of New Drugs from 1981 to 2014. *J Nat Prod* **2016**, *79* (3), 629–661. https://doi.org/10.1021/acs.jnatprod.5b01055.

(7) Liu, J. K. Natural Products in Cosmetics. *Nat Prod Bioprospect* **2022**, *12* (1). https://doi.org/10.1007/s13659-022-00363-y.

(8) González-Manzano, S.; Dueñas, M. Applications of Natural Products in Food. *Foods* **2021**, *10* (2). https://doi.org/10.3390/foods10020300.

(9) Rostagno, M. A.; Prado, J. M. *Natural Product Extraction: Principles and Applications*; RSC Publishing, 2017. https://doi.org/10.1039/9781849737579-fp001.

(10) Baran, P. S. Natural Product Total Synthesis: As Exciting as Ever and Here to Stay. *Journal of the American Chemical Society*. American Chemical Society April 11, 2018, pp 4751–4755. https://doi.org/10.1021/jacs.8b02266.

(11) Morrison, K. C.; Hergenrother, P. J. Natural Products as Starting Points for the Synthesis of Complex and Diverse Compounds. *Nat Prod Rep* **2014**, *31* (1), 6–14. https://doi.org/10.1039/c3np70063a.

(12) Akhtar, M. S.; Swamy, M. K.; Sinniah, U. R. *Natural Bio-Active Compounds*; Springer Singapore, 2019. https://doi.org/10.1007/978-981-13-7154-7.

(13) Atanasov, A. G.; Zotchev, S. B.; Dirsch, V. M.; Orhan, I. E.; Banach, M.; Rollinger, J. M.; Barreca, D.; Weckwerth, W.; Bauer, R.; Bayer, E. A.; Majeed, M.; Bishayee, A.; Bochkov, V.; Bonn, G. K.; Braidy, N.; Bucar, F.; Cifuentes, A.; D'Onofrio, G.; Bodkin, M.; Diederich, M.; Dinkova-Kostova, A. T.; Efferth, T.; El Bairi, K.; Arkells, N.; Fan, T. P.; Fiebich, B. L.; Freissmuth, M.; Georgiev, M. I.; Gibbons, S.; Godfrey, K. M.; Gruber, C. W.; Heer, J.; Huber, L. A.; Ibanez, E.; Kijjoa, A.; Kiss, A. K.; Lu, A.; Macias, F. A.; Miller, M. J. S.; Mocan, A.; Müller, R.; Nicoletti, F.; Perry, G.; Pittalà, V.; Rastrelli, L.; Ristow, M.; Russo, G. L.; Silva, A. S.; Schuster, D.; Sheridan, H.; Skalicka-Woźniak, K.;

Skaltsounis, L.; Sobarzo-Sánchez, E.; Bredt, D. S.; Stuppner, H.; Sureda, A.; Tzvetkov, N. T.; Vacca, R. A.; Aggarwal, B. B.; Battino, M.; Giampieri, F.; Wink, M.; Wolfender, J. L.; Xiao, J.; Yeung, A. W. K.; Lizard, G.; Popp, M. A.; Heinrich, M.; Berindan-Neagoe, I.; Stadler, M.; Daglia, M.; Verpoorte, R.; Supuran, C. T. Natural Products in Drug Discovery: Advances and Opportunities. *Nature Reviews Drug Discovery*., **2021**, pp 200–216. https://doi.org/10.1038/s41573-020-00114-z.

(14) Goss, R. J. M.; Shankar, S.; Fayad, A. A. The Generation of "UnNatural" Products: Synthetic Biology Meets Synthetic Chemistry. *Nat Prod Rep* **2012**, *29* (8), 870–889. https://doi.org/10.1039/c2np00001f.

(15) Sparks, T. C.; Hahn, D. R.; Garizi, N. V. Natural Products, Their Derivatives, Mimics and Synthetic Equivalents: Role in Agrochemical Discovery. *Pest Manag Sci* **2017**, *73* (4), 700–715. https://doi.org/10.1002/ps.4458.

(16) Najmi, A.; Javed, S. A.; Al Bratty, M.; Alhazmi, H. A. Modern Approaches in the Discovery and Development of Plant-Based Natural Products and Their Analogues as Potential Therapeutic Agents. *Molecules* **2022**, *27* (2). https://doi.org/10.3390/molecules27020349.

(17) Butler, M. S. The Role of Natural Product Chemistry in Drug Discovery. *J Nat Prod* **2004**, *67* (12), 2141–2153. https://doi.org/10.1021/np040106y.

(18) Maier, M. E. Design and Synthesis of Analogues of Natural Products. *Org Biomol Chem* **2015**, *13* (19), 5302–5343. https://doi.org/10.1039/c5ob00169b.

(19) Calixto, J. B. The Role of Natural Products in Modern Drug Discovery. *An Acad Bras Cienc* **2019**, *91*. https://doi.org/10.1590/0001-3765201920190105.

(20) Dias, D. A.; Urban, S.; Roessner, U. A Historical Overview of Natural Products in Drug Discovery. *Metabolites* **2012**, *2* (2), 303–336. https://doi.org/10.3390/metabo2020303.

(21) Fisher, M. H.; Mrozik, H. THE CHEMISTRY AND PHARMACOLOGY OF AVERMECTINS. *Annu. Rev. Pharmacol. Toxicol.* **1992**, *32*, 537–553.

(22) Hanessian, S.; Ugolini, A.; Dubé Daniel; Hodges, P. J.; André, C. Synthesis of (+)-Avermectin B1a. *J. Am. Chem. Soc* **1986**, *108* (15), 41.

(23) Yamashita, S.; Hayashi, D.; Nakano, A.; Hayashi, Y.; Hirama, M. Total Synthesis of Avermectin B1a Revisited. *Journal of Antibiotics* **2016**, *69* (1), 31–50. https://doi.org/10.1038/ja.2015.47.

(24) Krishna, S.; Bustamante, L.; Haynes, R. K.; Staines, H. M. Artemisinins: Their Growing Importance in Medicine. *Trends Pharmacol Sci* **2008**, *29* (10), 520–527. https://doi.org/10.1016/j.tips.2008.07.004.

(25) Cui, L.; Su, X. Z. Discovery, Mechanisms of Action and Combination Therapy of Artemisinin. *Expert Rev Anti Infect Ther* **2009**, *7* (8), 999–1013. https://doi.org/10.1586/ERI.09.68.

(26) Mutabingwa, T. K. Artemisinin-Based Combination Therapies (ACTs): Best Hope for Malaria Treatment but Inaccessible to the Needy! *Acta Trop* **2005**, *95* (3), 305–315. https://doi.org/10.1016/j.actatropica.2005.06.009.

(27) Avery, M. a.; Chong, W. K. M.; Jenning-White, C. Stereoselective Total Synthesis of (+)-Artemisinin, the Antimalarial Constituent of Artemisia Annua L. *J. Am. Chem. Soc* **1992**, *114*, 29.

(28) Yadav, J. S.; Satheesh Babu, R.; Sabitha, G. Stereoselective Total Synthesis of (+)-Artemisinin. *Tetrahedron Lett* **2003**, *44*, 387–389.

(29) Zhu, C.; Cook, S. P. A Concise Synthesis of (+)-Artemisinin. *J Am Chem Soc* **2012**, *134* (33), 13577–13579. https://doi.org/10.1021/ja3061479.

(30) Krieger, J.; Smeilus, T.; Kaiser, M.; Seo, E.; Efferth, T.; Giannis, A. Total Synthesis and Biological Investigation of (-)-Artemisinin:The Activity of Artemisinin Is Not Stereospecific. *Angewandte Chemie* **2018**, *130* (27), 8425–8428. https://doi.org/10.1002/ange.201802015.

(31) Mekhail, T. M.; Markman, M. Paclitaxel in Cancer Therapy. *Expert Opin. Pharmacother.* **2002**, *3* (6), 755–766.

(32) Nikolic, V. D.; Savic, I. M.; Savic, I. M.; Nikolic, L. B.; Stankovic, M. Z.; Marinkovic, V. D. Paclitaxel as an Anticancer Agent: Isolation, Activity, Synthesis and Stability. *Cent Eur J Med* **2011**, *6* (5), 527–536. https://doi.org/10.2478/s11536-011-0074-5.

(33) Li, B. J.; Wang, H.; Gong, T.; Chen, J. J.; Chen, T. J.; Yang, J. L.; Zhu, P. Improving 10-Deacetylbaccatin III-10-β-O-Acetyltransferase Catalytic Fitness for Taxol Production. *Nat Commun* **2017**, *8*. https://doi.org/10.1038/ncomms15544.

(34) Guéritte-Voegelein, F.; Sénilh, V.; David, B.; Guénard, D.; Potier, P. Chemical Studies of 10-Deacetyl Baccatin III. Hemisynthesis of Taxol Derivatives. *Tetrahedron* **1986**, *42* (16), 4451–4460.

(35) Wahl, A.; Guéritte-Voegelein, F.; Guénard, D.; Le Goff, M.-T.; Potier, P. REARRANGEMENT REACTIONS OF TAXANES: STRUCTURAL MODIFICATIONS OF 10-DEACETYLBACCATIN. *Tetrahedron* **1992**, *48* (34), 6965–6974.

(36) Potier, P. Search and Discovery of New Antitumour Compounds. *Chem Soc Rev* **1992**.

(37) Holton, R. A.; Somoza, C.; Kim, H.-B.; Liang, F.; Biediger, R. J.; Douglas Boatman, P.; Shindo, M.; Smith, C. C.; Kim, S.; Nadizadeh, H.; Suzuki, Y.; Tao, C.; Vu, P.; Tang, S.; Zhang, P.; Murthi, K. K.; Gentile, L. N.; Liu, J. H. First Total Synthesis of Taxol. 1. Functionalization of the B Ring. *J. Am. Chem. Soc.* **1994**, *116*, 5731–1598.

(38) Holton, R. A.; Kim, H.-B.; Somoza, C.; Liang, F.; Biediger, R. J.; Douglas Boatman, P.; Shindo, M.; Smith, C. C.; Kim, S.; Nadizadeh, H.; Suzuki, Y.; Tao, C.; Vu, P.; Tang, S.; Zhang, P.; Murthi, K. K.; Gentile, L. N.; Liu, J. H. First Total Synthesis of Taxol. 2. Completion of the C and D Rings. *J. Am. Chem. Soc* **1994**, *116*, 1599–1600.

(39) Nicolau, K. C.; Yang, Z.; Liu, J. J.; Ueno, H.; Nantermet, P. G.; Guy, R. K.; Clalborne, C. F.; Renaud, J.; Couladouros, E. A.; Paulvannan, K.; Sorensen, E. J. Total Synthesis of Taxol. *Nature* **1994**, *367*, 630–634.

(40) Nicolaou, K. C.; Guy, R. K. The Conquest of Taxol. *Angew. Chem. Int. Ed. Engl.* **1995**, *34*, 2079–2090.

(41) Danishefsky, S. J.; Masters, J. J.; Young, W. B.; Link, J. T.; Snyder, L. B.; Magee, T. V; Jung, D. K.; Isaacs, R. C. A.; Bornmann, W. G.; Alaimo, C. A.; Coburn, C. A.; Grandi, M. J. Di. Total Synthesis of Baccatin III and Taxol. *J. Am. Chem. Soc.* **1996**, *118*, 2843–2859.

(42) Morihira, K.; Hara, R.; Kawahara, S.; Nishimori, T.; Nakamura, N.; Kusama, H.; Kuwajima, I. Enantioselective Total Synthesis of Taxol. *J Am Chem Soc* **1998**, *120* (49), 12980–12981. https://doi.org/10.1021/ja9824932.

(43) Kanda, Y.; Nakamura, H.; Umemiya, S.; Puthukanoori, R. K.; Murthy Appala, V. R.; Gaddamanugu, G. K.; Paraselli, B. R.; Baran, P. S. Two-Phase Synthesis of Taxol. *J Am Chem Soc* **2020**, *142* (23), 10526–10533. https://doi.org/10.1021/jacs.0c03592.

(44) Kanda, Y.; Ishihara, Y.; Wilde, N. C.; Baran, P. S. Two-Phase Total Synthesis of Taxanes: Tactics and Strategies. *Journal of Organic Chemistry* **2020**, *85* (16), 10293–10320. https://doi.org/10.1021/acs.joc.0c01287.

(45) Iiyama, S.; Fukaya, K.; Yamaguchi, Y.; Watanabe, A.; Yamamoto, H.; Mochizuki, S.; Saio, R.; Noguchi, T.; Oishi, T.; Sato, T.; Chida, N. Total Synthesis of Paclitaxel. *Org Lett* **2022**, *24* (1), 202–206. https://doi.org/10.1021/acs.orglett.1c03851.

(46) Hu, Y. J.; Gu, C. C.; Wang, X. F.; Min, L.; Li, C. C. Asymmetric Total Synthesis of Taxol. *J Am Chem Soc* **2021**, *143* (42), 17862–17870. https://doi.org/10.1021/jacs.1c09637.

(47) Katrina Megget. *Semi-synthetic paclitaxel production starts in Italy*. https://www.outsourcing-pharma.com/ (accessed 2024-01-10).

(48) Malik, S.; Cusidó, R. M.; Mirjalili, M. H.; Moyano, E.; Palazón, J.; Bonfill, M. Production of the Anticancer Drug Taxol in Taxus Baccata Suspension Cultures: A Review. *Process Biochemistry* **2011**, *46* (1), 23–34. https://doi.org/10.1016/j.procbio.2010.09.004.

(49) Bassetti, B.; Ballini, R.; Ciceri, D.; Allegrini, P.; Palmieri, A. A Practical and Efficient Conversion of Luteolin into Luteoloside. *Synthesis (Germany)* **2021**, *53* (21), 4075–4078. https://doi.org/10.1055/a-1531-2385.

(50) Bassetti, B.; Hone, C. A.; Kappe, C. O. Continuous-Flow Synthesis of Δ9-Tetrahydrocannabinol and Δ8-Tetrahydrocannabinol from Cannabidiol. *Journal of Organic Chemistry* **2023**, *88* (9), 6227–6231. https://doi.org/10.1021/acs.joc.3c00300.

(51) Bassetti, B.; Ballini, R.; Allegrini, P.; Aldini, G.; Palmieri, A. Total Synthesis of 1''- and 2''-Hydroxycannabidiol Metabolites. *ChemistrySelect* **2023**, *8* (45). https://doi.org/10.1002/slct.202304489.

(52) Panche, A. N.; Diwan, A. D.; Chandra, S. R. Flavonoids: An Overview. *J Nutr Sci* **2016**, *5*. https://doi.org/10.1017/jns.2016.41.

(53) Lwashina, T. The Structure and Distribution of the Flavonoids in Plants. *J. Plant Res* **2000**, *113*, 287–299.

(54) Verma, A. K.; Pratap, R. The Biological Potential of Flavones. *Nat Prod Rep* **2010**, *27* (11), 1571–1593. https://doi.org/10.1039/c004698c.

(55) Hollman, P. C. H.; Katan, M. B. Dietary Flavonoids: Intake, Health Effects and Bioavailability. *Food and Chemical Toxicology* **1999**, *37*, 937–942.

(56) Terahara, N. Flavonoids in Foods: A Review. *Nat Prod Commun* **2015**, *10* (3), 521–528.

(57) Maleki, S. J.; Crespo, J. F.; Cabanillas, B. Anti-Inflammatory Effects of Flavonoids. *Food Chem* **2019**, *299*. https://doi.org/10.1016/j.foodchem.2019.125124.

(58) Pietta, P. G. Flavonoids as Antioxidants. *J Nat Prod* **2000**, *63* (7), 1035–1042. https://doi.org/10.1021/np9904509.

(59) Farhadi, F.; Khameneh, B.; Iranshahi, M.; Iranshahy, M. Antibacterial Activity of Flavonoids and Their Structure–Activity Relationship: An Update Review. *Phytotherapy Research* **2019**, *33* (1), 13–40. https://doi.org/10.1002/ptr.6208.

(60) Kopustinskiene, D. M.; Jakstas, V.; Savickas, A.; Bernatoniene, J. Flavonoids as Anticancer Agents. *Nutrients* **2020**, *12* (2). https://doi.org/10.3390/nu12020457.

(61) Ullah, A.; Munir, S.; Badshah, S. L.; Khan, N.; Ghani, L.; Poulson, B. G.; Emwas, A. H.; Jaremko, M. Important Flavonoids and Their Role as a Therapeutic Agent. *Molecules* **2020**, *25* (22). https://doi.org/10.3390/molecules25225243.

(62) Safe, S.; Jayaraman, A.; Chapkin, R. S.; Howard, M.; Mohankumar, K.; Shrestha, R. Flavonoids: Structure–Function and Mechanisms of Action and Opportunities for Drug Development. *Toxicol Res* **2021**, *37* (2), 147–162. https://doi.org/10.1007/s43188-020-00080-z.

(63) Punia Bangar, S.; Kajla, P.; Chaudhary, V.; Sharma, N.; Ozogul, F. Luteolin: A Flavone with Myriads of Bioactivities and Food Applications. *Food Biosci* **2023**, *52*. https://doi.org/10.1016/j.fbio.2023.102366.

(64) Imran, M.; Rauf, A.; Abu-Izneid, T.; Nadeem, M.; Shariati, M. A.; Khan, I. A.; Imran, A.; Orhan, I. E.; Rizwan, M.; Atif, M.; Gondal, T. A.; Mubarak, M. S. Luteolin, a Flavonoid, as an Anticancer

Agent: A Review. *Biomedicine and Pharmacotherapy* **2019**, *112*. https://doi.org/10.1016/j.biopha.2019.108612.

(65) D'Andrea, G. Quercetin: A Flavonol with Multifaceted Therapeutic Applications? *Fitoterapia* **2015**, *106*, 256–271. https://doi.org/10.1016/j.fitote.2015.09.018.

(66) Alizadeh, S. R.; Ebrahimzadeh, M. A. O-Glycoside Quercetin Derivatives: Biological Activities, Mechanisms of Action, and Structure–Activity Relationship for Drug Design, a Review. *Phytotherapy Research* **2022**, *36* (2), 778–807. https://doi.org/10.1002/ptr.7352.

(67) Chua, L. S. A Review on Plant-Based Rutin Extraction Methods and Its Pharmacological Activities. *J Ethnopharmacol* **2013**, *150* (3), 805–817. https://doi.org/10.1016/j.jep.2013.10.036.

(68) Frutos, M. J.; Rincón-Frutos, L.; Valero-Cases, E. Rutin. In *Nonvitamin and Nonmineral Nutritional Supplements*; Elsevier, 2018; pp 111–117. https://doi.org/10.1016/B978-0-12-812491-8.00015-1.

(69) Nüßlein, B.; Kreis, W. Purification and Characterization of a Cynaroside 7-O-β-D-Glucosidase from Cynarae Scolymi Folium. *Acta Hortic* **2005**, *681*, 413–420.

(70) Bouyahya, A.; Taha, D.; Benali, T.; Zengin, G.; El Omari, N.; El Hachlafi, N.; Khalid, A.; Abdalla, A. N.; Ardianto, C.; Tan, C. S.; Ming, L. C.; Sahib, N. Natural Sources, Biological Effects, and Pharmacological Properties of Cynaroside. *Biomedicine and Pharmacotherapy* **2023**, *161*. https://doi.org/10.1016/j.biopha.2023.114337.

(71) Sun, X.; Sun, G. B.; Wang, M.; Xiao, J.; Sun, X. B. Protective Effects of Cynaroside against H 2O 2-Induced Apoptosis in H9c2 Cardiomyoblasts. *J Cell Biochem* **2011**, *112* (8), 2019–2029. https://doi.org/10.1002/jcb.23121.

(72) Zou, Y.; Zhang, M.; Zhang, T.; Wu, J.; Wang, J.; Liu, K.; Zhan, N. Antioxidant and Anti-Inflammatory Activities of Cynaroside from Elsholtiza Bodinieri. *Nat Prod Commun* **2018**, *13* (11), 1501–1504.

(73) Szekalska, M.; Sosnowska, K.; Tomczykowa, M.; Winnicka, K.; Kasacka, I.; Tomczyk, M. In Vivo Anti-Inflammatory and Anti-Allergic Activities of Cynaroside Evaluated by Using Hydrogel Formulations. *Biomedicine and Pharmacotherapy* **2020**, *121*. https://doi.org/10.1016/j.biopha.2019.109681.

(74) Tabrez, S.; Rahman, F.; Ali, R.; Alouffi, A. S.; Akand, S. K.; Alshehri, B. M.; Alshammari, F. A.; Alam, A.; Alaidarous, M. A.; Banawas, S.; Bin Dukhyil, A. A.; Rub, A. Cynaroside Inhibits Leishmania Donovani UDP-Galactopyranose Mutase and Induces Reactive Oxygen Species to Exert Antileishmanial Response. *Biosci Rep* **2021**, *41* (1). https://doi.org/10.1042/BSR20203857.

(75) Ji, J.; Wang, Z.; Sun, W.; Li, Z.; Cai, H.; Zhao, E.; Cui, H. Effects of Cynaroside on Cell Proliferation, Apoptosis, Migration and Invasion Though the MET/AKT/MTOR Axis in Gastric Cancer. *Int J Mol Sci* **2021**, *22* (22). https://doi.org/10.3390/ijms222212125.

(76) Cao, Z.; Ding, Y.; Ke, Z.; Cao, L.; Li, N.; Ding, G.; Wang, Z.; Xiao, W. Luteoloside Acts as 3C Protease Inhibitor of Enterovirus 71 in Vitro. *PLoS One* **2016**, *11* (2). https://doi.org/10.1371/journal.pone.0148693.

(77) Kim, S. H.; Naveen Kumar, C.; Kim, H. J.; Kim, D. H.; Cho, J.; Jin, C.; Lee, Y. S. Glucose-Containing Flavones-Their Synthesis and Antioxidant and Neuroprotective Activities. *Bioorg Med Chem Lett* **2009**, *19* (21), 6009–6013. https://doi.org/10.1016/j.bmcl.2009.09.062.

(78) Ballini, R.; Gabrielli, S.; Palmieri, A. β-Nitroacrylates as Key Starting Materials for the Uncatalysed One-Pot Synthesis of Polyfunctionalized Dihydroquinoxalinone Derivatives, via an Anti-Michael Reaction. *Synlett* **2009**, No. 6, 965–967. https://doi.org/10.1055/s-0028-1088197.

(79) Ballini, R.; Gabrielli, S.; Palmieri, A. β-Nitroacrylates as Precursors of Tetrasubstituted Furans in a One-Pot Process and under Acidic Solvent-Free Conditions. *Synlett* **2010**, No. 16, 2468–2470. https://doi.org/10.1055/s-0030-1258031.

(80) Palmieri, A.; Petrini, M. Sulfonyl Azoles in the Synthesis of 3-Functionalized Azole Derivatives. *Chemical Record* **2016**, 1353–1379. https://doi.org/10.1002/tcr.201500291.

(81) Rossi, F. V.; Ballini, R.; Barboni, L.; Allegrini, P.; Palmieri, A. A Practical and Efficient Synthesis of (±)-Anatabine. *Synthesis (Germany)* **2018**, *50* (9), 1921–1925. https://doi.org/10.1055/s-0036-1591538.

(82) Chiurchiù, E.; Sampaolesi, S.; Allegrini, P.; Ciceri, D.; Ballini, R.; Palmieri, A. A Novel and Practical Continuous Flow Chemical Synthesis of Cannabidiol (CBD) and Its CBDV and CBDB Analogues. *European J Org Chem* **2021**, *2021* (8), 1286–1289. https://doi.org/10.1002/ejoc.202001633.

(83) Sun, D. Y.; Cheng, C.; Moschke, K.; Huang, J.; Fang, W. S. Extensive Structure Modification on Luteolin-Cinnamic Acid Conjugates Leading to BACE1 Inhibitors with Optimal Pharmacological Properties. *Molecules* **2020**, *25* (1). https://doi.org/10.3390/molecules25010102.

(84) Wang, Q. Q.; Cheng, N.; Zheng, X. W.; Peng, S. M.; Zou, X. Q. Synthesis of Organic Nitrates of Luteolin as a Novel Class of Potent Aldose Reductase Inhibitors. *Bioorg Med Chem* **2013**, *21* (14), 4301–4310. https://doi.org/10.1016/j.bmc.2013.04.066.

(85) Kappe, C. O.; Stadler, A.; Dallinger, D. *Microwaves in Organic and Medicinal Chemistry*; 2005.

(86) Chatterjee, A.; Sarkar, S.; Saha, S. K. Acacetin 7-O-β-D-Galarctopyranoside from Chrystanthemum Indicum. *Phytochemistry* **1981**, *20* (7), 1760–1781.

(87) Li, N. G.; Shi, Z. H.; Tang, Y. P.; Yang, J. P.; Duan, J. A. An Efficient Partial Synthesis of 4'-O-Methylquercetin via Regioselective Protection and Alkylation of Quercetin. *Beilstein Journal of Organic Chemistry* **2009**, *5*. https://doi.org/10.3762/bjoc.5.60.

(88) Xu, B.; Liang, G.; Wen, Z.; Hu, Z.; Yuan, J.; Chen, H.; Zhang, L. Synthesis of Quercetin Glycosides and Their α-Glucosidase Inhibitory Activities. *Heterocycles* **2016**, *92* (7), 1245–1260. https://doi.org/10.3987/COM-16-13455.

(89) Kimura, Y.; Kato, R.; Oyama, K.-I.; Kondo, T.; Yoshida, K. Efficient Preparation of Various O-Methylquercetins by Selective Demethylation. *Nat Prod Commun* **2016**, *11* (7), 957–961.

(90) Oyama, K. I.; Kondo, T. Total Synthesis of Apigenin 7,4'-Di-O-β-Glucopyranoside, a Component of Blue Flower Pigment of Salvia Patens, and Seven Chiral Analogues. *Tetrahedron* **2004**, *60* (9), 2025–2034. https://doi.org/10.1016/j.tet.2004.01.001.

(91) Hanuš, L. O.; Meyer, S. M.; Muñoz, E.; Taglialatela-Scafati, O.; Appendino, G. Phytocannabinoids: A Unified Critical Inventory. *Nat Prod Rep* **2016**, *33* (12), 1357–1392. https://doi.org/10.1039/c6np00074f.

(92) Andre, C. M.; Hausman, J. F.; Guerriero, G. Cannabis Sativa: The Plant of the Thousand and One Molecules. *Front Plant Sci* **2016**, *7*. https://doi.org/10.3389/fpls.2016.00019.

(93) Väisänen, T.; Batello, P.; Lappalainen, R.; Tomppo, L. Modification of Hemp Fibers (Cannabis Sativa L.) for Composite Applications. *Ind Crops Prod* **2018**, *111*, 422–429. https://doi.org/10.1016/j.indcrop.2017.10.049.

(94) Pisanti, S.; Bifulco, M. Medical Cannabis: A Plurimillennial History of an Evergreen. *J Cell Physiol* **2019**, *234* (6), 8342–8351. https://doi.org/10.1002/jcp.27725.

(95) Pollio, A. The Name of Cannabis: A Short Guide for Nonbotanists. *Cannabis Cannabinoid Res* **2016**, *1* (1), 234–238. https://doi.org/10.1089/can.2016.0027.

(96) Atakan, Z. Cannabis, a Complex Plant: Different Compounds and Different Effects on Individuals. *Ther Adv Psychopharmacol* **2012**, *2* (6), 241–254. https://doi.org/10.1177/2045125312457586.

(97) Gülck, T.; Møller, B. L. Phytocannabinoids: Origins and Biosynthesis. *Trends Plant Sci* **2020**, *25* (10), 985–1004. https://doi.org/10.1016/j.tplants.2020.05.005.

(98) Protti, M.; Brighenti, V.; Battaglia, M. R.; Anceschi, L.; Pellati, F.; Mercolini, L. Cannabinoids from Cannabis Sativa L.: A New Tool Based on HPLC-DAD-MS/MS for a Rational Use in Medicinal Chemistry. *ACS Med Chem Lett* **2019**, *10* (4), 539–544. https://doi.org/10.1021/acsmedchemlett.8b00571.

(99) Busardò, F. P.; Pérez-Acevedo, A. P.; Pacifici, R.; Mannocchi, G.; Gottardi, M.; Papaseit, E.; Pérez-Mañá, C.; Martin, S.; Poyatos, L.; Pichini, S.; Farré, M. Disposition of Phytocannabinoids, Their Acidic Precursors and Their Metabolites in Biological Matrices of Healthy Individuals Treated with Vaporized Medical Cannabis. *Pharmaceuticals* **2021**, *14* (1), 1–14. https://doi.org/10.3390/ph14010059.

(100) Lu, H. C.; MacKie, K. An Introduction to the Endogenous Cannabinoid System. *Biol Psychiatry* **2016**, *79* (7), 516–525. https://doi.org/10.1016/j.biopsych.2015.07.028.

(101) Calabrese, E. J.; Rubio-Casillas, A. Biphasic Effects of THC in Memory and Cognition. *Eur J Clin Invest* **2018**, *48* (5). https://doi.org/10.1111/eci.12920.

(102) Zou, S.; Kumar, U. Cannabinoid Receptors and the Endocannabinoid System: Signaling and Function in the Central Nervous System. *Int J Mol Sci* **2018**, *19* (3). https://doi.org/10.3390/ijms19030833.

(103) Pertwee, R. G. Cannabis and Cannabinoids: Pharmacology and Rationale for Clinical Use. *Research in Complementary Medicine* **1999**, *6* (3), 12–15.

(104) Kumar, R. N.; Chambers, W. A.; Pertwee, R. G. Pharmacological Actions and Therapeutic Uses of Cannabis and Cannabinoids. *Anaesthesia* **2001**, *56* (11), 1059–1068. https://doi.org/10.1111/j.1365-2044.2001.02269.x.

(105) Costa, B. On the Pharmacological Properties of Δ 9-Tetrahydrocannabinol (THC). *Chem Biodivers* **2007**, *4* (8), 1664–1677. https://doi.org/10.1002/cbdv.200790146.

(106) Parker, L. A.; Rock, E. M.; Limebeer, C. L. Regulation of Nausea and Vomiting by Cannabinoids. *Br J Pharmacol* **2011**, *163*, 1411–1422. https://doi.org/10.1111/j.1476-5381.2010.01176.x.

(107) Ben Amar, M. Cannabinoids in Medicine: A Review of Their Therapeutic Potential. *J Ethnopharmacol* **2006**, *105* (1–2), 1–25. https://doi.org/10.1016/j.jep.2006.02.001.

(108) Maccarrone, M.; Maldonado, R.; Casas, M.; Henze, T.; Centonze, D. Cannabinoids Therapeutic Use: What Is Our Current Understanding Following the Introduction of THC, THC:CBD Oromucosal Spray and Others? *Expert Rev Clin Pharmacol* **2017**, *10* (4), 443–455. https://doi.org/10.1080/17512433.2017.1292849.

(109) Tagen, M.; Klumpers, L. E. Review of Delta-8-Tetrahydrocannabinol (Δ8-THC): Comparative Pharmacology with Δ9-THC. *Br J Pharmacol* **2022**, *179* (15), 3915–3933. https://doi.org/10.1111/bph.15865.

(110) Leas, E. C.; Nobles, A. L.; Shi, Y.; Hendrickson, E. Public Interest in Δ8-Tetrahydrocannabinol (Delta-8-THC) Increased in US States That Restricted Δ9-Tetrahydrocannabinol (Delta-9-THC) Use. *International Journal of Drug Policy* **2022**, *101*. https://doi.org/10.1016/j.drugpo.2021.103557.

(111) Johnson-Arbor, K.; Smolinske, S. The Current State of Delta-8 THC. *American Journal of Emergency Medicine* **2022**, *56*, 259–261. https://doi.org/10.1016/j.ajem.2021.06.066.

(112) Erickson, B. E. Delta-8-THC Craze Concerns Chemists. *Chemical & Engineering News* **2021**, *99* (31).

(113) LoParco, C. R.; Rossheim, M. E.; Walters, S. T.; Zhou, Z.; Olsson, S.; Sussman, S. Y. Delta-8 Tetrahydrocannabinol: A Scoping Review and Commentary. *Addiction* **2023**, *118* (6), 1011–1028. https://doi.org/10.1111/add.16142.

(114) Britch, S. C.; Babalonis, S.; Walsh, S. L. Cannabidiol: Pharmacology and Therapeutic Targets. *Psychopharmacology (Berl)* **2021**, *238* (1), 9–28. https://doi.org/10.1007/s00213-020-05712-8.

(115) Crippa, J. A.; Guimarães, F. S.; Campos, A. C.; Zuardi, A. W. Translational Investigation of the Therapeutic Potential of Cannabidiol (CBD): Toward a New Age. *Front Immunol* **2018**, *9* (SEP). https://doi.org/10.3389/fimmu.2018.02009.

(116) Burstein, S. Cannabidiol (CBD) and Its Analogs: A Review of Their Effects on Inflammation. *Bioorg Med Chem* **2015**, *23* (7), 1377–1385. https://doi.org/10.1016/j.bmc.2015.01.059.

(117) Lazarini-Lopes, W.; Do Val-da Silva, R. A.; da Silva-Júnior, R. M. P.; Leite, J. P.; Garcia-Cairasco, N. The Anticonvulsant Effects of Cannabidiol in Experimental Models of Epileptic Seizures: From Behavior and Mechanisms to Clinical Insights. *Neurosci Biobehav Rev* **2020**, *111*, 166–182. https://doi.org/10.1016/j.neubiorev.2020.01.014.

(118) Urits, I.; Gress, K.; Charipova, K.; Habib, K.; Lee, D.; Lee, C.; Jung, J. W.; Kassem, H.; Cornett, E.; Paladini, A.; Varrassi, G.; Kaye, A. D.; Viswanath, O. Use of Cannabidiol (CBD) for the Treatment of Chronic Pain. *Best Pract Res Clin Anaesthesiol* **2020**, *34* (3), 463–477. https://doi.org/10.1016/j.bpa.2020.06.004.

(119) Bhunia, S.; Kolishetti, N.; Arias, A. Y.; Vashist, A.; Nair, M. Cannabidiol for Neurodegenerative Disorders: A Comprehensive Review. *Front Pharmacol* **2022**, *13*. https://doi.org/10.3389/fphar.2022.989717.

(120) Campos, A. C.; Moreira, F. A.; Gomes, F. V.; del Bel, E. A.; Guimarães, F. S. Multiple Mechanisms Involved in the Large-Spectrum Therapeutic Potential of Cannabidiol in Psychiatric Disorders. *Philosophical Transactions of the Royal Society B: Biological Sciences* **2012**, *367* (1607), 3364–3378. https://doi.org/10.1098/rstb.2011.0389.

(121) Bonaccorso, S.; Ricciardi, A.; Zangani, C.; Chiappini, S.; Schifano, F. Cannabidiol (CBD) Use in Psychiatric Disorders: A Systematic Review. *Neurotoxicology* **2019**, *74*, 282–298. https://doi.org/10.1016/j.neuro.2019.08.002.

(122) Atalay, S.; Jarocka-karpowicz, I.; Skrzydlewskas, E. Antioxidative and Anti-Inflammatory Properties of Cannabidiol. *Antioxidants* **2020**, *9* (1). https://doi.org/10.3390/antiox9010021.

(123) Beal, J. E.; Olson, R.; Laubenstein, L.; Morales, J. O.; Bellman, P.; Yangco, B.; Lefkowitz, L.; Plasse, T. F.; Shepard, K. V; John, S. Dronabinol as a Treatment for Anorexia Associated with Weight Loss in Patients with AIDS. *J Pain Symptom Manage* **1995**, *10* (2), 89–97.

(124) Bajtel, Á.; Kiss, T.; Tóth, B.; Kiss, S.; Hegyi, P.; Vörhendi, N.; Csupor-Löffler, B.; Gede, N.; Hohmann, J.; Csupor, D. The Safety of Dronabinol and Nabilone: A Systematic Review and Meta-Analysis of Clinical Trials. *Pharmaceuticals* **2022**, *15* (1). https://doi.org/10.3390/ph15010100.

(125) Abu-Sawwa, R.; Scutt, B.; Park, Y. Emerging Use of Epidiolex (Cannabidiol) in Epilepsy. *Journal of Pediatric Pharmacology and Therapeutics* **2020**, *25* (6), 485–499. https://doi.org/10.5863/1551-6776-25.6.485.

(126) De Vita, D.; Madia, V. N.; Tudino, V.; Saccoliti, F.; De Leo, A.; Messore, A.; Roscilli, P.; Botto, A.; Pindinello, I.; Santilli, G.; Scipione, L.; Costi, R.; Di Santo, R. Comparison of Different Methods for the Extraction of Cannabinoids from Cannabis. *Nat Prod Res* **2020**, *34* (20), 2952–2958. https://doi.org/10.1080/14786419.2019.1601194.

(127) Nahar, L.; Uddin, S. J.; Alam, M. A.; Sarker, S. D. Extraction of Naturally Occurring Cannabinoids: An Update. *Phytochemical Analysis* **2021**, *32* (3), 228–241. https://doi.org/10.1002/pca.2987.

(128) Monti, J. M.; Pandi-Perumal, S. R.; Murillo-Rodrìguez, E. *Cannabinoids and Sleep*; Springer, 2021. https://doi.org/10.1007/978-3-030-61663-2.

(129) Zamberletti, E.; Rubino, T.; Parolaro, D. Therapeutic Potential of Cannabidivarin for Epilepsy and Autism Spectrum Disorder. *Pharmacol Ther* **2021**, *226*. https://doi.org/10.1016/j.pharmthera.2021.107878.

(130) Bloemendal, V. R. L. J.; van Hest, J. C. M.; Rutjes, F. P. J. T. Synthetic Pathways to Tetrahydrocannabinol (THC): An Overview. *Org Biomol Chem* **2020**, *18* (17), 3203–3215. https://doi.org/10.1039/d0ob00464b.

(131) Cheng, L. J.; Xie, J. H.; Chen, Y.; Wang, L. X.; Zhou, Q. L. Enantioselective Total Synthesis of (-)-Δ8-THC and (-)-Δ9-THC via Catalytic Asymmetric Hydrogenation and S NAr Cyclization. *Org Lett* **2013**, *15* (4), 764–767. https://doi.org/10.1021/ol303351y.

(132) Schafroth, M. A.; Zuccarello, G.; Krautwald, S.; Sarlah, D.; Carreira, E. M. Stereodivergent Total Synthesis of Δ9-Tetrahydrocannabinols. *Angewandte Chemie - International Edition* **2014**, *53* (50), 13898–13901. https://doi.org/10.1002/anie.201408380.

(133) Ametovski, A.; Lupton, D. W. Enantioselective Total Synthesis of (-)-Δ 9 -Tetrahydrocannabinol via N-Heterocyclic Carbene Catalysis. *Org Lett* **2019**. https://doi.org/10.1021/acs.orglett.9b00198.

(134) Giorgi, P. D.; Liautard, V.; Pucheault, M.; Antoniotti, S. Biomimetic Cannabinoid Synthesis Revisited: Batch and Flow All-Catalytic Synthesis of (±)-Ortho-Tetrahydrocannabinols and Analogues from Natural Feedstocks. *European J Org Chem* **2018**, *2018* (11), 1307–1311. https://doi.org/10.1002/ejoc.201800064.

(135) Chiurchiù, E.; Sampaolesi, S.; Allegrini, P.; Ciceri, D.; Ballini, R.; Palmieri, A. A Novel and Practical Continuous Flow Chemical Synthesis of Cannabidiol (CBD) and Its CBDV and CBDB Analogues. *European J Org Chem* **2021**, *2021* (8), 1286–1289. https://doi.org/10.1002/ejoc.202001633.

(136) Aguillón, A. R.; Leão, R. A. C.; De Oliveira, K. T.; Brocksom, T. J.; Miranda, L. S. M.; De Souza, R. O. M. A.; De Souza, R. O. M. A. Process Intensification for Obtaining a Cannabidiol Intermediate by Photo-Oxygenation of Limonene under Continuous-Flow Conditions. *Org Process Res Dev* **2020**, *24* (10), 2017–2024. https://doi.org/10.1021/acs.oprd.0c00131.

(137) Bloemendal, V. R. L. J.; Spierenburg, B.; Boltje, T. J.; Van Hest, J. C. M.; Rutjes, F. P. J. T. One-Flow Synthesis of Tetrahydrocannabinol and Cannabidiol Using Homo- and Heterogeneous Lewis Acids. *J Flow Chem* **2021**, *11*, 99–105. https://doi.org/10.1007/s41981-020-00133-2/Published.

(138) Plutschack, M. B.; Pieber, B.; Gilmore, K.; Seeberger, P. H. The Hitchhiker's Guide to Flow Chemistry. *Chem Rev* **2017**, *117* (18), 11796–11893. https://doi.org/10.1021/acs.chemrev.7b00183.

(139) Marzullo, P.; Foschi, F.; Coppini, D. A.; Fanchini, F.; Magnani, L.; Rusconi, S.; Luzzani, M.; Passarella, D. Cannabidiol as the Substrate in Acid-Catalyzed Intramolecular Cyclization. *J Nat Prod* **2020**, *83* (10), 2894–2901. https://doi.org/10.1021/acs.jnatprod.0c00436.

(140) Jaidee, W.; Siridechakorn, I.; Nessopa, S.; Wisuitiprot, V.; Chaiwangrach, N.; Ingkaninan, K.; Waranuch, N. Kinetics of CBD, Δ9-THC Degradation and Cannabinol Formation in Cannabis Resin at Various Temperature and PH Conditions. *Cannabis Cannabinoid Res* **2022**, *7* (4), 537–547. https://doi.org/10.1089/can.2021.0004.

(141) Gaoni, Y.; Mechoulam, R. THE ISO-TETRAHYDROCANNABINOLS. *Isr J Chem* **1968**, *6*, 679–690.

(142) Colella, M.; Carlucci, C.; Luisi, R. Supported Catalysts for Continuous Flow Synthesis. *Top Curr Chem* **2018**, *376* (6). https://doi.org/10.1007/s41061-018-0225-0.

(143) Masuda, K.; Ichitsuka, T.; Koumura, N.; Sato, K.; Kobayashi, S. Flow Fine Synthesis with Heterogeneous Catalysts. *Tetrahedron* **2018**, *74* (15), 1705–1730. https://doi.org/10.1016/j.tet.2018.02.006.

Acknowledgments

The final part of this thesis is dedicated to acknowledge all the people who have been part of this crazy journey, all the people who have contributed to the work described in these pages. They are the best witness of my path, as a scientist and as a person.

For these same reasons, I want to thank my supervisor, Prof. Alessandro Palmieri, for the wise guidance over these years, for the experience and passion that he has for organic chemistry and for the work, and for all the knowledge that he tried to transfer me.
I want to express my gratitude to all the professors and researchers that I met during my PhD in Camerino, at all the conferences and meetings around Italy, and in my abroad period at the University of Graz. I want to thank Prof. C. O. Kappe for the incredible opportunity to work in his lab and with his team, filled with equally incredible and extremely passionate minds and people.

I want to thank all scientists of Indena SpA, for believing in me from day one, and supporting (also sponsoring) me, even if my previous experience was more pharmaceutical than chemical.
Thank you Daniele, if I am here now is for you.
A special mention to Prof. Simona Collina, my mentor at the University of Pavia, and to my first lab family.

A big part of this journey was (and is) represented by my colleagues, especially the ones that now I can call friends. Everyone taught me something, and supported me over these years (especially during the writing phase of this thesis). I am carrying you all with me today! I am not making names, no list is needed, you know it. We will drink together.

Growing up the circle of friends gets smaller, the people that remain are the one that are part of your inner tissue, the one that resemble you, the one that you actually choose to surround yourself with. Thank you to all the friends that I met around during my multiple experiences: from my hometown, in Spain and Austria, to the Marche, until reaching the top of the mountains.
Among these, a special mention to my anchors, my safe place: Giulia, Michela, Ardea.

Within this process of living the life, changing, making trials and errors, sometimes you find some answers, and sometimes these answers have the shape of a person, that bring everything together, that links the dots of who you already are. Lorenzo, you are my present. Together we are the home in which I want to live in, the garden where we are continuously sowing our future. If you didn't dump me in these last few months, you're definitively screwed. Ti amo proprio.

Marina. Gigi. Lorenzo. E tutti nostri cani. Nonni. Grazie, per tutte le cose materiali, e infinitamente di più per l'amore, la cura, i valori, il tempo, la comprensione, i consigli. Mi dispiace ogni giorno di esservi fisicamente distante, ma spero di potervi ripagare di tutto. Vi porto sempre con me. Vi voglio bene.

Thank you Camerino, you are the best mirror of my personality. You brought me truth, air, and peace. Resisti.

Continuiamo a "fluire con il mare della vita". (Qualcuno lo sapeva già anni fa)
Il cammino è sempre da ricominciare.